Development of diffuse large B-cell lymphoma mouse models and role of CXCR4 in dissemination

Desarrollo de modelos murinos de linfoma difuso de células grandes B y papel de CXCR4 en diseminación

María José Moreno Jiménez

UNIVERSITAT DE BARCELONA

Universitat de Barcelona
Facultat de Biologia
Departament de Bioquímica i Biologia molecular
Programa de Doctorado en Biomedicina

Development of diffuse large B-cell lymphoma mouse models and role of CXCR4 in dissemination

Desarrollo de modelos murinos de linfoma difuso de células grandes B y papel de CXCR4 en diseminación

María José Moreno Jiménez

2014

Universitat de Barcelona
Facultat de Biologia
Departament de Bioquímica i Biologia molecular
Programa de Doctorado en Biomedicina

Development of diffuse large B-cell lymphoma mouse models and role of CXCR4 in dissemination

Memoria de tesis doctoral presentada por

María José Moreno Jiménez

Para optar al grado de

Doctora por la Universitat de Barcelona

Directores de tesis: Dr. Ramon Mangues Bafalluy y Dra. Isolda Casanova Rigat

del Grup d'Oncogènesi i Antitumors de l'Institut d'Investigacions Biomèdiques Sant Pau

Tutora: Dra. Marta Cascante Serratosa

Programa de Doctorado en Biomedicina

Dr. Ramon Mangues — Dra. Isolda Casanova

Dra. Marta Cascante — María José Moreno

A mis padres

"The best way to make children good is to make them happy"

"El medio mejor para hacer buenos a los niños es hacerlos felices"

Oscar Wilde

A Adri

"Dejarse llevar suena demasiado bien.

Jugar al azar,

nunca saber dónde puedes terminar...

o empezar"

Copenhague, Vetusta Morla

Un día en el mundo, 2008

Acknowledgments

"A veces la impaciencia

da más frutos que los más profundos cálculos"

William Shakespeare

Quien iba a decir que llegaría este momento taaaaan rápido… La verdad es que cuando decidí hacer una tesis doctoral afronté la decisión con mucha ilusión pero también con miedo, miedo de no ser capaz de estar al nivel de todo el sacrificio que requiere este mundillo de la investigación. Y la verdad es que aunque no ha sido un camino de rositas, ha merecido la pena y he aprendido mucho de esta experiencia. A día de hoy (a punto de depositar la tesis), puedo decir que al final todos los miedos y obstáculos se superan.

Llegados a este punto, me gustaría agradecer a todas las personas que han estado ahí, ya sea a nivel de jefes, compañeros, amigos o familiares.

En primer lugar, doy las gracias a mis directores de tesis, Ramon e Isolda, por confiar en mí y darme la oportunidad de realizar la tesis en el Grupo de Oncogénesis y Antitumorales. Durante estos 4 años he aprendido mucho de vosotros. También doy las gracias al Dr Jordi Sierra por todo su apoyo a lo largo de esta tesis doctoral. Además agradezco al Dr Sergio Serrano, a la Dra Adela Mazo y a la Dra Anna Bigas por haber sido parte del tribunal de tesis. También muchas gracias al Dr Pep Nomdedeu, a la Dra Silvia Vidal y al Dr Simo Schwartz por aceptar ser el tribunal suplente.

Como no, agradecer a todos los compañeros del *GOA club* la ayuda recibida y los buenos momentos compartidos. Cristina e Irene, porque sois las que habéis estado ahí durante los últimos 2 años como compañeras y como

amiguísimas, para los buenos momentos y también para los no tan buenos. Irene, aunque nos conocemos desde hace poco, rapidísimamente te has convertido en una más del grupo, menudas charletas trascendentales y de apoyo hemos llegado a tener! A Cristina porque además de ser una buena amiga de esas de toda la vida (y prima), has demostrado ser una magnífica compañera! También gracias por tu ayuda con todo el experimental, sobre todo en esta última etapa. A Rebeca, porque aunque en realidad no estuvimos mucho tiempo juntas en el labo, te has convertido en mi amiga del alma, muchas gracias por tu apoyo a nivel científico, y sobre todo, por demostrar que a las amigas de verdad no les importa la distancia. Al doctor remamadísimo Marcelinho! Que aunque al principio parecías estirado y serio… (jajajaja), me encanta tu buen humor y que siempre estés ahí para ayudarme, escucharme y aconsejarme; te has convertido en un gran amigo y compañero! Muchas gracias por tu optimismo y por esos cafés matutinos que nos tomábamos junto con Irene y Cris! Menudo cuarteto! Echaré mucho de menos esos cafelillos! ;) A Rous, que aunque tampoco hemos coincidido mucho en el GOA, he aprendido mucho de ti, sobre todo al principio mientras tu escribías la tesis y yo te inundaba con mis preguntas sobre los ratatuis y el background de las células! Y porque siempre has estado ahí para echarnos unas buenas risas!

La lista sigue…. Gracias a todas las chicas por los buenos ratos en las comidas, risas y desahogos, Pati, Carmen, Montse, Laura… Pati a ti también gracias por resolverme todas mis dudas de formato con el word, maquetado de tesis, etc, qué pesada que soy, jajaja! También muchas gracias a Montse e Iris por todo el trabajo de histología e immunos, gracias a Montse por sus charletas en momentos de saturación y por iniciarme en el mundo scrapero! También muchas gracias a Marta Soler por su ayuda con los FACs y la facilidad que ofrece para usar su servicio. Y como no, muchas gracias a Sergi del estabulario

del ICCC, por estar siempre ahí cuando he tenido dudas con los animales o he necesitado consejos.

Y a todos los demás compis y excompis del GOA que también habéis estado ahí, Miguel Ángel, Marta, Víctor, Carlos, Virtu, Olga, Everton... A Miguel Ángel muchas felicidades en tu nueva etapa como papi! Y a Víctor, felicidades y ánimo con tu nueva etapa post-doctoral!

Espero no dejarme a ningún compañero de Sant Pau… de todos modos, si estás leyendo esto, muchas gracias también! ;)

Y ahora viene la parte más personal, esa que no se me da tan bien y que por tanto intentaré que sea breve… Mis amigos y familia. La verdad es que agradezco poder contar con vosotros y que seáis un soporte tan importante para mí, siempre va bien sentirte apoyada y querida. Mis amigos, Suárez, Cañi, Víctor, Belén, Irene, Mofi, Rebe, Carlos, Javi, Karel… Todos vosotros me habéis aguantado en esos momentos de saturación mental post-día-duro-de-tesis. Muchas gracias por los buenos momentos compartidos, se aproximan días de jolgorio y celebración! Preparaos bigoteros y bigoteras porque *la nit de Sant Joan* está a la vuelta de la esquina!

No querría concluir este apartado sin incluir a otros amigos que, aunque no nos vemos tan a menudo, también son muy importantes para mi, Pati, Carlos, las parkinianas (ibicencas y andaluzas), la Rusa, Marteta y compis Biotech (Clemen, Flequi, Sonia, Laura, Raquel…).

Y como lo mejor siempre se deja para el final… Adri, muchas gracias por compartir tu vida conmigo, gracias por tu apoyo, por estar siempre ahí para sacarme unas risas, por hacer que los días grises se conviertan en los más

soleados, por ser tú por encima de todo, y por hacerme taaaan feliz días tras día! Ah! Y como no, por nunca perder la ilusión por la vida, jajajaja! ;)

Papá, mamá, muchísimas gracias por todo el amor y educación que me habéis dado, sin vosotros no sería quien soy ahora ni hubiese llegado hasta aquí. Papis, Carlos, Víctor, juntos hemos superado momentos difíciles y ahora toca seguir disfrutando de lo lindo! Carlos a ver si te aplicas más en clase y te haces futbolista de éxito! Víctor, has demostrado superación absoluta, seguro que en esta nueva etapa encontrarás tu camino!

Content

"The truth is what is, and remains true even if one thinks the other way around"

"La verdad es lo que es, y sigue siendo verdad aunque se piense al revés"

Antonio Machado

LIST OF TABLES

LIST OF FIGURES

ABBREVIATIONS

ABC: Activated B cells

ALL: Acute lymphoblastic leukaemia

AML: Acute myelogenous leukaemia

ASCT: Autologous Stem Cell Transplantation

BCR: B-cell Receptor

BLI: Bioluminescence Imaging

BM: Bone marrow

B-CLL: B-cell chronic lymphocytic leukaemia

B-NHL: B-cell NHL

CHOP: Cyclophosphamide, Doxorubicin, Vincristine, and Prednisone

CNS: Central nervous system

CR: Complete Remission

CSR: Class-Switch Recombination

CXCR4: C-X-C chemokine receptor type 4

DLBCL: Diffuse Large B cell Lymphoma

DMSO: Dimethil sulfoxide

ECOG: Eastern Cooperative Oncology Groups

FDA: US Food and Drug Administration

FDC: Follicular Dendritic Cell

GCB: Germinal Center B-cell

GEM: Genetically Engineered Mice

GEP: Gene Expression Profiling

GFP: Green Fluorescent Protein

HL: Hodgkin Lymphoma

HSC: Haematopoietic Stem Cells

HSCT: Hematopoietic Stem Cell Transplantation

ICE: Ifosfamide-Carboplatin-Etoposide

Ig: Immunoglobulin

IPI: International Prognostic Index

iv: Intravenous

LDH: Lactate Dehydrogenase

LN: Lymph nodes

Luc: Luciferase

MFI: Mean fluorescence intensity

MM: Multiple myeloma

MTD: Maximum Tolerated Dose

NF-*k*B: Nuclear factor- Kappa B

NHL: Non-Hodgkin Lymphoma

NOD: Non-Obese Diabetic

OS: Overall Survival

PFS: Progression-Free Survival

PI: Propidium Iodide

PMBL: Primary Mediastinal Large B-cell lymphoma

R-CHOP: Rituximab and CHOP

R-IPI: Revised IPI

REAL: Revised European-American Lymphoma

RICE: Rituximab and ICE

Sc: Subcutaneous

SCID: Severe Combined Immunodeficiency

SDF-1: Stromal Cell-Derived Factor-1

SHM: Somatic Hypermutations

TMA: Tissue microarray

T-NHL: T-cell NHL

WF: Working Formulation

WHO: World Health Organization

“Je donnerais tout ce que je sais, pour la moitié de ce que je ne sais pas”

“Daría todo lo que sé por la mitad de lo que ignoro”

René Descartes

INTRODUCTION

1. LYMPHOMA

1.1 DEFINITION

Lymphomas are a heterogeneous group of malignancies arising from the lymphopoietic system. This diverse group of neoplasms is estimated to account for around 3-4% of cancers world-wide.[1,2] Genomewide molecular profiling has revealed new subtypes of lymphoma that originate from lymphocytes that differ in their developmental stage and that use distinct oncogenic pathways.[3]

1.2 CLASSIFICATION OF LYMPHOMAS

1.2.1 Hodgkin and non-Hodgkin lymphomas

Lymphoid malignancies are classified in two main groups: Hodgkin lymphoma (HL), and non-Hodgkin lymphoma (NHL).

Hodgkin lymphoma (HL): This malignancy is characterized by easily detected large polynuclear Reed-Sternberg cells. According to differences in the morphology and phenotype of the lymphoma cells and the composition of the cellular infiltrate, Hodgkin lymphoma is subdivided into classical Hodgkin lymphoma and nodular lymphocyte-predominant Hodgkin lymphoma. The incidence of HL is lower than the so-called non- Hodgkin lymphoma.[2]

Non-Hodgkin lymphoma (NHL): This subtype of lymphoma is composed by a heterogeneous group of more than 30 malignancies arising from lymphoid tissue, with diverse clinical and biological features. NHL is classified in two main subgroups: B-cell non-Hodgkin lymphoma (B-NHL) and T-cell and natural-killer cell non-Hodgkin lymphoma (T-NHL).[4] In most European countries, NHL

mortality rose up to the mid 1990s, and started to decline in the following decade.[5] The most common NHL subtypes in developed countries are diffuse large B-cell lymphoma (about 30%) and follicular lymphoma (about 20%). All other NHL subtypes have a frequency of less than 10%.[6] Diffuse large B-cell lymphoma (DLBCL) is the disease studied in this PhD thesis.

1.2.2 Classification of non-Hodgkin lymphomas

Many systems have been developed over the time to classify lymphomas, reflecting increased understanding of the morphology, immunology and molecular genetics of the disease.[7] The classification of NHL has considerably changed over the past years. The oldest classification known for this malignancy is the Rappaport system. This classification system is based on the cell morphology and proposed a separation of NHL into two clinically useful categories: those with a favorable prognosis (nodular lymphomas) and those with an unfavorable prognosis (diffuse lymphomas).[8] In 1982, the international Working Formulation (WF) sponsored by the National Cancer Institute introduced a new classification system that included the Rappaport and the immunologically oriented Lukes and Collins and Kiel systems. The WF classification excluded the Hodgkin lymphoma and is based on the aggressiveness and morphology of lymphoma cells. This classification of NHL introduced 3 categories: low, intermediate, and high-grade lymphoma types.[9]

From the early 1990s, observations related to the immunology and genetics of lymphomas allowed the identification of previously unrecognized subtypes. The recognition of these new entities led to a new classification proposed by the Revised European-American Lymphoma (REAL). This new classification included not only morphologic subgroups, but also immunophenotypes,

genetic abnormalities, and clinical observations.[10] The World Health Organization (WHO) accepted and updated the REAL classification and is currently the gold standard used throughout the world.[11] The WHO classification subdivides lymphomas into those of B-cell versus T- and NK-cell origin.[12] This classification has been updated in 2001[13] and more recently in 2008.[14] In **Table 1**, the WHO 2008 modified classification is shown for B-cell and T-cell and NK-cell neoplasms. The complete classification of lymphomas is enclosed in **Appendix I**.

Table 1. WHO 2008: NHL B-cell neoplasms. [14]

B-CELL NEOPLASMS
I. Precursor B-cell neoplasm
Precursor B-lymphoblastic leukaemia/lymphoma (B-ALL/LBL)
II. Mature (peripheral) B-cell neoplasms
B-cell chronic lymphocytic leukaemia/small lymphocytic lymphoma
B-cell prolymphocytic leukaemia
Lymphoplasmacytic lymphoma
Splenic marginal zone lymphoma
Hairy cell leukaemia
Plasma cell myeloma/Plasmacytoma
Extranodal marginal zone B-cell lymphoma of mucosa-associated lymphoid tissue (MALT lymphoma)
Mantle cell lymphoma
Follicular lymphoma
Nodal marginal zone B-cell lymphoma
Diffuse large B-cell lymphoma (DLBCL), not otherwise specified
Burkitt lymphoma
T-CELL AND NK-CELL NEOPLASMS
I. Precursor T-cell neoplasms
Precursor T-lymphoblastic lymphoma/leukaemia
II. Mature (peripheral) T-cell neoplasms
T-cell prolymphocytic leukaemia
T-cell granular lymphocytic leukaemia
Aggressive NK-cell leukaemia
Adult T-cell lymphoma/leukaemia (HTLV1+)
Extranodal NK/T-cell lymphoma, nasal type
Enteropathy-type T-cell lymphoma
Hepatosplenic gamma/delta T-cell lymphoma
Subcutaneous panniculitis-like T-cell lymphoma
Mycosis fungoides/Sezary's syndrome
Anaplastic large cell lymphoma, primary cutaneous type
Peripheral T-cell lymphoma, unspecified
Angioimmunoblastic T-cell lymphoma
Anaplastic large cell lymphoma, primary systemic type
HODGKIN DISEASE/LYMPHOMA
I. Lymphocyte predominance
II. Nodular sclerosis
III. Mixed cellularity
IV. Lymphocyte depletion
V. Lymphocyte-rich classical Hodgkin disease

2. NORMAL B CELLS

2.1 BIOLOGY OF B CELLS

The main task of the immune system is to recognize foreign antigens and invading organisms (viruses, bacteria, fungi, protozoa, etc). This task is accomplished by two different mechanisms, known as natural and adaptive immunity. The natural or inborn immunity is the first line of defens and consists of the non-specific complement system, macrophages and natural killer cells. In contrast, the adaptive immunity is based on the ability of B and T lymphocytes to respond specifically and selectively to different antigens.

B lymphocytes are small (6-10 μm) cells that have a dense nucleus and little cytoplasm. They were discovered together with T cells in the early 1960s and can be distinguished phenotypically by analysis of cell surface markers.[15] B lymphocytes are generated from hematopoietic stem cells (HSC) within the bone marrow in a multistep differentiation process.[16] Their development involves several differentiation stages and the successive acquisition of properties that are essential for the correct function of mature B cells. In the marrow, a primary B-cell repertoire is produced through several immunoglobulin (Ig) gene rearrangements steps to form an antigen B-cell receptor (BCR); then, in the secondary lymphoid organs, a secondary B-cell repertoire is generated through somatic hypermutation and class-switch recombination upon antigen encounter (**Figure 1**).

Hence, the B cells leaving the bone marrow are mature lymphocytes that express a functional and selected BCR. These cells have not been exposed to external antigens and are known as “naïve B cells”. Then, they leave the bone marrow to circulate through the blood stream for antigen encounter within the

secondary lymphoid organs (spleen, lymph nodes and mucosa-associated lymphoid tissues). Antigen binding is required for the final stages of B cell development. Antigen-activated B cells may enter the germinal center microenvironment (found in the cortex of lymph nodes), where they will undergo clonal expansion.[17] Once activated, B cells are transformed into large and proliferating cells, known as centroblasts that may form the germinal center structure. The subsequent cell division of the centroblasts leads to the expansion of specific clonal lineages that will react against one specific antigen. Then, centroblasts differentiate into centrocytes (small non-proliferating lymphocytes) that will be positively selected by antigen-presenting follicular dendritic cells (FDC) and T-cells. Some of these selected centrocytes may be differentiated into Ig-secreting plasmablasts and others may migrate to the marginal zone as memory B cells.[18,19] In the germinal center, following the antigen encounter and the clonal expansion, two types of genetic changes take place. First, the somatic hypermutations (SHM) in the variable region of the Ig genes that increase the affinity and specificity of B-cell receptor for the antigen. And then, the class-switch recombination (CSR), to allow those modified antigen-binding sites to be expressed with all possible Ig constant regions and carry out a variety of effector functions throughout the body (**Figure 1**).

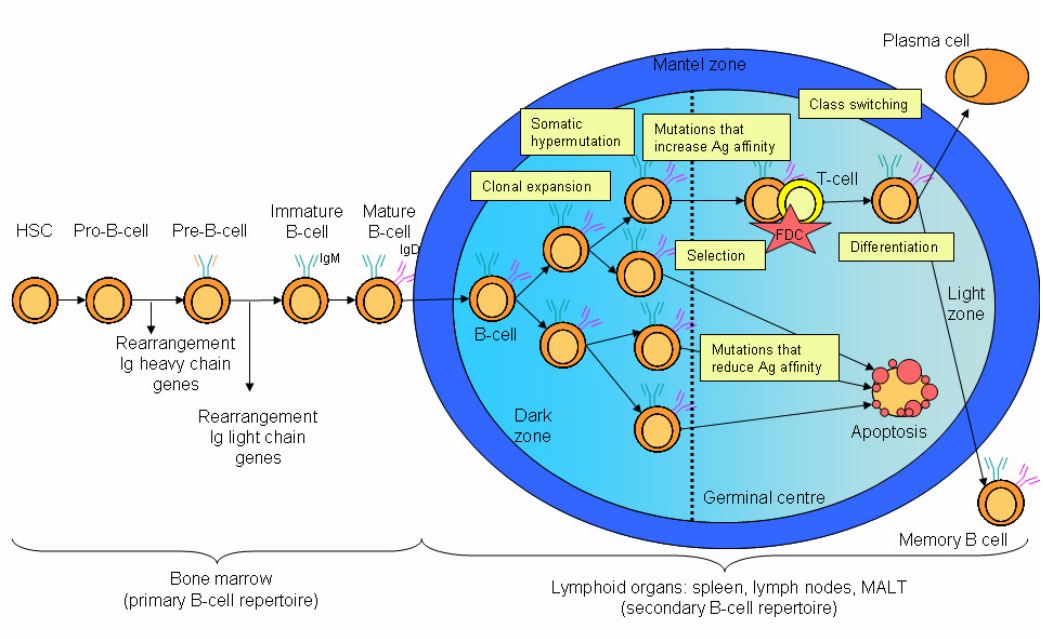

Figure 1. B-cell development diagram. Schematic representation of the events in the development of primary and secondary B cell repertoire. Ig, immunoglobulin; Ag, antigen; HSC, haematopoietic stem cell; MALT, mucosa-associated lymphoid tissue. (Adapted from references 20,21).

2.2 B-CELL DIFFERENTIATION AND REARRANGEMENT

The earliest B cells in the bone marrow are known as the progenitor B cells or pro-B cells. These cells are committed to the lymphoid lineage and differ from HSC in the expression of B-cell molecules, such as CD19 and CD79A, and also by their ability to rearrange Ig genes. This rearrangement process is known as VDJ rearrangement and implies highly regulated recombinant events resulting in a functional BCR or IgM expression in the membrane of B lymphocytes.

The B-cell receptor (BCR) is a transmembrane receptor composed of two identical heavy-chain and two identical light-chain immunoglobulin (Ig)

polypeptides that are covalently linked by disulphide bridges (**Figure 2A**). Other components of the BCR receptor are the CD79A and CD79B molecules, which contain cytoplasmic immunoreceptor tyrosine-based activation motifs to transmit signals following the BCR crosslinking.[16] The BCR receptor is generated in the early stages of B-cell maturation in the bone marrow. To generate the variable region of the BCR, the genes of this region are assembled by somatic recombination of variable (V), diversity (D) and joining (J) segments for the heavy chains, and V and J segments for the light chains (**Figure 2**B). Hence, as there are many different V, D and J segments in the germline, a wide repertoire of BCR receptors with different antigen recognition can be generated.[21]

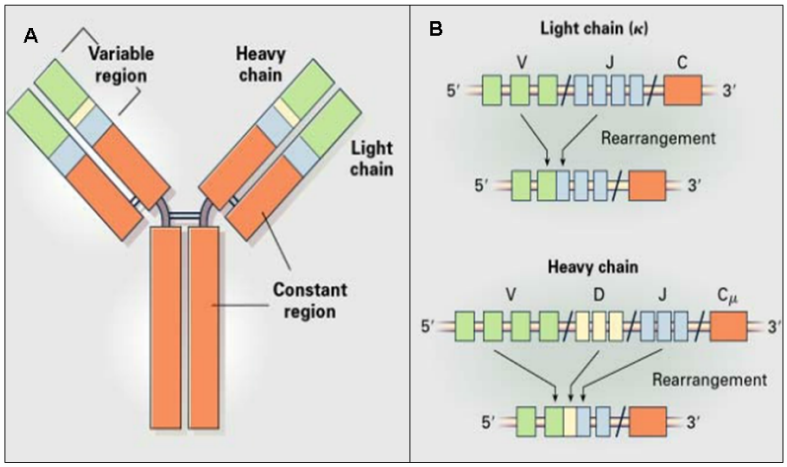

Figure 2. BCR structure and V(D)J recombination in B-cell development. (A) The BCR receptor consists of two identical heavy chains and two identical light chains. (B) Somatic recombinations in the variable-region genes for the heavy and light chains of the B-cell receptor (Adapted from reference 22).

As previously mentioned, the development of B cells occurs through several main stages, resulting in a functional BCR expressed in the cell membrane (**Figure 1 and 3**):

1) **Pro-B cell**: Characterized by rearrangement of the Ig heavy chain genes. The constant region of the heavy chain is rearranged and further rearrangements attach the variable genes to the constant segment.

2) **Pre-B cell**: Characterized by rearrangement of the Ig light chain genes. The heavy chains are joined to the light chains and rearrangement of the Ig light chain genes lead to the expression of IgM or BCR molecule in the membrane.

3) **Immature B cell**: Characterized by the expression of functional IgM or BCR on cell surface. The contact between IgM and the antigen leads to the apoptosis of cells that have generated autoreactive IgM. The selected immature B cells migrate from the bone marrow to the lymph nodes where they will be further selected to generate the mature B-cell.

4) **Mature B cell**: Naïve mature B cells that have not been exposed to the antigen, express both IgM and IgD molecules in their surface, made from alternatively spliced heavy-chain transcripts.[21] Antigen encounter leads to activation of mature B cells in peripheral lymphoid tissues where class switch recombination (CSR) occurs. During the CSR, the exons for the constant domain of the heavy chain of IgM are swapped with downstream exons to generate different classes of antibody, such as IgG, IgE or IgA. Gene rearrangements will also take place in peripheral B cells undergoing somatic hypermutation (SHM) to increase antibody-binding specificity.[23]

During the described B-cell development, several DNA breaks are generated in the process of immunoglobulin gene rearrangement in the bone marrow and also in the processes of SHM and CSR in the germinal center.[24] These DNA breaks are dangerous mechanisms that might pre-dispose to chromosomal translocations. In lymphomas, chromosomal translocations are typically

associated with inappropriate oncogene expression that gives place to the disease.[25,26]

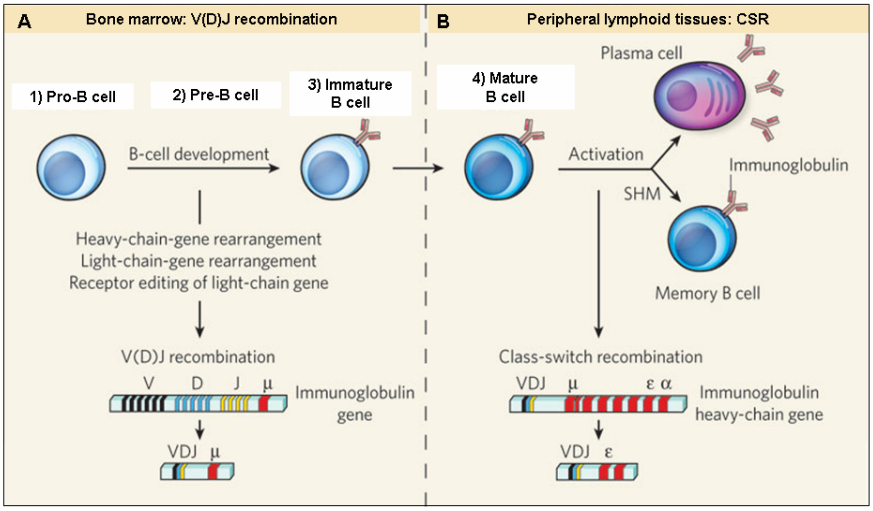

Figure 3. Immunoglobulin gene rearrangements. (A) Recombination of variable (V), diversity (D) and joining (J) segments of immunoglobulin genes generates B-cell receptors during development in the bone marrow. (B) Class-switch recombination occurs after activation of mature B cells in peripheral lymphoid tissues to generate a different antibody class. Activated B cells also undergo somatic hypermutation as they develop into memory B cells (Adapted from reference 23).

2.3 CELLS OF ORIGIN OF B-CELL LYMPHOMAS

Historically, the relationship between normal and malignant B cells has been established by a combination of microscopic appearance and immunophenotype. It has been observed that most B-cell malignancies seem to be "frozen" at particular stages of normal B-cell development, which reflects their origin. However, oncogenic translocations might occur at an early stage of B-cell differentiation, after which the transformed B cell might differentiate further and get "frozen" at a later stage. The important fact is that the tumor phenotype will influence its clinical behavior.[25] Therefore, analysis of the BCR

structure and expression patterns of differentiation markers are routinely used to determine the origin of several human B-cell lymphomas.[22]

One of the main concepts emerging from these studies is that most types of B-cell lymphomas are derived from the germinal center or from post-germinal center B-cells.[22,27] Gene-expression profiles have shown a relationship between stages of B-cell differentiation and several types of B-cell lymphomas. Based on these profiles two main subtypes of diffuse large B-cell lymphoma (DLBCL) have been identified, one resembling germinal center B-cells (GCB) and another resembling activated B-cells (ABC). As shown in **Figure 4**, human B-cell lymphomas are assigned to their normal counterparts that have been transformed during the B-cell development stages. Tumors corresponding to almost all stages of B-cell development have been found in humans. Moreover, most lymphoid tumors have gene rearrangements characteristic of the cell type from which they arose.[28]

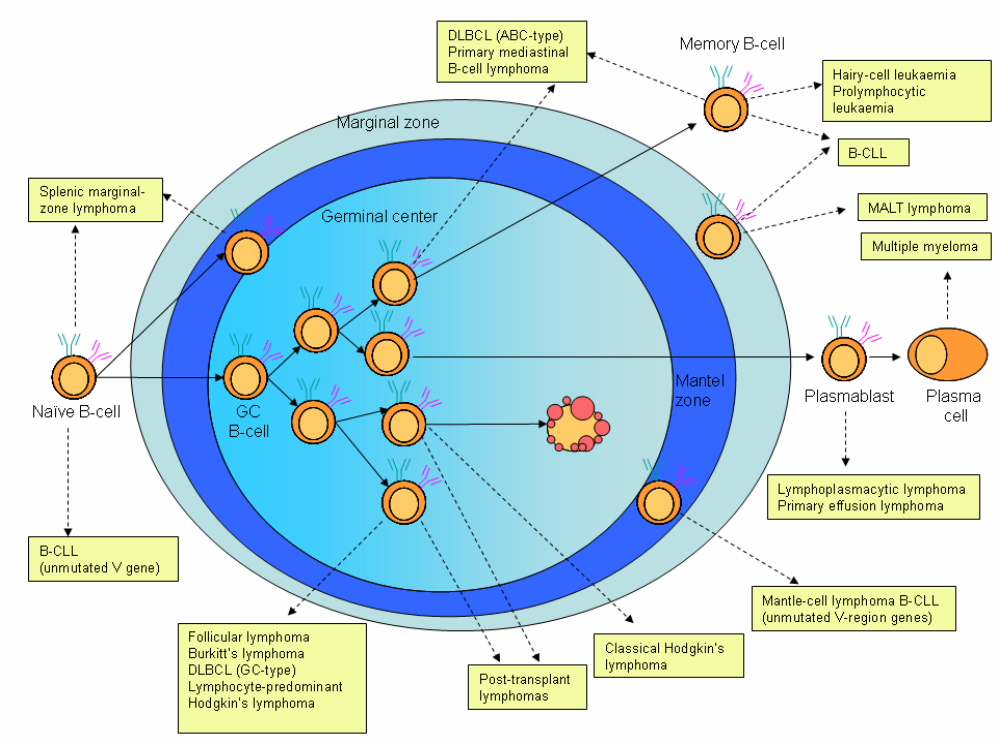

Figure 4. Cellular origin of human B-cell lymphomas. Human B-cell lymphomas are assigned to their proposed normal B-cell counterpart. Most lymphomas are derived from germinal-center B-cells (GCB) or from activated B–cells (ABC) that have passed through the germinal center.[20] B-CLL, B-cell cronic lymphocytic leukaemia; MALT, mucosa-associated lymphoid tissue; GC, germinal center.

3. DIFFUSE LARGE B-CELL LYMPHOMA

Diffuse large B-cell lymphoma (DLBCL) is the most frequent lymphoma in adults accounting for 30% of all non-Hodgkin lymphoma (NHL) cases.[20] DLBCL is a clinically and biologically heterogeneous group of lymphomas composed of malignant large B cells and is characterized as an aggressive disease.[29]

3.1 ETIOLOGY AND CLINICAL FEATURES

DLBCL is a lymphoma characterized by the presence of large neoplastic cells with a diffuse growth pattern. Within cellular morphology three variants are the most commonly seen: centroblastic, immunoblastic, and anaplastic. Centroblastic DLBCL is the most common form, with tumor cells having vesicular chromatin, small cytoplasm and multiple small nucleoli. In the immunoblastic variant, tumor cells resemble immunoblasts and contain basophilic cytoplasm and a central nucleolus. Although sometimes the tumour can be monomorphic, composed almost entirely of centroblasts, usually the tumors are polymorphic with a mixture of centroblastic and immunoblastic cells. The third morphologic variant, anaplastic, consists of tumour cells that are very distinct from their normal B cell counterparts. The cells are generally very large with a round, oval, or polygonal shape and pleomorphic nuclei resembling Hodgkin or Reed-Sternberg cells.[30]

Initial diagnosis of large cell lymphomas is more common in the elderly, around the seventh decade, though they are not restricted to any particular group of age.[31] Usually patients present a growing, painless lymph node. However, in 40% of patients, the initial infiltrated site is extra-nodal (outside the lymph nodes), commonly involving the gastrointestinal and genitourinary

tracts, skin, central nervous system, lungs, or the bones.[32] In up to 15% of patients, bone marrow is also involved, about one-third of the patients present B-symptoms (fever, night sweats, and weight loss), almost 50% have Ann Arbor system stage III/IV disease (**Table 2**), and more than 50% have an elevated serum lactate dehydrogenase (LDH) level.[33]

Table 2. Ann Arbor Staging System for non-Hodgkin Lymphoma.[34]

Stage	Spread of disease
I	Involvement of a single lymph node region or of a single extranodal organ or site (I_E)
II	Involvement of two or more lymph node regions on the same side of the diaphragm, or localized involvement of an extranodal site or organ (II_E) and one or more lymph node regions on the same side of the diaphragm
III	Involvement of lymph node regions on both side of the diaphragm, which may also be accompanied by localized involvement of an extranodal organ or site (III_E) of spleen (III_S) or both (III_{SE})
IV	Diffuse or disseminated involvement of one or more distant extraanodal sites.

The stages are described by Roman numerals (I-V). Lymphomas that affect an organ outside of the lymph system (an extranodal organ) have E added to their stage (for example, stage IIE), while those affecting the spleen have an S added.

For the majority of DLBCL patients, the etiology of the disease is unknown.[33] However, several factors are considered to potentially confer increased risk such as immunosuppression (including AIDS, and iatrogenic etiologies related to transplantation or autoimmune diseases), pesticides, ultraviolet radiation, hair dyes, and diet.[35]

3.2 CLASSIFICATION

As its name implies, DLBCL is a neoplasm of large B cells with diffuse growth that presents multiple morphologic variants. Several classifications have been established over the time reflecting the clinically heterogeneity of the pathology. In 2008 the World Health Organization (WHO) published a modified and updated DLBCL classification.[36] This new classification recognizes multiple morphologic variants based on an improved understanding of the variety of molecular abnormalities associated with the pathology (**Table 3**).[32] The classification of DLBCL has notably changed over recent decades, and will continue to do so as new diagnostic methods and techniques are developed.

Table 3. World Health Organization classification of the Large B-cell Neoplasms.[32]

DLBCL classification
Diffuse large B-cell lymphoma (DLBCL), NOS
T-cell/histiocyte rich large B-cell lymphoma
Primary DLBCL of the CNS
Primary cutaneous DLBCL, leg type
EBV^+ DLBCL of the elderly*
DLBCL associated with chronic inflammation
Lymphomatoid granulomatosis
Primary mediastinal (thymic) large B-cell lymphoma
Intravascular large B-cell lymphoma
ALK^+ large B-cell lymphoma
Plasmablastic lymphoma
Large B-cell lymphoma arising in HHV8-associated multicentric Castleman disease
Primary effusion lymphoma
B-cell lymphoma, unclassifiable, with features intermediate between diffuse B-cell lymphoma and Burkitt lymphoma
B-cell lymphoma, unclassifiable, with features intermediate between diffuse large B-cell lymphoma and classical Hodgkin lymphoma

NOS indicates not otherwise specified; CNS, central nervous system.
*Provisional entities for which the WHO Working Group felt there was insufficient evidence to recognize as distinct diseases at this time.

3.3 GENETIC ALTERATIONS IN DLBCL

Studies over the past decade have revealed that DLBCL compromises distinct molecular subgroups with different gene signatures and oncogenic pathways involved.[37] Accumulative studies have reported the high complexity of the DLBCL genome compared with other B cell malignancies, with an average of 30 to more than 100 lesions per case and high variability between patients.[38] As shown in **Figure 5**, somatic hypermutation of oncogenes occurs in a 50% of DLBCL cases.[39] Some of these mutable genes are also susceptible to chromosomal translocations. Here, we will explain some of the most common translocations and other genetic alterations involved in the DLBCL malignancy.

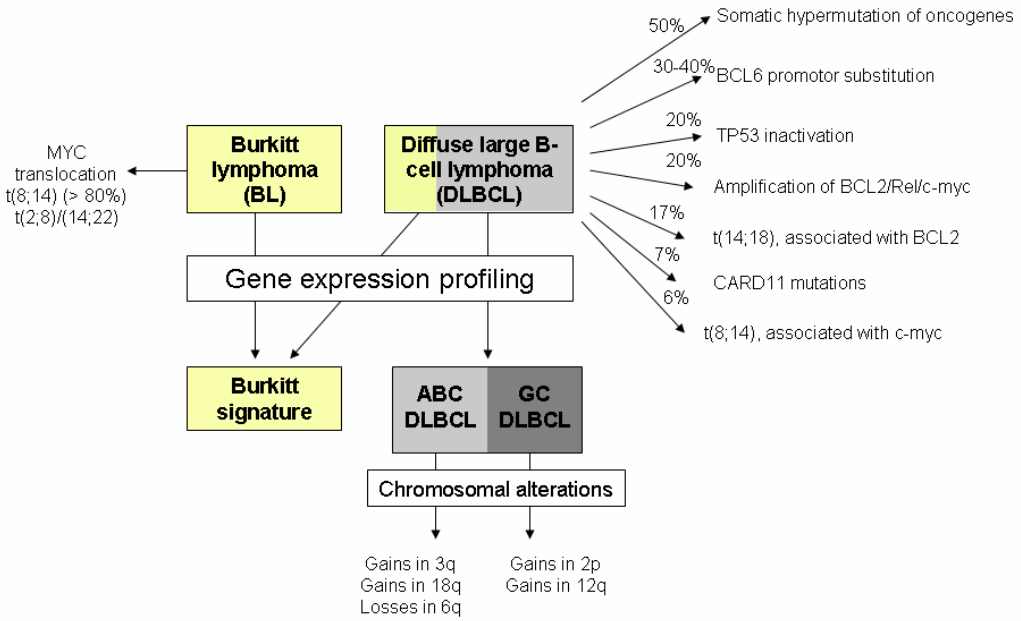

Figure 5. Molecular features of diffuse large B-cell and Burkitt lymphomas. Common genetic alterations and molecular signatures defined by gene-expression profiling are included.[39]

Reciprocal chromosomal translocations that involve one of the Ig (immunoglobulin) loci and a proto-oncogene are common alterations in many types of B-cell lymphomas. Consequently, the oncogene comes under the control of the active Ig locus, causing its constitutive expression.[26] As observed in **Figure 5**, the most frequent chromosomal translocations described in DLBCL are associated with BCL6, BCL2 and MYC genes.[20,39]

MYC: This is a pleiotropic transcription factor involved in many aspects of cellular development and physiology.[40] It was involved in the first chromosomal translocation associated with a lymphoproliferative disorder. The gene is associated with the translocation t(8;14)(q24;q32). The translocation juxtaposes the MYC gene in chromosome region 8q24 next to the IgH locus in chromosome region 14q32, leading to overexpression of the transcription factor MYC.[41] This translocation is observed in up to 6-30% of DLBCL cases.[39,42,43]

BCL2: This gene was discovered due to its implication in the translocation t(14;18)(q21:q34). This translocation causes constitutive overexpression of BCL2 by juxtaposing it to immunoglobulin heavy chain gene enhancer elements. BCL2 overexpression has been shown to inhibit apoptosis and to block chemotherapy-induced cell death.[41] Although the overexpression of BCL2 is usually associated with the t(14;18) translocation, it has also been detected in DLBCL patients with no translocation. This translocation has 20% of incidence in DLBCL patients.[44,45]

BCL6: This gene was discovered due to its involvement in chromosomal translocations t(11;14)(3q27) detected in NHL. These rearrangements juxtapose heterologous sequences derived from other chromosomes to the BCL6 coding

domain, causing a deregulation of the protein expression. The most frequent BCL6 rearrangement was detected in the 14q32 region. BCL6 is a transcription factor that plays a critical role in cell proliferation and differentiation. The rearrangements of BCL6 transcription factor are found in 30-40% of DLBCL cases. Furhtermore, independent of the rearrangements associated with BCL6 translocations, somatic-point-mutations have been described in the 5' non-coding region of this gene in 70% of DLBCL cases.[41]

Recently, it has been described that MYC aberrations are usually associated with complex karyotypes and with other cooperating genetic lesions such as BCL2 and BCL6 rearrangements, defining the so-called "double-hit" and "triple-hit" DLBCL.[43,46] MYC status together with BCL2 and BCL6 expression have been associated with prognosis and probably, in the near future, they will have an impact on defining the most appropriate treatment for DLBCL patients.[46,47]

In addition, some other genetic alterations have been described in DLBCL patients causing genome inestability. Some of these alterations are the already mentioned aberrant somatic hipermutations of proto-oncogenes,[48] mutations of the tumor suppressor TP53, amplification of BLC2/Rel/c-myc genes or genetic lesions leading to constituve activity of NF-κB like mutations in the oncogene CARD11 or MYD88 (**Figure 5**).[38,49,50]

Moreover, there is increasing evidence that epigenetic changes, such as DNA methylation, may play an important role in DLBCL pathogenesis and chemoresistance.[51-54] Further studies and clinical trials will be needed to define new treatment approaches to target this deregulated genes.

3.4 PROGNOSTIC FACTORS IN DLBCL

3.4.1 Clinical prognostic factors: The International Prognostic Index (IPI)

The International Prognostic Index (IPI) originally proposed in 1993, remains the routinely used tool to classify and predict outcome for DLBCL patients (**Table 4**).[32] The IPI scoring system is a clinical and biological score that stratifies DLBCL patients into four prognostic groups with distinct median overall survivals.[55] The IPI score is based in several factors related with the patient's characteristics (age, performance status), disease extension and tumor growth (disease stage, lactate dehydrogenase [LDH] level in the serum and extranodal involvement). To calculate the IPI score of a patient, one point is given for each of the following factors: Age > 60 years, Eastern Cooperative Oncology Groups (ECOG) performance status ≥ 2 (**Table 5**), Ann Arbor stage III/IV disease, elevated LDH, and involvement of >1 extranodal site. The total account of points forms the IPI score, ranging from 0 to 5 and correlating with the state of the disease. Another scoring system was generated to classify young patients with aggressive lymphomas, the age-adjusted international prognostic index (**Table 4**). Depending on the risk factors punctuation, DLBCL patients are distributed in 4 groups: low, low intermediate, high intermediate and high IPI, with an overall survival (OS) ranging from 26 to 83% over 5 years.[56]

Table 4. Expected outcome for DLBCL patients according to risk groups of the International Prognostic Index and the revised International Prognostic Index.[32]

Risk group	Risk factors	CR (%)	5-years OS (%)
International Prognostic Index for patients of all ages			
Low	0-1	87 %	73 %
Low intermediate	2	67 %	51 %
High intermediate	3	55 %	43 %
High	4-5	44 %	26 %
International Prognostic Index for patients aged ≤ 60 anys			
Low	0	92 %	83 %
Low intermediate	1	75 %	69 %
High intermediate	2	57 %	46 %
High	3	46 %	32 %
Revised International Prognostic Index			
Risk group	**Risk factors**	**4-year PFS (%)**	**4-year OS (%)**
Very good	0	94	94
Good	1,2	80	79
Poor	3-5	53	55

CR, complete remission; OS, overall survival; PFS, progression-free survival.

Table 5. ECOG (Eastern Cooperative Oncology Group) performance status.[57]

Grade	ECOG
0	Fully active, able to carry on all pre-disease performance without restriction
1	Restricted in physically strenuous activity but ambulatory and able to carry out work of a light or sedentary nature
2	Ambulatory and capable of all self-care but unable to carry out any work activities. Awake and active more than 50% of the day hours
3	Capable of only limited self-care, confined to bed or chair more than 50% of the day hours
4	Completely disabled. Cannot carry on any self-care. Totally confined to bed or chair
5	Dead

With the recent incorporation of rituximab to standard therapy, several studies were conducted and confirmed that although the IPI scoring system remained prognostic, it no longer distinguished 4 outcome groups. With redistribution of the IPI factor into a revised IPI (R-IPI), 3 new categories were established that conferred more accuracy in the outcome prediction (**Table 4**).[32] However, several studies have refused this revised classification,[58,59] and currently the original IPI remains the validated measure for assessing DLBCL risk.

3.4.2 Biological prognostic factors that define DLBCL subtypes

It has been established that differences in the clinical features and treatment responses are also dependent on genetic and molecular factors that are associated with disease aggressiveness.[55] DLBCL is classified in 3 main subtypes according to gene expression patterns. The first group has a gene expression profile similar to normal germinal center B cells and was termed as the GCB subtype. The second group displays a gene signature similar to activated B cells and was referred to the ABC subtype.[60] A third uncommon subtype is the primary mediastinal large B-cell lymphoma (PMBL). This third subtype usually appears in the anterior mediastinum of younger patients showing intermediate features between DLBCL and Burkitt lymphomas.[14] It has been reported that patients in the GCB subgroup have a higher 5-years survival rate after chemotherapy than the ABC and type 3 subgroups (60% *vs* 35%; $P < 0.001$) (**Figure 6**).[32]

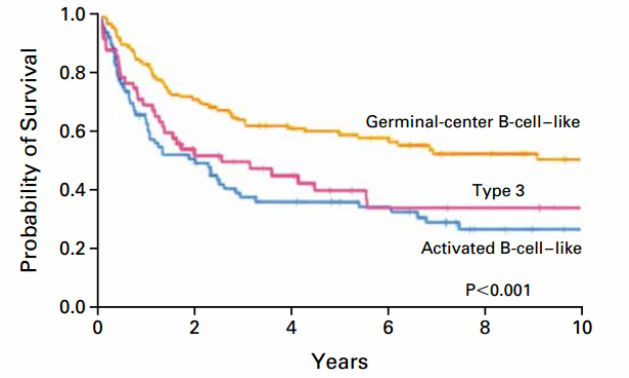

Figure 6. Overall survival of DLBCL patients after chemotherapy according to the gene-expression subgroups.[60]

As noted, GCB, ABC and PMBL subtypes of DLBCL are not just associated with prognosis but they are also biologically distinct entities associated with different oncogenic pathways. For example, translocation of BCL2 (t(14;18)) is more commonly detected in GCB DLBCL, whereas BCL6 translocation is more frequent in ABC DLBCL.[61,62] In addition, several studies demonstrated that the activation of nuclear factor-kappaB (NF-*k*B) pathway is more frequently observed in the ABC and PMBL subtypes.[63]

The classification of molecular subtypes based on genetic features was shown to predict survival independently of the IPI risk. However, gene expression profiling (GEP) never moved easily into clinical routine. At present, immunohistochemical algorithms have been validated for classification of DLBCL into the 2 major subtypes: GCB and ABC. The algorithm proposed by Hans *et al* (**Figure 7A**)[64] was based on 4 markers (CD20, CD10, BCL6 and MUM1) to distinguish between the 2 DLBCL subtypes. Later, the algorithm was improved by adding the markers CGET1 and FOXP1. The new algorithm presented 93% concordance with GEP and was an independent predictor of survival in multivariate analysis (**Figure 7B**).[65] However, several studies have

indicated that these algorithms based on immunohistochemical analysis did not provide prognostic information in the rituximab era.[66]

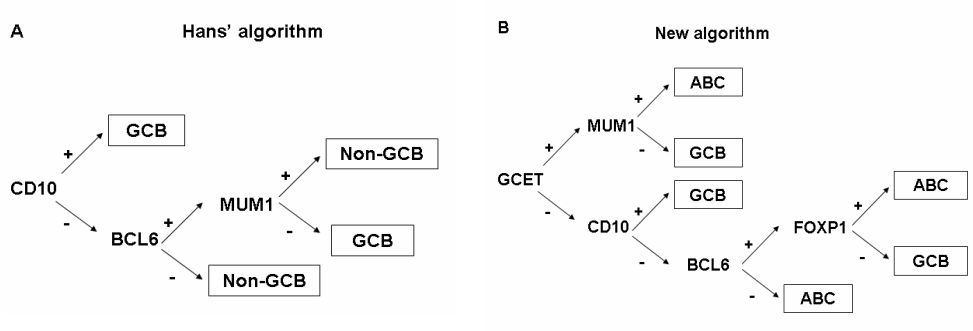

Figure 7. The Hans' (A) and the new (B) algorithms based on immunohistochemical analysis to classify DLBCL subtypes.[65]

3.5 DLBCL TREATMENT

At the present time, the clinical approach to treat DLBCL does not take into account the distinct biology of the disease subtypes. The treatment algorithms are based in the state of the malignancy, differing between patients with local (Ann Arbor I and II) or with advanced disease (Ann Arbor III and IV).[67]

3.5.1 First line treatment: localized *vs* advanced DLBCL

3.5.1.1 Treatment for localized DLBCL

25% of DLBCL patients present a localized lymphoma at the time of diagnosis, usually defined as stage I or II (measuring less than 10 cm of tumor diameter). In 1993, the United States Intergroup trial, reported that the anthracycline-based regimen (CHOP: cyclophosphamide, doxorubicin, vincristine and prednisone) was associated with similar complete response

rates (CR), progression-free survival (PFS) and overall survival (OS) compared with other complex regimens associated with higher toxicity.[68] Hence, CHOP therapy became the gold standard for the treatment of localized DLBCL since its first description in 1970.[69]

Several clinical studies suggested that patients with localized DLBCL receiving shortened courses of chemotherapy followed by radiation demonstrated a significant better outcome.[70] However, other studies showed that consolidation by radiotherapy did not prove any clear benefits in localized aggressive lymphomas of young patients.[71]

In 1997, the anti-CD20 antibody rituximab was the first antibody approved by the US Food and Drug Administration (FDA) for the treatment of NHL and specifically for DLBCL.[72] Although its mechanism of action has not been completely elucidated, several actions have been postulated, including complement-mediated toxicity.[72] Multicenter trials have demonstrated a favorable response in patients who received rituximab and CHOP (R-CHOP) compared with those receiving CHOP alone.[73] In addition, the GELA group reported that rituximab was effective in both young and old DLBCL patients, demonstrating that the effect of the anti-CD20 antibody was age independent.[58,73] In summary, R-CHOP combined with field radiation is the standard of care for most patients with localized DLBCL.

3.5.1.2 Treatment for advanced DLCBL

Following the United States Intergroup trial published in 1993, systemic CHOP emerged as a time-tested standard of care also for the treatment of advanced and disseminated DLBCL.[68] When combined with rituximab, patients in all risk groups showed an improved overall survival. Randomized studies in Europe and in the United States, have demonstrated that rituximab clearly adds benefit to several chemotherapy regimens based on CHOP.[33] Patients with disseminated DLBCL that present adverse features are also treated with investigational therapy or subjected to stem cell transplantation.[74] Hence, the standard of care for advanced-stage DLBCL is also based on the combination of rituximab with CHOP,[70] followed by transplantation in patients that show adverse features.

Patients with CNS involvement

Central nervous system (CNS) metastasis is one of the most serious complications for patients with advanced stage of DLBCL. The incidence of CNS relapse in patients with DLBCL has been reported to be between 1.1 and 10.4%.[75] Metastases to the CNS usually involve the cerebrospinal fluid and meninges, and solid parenchymal brain metastasis can also be detected. Although this complication is relatively uncommon, it is usually fatal.[76] For that reason patients with disseminated DLBCL who have a high risk for developing CNS metastasis typically receive prophylactic therapy. The most used prophylactic therapy is intrathecal methotrexate with or without intravenous injection of high-dose methotrexate. However, the use of drugs to prevent CNS involvement in patients remains controversial due to the complex route of administration and the lack of clear benefits for DLBCL patients.[77]

3.5.2 Salvage treatment for patients with relapsed DLBCL

Although the addition of rituximab to the standard chemotherapy has improved the treatment of DLBCL patients,[33,78] their overall survival remains poor, ranging from 30 to 50% over 5 years, and 30-40% of patients still relapse.[58] The standard approach for patients with relapsed DLBCL has been to proceed toward salvage therapy and consolidation with autologous stem cell transplantation (ASCT).[32] The salvage therapy is based on the combination of several drugs such as ifosfamide-carboplatin-etoposide (ICE) regimen or the addition of rituximab (RICE), which are effective and dose-intense regimens with minimal extramedullary toxicity.[79] Salvage therapy followed by transplantation have improved patient outcome compared with the conventional salvage therapy.[80] According to these observations, high-dose therapy followed by ASCT became the treatment of choice for relapsed or refractory patients who respond to salvage therapy.[67,81] For patients that do not achieve remission after ASCT, a hematopoietic stem cell transplant (HSCT) is the only remaining option. However, in many cases HSCT availability is limited by patient age, treatment-related morbidities, and poor performance status. An alternative to these patients would be to try new therapies that may improve their outcome.[70]

3.5.3 Novel therapies for DLBCL

Despite the success of the anti-CD20 antibody rituximab and the ASCT consolidation, some patients with advanced stage disease do not respond to R-CHOP based therapy. Major improvements in the treatment of DLBCL will probably be based on the incorporation of novel agents to the standard treatment of patients.

3.5.3.1 Anti-CD20 antibodies

Several novel antibodies against CD20 and other cellular markers are currently under study for the treatment of DLBCL. Some of these antibodies such as Ofatumumab, Obinutuzumab and Veltuzumab, are being evaluated in combination with traditional chemotherapy regimens.[70,82,83] Different mechanisms of action for therapeutic monoclonal antibodies have been suggested including (1) complement-mediated lysis and phagocytosis, (2) antibody-dependent cell mediated cytotoxicity, (3) physiologic activation or deactivation of target receptor, (4) enhanced effect of chemotherapy, (5) induction of secondary immune reactions, and/or (6) delivery vehicles for targeting radioisotopes, other drugs, or toxins.[72]

3.5.3.2 Agents against novel targets

- **Targeting tumor cells:** Several clinical trials are being conducted with humanized antibodies against cell membrane proteins such as Epratuzumab (a monoclonal antibody against CD22 B-cell marker),[84] Dacetuzumab (an anti-CD40 antibody),[85] Blinatumomab (a bi-specific antibody for B-cell CD9 marker and T-cell CD3 marker), amongst others.[70]

- **Antibody-drug conjugates:** These conjugates are used to deliver targeted cytotoxic agents. Several compounds are being investigated such as Inotuzumab ozogamicin, an antibody against CD22 that is conjugated with calicheamicin. This drug showed high levels of cytotoxic activity in B-cell lines, delivering the calicheamicin directly to the target cells. Successful results have been reported using the agent in combination with rituximab to

treat patients with recurrent DLBCL and also as a salvage regimen prior to autologous HSCT.[32]

- **Lenalidomide:** This is an immunomodulatory agent which mechanism of action is not clearly understood. It has been reported that this drug may enhance the cytotoxic activity of T and NK cells and that it may also upregulate tumor suppressor genes. Efforts are currently ongoing to combine this agent with standard chemotherapy for salvage chemotherapy and maintenance following autologous transplantation.[70]

- **Bortezomib:** It is a proteasome inhibitor that when combined with chemotherapy, improves the outcome in patients with the non-GCB subtype of DLBCL.[86]

- **Radioimmunotherapy:** It has been approved for the treatment of indolent and transformed lymphoma. Phase II studies reported promising results with ibritumomab tiuxetan and iodine-131 tositumomab consolidation after standard R-CHOP therapy for patients with *de novo* DLBCL.[87]

- **Other agents:** Several inhibitors are currently under evaluation and studies are ongoing combining drugs with diverse mechanisms of action with standard therapies. Some of these novel drugs are inhibitors of VEGF, inhibitors of the protein kinase PKC-beta, inhibitors of bcl-2, inhibitors of the B-cell receptor pathway such as Syk (a tyrosine kinase downstream of the B-cell receptor) and Btk (protein required for B-cell receptor signaling), inhibitors of m-TOR apoptosis pathway, and inhibitors of histone deacetylase.[33,70]

4. MOUSE MODELS IN CANCER AND IN DLBCL RESEARCH

4.1 MOUSE MODELS IN CANCER RESERCH

Animal models are useful tools to understand the mechanisms of malignancies and to evaluate new treatments. The laboratory mouse (*Mus musculus*) is one of the best model systems used for the study of cancer. Some advantages of the laboratory mouse are: its small size and propensity to breed in captivity, its short lifespan (3 years), the physiological and molecular similarities to humans, having an entirely sequenced genome and also the easiness in being genetically modified.[88,89] *M. Musculus* cancer models have progressed through several phases of increasing complexity, going from tumors raised in syngeneic fully immunocompetent hosts to immunodeficient xenograft models derived from human tumor cells, and tumors spontaneously growing in several genetically engineered mice (GEM). These models are used to study the factors involved in malignant transformation, invasion and metastasis, and also to evaluate response to therapy.[90]

Although mice and humans are at least 95% identical at a genomic level, their respective phenotypes are very different. Differences have also been observed in several studies on therapeutic drugs, which showed good results in mice but failed to provide similar efficacy in humans.[89] Here, we will discus the different mouse models used in the study of cancer (**Figure 8**) and we will explain the strength and limitations of each model type (**Table 6**). It is important to consider that animal studies are required before the human administration of new drugs. However, due to the inherent biologic differences between species, results obtained in animals are often not fully or directly applicable to the clinic.

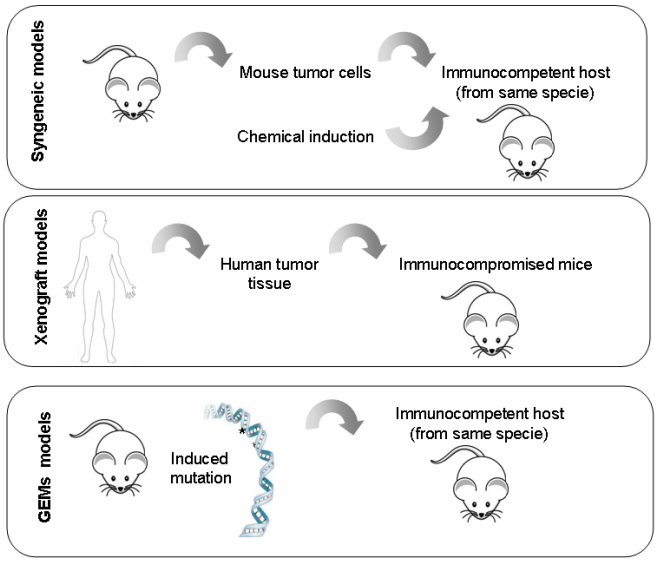

Figure 8. Mouse models used in cancer research (adapted from reference 90).

Table 6. Mouse models in cancer research: strength and limitations.[89,91]

	Material	Site	Advantages	Limitations
Syngeneic	- Chemical induction - Injection of cells/explants from the same species	- Predominantly subcutaneous - Orthotopic	- Immunocompetent - Low cost - Simple - Reproducibility of tumor properties - Short latency - Wide range of metastatic sites	- Poor representation of human disease - Lack of homology in target molecules between species - Limited mouse cell lines
Xenografts	- Injection of human cell lines or explants	- Subcutaneous (unnatural site)	- Characterized cell lines and human samples - Simple - Expression of human targets - Reproducibility - Homogeneity in tumor characteristics	- Immunosuppressed - Costly host and housing
		- Orthotopic (primary tumor source site)	- Characterized cell lines and human samples - Mimics human carcinogenesis and metastasis - Expression of human targets - Reproducibility - Homogeneity in tumor characteristics	- Immunosuppressed - Costly host and housing - Surgical skills - Limited engraftment - Non-homogeneity of tumor growth rates
GEM	- Mutation, deletion or overexpression of genes involved in transformation		- Controlled cancer progression in selected organs - Clinically relevant mutations are introduced - Mimics human carcinogenesis - Immunocompetent	- Costly - Variations in tumor growth rates - Limited and/or atypical metastastatic spread - Long latency

4.1.1 Syngeneic mouse models

Syngeneic models enable the study of transplantable mouse tumors within an intact mice environment. Carcinogenesis is usually induced using chemical or surgical interventions and then, material from this first tumor (cells or explants) is introduced into host of the same mouse strain.[89] These models are useful for the evaluation of therapies that require immune response or that target specific components of the tumor microenvironment.[92] The syngeneic models present some advantages such as the ease of their implementation, the low cost, and the reproducibility of tumor histology and growth rate. Furthermore, the interaction of the introduced malignant cell lines with the host stroma is favored.[89] However, these models fail to adequately represent the human situation and have limitations when they are used to study cancer metastasis.[91] In addition, as modern therapies are directed towards specific cancer targets, the lack of homology between mouse and human target bio-molecules is also a limitation for the use of syngeneic models.[93]

4.1.2 Xenograft mouse models

Xenograft models are one of the most widely used systems to study human cancer. These models permit a rapid and easy *in vivo* evaluation of drugs efficacy and growth of human tumor cells in immunocompromised mice.[94] The most frequently used immunosuppressed hosts to avoid rejection of human cells are the nude athymic mice (*nu/nu*), the severe combined immunodeficiency mice (*SCID*) and the hybrid strain NOD (non-obese diabetic)/SCID, with different immune deficiencies.[89] In **Table 7**, a summary of immunodeficient mouse models and their most common applications are presented.[95] Human tumors cells or tissues are usually implanted in the

immnodeficient mice into ectopic (e.g. subcutis) or orthotopic sites (into the organ in which the tumor originates).[94] In addition, patient-specific models have been proposed to be used for improving the clinical translation of the preclinically evaluated treatments.[96,97]

Xenograft models have been used for decades but recent information regarding the important influence of the tumor microenvironment (stromal and immune cells, vasculature and lymphatic circulation) on tumor progression and growth has led to the use of GEM tumor models using immunocompetent mice,[98] as well as to the use of primary human tumor xenografts in humanized mouse models.[88] However, xenograft models present some advantages such as the broad spectrum of available tumor types (patient explants and cell lines), the possibility of *ex vivo* genetic or therapeutic manipulation before xenotransplantation, rapid analysis of human tumor response to therapeutic agents, and a realistic incorporation of clonal and genetic heterogeneity observed in patients.[90,92]

Orthotopic xenograft models: In these models, tumor cells are inoculated in the organ where the primary tumor grows, so the effect of the tumor on its microenvironment can be modulated. As the xenograft grows in the tissue of origin, it might reproduce the human carcinogenesis and later metastatic events.[89] Conversely, these models are time consuming, expensive and technically challenging (surgical manipulation often needed), and mice usually have to be sacrificed due to primary tumor growth, sometimes even before disease spread has occurred.[90]

Subcutaneous xenograft models: These xenografts remain the most widely used models to test and to develop novel anticancer drugs.[88] Although it has

been reported that some drugs showing good results in mice failed to provide efficacy in humans, these models are still being used due to several advantages. Subcutaneous models are simple to generate, reproducible and present homogeneity in tumor histology and growth rates which is required in preclinical drug evaluation. In addition, there are available human tumor cell lines and databases reporting drug efficacy. [99]

Table 7. Spontaneous and transgenic immunodeficient mouse models and applications.[95]

Mouse Strain	Immune deficiency	Applications
Nude (*nu/nu*)	- Mice are athymic - The mutation at Foxn1 gene blocks thymus-derived T cells - Mice have highly activated NK cells	- Transplantation of murine and human tumors for imaging, metastasis and new therapies evaluation
Scid (*scid*)	- B and T cells deficiency - Spontaneous generation of mouse T and B cells with age - Mutation of Prkdc/*scid* protein	- Transplantation of murine and human tumors for imaging, metastasis and new therapies evaluation - Low levels of engraftment of human PBMC and HSCs.
NOD-*Scid*	- NK cell dysfunction, low cytokine production and T and B cell dyregulation - Insulitis- and diabetes free - Innate immune defects due to interactions between insulin-dependent susceptibility genes and Prkdc/*scid* genes	- High levels of engraftment compared with the *Scid* mouse models
NOD-*Scid* IL2rγ*null* (NSG)	- Deletion of multiple genes causes severe impairment in T and B-cell development and absence of NK cells	- Increased levels of human tissue engraftment
NOD-scid-B2mnull (NSG B2m)	- Deletion of multiple genes causes severe impairment in T- and B-cell development and absence of NK cells	- Similar to NOD-scid IL2rγnull

NK, natural killers; PBMC, peripheral blood mononuclear cells; HSC, haematopoietic cells; NOD, non-obese diabetic. *Scid*, severe combined immunodeficiency.

4.1.3 Genetically engineered mouse models (GEM)

Despite the availability of human tumor cell lines, naïve cell lines can also be genetically modified through the introduction of genetic mutations associated with particular human malignancies.[94] The genes involved in the transformation of malignant cells can be overexpressed, mutated or even deleted and the effects of these alterations or the response to therapy can be studied *in vivo*. These genetically engineered mice are usually generated by exchange of the endogenous gene by the mutant gene to mimic human carcinogenesis (*Knock-in* mice), and they can also be manipulated to disrupt a gene leading to suppression of its function *(knock-out* mice).[89] These models are useful tools for the evaluation of specific mutations, deletions or gene amplifications during mice tumor progression; however, they cannot fully reproduce the genetic complexity of human tumors, especially the metastatic phenotype. Furthermore, genetically engineered models are not suitable for evaluating the anti-tumor activity of drugs that are specific for human tumor-associated antigens.[100] Moreover, the appearance of tumors at different stages and at different time periods within the same GEM models complicates the use and raises the price of these models for drug evaluation. Since drug evaluation requires the comparison of vehicle-treated and agent-treated groups of mice bearing homogenous tumors to statistically test drug efficacy, the GEM models are not appropriate for these studies. Nonetheless, these models present several advantages: mice are immunocompetent resembling the human tumor microenvironment, specific genetic abnormalities of human tumors can be induced at specific ages and tissues in mice, and therapeutic approaches can be tested at various stages of the disease. However, it is difficult and expensive to generate and maintain these models, they do not mimic the complexity of human tumors and they take long time to generate spontaneous tumors.[90]

4.2 MOUSE MODELS IN DIFFUSE LARGE B-CELL LYMPHOMA

Modeling human disease in mice has reached a great relevance in the field of haematological malignancies research. The mouse has become an important tool for understanding the molecular basis of many of these heamatological diseases. Most cancer types arise from the accumulation of several genetic changes in somatic cells. In human lymphomas and leukaemias these genetic alterations are often due to chromosomal rearrangements, which are more rarely observed in solid tumors. Frequently, these rearrangements are chromosomal translocations and/or inversions that result in inappropriately high expression of proto-oncogenes, or in the generation of fusion genes that encode chimeric oncoproteins, which are associated with specific types of lymphomas or leukaemias.[101] Thus, the development of mouse models of specific subtypes of these malignancies can be a useful tool for preclinical drug testing and to further investigate molecular aspects of these diseases.

4.2.1 Syngeneic mouse models of DLBCL

Syngeneic models are used to study the inter-relationship between the immune system and the neoplastic lesion caused by lymphomas. Syngeneic models of disseminated B-cell lymphomas have been described using tumor cells derived from the immunocompetent host Balb/c.[102-104] The most frequently used cells to develop the syngeneic models are the established cell lines A20 and BCL1.[105,106] These cell lines were described as lymphoid lines presumably of B cell origin at various stages of differentiation but they are not defined as specific lymphoma subtypes. The intravenous injection of these cell lines generates a disseminated lymphoma in Balb/c mice that is used as a model for the study of DLBCL.[107] However, there are several differences

between human and mice lymphomas that deserve consideration for the study of the disease, such as the clinical features and the morphology and genetic characteristics.[108] Hence, the mentioned differences between lymphomas in the two species have to be considered when studying the molecular mechanisms or the efficacy of a new drug in these models. These factors may limit the clinical translation of the findings.

4.2.2 Xenograft mouse models of DLBCL

The transplantation of human tumor cells into immunodeficient mice has been used extensively for the study of tumor biology and its response to treatment since the late 1960s. Mice bearing the *Nude* or the *SCID* mutation have been considered the standard model to evaluate human malignancies *in vivo.* However, these mouse strains have some residual immunity that limits the post-transplant growth of human hematopoietic malignancies.[109] Studies have revealed that the *NOD/SCID* strain is a more useful strain for human lymphoma xenotransplantation, showing higher levels of engraftment. *NOD/SCID* mice transplanted intravenously (*iv)* with tumor cells reported significantly superior engraftment compared with *SCID* mice. In addition, subcutaneous (*sc*) xenograft transplant of lymphoid malignancies in *Nude* and *SCID* mice also showed lower engraftment, compared with the NOD/SCID model.[110-112]

Most preclinical models of human lymphomas still rely upon subcutaneous xenograft models of the most aggressive lymphomas, such as Burkitt lymphoma. Although these models have served a role in developing new drugs for these diseases, they do not represent the heterogeneous biology of the different lymphoma types found in patients.[99] Some authors have

intraperitoneally injected lymphoma cells in mice, leading to local tumor growth which does not resemble the natural history of the corresponding haematologic disease.[113] Dissemination to bone marrow, liver, lung, spleen and central nervous system are observed more commonly following the intravenous administration of the aggressive and human Burkitt lymphoma cells.[114] For that reason, intravenous injection of this lymphoma subtype has been widely used to study molecular pathways and new treatments for B-cell malignancies.[115,116] However, Burkitt lymphoma does not share the same molecular basis, prognosis and treatment with the majority of B-cell lymphomas, and neither with DLBCL.

Our group has recently developed a xenograft DLBCL model by subcutaneously preconditioning lymphoma cells to increase their aggressiveness. Cells were subcutaneously inoculated in mice and then the tumors where extracted, disaggregated and intravenously injected into new hosts. These mice successfully developed a quick and disseminated DLBCL that reproduced the clinical features of the disease.[117]

4.2.3 Genetically engineered mouse models (GEM) that develop DLBCL

Several strategies have been applied to develop genetically engineered models of haematological malignancies, generally involving knock-in or knock-out of certain genes implicated in the diseases. B-cell malignancies often involve translocation of an oncogene, like myc or bcl-2 to an immunoglobulin locus, resulting in its deregulated expression. These translocations can be studied in GEMs by inserting an immunoglobulin regulatory element upstream of the gene or oncogene of interest in B-cells. The impact of the deregulation of an oncogene can be studied in the appropriate cell type, evaluating how it

affects cell cycling, differentiation, and apoptosis.[118] Some authors have described transgenic mice over-expressing c-Myc, Bcl-2 or Bcl-6 under the control of an immunoglobulin promotor.[119-121] However, these transgenic mice generate lymphomas at a low incidence, they need long time to develop and they usually coexist with some other lymphomas subtypes.[100,101] In addition, although initiated by a comparable genetic event, many tumor-suppressor knockout mice and oncogene-expressing transgenic mice do not precisely recapitulate the corresponding human malignancies.[122] Furthermore, the secondary genetic events acquired during tumor development in transgenic mice are often poorly characterized, making it difficult to compare the findings with the tumorigeneic process in humans.[123]

In summary, there is a need to improve mouse models of lymphoma and also to develop new models that may increase the accuracy as preclinical tools in identifying effective therapies against these diseases. Moreover, it is necessary to develop animal models for each of the various lymphoma subtypes, so that drug screening and development can be more focused on the specific biological targets.[99] In this thesis, we develop several DLBCl xenograft mouse models that reproduce the clinical features observed in patients.

5. CHEMOKINE RECEPTORS

Chemokine receptors form a large family of proteins that mediate the chemotaxis of cells towards a gradient of chemokines.[124] These receptors are seven-transmembrane proteins that are coupled to G-proteins. One of the intracellular loops of the chemokine receptors couples with heterotrimeric G-proteins, mediating ligand binding to the receptor which initiates a cascade of signal transduction events.[125] Chemokine receptors are classified into four groups (CXC, CC, C, and CX3C) based on the position of the first two cysteines.[126] Generally, these receptors exhibit promiscuity and redundancy, being able to bind multiple ligands. In turn, some chemokines also bind to multiple receptors. However, as observed in **Figure 9**, certain chemokines interact with single receptors and some receptors bind only one chemokine.[127]

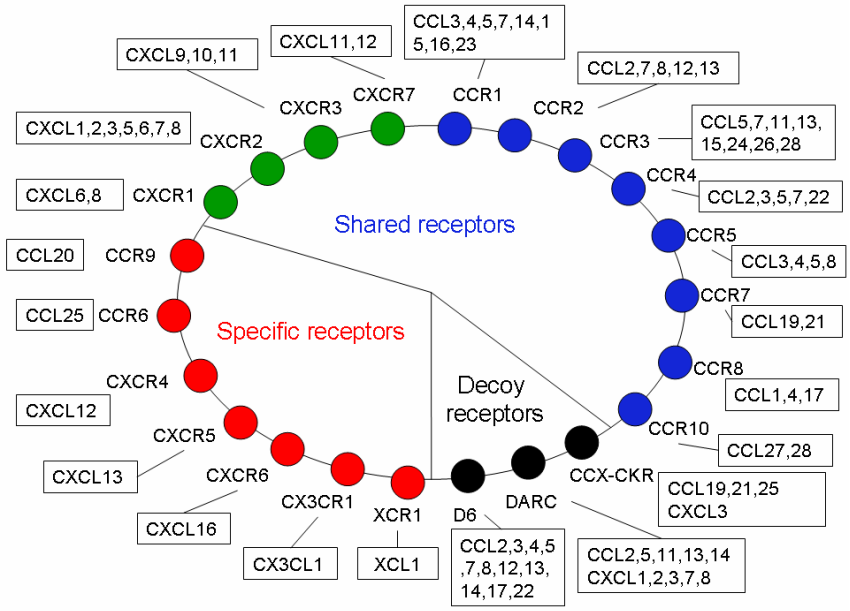

Figure 9. Chemokine receptors and their ligands. Most chemokines can bind multiple receptors, and a single receptor can bind multiple chemokines as shown for most CC (green) and CXC (blue) chemokines. Decoy receptors (black) can also interact with multiple chemokines. By contrast, a minority of receptors (red) have only one ligand.[127]

To date, more than 20 chemokine receptors have been described. Together with their ligands, they play important roles in several pathological processes such as inflammation, infection, tissue injury, allergy, cardiovascular diseases, and growth and dissemination of malignant tumors.[128]

5.1 CHEMOKINE RECEPTOR CXCR4

One of the best studied chemokine receptors is the highly conserved transmembrane protein C-X-C chemokine receptor type 4 (CXCR4), also known as CD184 or fusin. This receptor has a single ligand, the chemokine CXCL12, also known as SDF-1 (Stromal cell-derived factor-1[129]). Recent reports have identified the CXCR7 as the second SDF-1 receptor.[130] The SDF-1 chemokine can be expressed in two major isoforms: SDF-1α and SDF-1β, being the first the predominant one. The chemokine is secreted by several cell types such as marrow stromal and endothelial cells, lymph node stromal cells, heart, skeletal muscle, liver, brain, and kidney parenchymal cells, and its secretion increases following tissue damage.[23,131]

CXCR4 functions as a classical chemokine receptor in the adults and, together with its ligand, is essential for development and hematopoiesis.[132] Expression of CXCR4 is detected in several tissues, with predominant expression on the surface of hematopoietic cells such as T and B lymphocytes and early hematopoietic progenitor cells in the bone marrow.[133] The receptor and its ligand are critically involved in the trafficking and homing of normal lymphocytes.[134] They are also essential for normal B-cell development and are involved in diverse aspects of B-cell homeostasis, including retention of B-cell precursors on the bone marrow and B cell homing to lymph nodes.[135]

In addition to the implication of CXCR4 in physiological processes, the receptor has also been described in several diseases. CXCR4 was first discovered due to studies focused on its role as a co-receptor in the pathogenesis of HIV, in which this receptor is essential for the entry of HIV virus into CD4+ T cells.[132] The CXCR4/SDF-1 axis is also involved in inflammatory diseases such as rheumatoid arthritis and chronic lung inflammatory processes, among others. In these diseases, up-regulation of SDF-1 chemokine leads to the recruitment of inflammatory CXCR4+ cells.[136] Furthermore, the CXCR4 receptor is overexpressed in more than 20 human cancer types and, together with its ligand, is involved in cancer cell migration and invasion.[137]

5.1.1 CXCR4/SDF-1 pathway

Cells expressing CXCR4 on their surface migrate towards chemotactic gradients of its specific ligand SDF-1 (CXCL12). The binding of the chemokine SDF-1 to CXCR4 initiates signaling pathways which can result in a variety of responses such as chemotaxis, increase in intracellular calcium, cell survival and/or proliferation, and gene transcription. CXCR4 is coupled to an intracellular heterotrimeric G-protein composed of Gα, Gβ and Gγ subunits. Activation by SDF-1 binding, leads to subunit dissociation and each G-protein subunit stimulates different pathways (**Figure 10**).[138] Some of the most relevant effects on signaling pathways are:

- Activation of PI3K leading to phosphorilation of the kinase AKT and focal adhesion proteins, which are respectively associated with cell survival and chemotaxis.
- Activation of MEK1/2 and ERK1/2 which lead to changes in gene expression, cell cycle progression and chemotaxis.

- Activation of IP3 and DAG that stimulate the mobilization of calcium from intracellular stores. This calcium flux can be measured and is frequently used to evaluate chemokine activity.

After ligand binding, CXCR4 signaling is rapidly desensitized by internalization of the receptor. The intracellular C-terminus of CXCR4 is phosphorylated after ligand binding and the receptor is recruited by β-arrestin and clathrin-mediated endocytosis and degradated in lysosomes or recycled back to the membrane.[132]

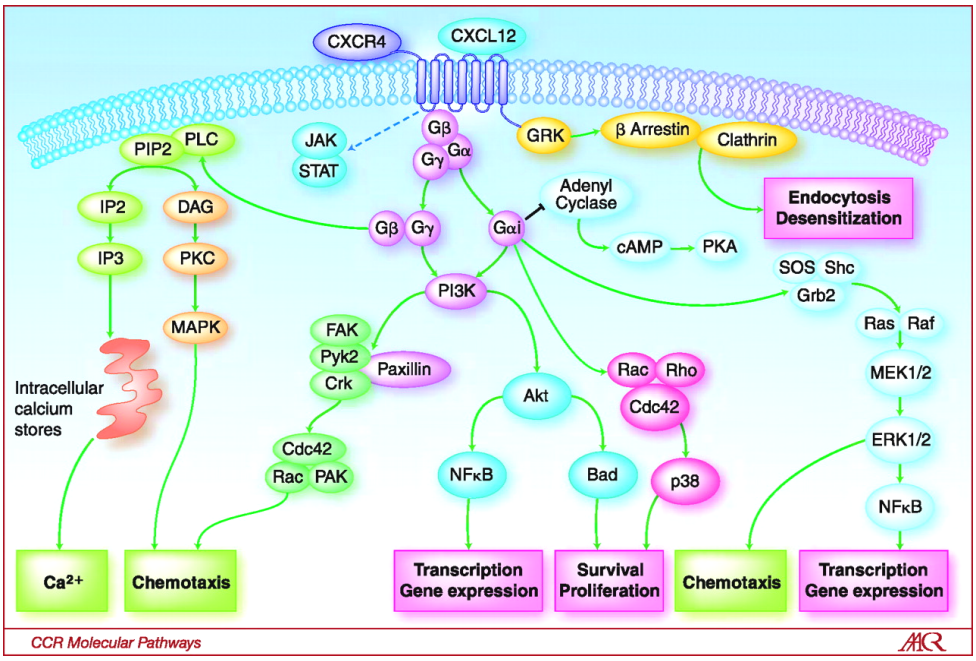

Figure 10. SDF-1/CXCR4 intracellular signal transduction pathways. The figure described some of the key signaling pathways involved in CXCR4 signal transduction. These pathways may be tissue-dependent and may differ between cell types.[138]

5.1.2 CXCR4 and cancer

Overexpression of CXCR4 receptor has been described in several malignancies, including solid and haematological tumors. Here, we summarize the human cancers for which the receptor has been reported to play a role in the disease aggressiveness.

5.1.2.1 CXCR4 in solid tumors

A decade ago, overexpression of CXCR4 was first described in human breast cancer cell lines and in primary and metastatic breast tumors.[139] Nowadays, overexpression of CXCR4 has been found in more than 20 human neoplasms including pancreatic, ovarian, lung, breast, colorectal and brain tumors,[140-142] in which this receptor promotes metastasis, angiogenesis and tumor growth or survival.[137] Several preclinical models revealed that the metastasis of cancer cells is mediated by CXCR4 activation and directed tumor cell migration towards SDF-1 expressing organs. These findings have been described in preclinical thyroid, melanoma, prostate, and colon cancer models.[143-146] For example, breast cancer studies reported that bone marrow, liver, lungs, and lymph nodes exhibit expression of SDF-1 chemokine and represent the most common organs for breast cancer metastasis. Furthermore, metastatic mouse models provided evidence that targeting CXCR4 decreased the spread of cancer cells, therefore inhibiting metastasis development in several neoplasms, such as breast, colorectal and prostate cancer.[124]

In clinical studies, CXCR4 receptor has been associated with enhanced metastasis and decreased survival, and described as a prognostic marker in several neoplasms correlating with disease aggressiveness.[147-150]

5.1.2.2. CXCR4 in haematological tumors

Overexpression of CXCR4 has also been reported in several haematological neoplasms. The receptor and its ligand have been described in the migration and trafficking of malignant B cells in several haematological malignancies such as Burkitt lymphoma,[134] acute myelogenous leukaemia (AML),[151] acute lymphoblastic leukaemia (ALL),[152] and B-cell chronic lymphocytic leukaemia (B-CLL). [153-155]

Furthermore, studies in leukaemia have indicated that CXCR4/SDF-1 signaling in the bone marrow niche may contribute to resistance to chemotherapy. As the SDF-1-CXCR4 interaction is considered essential for attracting tumour cells to the bone marrow, CXCR4 inhibitors have been explored as chemosensitising agents. Multiple preclinical studies in mouse models of leukaemia have provided evidence for the greater benefits of combining CXCR4 inhibition with conventional chemotherapy compared with chemotherapy treatment alone.[156,157]

CXCR4 and B-cell malignancies

The overexpression of CXCR4 has also been described in B-cell lymphomas. In fact, CXCR4 overexpression has been detected in a wide range of NHL cell lines and primary cells, and has been related with dissemination to lymphoid organs.[153,154] These studies suggested a possible role of the receptor in the migration and progression of tumor cells in NHL patients. Trentin *et al* showed that although CXCR4 is also expressed on normal B lymphocytes, it transduces a low migratory activity with respect to CXCR4 expressed on malignant B cells. López-Giral *et al* revealed that the chemotaxis pattern of different B cell populations was related to the levels of chemokine receptor expression. Their

studies provided evidence supporting that CXCR4, together with other receptors like CXCR5 and CCR7, were involved in the pattern of lymphoid organ infiltration observed in B-cell cronic lymphocytic leukaemia (B-CLL).[153]

Due to the pivotal role of CXCR4 in cancer progression and dissemination, several inhibitors of CXCR4 have been developed and studied as potential anti-cancer drugs to treat lymphoma patients. Pre-clinical studies showed that neutralization of CXCR4 inhibits migration and prevents *in vivo* growth of Burkitt lymphoma cells.[134,152] Bertolini *et al* reported that neutralization of CXCR4 before intravenous injection of lymphoma cells lead to an increased number of circulating cancer cells. These studies confirmed that this receptor plays a crucial role in tumor cell extravasation. Moreover, Beider *et al* described that the CXCR4-antagonist BKT140 exhibits anti-lymphoma effects both *in vitro* and *in vivo*. This antagonist synergizes with rituximab and targets lymphoma cells in the bone marrow microenvironment, overcoming the stroma-induced resistance to rituximab.[134] Another CXCR4 antagonist has shown benefits as monotherapy in Burkitt tumor-bearing mice and is currently in phase I for the treatment of relapsed AML, NHL, B-CLL, and multiple myeloma (MM).[158]

Taken together, these data indicate that CXCR4 plays an important role in tumour metastasis of B-cell lymphomas. However, most of the preclinical studies have been conducted using Burkitt cells and no data have been published on the role of CXCR4 receptor in dissemination or its prognostic value in DLBCL.

5.1.3. CXCR4 inhibitors in the clinic

The chemokine receptors CXCR4 and CCR5 were first described as coreceptors for the HIV-1 entry into $CD4^+$ T-cells. Although several CXCR4 inhibitors were developed to treat HIV, some of which are highly active and orally bioavailable, they are still at preclinical stages or have failed to complete their drug development process.[159] However, clinical applications for CXCR4 inhibitors others than anti-HIV therapy have been considered. It was reported that the inhibitor AMD3100 (Mozobil, Plerixafor) induced an increased amount of white blood cells after its injection in healthy volunteers. This finding led to the observation that AMD3100 mobilizes CD34+ haematopoietic stem cells and progenitor cells from the bone marrow to the peripheral blood. Later, AMD3100 was approved for the use in NHL and MM patients in combination with granulocyte colony-stimulating factor (G-CSF) to mobilize haematopoietic stem cells to the peripheral blood for autologous transplantation.[160] More recently, CXCR4 inhibitors have been used in the treatment of haematologic malignancies:

- AMD3100: Several preclinical studies in mouse models of leukaemia showed greater benefits of combining the CXCR4 antagonist plerixafor with conventional chemotherapy, compared to chemotherapy alone.[156,157] Clinical trials have been carried out using plerixafor combined with intensive chemotherapy treatment in a small group of relapsed AML patients. Although no definitive results were obtained in these clinical trials, the data are encouraging to further investigate the properties of plerixafor in cancer treatment.[161] In addition, it has also been shown that the drug is safe when given in combination with rituximab to B-CLL patients [162] Hence, the studies performed until now in AML and B-CLL show that the combination of

plerixafor with conventional chemotherapy appears to have an increased antitumor effect, is safe and does not affect haematological recovery.

- CTCE-9908: This SDF-1 peptide analogue (Chemokine Therapeutics Corp. Vancouver, Canada) is another inhibitor of the CXCR4/SDF-1 pathway. This drug was able to reduce the number of metastases in preclinical models of osteosarcoma and melanoma and was tested as monotherapy in solid tumours.[163] Furthermore, several clinical trials (phase I/II) are currently being conducted to inhibit CXCR4 receptor in malignancies such as brain tumors, MM, B-CLL, small lymphocytic leukaemias, and also in NHL patients that previously failed HSCT.[124]

Although the use of CXCR4 inhibitors or blocking agents in the clinic setting seems to add benefits in the current treatment of patients, it is necessary to validate these results in further clinical trials in independent series and with larger number of patients.

6. ANTITUMOR EFFECT OF THE FOCAL ADHESION INHIBITOR E7123

6.1. CELECOXIB, E7123 PARENTAL COMPOUND

The COX-2 selective inhibitor celecoxib was initially developed to relief pain and inflammation without the gastrointestinal toxicities associated with nonselective non-steroideal anti-inflammatory drugs. Later, administration of celecoxib was reported to significantly decrease the occurrence of sporadic colorectal adenomas, supporting a critical role for COX-2 in tumorigenesis.[164]

Because of the apparent role of COX-2 in various tumors, COX-2 inhibitors like celecoxib have been evaluated as potential antitumor agents. Celecoxib has been evaluated in clinical trials in combination with chemotherapy to treat patients with glioblastoma, melanoma, breast, pancreatic and colorectal cancers, amongst others.[165-169] Celecoxib has also shown benefits when given at high-dose in combination with low-dose of cyclophosphamide to treat relapsed DLBCL patients in phase II trials. However, if celecoxib is given at high-dose, a close surveillance is recommended for these patients to avoid unfrequent but sometimes lethal toxicity.[170]

The mechanism of the antitumor effect of celecoxib has not been clearly elucidated and its use in the clinic is still controversial. Given the cardiovascular side effects of celecoxib due to its inhibition of COX-2, new studies emerged to find cellular effects independent of COX-2 inhibitory activity. Our group showed that celecoxib had antitumor effect against colorectal tumor cells independent of COX-2 inhibition. The mechanism involved in this cytotoxicity was described to be the inhibition of focal adhesion signaling.[171]

6.2. THE FOCAL ADHESION INHIBITOR, E7123

After showing that celecoxib induced cytotoxicity by inhibition of focal adhesion signaling,[171] the relationship between the structure and the activity of a series of celecoxib-derived compounds was analyzed. The goal was to identify new chemical structures that maintained the antitumor effect by inhibition of the focal adhesion signaling without inhibiting COX-2. Five different compounds were studied and E7123 drug was selected for further development (**Figure 11**). After that, our group showed that E7123 was significantly more potent than celecoxib in inducing cell death in acute myeloid leukaemia cells.[172] In addition, we recently described the *in vitro* antitumoral effect of E7123 against DLBCL cell lines and also the *in vivo* effect of the drug in a subcutaneous mouse model of this pathology.[173]

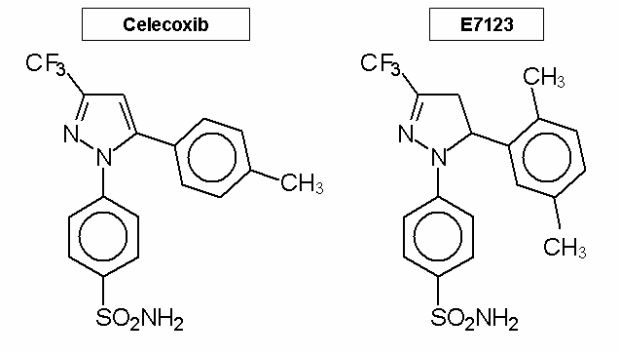

Figure 11. Chemical structure of celecoxib and its derivative E7123. Changes in the position of the substituents in the phenil group alter its antitumor potency.

The mechanism involved in this cytotoxicity was proven to be the inhibition of the focal adhesion signaling. The focal adhesion complexes are structures composed of transmembrane receptors (integrins), structural proteins (i.e., vinculin, talin, paxilin…) and signaling proteins (i.e., FAK, p130Cas, HEF1,

Pyk2...). These structures link the actin filaments of the cytoskeleton with the extracellular matrix and activate various protein kinases, such as the focal adhesion kinase (FAK) and the Src family kinases.[174] The mechanism of action of E7123 in DLBCL cells was also described by our group. Its mechanism is based on the inhibition of the focal adhesion signaling inducing dephosporylation of FAK, PYK2 and LYN, and proteolysis of p130Cas. We also reported that these proteins were expressed in DLBCL patient samples, suggesting the potential use of E7123 to treat DLBCL patients.[173]

Furthermore, it has been reported that the integrin β1 is essential for the interaction between tumor cells and the brain vessels promoting proliferation and metastasis within the brain in carcinomas and lymphomas.[175-177] This adhesion to the vascular basement membrane of the brain mediated by integrin signaling is a critical step in the CNS metastasis.[177] Considering that the CNS involvement is a fatal complication in DLBCL patients and the reported lack of benefits in the current prophylactic protocols, the novel drug E7123 merits futher studies to evaluate its role in the prevention of CNS progression.

“They did not know it was impossible so they did it”

“Lo consiguieron porque no sabían que era imposible”

Mark Twain

OBJECTIVES

1. To develop bioluminescent xenograft mouse models of disseminated DLBCL which reflect this human pathology and that are useful for the evaluation of novel antitumor drugs.

1.1. To compare the *in vivo* dissemination and aggressiveness of mouse models derived from DLBCL cell lines after the intravenous injection of subcutaneous preconditioned or non-preconditioned cells.

1.2. To validate the use of the disseminated DLBCL models for antitumor drug evaluation by testing their response to cyclophosphamide.

2. To evaluate the *in vivo* antitumor effect of an inhibitor of focal adhesion signaling, E7123, in a model of DLBCL with CNS involvement.

3. To study the role of CXCR4 receptor in the migration and dissemination of DLBCL cells.

3.1. To study the role of CXCR4 in cell line migration *in vitro*.

3.2. To evaluate membrane CXCR4 levels in the disseminated DLBCL mouse models and the correlation with lymphoma dissemination and/or aggressiveness.

3.3. To evaluate if the CXCR4 antagonist, AMD3100, inhibits cell dissemination in a DLBCL mouse model.

3.4. To assess the prognostic value of membrane CXCR4 levels in lymph node biopsies from DLBCL patients.

“Science is not religion. If it were, we'd have a much easier time raising money”

“La ciencia no es una religión. Si lo fuese no tendríamos problemas para conseguir dinero”

Leon M. Lederman

MATERIALS AND METHODS

1. *IN VITRO* EXPERIMENTS

1.1. CELL CULTURE

1.1.1 Cell lines

All cell lines were cultured in specific media supplemented with 10% human or fetal bovine serum, 1% glutamine, 100 U/ml penicillin/streptomycin (Life Technologies) in a humidified atmosphere at 37°C in 5% CO_2.

- **293T**

Human cell line 293T, originally derived from human embryonic kidney cells, was obtained from American Type Culture Collection (ATCC). This cell line is a highly transfectable derivative of the 293 cell line into which the temperature sensitive gene for SV40 T-antigen was inserted. Because of that, transfected plasmids containing SV40 as origin of replication can be replicated, amplified and transiently expressed within this cell line.
In this thesis, 293T cells were used as a virus packaging cell line for lentiviral production. 293T cells were cultured in supplemented Dulbecco's modified eagle medium-high glucose (DMEM, Life Technologies).

- **Germinal center DLBCL cells (GCB): Toledo, OCI-Ly19, KARPAS-422 and HT**

HT, Toledo, KARPAS-422 and OCI-Ly19 are human GCB-DLBCL cell lines. Cells were cultured in supplemented RMPI 1640 media (Life Technologies). HT, KARPAS-422 and OCI-Ly19 cell lines were obtained from DSMZ - German collection of microorganisms and cell cultures. Toledo cell line was kindly provided by Dr Piris (CNIO, Madrid).

- **Activated DLCBL cells (ABC): SUDHL-2, OCI-Ly-10, RIVA**

SUDHL-2, OCI-Ly10 and RIVA are human ABC-DLBCL cell lines. Cells were cultured in supplemented IMDM media (Life Technologies). OCI-Ly-10 cells were cultured with 10% human serum (from human male AB plasma, Sigma-Aldrich) instead of fetal bovine serum and with 50 µM 2-mercaptoethanol. These cell lines were kindly provided by Dr L. Pasqualucci (Columbia University Medical Center, NY).

1.1.2 Thawing frozen cells

Frozen cells were stored in cryotubes in liquid nitrogen tanks. Cryotubes were placed in a 37°C bath for 1-2 minutes to thaw frozen cells. Cells were transferred to a 10 ml-tube containing culture media and centrifuged at 1500 rpm for 5 minutes to remove the toxic dimethil sulfoxide (DMSO) from the freezing media. Then, cells were resuspended in prewarmed media and cultured at 37°C with 5% CO_2.

1.1.3 Subculture of cells

Adherent cells

For subculturing adherent 293T cells, the media was removed and the monolayer of cells was washed with phosphate buffered saline (PBS). Trypsin-EDTA (Life Technologies) was added onto the cell monolayer and the cells were incubated at 37°C for 2-5 minutes. After that time, the side of the flasks was gently tapped to release any remaining attached cells. Then, cells were resuspended in fresh serum-containing media to inactivate the trypsin and seeded into new flasks.

Suspension cells

All DLBCL cell lines grew in suspension and had a doubling time of approximately 48 hours. Every 2 days the cell lines were maintained or expanded by spinning them at 1500 rpm for 5 minutes and then cells were resuspended in the appropriate volume of media. When an experiment was carried out, cells were counted using the Automated Scepter™ 2.0 Cell Counter (EMD Millipore) and the required number of cells was transferred to a new labeled flask or plate containing pre-warmed media.

1.1.4 Cell cryopreservation

Cells were centrifuged at 1500 rpm for 5 minutes and resuspended in freezing medium containing 90% FBS and 10% dimethil sulfoxide (DMSO). DMSO was used as a cryoprotectant. Thus, when added to cell media it reduced ice formation and prevented cell death during the freezing process. Aliquots of 1 ml containing $1\text{-}5\cdot10^6$ cells were prepared in cryotubes and held in freezing containers (Frosty, Nalgene) at -80°C. After 24 hours, cells were transferred to a liquid nitrogen tank for long-term conservation.

1.1.5 Cell counting

Scepter™ 2.0 Cell Counter (EMD Millipore) was used for cell counting. A single-cell suspension was prepared in a total volume of 100 µL culture media and at a concentration of $1\cdot10^4$ - $5\cdot10^5$ cells/ml (operating range of the Scepter). The automated cell counter uses the Coulter principle of impedance-based particle detection to count every cell in the sample. Once counting was complete, the upper and lower gates were adjusted to select the population of

viable cells. After gating, the concentration and average cell size of the sample were automatically obtained.

1.1.6 Paraffin-embedded cell lines

Cell lines were paraffin-embedded to perform histological and immunohistochemical analysis. About $20 \cdot 10^6$ cells were centrifuged at 1500 rpm for 5 minutes. The obtained pellet was suspended adding equal portions of human plasma and thrombin (from human plasma, SIGMA-ALDRICH), that was then mixed to obtain a cell lump. This lump was fixed in buffered formaldehyde and paraffined.

1.1.7 Flow cytometry analysis

Fluorescence-activated cell sorting (FACS) analysis was performed to detect GFP positive cells and CXCR4 expression in cell membrane. Data were obtained with the FACSCalibur (BD) and analyzed using Cell Quest Pro software. Results were expressed as mean fluorescence intensity (MFI) ± standard deviation.

1.1.7.1 Quantification of GFP positive cells

Quantification of GFP positive cells was conducted to titrate the lentiviral particles in 293T cells and to detect lentiviral infection in DLBCL cells. One million cells were centrifuged at 1500 rpm for 5 minutes, washed twice with PBS and resuspended in 400 µL of the buffer containing 0.5% of albumin. Parental non-fluorescent cells were used as control for each cell line. Data acquisition was performed by flow cytometry with the 488 nm excitation laser.

1.1.7.2 Quantification of CXCR4 expression and internalization

One million cells were washed in PBS containing 0.5% bovine serum albumin (PBS-BSA) and incubated for 30 minutes at 4°C with PE-Cy5 mouse anti-human CXCR4 monoclonal antibody or PE-Cy5 mouse IgG2a (BD Biosciences) as an isotype control. 5 µL of each antibody were added to a total volume of 100 µL of cells in PBS-BSA. Unbound antibody was removed by two washes with PBS-BSA. Then, the cells were resuspended in 400 µL PBS-BSA and data acquisition was performed using flow cytometry with the 633 nm excitation laser.

The internalization of CXCR4 was evaluated by incubating cells with 100 ng/ml SDF-1α (Prospec-Tany TechnoGene) or 10 µg/ml AMD3100 (Sigma-Aldrich). Cells were incubated with SDF-1α for 2 hours or with AMD3100 for 1 hour and then washed twice with PBS. Cell surface expression of CXCR4 was detected by flow cytometry and compared with control cells (incubated with saline solution).

1.1.8 Cell sorter separation

After lentiviral infection of DLBCL cells, GFP positive cells were sorted using the FACSAria cell sorter (BD Biosciences). Ten million infected cells were centrifuged at 1500 rpm for 5 minutes and resuspended in 2 ml of media. For each infected cell line, one million of control cells were used to establish the separation settings. Cells expressing GFP expressed also the luciferase gene. These cells were selected and used for all *in vitro* and *in vivo* experiments.

SUDHL-2 cells transfected with pCXCR4 plasmid and selected with geneticin (See "*Nucleofection and selection of clones*") were also subjected to cell

separation. To detect CXCR4-expressing cells, the samples were incubated with PE-Cy5 mouse anti-human CXCR4 monoclonal antibody, following the procedure described in "*Quantification of CXCR4 expression and internalization*" section. Cells were resuspended in fresh media and subjected to cell separation.

1.1.9 Luciferase activity *in vitro*

The Luciferase Assay System (Promega) was used to determine whether the infected cell lines expressed the reporter *Luciferase* gene. Cells were washed with PBS and cell lysates were prepared using 200 µL of 1X lysis reagent (CCLR, Cell Culture Lysis Reagent). To quantify luminescence, 20µl of cell lysate were mixed with 100µl of Luciferase Assay Reagent (LAR) and the produced light (Relative Light Units, RLU) was measured using a microplate reader equipped with luminescence detection (Infinite® 200 Pro, Tecan).

1.1.10 Cell migration assay

Migration assays were performed using 8-µm pore size Transwell (Corning Costar, Corning). $5 \cdot 10^5$ cells were suspended in 100 µl of serum-free media and incubated at 37°C for 2 hours in the presence or absence of the CXCR4 inhibitor AMD3100 (10 µg/ml, Sigma-Aldrich). Then, cells were added to the upper compartment of the transwells and the lower compartment was filled with 600 µL of serum-free media with or without 100 ng/ml of human SDF-1α (Prospec-Tany TechnoGene). The amount of cells migrating within 24 hours to the lower compartment was quantified using the Scepter 2.0 Handheld Automated Cell Counter (Millipore). Results are expressed as the total number of cells that migrated to the lower chamber ± standard deviation.

1.1.11 Apoptosis Test

The Annexin V-FITC Apoptosis Detection Kit (Calbiochem/EMD Millipore, Darmstadt, Germany) was used to evaluate if AMD3100 induced apoptosis in DLBCL cells. The protocol is based on the detection of annexins that bind to membrane phosphatidylserine and are used to quantify apoptotic cells by flow cytometry. After initiation of apoptosis, the phosphatidylserine loses its distribution in the phospholipid bilayer and translocates to the extracellular membrane, which is detectable with fluorescently labeled Annexin V-FITC. In early stages of apoptosis, the plasma membrane excludes viability dyes such as propidium iodide (PI), therefore cells which display only Annexin V staining are in early stages of apoptosis. During late-stage apoptosis, loss of cell membrane integrity allows annexin-V binding to cytosolic phosphatidylserine, as well as cell uptake of PI.

For each condition, $5 \cdot 10^5$ cells were centrifuged at 1000 g for 5 minutes and washed with PBS. Cells were resuspended in 0.5 ml cold 1x Binding Buffer and 1.5 µL of Annexin V-FITC were added. After 15 minutes incubation at room temperature in the dark, cells were centrifuged again and then resuspended in 0.5 ml cold 1x Binding Buffer. 10 µl of Propidium Iodide were added to each sample and then apoptosis was evaluated by flow cytometry. The 488 nm excitation laser was used to measure annexin-V staining and the 633 nm excitation laser was used to measure PI staining.

1.1.12 XTT Cell Viability Assay

Antitumor activity was evaluated measuring cell metabolic capacity (viability), using the colorimetric cell proliferation kit II (XTT, Roche Diagnostics)

and following the manufacturer's recommendations. During the assay, the yellow tetrazolium salt XTT is reduced to a highly colored formazan dye by dehydrogenase enzymes present in metabolically active cells. This conversion only occurs in viable cells and the amount of the formazan produced is proportional to the viable cells in the sample.

To quantify cell viability, $30 \cdot 10^4$ cells were seeded into 96-well plates in 100 µL of media and incubated at 37°C for 24 hours. Then, cells were exposed to the tested drug for 48 hours and assessed for viability. The XTT cell viability reagents were thawed just before its use and the electron coupling solution was mixed with the XTT reagent (1:50 volume ratio) to make XTT detection solution. 50 µl of the mixture were added to each well (which contains 100 µl/well culture medium) and the plate was returned to the incubator. After 4 hours incubation, cell viability was quantified by measuring the absorbance at 450 nm wavelength using a spectrophotometer (BMG Labtech). Assays were carried out in triplicates, exposing cells to the drug or vehicle for 48 hours.

1.2 GENETIC ENGINEERING METHODS

1.2.1 Plasmid constructions

Lentiviral plasmids

Four plasmids were used to obtain bioluminescent DLBCL cells. First, the *Luciferase* gene was obtained from the pPK-CMV-F3 C-Luc plasmid. Then, the gene was introduced into the pSIN-DUAL-GFP1-GFP2 plasmid. Finally, the plasmid pSIN-DUAL-GFP1-Luciferase together with two lentiviral plasmids coding for envelope and packaging proteins were used to generate lentiviral particles in 293T cells. pSIN-DUAL-GFP1-GFP2, pCMV-dR 8.91 and pVSV-G

plasmids were kindly provided by Dr Mary Collins (College Medical School, Cleveland, OH). All these plasmids contained the ampicilin-resistance gene to select bacteria cells containing the plasmid.

- **pPK-CMV-F3 C-Luc** (Promokine): This construct contains the G3 firefly *Luciferase* gene, a reporter gene useful to follow the dissemination or tumor growth of lymphoma cells *in vivo*.

- **pSIN-DUAL-GFP1-GFP2**: This plasmid contains 2 GFP (Green Fluorescent Protein) reporter genes. The GFP2 gene was useful to detect the fluorescent protein in transfected cells in order to quantify the transfection efficiency by flow cytometry. The GFP1 gene was replaced by the *Luciferase* gene. The generated plasmid, pSIN-DUAL-GFP1-Luciferase, was transfected into 293T cells together with pCMV-DR 8.91 and pVSV-G lentiviral plasmids to produce lentiviruses able to infect DLBCL cells.

- **pCMV-dR 8.91**: Packaging plasmid that regulates the synthesis of viral proteins and the virus replication.

- **pVSV-G**: Envelope plasmid that contains proteins related to the formation of the viral envelope.

pCXCR4 plasmid

The **pCXCR4** plasmid was used to transfect DLBCL cells. This plasmid was kindly provided by Dr. Jun Komano (Osaka Prefectural Institute of Public Health, Osaka, Japan). The plasmid was introduced by nucleofection into SUDHL-2 cells which originally did not express CXCR4. This plasmid contains a kanamicine/neomycin-resistance gene that permits selection with antibiotics

(see "*Nucleofection and selection of clones*" section) and the CXCR4 gene is placed under the control of the constitutive CMV (cytomegalovirus) promoter.

1.2.2 Bacterial transformation

E.coli DH5α competent bacteria cells (Invitrogen) were used for transformation porpuses. Under sterile conditions, 50 µl of competent cells were thawed on ice and 2 µl of plasmid DNA were added to the cells (1-10 ng DNA). Cells were incubated on ice for 30 minutes and subjected to a 42°C heat shock for 45 seconds. Afterwards, cells were kept on ice for 2 additional minutes and then 500 µl of pre-warmed S.O.C media (0.5% Yeast Extract, 2% Tryptone, 10 mM NaCl, 2.5 mM KCl, 10 mM MgCl2, 10 mM MgSO4 and 20 mM Glucose) were added. After 1 hour of shaking, 50, 100 and 200 µL of cells were spread in LB-agar plates with the appropriate antibiotic (25 µg/ml Ampicillin or 30 µg/ml Kanamycin) and incubated at 37^{o}C overnight.

Bacterial cells that grew in the LB-agar plates were those that had incorporated the plasmid, which confered resistance to the antibiotic. A sterile loop was used to pick a single colony and the bacterial cells were transferred to a 50 ml tube and incubated at 37°C overnight in their suitable growth medium (LB media supplemented with the appropriate antibiotic).

LB liquid media was prepared with 10 g of casein peptone, 5 g of yeast extract, 10 g of NaCl, and 1 liter of distilled water; the pH was adjusted to 7.0 ± 0.2 with NaOH and the mixture was autoclave for 25 min at 120°C. LB-Agar was prepared with 15 g/L of agar in LB media, and then the mixture was also autoclaved and poured into petri plates.

1.2.3 Generation of bacterial glycerol stocks

For long-term storage of bacterial stocks, cells were frozen using a solution of 15 % of glycerol as a cryoprotectant. Equal amounts of 30% glycerol and culture broth were mixed, dispensed into cryotubes and then frozen at -80^{o}C.

To recover frozen bacteria, a portion of the frozen stock was scraped off and then grown in LB media containing the appropriate antibiotics. The stock tube was returned to –80°C and freeze-thaw cycles were avoided to maintain the bacterial viability. Bacterial cells that grew in the LB media were spread into LB-Agar plates also containing the appropriate antibiotics.

1.2.4 Recovery of plasmid DNA from bacterial stock

Plasmid DNA from bacterial cells was purified using Qiagen Miniprep or Maxiprep kits. First, the Miniprep kit was used to purify and check the bacterial plasmid DNA. The DNA was analyzed by digestion using appropriate restriction enzymes followed by an agarose gel to verify the length of the obtained fragments. Then, we evaluated the quality of the purified plasmid DNA by measuring its absorbance using a Nanodrop spectrophotometer (Thermo Scientific). The ratio of absorbance at 260 nm and 280 nm was used to assess the purity of the DNA. A ratio of ~1.8 was considered as “pure” DNA. Once the plasmid DNA was checked, the Qiagen Maxiprep Endofree kit was used to obtain the lentiviral plasmids (following the manufacturer’s instructions). This kit was used to obtain higher amounts of DNA achieving from 300 to 800 µg of plasmid DNA from a bacterial cell culture of 100-150 ml. This purified DNA was also quantified and evaluated to check the length of the fragments and its purity.

1.2.5 DNA digestion using restriction enzymes

The *Luciferase* gene from the plasmid pPK-CMV-F3 C-Luc was subcloned into pSIN-DUAL-GFP1-GFP2 plasmid. The resulting plasmid contained the *GFP* and *Luciferase* reporter genes, for *in vitro* and *in vivo* monitoring, respectively. The pSIN-DUAL-GFP1-GFP2 plasmid was digested with *KpnI* and *XhoI* restriction enzymes. Hence, the opened plasmid with cohesive endings could be ligated with the *Luciferase* gene (*Luc*). The *Luc* gene was cut off from its original plasmid using the same digestion enzymes. 10-15 µg of DNA were digested with 2 µl of each restriction enzyme (50 U/µL, Invitrogen) and mixed with 3µl of digestion buffer and distilled water in a total volume of 30 µl. The digestions were incubated overnight in a water-bath at 37°C.

1.2.6 DNA electrophoresis

An agarose gel was prepared to check and purify the DNA of interest: the linearized plasmid and the *Luciferase* gene. 1% agarose gel was prepared by dissolving 1 gram of agarose in 100 ml of 1x TAE buffer (diluted from 5x TAE: 2M Tris-Base, 1M boric acid and 50 mM EDTA, pH 8). The microwave was used to dissolve the agarose, avoiding over-boiling of the mix. Once the agarose was cooled, 5 µL of ethidium bromide were added and the gel was poured into a tray containing a comb (for wells formation). When the gel was solid, the comb was taken off, and the agarose gel was inserted in the electrophoresis chamber. Then, samples were mixed with 6x loading buffer and loaded in the gel for DNA separation. 1 Kb marker (Promega) was used as a control DNA to check the size of the digested fragments. The gel was covered with buffer (about 2 mm). Finally, electrodes were attached to the chamber and power was turned on to 100 volts for approximately 60 - 120 minutes.

1.2.7 Recovery of DNA fragments from agarose gels

DNA fragments obtained from the agarose gel separation were recovered and purified in order to use them for subcloning purposes. As ethidium bromide binds to DNA and fluoresces under ultraviolet light, an ultraviolet-trans-illuminator was used to see and detect the DNA fragments. Once the bands of interest were detected, which could be a gene or a linearized plasmid, they were cut out from the gel using a scalpel. The pieces of gel containing the DNA of interest were then purified using the Gel extraction kit protocol (Qiagen) and following the manufacturer's instructions.

1.2.8 Ligation

A new construct was obtained by performing a ligation of fragments from different plasmids, the Luc gene and the opened pSIN-DUAL-GFP1 plasmid. Different insert/plasmid ratios (2/1, 4/1, 6/1) were mixed to optimize the ligation reaction. Then, 1 µL of T4 DNA ligase (Invitrogen) per each 100 µg of plasmid was added to the mix, together with the required ligation buffer. The reaction took place overnight at 16°C. The obtained ligated constructs were then transformed into DH5 alpha bacterial competent cells and incubated at 37°C overnight in LB-Agar plates containing ampicilline. Then, single colonies were picked from LB-Agar plates and grown in LB-Ampicilline media. Plasmid DNA was purified (Miniprep protocol, Qiagen) and digested with restriction enzymes to verify the identity of the new vector.

1.2.9 Nucleofection and selection of clones

The SUDHL-2 cell line was transfected with pCXCR4 plasmid by nucleofection. The nucleofection process is based on the physical method of electroporation and uses a combination of electrical parameters, generated by a device called Nucleofector (Amaxa®), with cell-type specific reagents to introduce DNA directly into the cell nucleus. The protocol for nucleofection of suspension cell lines was used, $1 \cdot 10^6$ cells were transfected with 1 µg of pCXCR4 plasmid in 100 µL of Solution L. 48 hours post-transfection, CXCR4 expression was quantified by flow cytometry using the fluorescent PE-Cy5 mouse anti-human CXCR4 monoclonal antibody (See "*Flow cytometry analysis*"). After selection of the GFP positive cells, stable clones were obtained through selection in medium containing 0.2-1.4 mg/ml of geneticin (G418, Life Technologies) for a period of at least 4 weeks.

1.3 CELL LINE INFECTION USING LENTIVIRAL PARTICLES

1.3.1 Production of lentiviral particles

Due to the difficulty of transfecting haematologic cells, lentiviral particles were produced to infect DLBCL cells. As mentioned before, the GFP2 gene was replaced by the Luciferase gene to obtain the pSIN-DUAL-GFP1-Luciferase plasmid. Then, we used the 293T cell line to produce lentiviral particles expressing the vector. 60-mm petri dishes were treated with poly-L-lysine (Sigma-Aldrich) to avoid cell detachment and 293T cells ($3 \cdot 10^6$) were seeded using antibiotic-free DMEM media to produce the lentiviral particles. The cells were cotransfected with 2.25 µg of the pSIN-DUAL-GFP1-Luciferase plasmid, 1.5 µg of pCMV-dR 8.91 gag-pol expression vector, and 0.75 µg of pVSV-G virus

envelope expression vector using Lipofectamine 2000 (Invitrogen) in Opti-Mem media. The mixture was incubated for 20 minutes at room temperature and then added to the cells. Then, after 16 hour incubation at 37°C, fresh media was added to the cells (50% Optimem / 50% DEMEM with 2% FBS). After 48 hours of transfection, lentiviral particles from the supernatants were harvested, passed through a 0.45 µm filter, and stored at -80°C.

1.3.2 Virus titration

The produced lentiviral particles were titrated by infecting 293T cells with different dilutions of the supernatants containing the viruses. These cells were used because they are highly infectable. 293T cells were seeded in 12-well plates ($1.5 \cdot 10^5$) and the following day, several viral dilutions (½, 1/10, 1/100 and 1/1000) in a volume of 400 µL were added to the cells. After 6 hours of incubation at 37°C, 500 µL of fresh DMEM media were added to the cells and after 48 hours, the percentage of infected cells was quantified by flow cytometry. Cells were treated with trypsin to detach them from the wells and centrifuged at 1500 rpm for 5 minutes. Then, cells were washed twice with PBS and resuspended in 400 µL of PBS for flow cytometry analysis (see "Quantification of GFP positive cells"). For each dilution of the viruses a percentage of GFP positive cells was obtained and was linearly interpolated into percentage of infected cells. The percentage of infected cells was expressed as transduction units (tu) and considering the volume of the supernatant that was added to the cells, we obtained transduction units per milliliter (tu / ml). Lentiviral stocks of > 10^6 tu / ml were considered optimal for infection.

1.3.3 DLBCL cell lines infection with lentiviruses

Several DLBCL cell lines were infected with the lentiviral particles: GC-DLBCL cell lines (Toledo, HT, KARPAS-422, OCI-Ly19) and ABC-DLBCL cell lines (SUDHL-2, RIVA, OCI-Ly10). Cells were seeded at a concentration of $2 \cdot 10^5$ cell/ml (200 µL) in 12-well plates and then infected using different viral multiplicity of infection (MOI, number of lentiviral particles per cell). Different volumes of the viral supernatants were added to obtain the different MOIs (0.5 - 1 - 2). After 6 hours incubation at 37°C, fresh media was added to the cells to a total volume of 500 µL. The percentage of infection was quantified by cytometry 48 hours post-infection. Then, cell sorting was performed to select the GFP possitive cells in order to obtain a homogeneous population expressing the vector. Luciferase activity was also measured according to Promega Luciferase Assay System Protocol (See "*Luciferase activity in vitro*").

1.4 RT-PCR TO QUANTIFY CXCR4 EXPRESSION

The levels of CXCR4 mRNA expression from cell lines were measured on a 7900 HT Fast-Real Time PCR System (Applied Biosystems). Total RNA was isolated using TRIzol Reagent (Life Technologies) according to the manufacturer's instructions. cDNA was synthesized from 1.5 µg of total RNA using the High Capacity Reverse Transcription Kit (Applied Biosystems). Cycling conditions for cDNA systhesis were 10 minutes at 26°C, 2 hours at 37°C and 3 minutes at 90°C. Real-time PCR was performed using pre-designed Taqman® Gene Expression primer and probe assays for CXCR4 (Hs00607978_s1) and HPRT1 (Hs99999909_m1) (Applied Biosystems). 2 µL of cDNA were used as template; 10 µL of Taqman Master Mix (Life Technologies) were mixed with template and primers to a total volume of 20 µL. Cycling conditions were 2

minutes at 50°C, 10 minutes at 95°C and 40 cycles of 15 seconds at 95°C followed by 1 minute at 60°C. Experiments were done in triplicate for each sample and were repeated at least twice. Ct values were normalized against HPRT1 as a housekeeping gene.

2. IN VIVO EXPERIMENTS USING NOD/SCID MICE

2.1 NOD/SCID MICE

NOD/SCID female mice (4 weeks old) were obtained from Charles River Laboratories. Mice were housed in microisolator units with sterile food and water *ad libitum*. During the experimental work, animals were monitored every other day and a loss of 15% in body weight or signs of sickness were considered as the endpoint. In addition, bioluminescence (BLI) was monitored as described below. All procedures involving mice were approved by the Hospital de la Santa Creu i Sant Pau Animal Ethics Committee according to established guidelines.

2.2 CELL LINES

Several DLBCL luminescent cell lines were used for the *in vivo* experiments: SUDHL-2, RIVA, OCI-Ly10 (ABC-DLCBL), and Toledo, HT, KARPAS-422 and OCI-Ly19 cells (GCB-DLBCL). All cell lines expressed the G3 firefly luciferase gene which allows to non-invasively monitor the cells after their injection in mice.

2.3 IMPLANTATION TECHNIQUES

Two types of implantation techniques were used for the *in vivo* experiments: 1) the subcutaneous (sc) injection of cells into the flanks of mice and, 2) the intravenous (iv) injection of cells in the tail vein. In these studies, the subcutaneous conditioning of the cells prior to their intravenous injection was compared with the direct intravenous injection of the cells. Engraftment, dissemination and mouse survival times were compared between groups.

2.3.1 Subcutaneous (sc) injection

NOD/SCID mice were anesthesized with 100 mg/kg ketamine (Ketolar, Parke Davis SL, Pfizer) and 10 mg/kg xylazine (Rompun, Bayer). Mice were subcutaneously inoculated in both flanks with $10 \cdot 10^6$ of DLBCL cells (resuspended in 100 µL of saline solution) using an insulin syringe of 25G needle.

2.3.2 Intravenous (iv) injection

Subcutaneously conditioned cells and non-conditioned cells were centrifuged at 1500 rpm for 5 minutes and suspended in 100 µL of saline solution per mouse. The animals were intravenously injected with $20 \cdot 10^6$ cells via the tail vein using a insulin syringe of 25G needle.

2.4 EXTRACTION AND DISAGGREGATION OF SUBCUTANEOUS TUMORS

When subcutaneous tumors achieved a volume of 800-900 mm^3, mice were euthanized by cervical dislocation. Tumor pieces were extracted, placed in a sterile petri dish containing the appropriate culture medium, and mechanically disaggregated with tweezers until a single-cell suspension was obtained. For the intravenous injection into new mice, cells were cultured for 15 hours, filtered through a cell strainer and suspended in 100 µL of saline solution per mouse.

2.5 MONITORING OF CELLS: BLI IMAGING AND QUANTIFICATION

We monitored subcutaneous tumor growth and dissemination of intravenously injected DLBCL cell lines capturing bioluminescence (BLI) once a week using either the IVIS-2000 (Xenogen) imaging system or the ORCA-II Deep Cooling BTW Imaging System (Hamamatsu Photonics). Mice were anesthetized with 3% isoflurane and maintained with 1.5% isoflurane in oxygen or with ketamine-xylazine, for the IVIS and the BTW imaging systems, respectively. BLI was captured 10 minutes after the intraperitoneal injection of firefly D-luciferin (2.25mg/mouse, Perkin Elmer) and the animals were exposed for 2 minutes in order to acquire the images. To maximize the sensitivity, dorsal images were taken from subcutaneously injected mice and ventral images were taken from intravenously injected mice.

BLI pictures were quantified using Living Imaging Software (Version 4.2, Xenogen). Images from experimental sets were loaded and global bioluminescence was taken as region of interest. Baseline signals obtained from each mouse on day 7 post injection of cells were used for the comparison with the signals obtained over time. The bioluminescence of images taken with the IVIS system was evaluated as total photon flux and expressed as photons/sec (p/s). The bioluminescence of images taken with the BTW system was evaluated as total photons and expressed as Photon Counts (PHCs). The net number of PHC was calculated using the formula: [Total number of PHC in the area of interest- (Number of pixels in the area of interest x Average background PHC per pixel)].

2.6 NECROPSY AND TISSUE PROCESSING

2.6.1 Necropsy, macroscopic and histopathologycal analyses

At the end of all *in vivo* experiments, mice were euthanized and analyzed for macroscopic signs of lymphoma development. Furthermore, histological analyses were performed using paraffin-embedded sections of potentially infiltrated organs, including cervical, axillary, inguinal, caudal, mesenteric, mediastinal and renal lymph nodes, brain, spleen, liver, kidneys, and bone marrow from cranium, femur and vertebral column. Tissue sections were stained with hematoxylin and eosin (H&E) staining, following the standard protocol.

2.6.2 Immunohistochemical analysis

Immunohistochemical analysis was performed in tissue samples, cell lines or sections of infiltrated organs to detect CD10, MUM1, BCL6 (DAKO) or CXCR4 (Abcam) expression (**Table 8**). 4 µM-thick sections were incubated at 58**°**C for 1 h and then dewaxed in xylene, rehydrated through a graded ethanol series and washed with phosphate-buffered saline. Heat-induced epitope retrieval was done by immersing the sections in sodium citrate buffer (pH 6.0) and incubating them at 97**°**C for 20 minutes in a DAKO PTLink. The immunohistochemical reactions were visualized following the biotin-free EndVision system (DAKO) using diaminobenzidine. The reactions were performed in a DAKO Autostainer Link48.

Table 8. Primary antibodies used for the immunohistochemical analysis.

Primary antibody	Dilution	Clone	Marca comercial
CD10	Pre-diluted*	Mouse	Dako
MUM1	Pre-diluted*	Mouse	Dako
BCL6	Pre-diluted*	Mouse	Dako
CXCR4	1:300	Rabbit	Abcam

* Dako pre-diluted antibodies which concentrations are unknown.

2.6.3 Image acquisition and quantification

CXCR4 expression was quantified in cell lines and infiltrated organs by assigning an H-score (0-300), resulting from the product of the intensity (0-3) and the percentage of staining (0-100), observed under microscopic analysis. We also evaluated whether tumor samples of DLBCL patients were positive or negative for CXCR4 expression in the cell membrane (presence or absence of the receptor) and used dichotomized values for statistical analysis. Two independent observers evaluated all samples using an Olympus BX51 microscope. Images were acquired using an Olympus DP72 digital camera and processed with the Olympus Cell^{D} Imaging 3.3 software (Olympus Corporation).

2.7 DRUG ADMINISTRATION

2.7.1 Therapeutic validation of DLBCL mouse model using cyclophosphamide

Cyclophosphamide (Genoxal®) was chosen as a clinically used drug for the validation of our DLBCL mouse model. Cyclophosphamide is routinely given to DLBCL patients and it is a stable and non-vesicant drug when intravenously injected in mice. First of all, healthy NOD/SCID mice were used to establish the

Maximum Tolerated Dose (MTD) of cyclophosphamide in this mouse strain. 12 mice were randomly divided into four groups and intravenously injected in the tail vein with 60, 75, 100 or 120 mg/kg of cyclophosphamide per 3 days a week (Monday, Wednesday and Friday). 7 and 9 doses were given for the low (60 and 75 mg/kg cyclophosphamide) and high concentration groups (100 and 120 mg/kg cyclophosphamide), respectively.

When the MTD for cyclophosphamide was established, Toledo-Sc cells were intravenously injected in 20 mice which were randomly distributed into two groups that received either vehicle (saline solution) or 75 mg/kg of cyclophosphamide every 2 days during 7 administrations. Treatment was initiated 7 days after cell injection. Once a week, mice were non-invasively monitored using the IVIS system to quantify the BLI signal.

2.7.2 Blockage of CXCR4 by AMD3100

The CXCR4 inhibitor AMD3100 was used to block CXCR4 activity in DLBCL cells *in vivo*. Mice were intravenously injected with $20 \cdot 10^6$ AMD3100-pretreated OCI-Ly10 cells (n=10) or with untreated OCI-Ly10 cells (n=10). OCI-Ly10 cells were pre-treated by incubation with AMD3100 (10 µg/ml, Sigma-Aldrich) for 30 minutes at 37°C. Mice injected with AMD3100-pretreated cells were administered daily with intraperitoneal AMD3100 (10 mg/kg), whereas control mice were treated with vehicle (saline solution) using the same administration interval until the end of the experiment. All the doses were established in accordance with the dosage genearally used in reported experiments from the literature. BLI images were taken weekly to follow the dissemination of DLBCL cells, and mice were evaluated daily to monitor their weight and to detect signs of toxicity. All mice were euthanized 4 weeks after cell injection. We evaluated

the effect of AMD3100 by comparing the infiltration pattern and bioluminescent signal emitted in the different organs between treated and non-treated groups.

2.7.3 E7123 treatment of the DLBCL model with CNS involvement

2.7.3.1 E7123 preparation and administration to mice

E7123 was dissolved using polietilenglycol-400 (PEG-400) and fetal bovine serum (FBS) in a 3:1 proportion. First of all, the E7123 powder was dissolved with PEG-400 using a mechanical mixer (Pestle Mixer Motor, VWR International) at room temperature. Then, FBS was added to the mixture and mice were orally administered with 75 mg/kg of E7123 using a cannula to reach the stomach of the animals.

2.7.3.2 Evaluation of E7123 antitumor activity

HT-Sc cells obtained from the disaggregation of subcutaneous tumors were intravenously injected in 20 mice to evaluate the antitumor effect of E7123. Mice were randomly divided into 2 groups and were orally administered with E7123 (75 mg/kg) or vehicle (PEG:FBS) every day until they were euthanized. Bioluminescence images were taken weekly to follow the dissemination of lymphoma cells. A loss of 15% in body weight or the appearance of motor problems or evident signs of sickness were considered as the endpoint. We evaluated the antitumor effect of E7123 by comparing survival time, infiltration pattern and bioluminescent signal between treated and non-treated groups.

3. ANALYSIS OF DLBCL PATIENT BIOPSIES

3.1 TISSUE MICROARRAYS OF DLBCL PATIENTS

Forty-two lymph node biopsies from patients with primary nodal DLBCL who were diagnosed in our institution, between 2007 and 2012 based on the World Health Organization criteria, were used. Patients with follicular lymphoma or indolent lymphomas with subsequent transformation into DLBCL were excluded. Patients with central nervous system involvement or with HIV-associated lymphomas were also excluded. All 42 patients received rituximab in their treatment; 87% were treated with R-CHOP chemotherapy and 13% received other chemotherapeutic agents in combination with rituximab. **Table 17** from the "*Results*" section shows the main features of the patient series. The Institutional Review Board at Hospital de la Santa Creu i Sant Pau approved the study and informed consent was provided according to the declaration of Helsinki and obtained from patients.

3.2. HISTOLOGY AND IMMUNOHISTOLOGICAL EVALUATION OF DLBCL TISSUE MICROARRAYS

Forty-two lymph node biopsies from DLBCL patients were evaluated by a pathologist to confirm their diagnosis. Then, two tissue microarrays (TMA) containing duplicated tumor samples were generated using an automated tissue microarray device (Beecher Instruments, Silver Spring). Tissue cylinders of 1 mm of diameter were punched out from each tumor and normal tissues were included in the TMA as control. All samples in the TMA were evaluated by immunohistochemical analysis to detect CXCR4 expression (see "*Immunohistological analysis*").

4. STATISTICAL ANALYSIS

In the studies performed during this PhD, we have evaluated categorical and continuous data. The results with categorical data are reported as number of cases (n) followed by the percentage (%). Contingency tables were used to evaluate differences between groups using the Chi-square or the Fisher's exact tests. The results of continuous data are reported as mean ± standard deviation for experiments performed in 3 replicates and were analyzed using the non-parametric Mann–Whitney test.

Survival rates were estimated by the Kaplan-Meier method and differences between groups were compared using the Log-rank test. In mice, overall survival (OS) was defined as the time from the day of cell injection to the end-point. In DLBCL patients, progression-free survival (PFS) was calculated from the onset of treatment until relapse or death; OS was defined as the time between the onset of treatment and death or date of the last follow-up evaluation.

Univariate and multivariate analyses of the prognostic effect of the studied variables were done using the COX proportional hazard model using dichotomized values. Only significant factors for the univariate analysis were included in the multivariate analysis. Correlations between clinico-pathological variables and CXCR4 expression were tested using Fisher's exact test. Results were considered significantly different at $P \leq 0.05$. Statistical calculations were performed using SPSS software (version 21).

“No good deed is lost in this world. In some place, it will remain forever”

“Ninguna acción buena se pierde en este mundo. En algún lugar quedará para siempre”

Vicent Ferrer

RESULTS

1. DLBCL MOUSE MODELS DEVELOPMENT AND VALIDATION

One of the main goals of this thesis was to develop bioluminescent DLBCL mouse models able to reproduce the clinical features of this disease. These mouse models will be useful for the study of DLBCL pathology and to evaluate the antitumor effect of new drugs. Previously, our group developed disseminated GCB-DLBCL mouse models by performing subcutaneous-conditioning of the cells to increase their aggressiveness prior to their intravenous injection.[117]

To develop luminescent mouse models, several DLBCL cell lines (SUDHL-2, RIVA, OCI-Ly10, OCI-Ly19, Toledo, KARPAS-422 and HT) were transduced with lentiviral particles to express the *Luciferase* reporter gene. Then, we evaluated if the different DLBCL cell lines were able to grow and survive in the subcutis of NOD/SCID mice. The cell lines that were able to subcutaneously grow in mice were selected to develop the mouse models. The selected luminescent cell lines were injected in mice, with and without the subcutaneous preconditioning, and the generated models were monitored to evaluate their engraftment, infiltration pattern and survival time. Furthermore, the use of the disseminated DLBCL models for antitumor drug evaluation was validated by testing its response to cyclophosphamide.

1.1 LUMINESCENT DLBCL CELLS

Luminescent DLBCL cells were obtained to non-invasively follow their dissemination in NOD/SCID mice. Due to the limitation of transfecting haematologic cells by conventional transfection methods, we used lentiviral vectors to transduce the cells (explained in "*Material and Methods*"). The

DLBCL cell lines were infected with the lentiviral particles so that they incorporated the pSIN-DUAL-GFP1-Luciferase plasmid into their DNA. This plasmid was obtained by digesting the original pSIN-DUAL-GFP1-GFP2 with *KpnI* and *XhoI* restriction enzymes and replacing the GFP2 by the *Luciferase* gene (**Figure 12**). Hence, the *GFP* and *Luciferase* reporter genes were constitutively expressed by the cells, allowing the *in vitro* and *in vivo* detection, respectively.

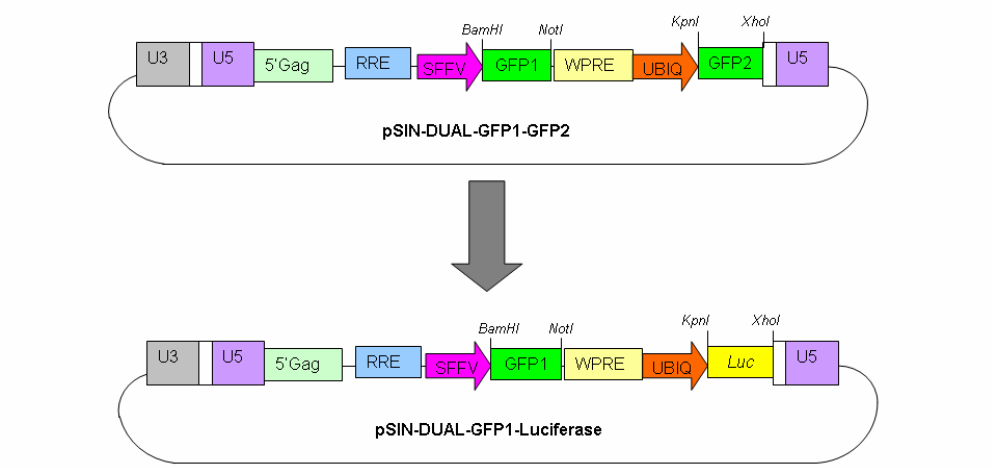

Figure 12. Generation of the pSIN-DUAL-GFP1-Luciferase plasmid. The pSIN-DUAL-GFP1-GFP2 plasmid was digested with Kpn*I* and *XhoI* restriction enzymes and the GFP2 was replaced by the *Luciferase* gene.

The efficiency of infection of DLBCL cell lines was evaluated by quantifying the GFP positive cells by flow cytometry and the luciferase activity using a luminescence microplate reader. The percentage of GFP positive cells after lentiviral infection was different for each cell line, ranging from 6.51 to 28.81% (%GFP Pre-sorter, **Table 9**). Cells expressing GFP were selected using a Cell Sorter to obtain a homogenous population of infected cells. Once the positive cells were selected and grown, they were evaluated again by flow cytometry. In all cases, the cells selected for injection into mice contained more than 90% of fluorescent cells in the population (%GFP Post-sorter, **Table 9**).

Representative cytometry histograms for Toledo cells are shown in **Figure 13**. The percentage of GFP positive cells are shown for non-infected (control) and infected cells after their selection by cell sorting. Moreover the sorted cells were luminescent as shown in **Table 10**, in which the emitted light (Relative light units) from control cells was compared with the emitted light from infected and sorted cells. Hence, the cells were successfully expressing the *GFP* and the *Luciferase* reporter genes for *in vitro* and *in vivo* monitoring, respectively.

Table 9. Percentage of GFP positive DLBCL cells before and after their selection by cell sorting.

Cell Line	%GFP Pre-sorter	%GFP Post-sorter
SUDHL-2	10.24	95.20
RIVA	28.81	98.93
OCI-Ly-10	14.89	94.29
OCI-Ly-19	17.75	96.39
TOLEDO	10.27	92.12
KARPAS-422	6.51	91.41
HT	8.32	92.71

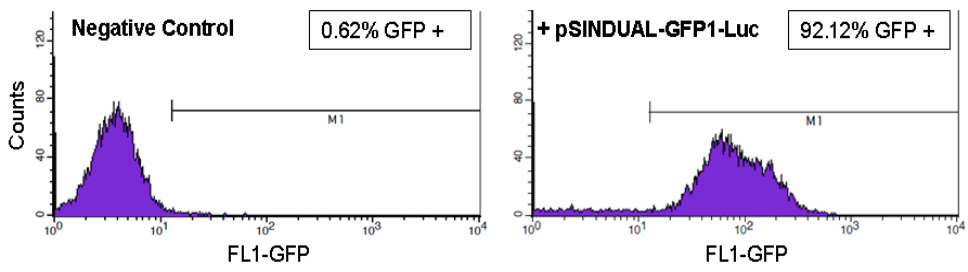

Figure 13. Cytometry histograms of Toledo cells infected with lentiviral particles containing the pSIN-DUAL-GFP1-Luciferase plasmid. The percentage of cells expressing the GFP fluorescent protein is shown for control and infected cells after their selection by cell sorting.

Table 10. Luminiscence quantification of parental and GFP-sorted cell lines.

	Relative Light Units (RLU)	
Cell Line	**Parental cells**	**GFP-Sorted cells**
SUDHL-2	113	196585
RIVA	122	105595
OCI-Ly-10	109	87222
OCI-Ly-19	102	17734
TOLEDO	106	69401
KARPAS-422	99.5	105398
HT	28	93839

1.2 SUBCUTANEOUS CONDITIONING OF DLBCL CELLS ENHANCED THEIR AGGRESSIVENESS

We wanted to evaluate if the subcutaneous conditioning of DLBCL luminescent cells would enhance their aggressiveness when injected into new mice. To that aim, first we had to evaluate if DLBCL cells were able to grow when injected subcutaneously into NOD/SCID mice. A total of 6 mice per each cell line were subcutaneously injected with $10 \cdot 10^6$ cells of luminescent SUDHL-2, RIVA, OCI-Ly10, OCI-Ly19, Toledo, KARPAS-422 or HT. The growth of the tumors was followed once a week by BLI imaging. In **Figure 14** representative BLI images of subcutaneous tumor growth are shown for the Toledo cell line. From the first week after cell injection, luminiscence was detected in the flanks of mice and, as observed in the images, the BLI signal increased over the time. The subcutaneous tumors were extracted 34 days after the injection of Toledo cells.

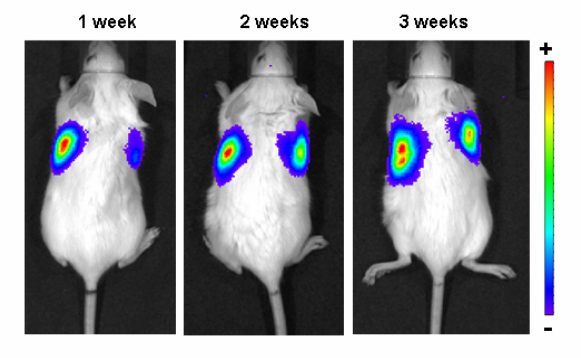

Figure 14. Bioluminescent images of subcutaneous tumors of Toledo cells growing in NOD/SCID mice. Toledo cells were injected in the flanks of mice and bioluminescent images were taken once a week from day 7 after cell injection. The same process was followed for SUDHL-2, RIVA, OCI-Ly10, OCI-Ly19, KARPAS-422 and HT cells. Arbitrary color bars illustrate relative light intensity levels of firefly luciferase, ranging from low (blue) to high (red).

The subcutaneous tumors were extracted when they reached a volume of 800-900 mm^3. **Table 11** shows the percentage of engraftment and the time that each cell line took to develop the tumors. The percentage of subcutaneous tumors engraftment of OCI-Ly-19 and KARPAS-422 cells was the lowest, 25 and 31.3%, respectively. In contrast, the engraftment of the other cell lines was higher, ranging from 48.8 to 91.6%. SUDHL-2, RIVA, OCI-Ly10 and Toledo cells took between 24 and 34 days to reach a volume of 800-900 mm^3, whereas HT took 56 days. Based on the percentage of subcutaneous engraftment, we selected SUDHL-2, RIVA, OCI-Ly10, Toledo and HT cells to develop disseminated DLBCL mouse models by intravenous injection of the conditioned cells.

Table 11. Percentage of subcutaneous (Sc) tumors that grew in NOD/SCID mice and the time they took to reach a volume of 800-900 mm^3. Mice were injected with $10 \cdot 10^6$ of cells in both flanks.

Cell Line	% Sc Tumors	Time (days)
SUDHL-2	83.3	24
RIVA	75	28
OCI-Ly-10	91.6	25
TOLEDO	87.5	34
OCI-Ly-19	25	42
KARPAS-422	31.3	85
HT	48.8	56

The subcutaneous tumors derived from SUDHL-2, RIVA, OCI-Ly10, Toledo and HT cells were extracted, disaggregated and incubated at 37°C. After 15 hours the suspension of conditioned cells was intravenously injected in new mice. In addition, control groups of mice were intravenously injected with non-conditioned cells (**Figure 15**). The BLI was followed weekly and the engraftment, infiltration pattern and survival times were compared between groups. The mouse model obtained with the subcutanously conditioned HT cells generated a DLBCL mouse model with central nervous system involvement and was used to test a new antitumor drug (explained in the section "*A novel inhibitor of focal adhesion increases survival in a xenograft model of DLBCL with central nervous involvement").*

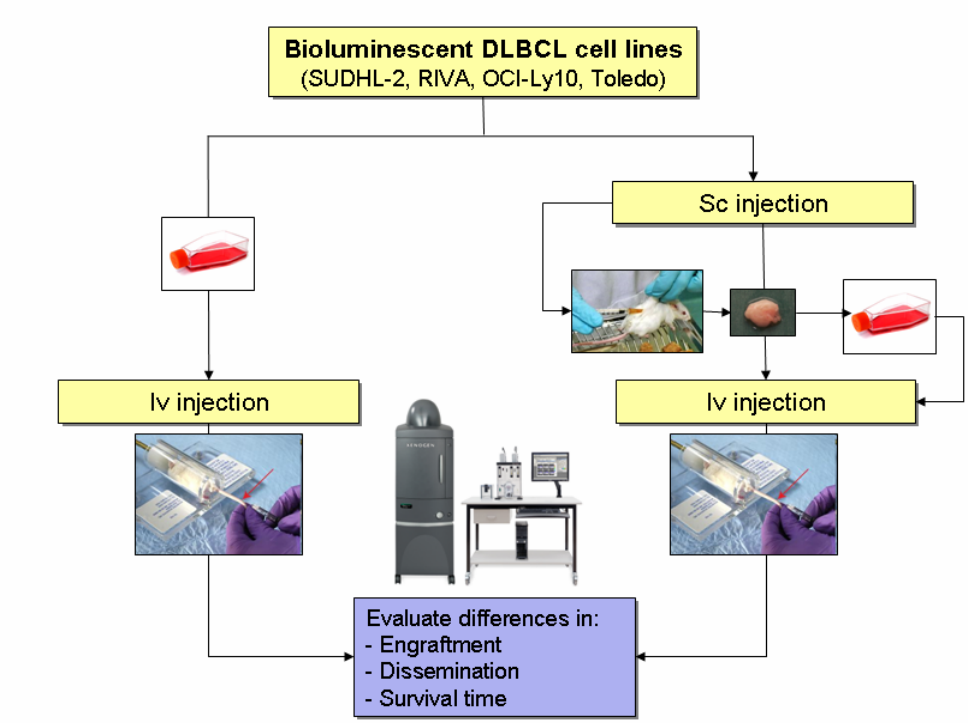

Figure 15. Diagram showing *in vivo* experiments to compare the aggressiveness of subcutaneously conditioned and non-conditioned cells in NOD/SCID mice. Subcutaneous tumors were grown, extracted, disaggregated and the resulting cell suspension was intravenously injected in mice. Engraftment, dissemination and survival time were compared with a group of mice intravenously injected with non-conditioned cells. The cell lines used for the *in vivo* experiment were SUDHL-2, RIVA, OCI-Ly10 and Toledo.

A summary of the infiltrated organs for each group of mice together with the survival times and the engraftment (positive mice that developed lymphoma) are shown in **Table 12**. The aggressiveness of the cells was increased for subcutaneously conditioned RIVA-Sc and Toledo-Sc cells. In contrast, the OCI-Ly10-Sc cells decreased their aggressiveness in mice when compared with the non-conditioned cells. In the case of the SUDHL-2 cells, there were no differences between groups.

Thus, the effect of the subcutaneous preconditioning of DLBCL cells depends on the cell line:

- OCI-Ly10: This is the most aggressive cell line. When the cells were intravenously injected in mice they presented a rapid dissemination to lymph nodes (LN), bone marrow (BM) and central nervous system (CNS) and developed lymphoma in all mice in less than a month. However, the subcutaneous-conditioned cells, OCI-Ly10-Sc, showed a decrease in LN infiltration (66%) and a significant increase in the survival time.

- RIVA: The intravenously injected RIVA cells showed a 83,3% of engraftment and the infiltration of LN was observed in 60% of the mice; furthermore, the CNS and the cranium were infiltrated in the 83% of the injected mice, and no infiltration of column or femur was detected. When the cells were subcutaneously conditioned, they showed a 100% of engraftment and infiltration of LN and cranium in all mice. These mice also showed a 83% of vertebral column or femur infiltration. Furthermore, they presented a significant decrease in the survival time.

- Toledo: The intravenously injected Toledo cells showed a 100% of engraftment. In 38 days approximately, all mice presented BM and CNS infiltration and 88.8% of the mice showed LN infiltration. The aggressiveness of the cells was increased with the subcutaneous conditioning leading to a decrease survival time of mice. However, the infiltration pattern was almost the same as that observed in the non-conditioned cells.

- SUDHL-2: There were not statistically differences between the subcutaneous conditioned and the non-conditioned SUDHL-2 cells injected in mice. Both

groups of mice, injected with the conditioned or with the non-conditioned SUDHL-2 cells, showed low engraftment and long survival times.

Table 12. Histopathological features and clinical evolution of NOD/SCID mice intravenously (iv) injected with DLBCL cell lines or with subcutaneously conditioned cells (Sc-iv).

	OCI-Ly10		**RIVA**		**SUDHL-2**		**Toledo**	
	iv	**Sc-iv**	**iv**	**Sc-iv**	**iv**	**Sc-iv**	**iv**	**Sc-iv**
Positive mice, n(%)	6/6 (100)	6/6 (100)	5/6 (83.3)	6/6 (100)	3/6 (50)	2/6 (33)	9/9 (100)	10/10 (100)
Survival time of mice with lymphoma[1]**,** days	29.6 ± 0.5	37.4 ± 0.8*	81.6 ± 9.5	52.7 ± 8.1*	67.3 ± 21.5	52 ± 35.4	37.8 ± 6.2	27.7 ± 1.5*
Mice with LN infiltration, n(%)	6/6 (100)	4/6 (66)	3/5 (60)	6/6 (100)	0/6 (0)	0/6 (0)	8/9 (88.8)	8/10 (80)
Mice with BM infiltration, n(%)	6/6 (100)	6/6 (100)	5/6 (83.3)	6/6 (100)	2/6 (33)	1/6 (16)	9/9 (100)	10/10 (100)
Vertebral column or Femur, n(%)	6/6 (100)	6/6 (100)	0/6 (0)	5/6 (83)*	2/6 (33)	0/6 (0)	9/9 (100)	10/10 (100)
Cranium, n(%)	6/6 (100)	6/6 (100)	5/6 (83.3)	6/6 (100)	1/6 (16.6)	0/6 (0)	9/9 (100)	10/10 (100)
Mice with CNS infiltration, n(%)	6/6 (100)	6/6 (100)	5/6 (83.3)	6/6 (100)	0/6 (0)	0/6 (0)	9/9 (100)	10/10 (100)

Positive mice are those that developed lymphoma. P values were calculated using the Log-rank test for survival time and Fisher's exact test for categorical variables. [1]Values represent the mean ± standard deviation. *Statistically significant differences between groups for histopathological features or clinical evolution when comparing groups of NOD/SCID mice intravenously injected with DLBCL cell lines (iv) and mice intravenously injected with subcutaneously-conditioned cells (Sc-iv), P <0.05. LN, lymph nodes; BM, bone marrow; CNS, central nervous system.

Next, we evaluated if the DLBCL cells mantained their original immunophenotype in the infiltrated tissues. Based on the Han's algorithm we determined the expression of CD10, BCL6 and MUM1 markers in cells and in infiltrated lymph nodes (LN). The immunophenotype of SUDHL-2 cell line was analyzed in infiltrated bone marrow (BM) because the cells did not infiltrate the LN. OCI-Ly10, RIVA and SUDHL-2 cell lines did not express CD10, a germinal center marker. In contrast, they did expres BCL6 and MUM1 markers as expected for ABC-DLBCL cells. Toledo cell line was positive for CD10 expression (**Figure 16**), as expected for GCB-DLBCL cells.

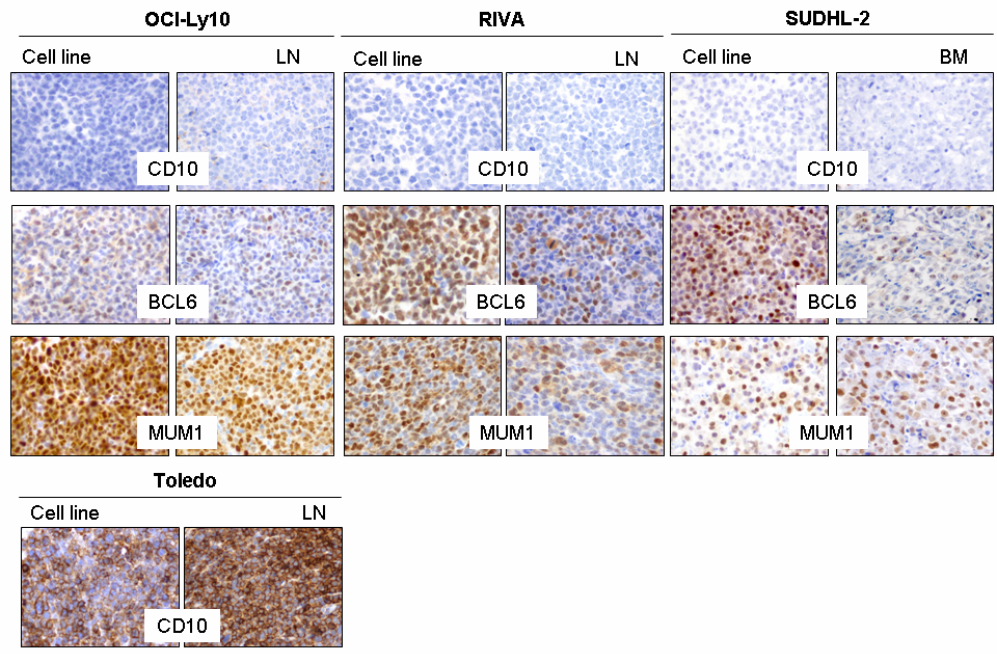

Figure 16. DLBCL cells maintained their original immunophenotype after injection into mice. Expression of CD10, BCL6 and MUM1 was analyzed by IHC in cell lines and in representative sections of infiltrated LN or BM of OCI-Ly10, RIVA, SUDHL-2 and Toledo injected mice. The immunohistochemical phenotype of SUDHL-2 cell line was analyzed in infiltrated BM because they did not infiltrate the LN. Original magnification x400. LN, lymph nodes; BM, bone marrow; IHC, immunohistochemistry.

In summary, all DLBCL cells maintained their CD10, BCL6 or MUM1 markers in the infiltrated tissues. Hence, we confirmed that the cells that infiltrated the different organs and that derived from the DLBCL cell lines, maintained their germinal (Toledo) or activated phenotypes (OCI-Ly10, RIVA and SUDHL-2).

We also evaluated the survival time of each group of mice, comparing the mice injected with the subcutaneous-conditioned cells with mice injected with the non-conditioned cells. The Kaplan-Meier survival curves for each group of mice are shown in **Figure 17**. For RIVA and Toledo injected mice there was a significant decrease in the survival time of mice injected with the subcutaneous-conditioned cells compared with mice injected with the non-conditioned cells. In contrast, mice injected with conditioned OCI-Ly10-Sc cells showed an increased survival time compared with the non-conditioned cells. Finally, for the SUDHL-2 cell line there were no statistically significant differences for the survival time between the two compared groups. The survival curves were not plotted for this cell line because of its low engraftment in mice.

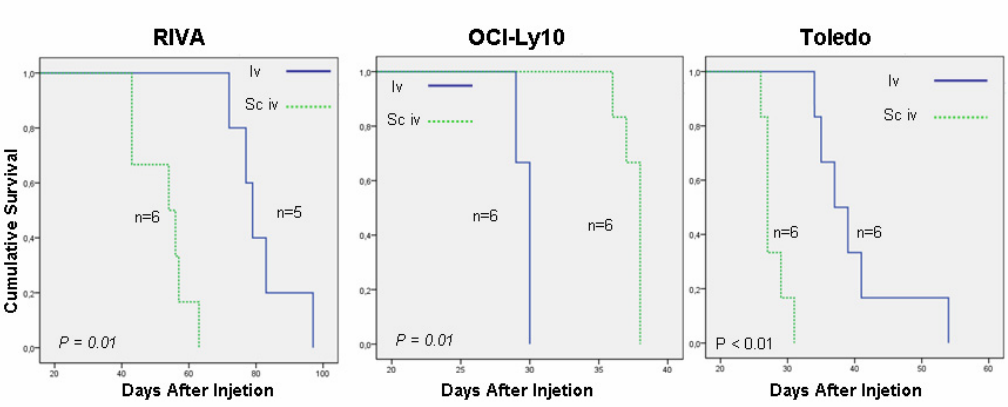

Figure 17. Kaplan-Meier analysis of NOD/SCID mice intravenously injected with subcutaneously conditioned (Sc-iv) or non conditioned cells (iv). The differences between groups were calculated using the Log-rank test.

In summary, the direct intravenous injection of Toledo and OCI-Ly10 cells generates DLBCL models with high engraftment, dissemination and short mouse survival time. Moreover, the subcutaneous conditioning of RIVA and Toledo cells increased the model aggressiveness compared to the direct injection of the cells. The described xenograft models do replicate the clinico-pathological features observed in DLBCL patients.

1.3 ANTITUMOR EFFECT OF CYCLOPHOSPHAMIDE IN A DLBCL XENOGRAFT MOUSE MODEL

As previously mentioned, one of the main objectives of this thesis was to develop bioluminescent mouse models to study DLBCL malignancy and to evaluate novel antitumor drugs. Once the models were developed, we wanted to test the antitumor effect of a drug routinely used for the treatment of DLBCL patients. Cyclophoshamide together with rituximab, doxorubicin, vincristine and prednisone are the drugs used for the standard treatment of DLBCL patients. Cyclophoshamide was selected to be used in the *in vivo* studies due to its stability and non-vesicant properties when intravenously injected in mice.

1.3.1 Antitumor evaluation of cyclophosphamide *in vitro*

We wanted to validate the use of the disseminated DLBCL model derived from Toledo-Sc cells for antitumor drug evaluation by testing its response to cyclophosphamide. To that aim, we first evaluated the *in vitro* antitumor effect of cyclophosphamide in the Toledo cell line in culture. However, as cyclophosphamide has to be activated by hepatic enzymes to be converted into

its active metabolite, we used an active cyclophosphamide analogue known as mafosfamide (Sigma).

The antitumor effect of mafosfamide was evaluated in Toledo cells using different concentrations of the drug (0.5-50 µM). Cell viability was assessed by using the Cell proliferation kit II (XTT, Roche) and following the manufacturer's instructions. As shown in **Figure 18**, mafosfamide induced cell death after 48 hours of exposure. Furthermore, the cytotoxic effect of the drug was dose-dependent.

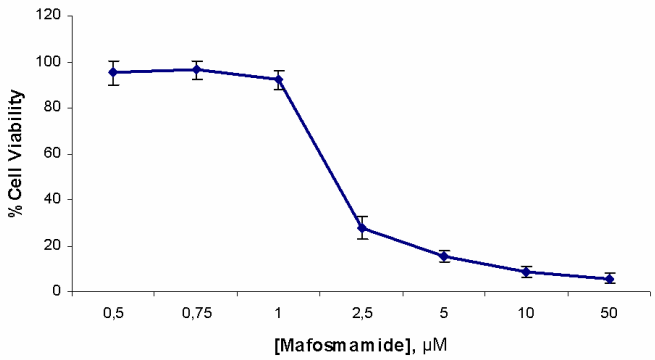

Figure 18. Cell viability in the Toledo cell line exposed to mafosfamide (0.5-50 µM) for 48 hours. IC_{50} value 1.9 ± 0.1 µM.

1.3.2 Maximum Tolerated Dose (MTD) of cyclophosphamide in NOD/SCID mice

To determine the dose of cyclophosphamide that could be administered intravenously into DLBCL mouse models, we had first to evaluate the drug toxicity in healthy mice. Non-tumor bearing mice were used to establish the Maximum Tolerated Dose (MTD) of cyclophosphamide (Genoxal®). As explained in "*Materials and Methods*", 12 mice were randomly divided into four groups and intravenously injected with 60, 75, 100 or 120 mg/kg of

cyclophosphamide 3 days a week, for a total of 7 to 9 doses. As shown in **Table 13 and Figure 19**, the group that showed less drug toxicity was the one administered with 60 mg/kg of cyclophosphamide. Although one mouse was euthanized due to weight loss, 2 mice were alive at the end of the treatment.

Table 13. Evaluation of cyclophosphamide toxicity in healthy NOD/SCID mice and establishment of the Maximum Tolerated Dose (MTD).

	60 mg/kg, x 9	**75 mg/kg, x 9**	**100 mg/kg, x 7**	**120 mg/kg, x 7**
Mice euthanized by toxicity, n(%)	1 (33.3)	3 (100)	2 (66.7)	3 (100)
Survival time, days	90.6 ± 49	39.7 ± 17.6	74.7 ± 28.3	12.0 ± 1.7

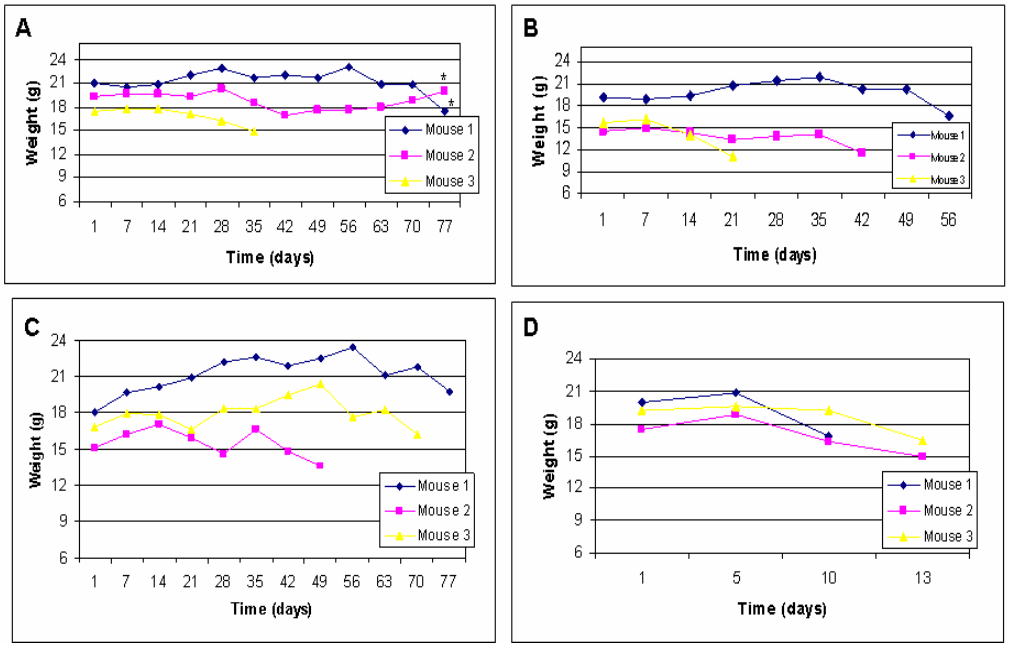

Figure 19. Evaluation of weight loss in healthy NOD/SCID mice administered with cyclophosphamide. Mice were divided in 4 groups of 3 animals and intravenously injected with (A) 60 mg/kg x 9 doses, (B) 75 mg/kg x 9 doses, (C) 100 mg/kg x 7 doses, or (D) 120 mg/kg x 7 doses of cyclophosphamide and the weight was monitored daily. *, mice were euthanized at day 119 without any sign of toxicity.

It is important to mention that the mouse that showed weight loss in the group administered with 60 mg/kg of cyclophosphamide was the one with the

lowest weight at the beginning of the treatment. In contrast, in the group of 75 and 120 mg/kg all mice died before the end of the treatment, and 2 mice in the group of 100 mg/kg had to be also euthanized due to weight loss.

Hence, the group of mice injected with 9 doses of 60 mg/kg of cyclophosphamide showed less signs of drug toxicity than the other groups of mice. In order to assess cyclophosphamide antitumor activity in mice injected with DLBCL cells, we decided to use the same dose (60 mg/Kg) of cyclophosphamide but to administer a total of 7 doses every two days to mice injected with DLBCL cells, instead of 9 doses three days a week.

1.3.3 Antitumor effect of cyclophosphamide in a DLBCL mouse model

Once the MTD for cyclophosphamide was established in the NOD/SCID strain, we evaluated the antitumor effect of the drug in the disseminated DLBCL mouse model derived from Toledo-Sc cells. To that aim, Toledo cells were subcutaneously grown in NOD/SCID mice. Then, the Toledo-Sc cells obtained from tumors were intravenously injected in 20 mice and randomly divided into two groups receiving either vehicle or cyclophosphamide (60 mg/kg) every 2 days for 7 administrations. Mice were treated from day 7 after cell injection, when DLBCL cells had disseminated to LN, BM and CNS. Once a week, mice were non-invasively monitored using the IVIS system to quantify the BLI signal emitted by lymphoma cells. As observed in **Figure 20**, after 1 week of Toledo-Sc cell injection, the cells were fully disseminated in both groups of mice. After 2 weeks of cell injection and following the administration of vehicle or cyclophospamide, the BLI signal decreased in the group of mice treated with the drug (**Figure 20**). This decrease in the BLI signal in the treated group caused by the antitumor effect of cyclophosphamide was maintained during all the

treatment. As shown in the BLI images, at week 3 and 4 after cell injection, there was an important reduction in lymphoma cells dissemination in the drug-treated mice compared with control mice.

As observed in the BLI variation plot, after 10 days of cell injection there is a rapid increase in the BLI signal for the vehicle group. From day 12 after cell injection and until the end of treatment, the BLI signal was significantly higher in the vehicle group compared with the drug-treated group. In the cyclophosphamide-treated mice the BLI increased from approximately day 30, when the treatment was already finished (**Figure 21**).

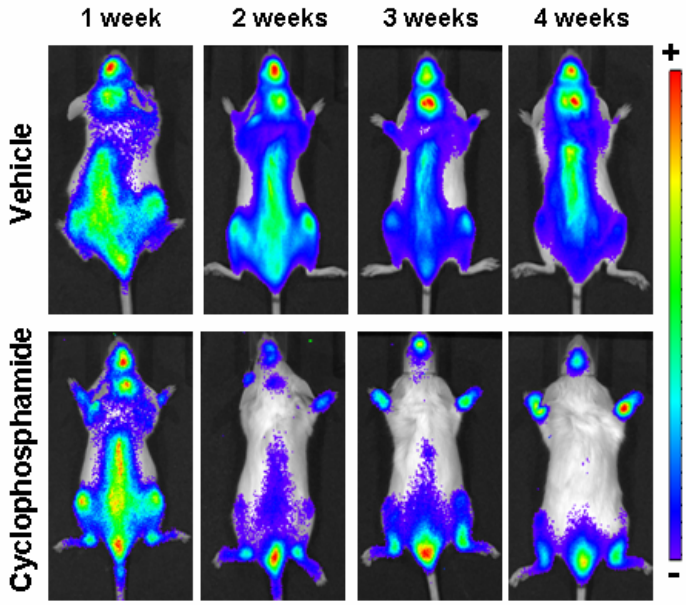

Figure 20. Dissemination of Toledo-Sc cells in NOD/SCID mice treated with vehicle (top panel) or cyclophosphamide (bottom panel). The BLI signal decreased over time in cyclophosphamide-treated mice and increased in the non-treated mice (vehicle). BLI images after 1, 2, 3 and 4 weeks after injection of cells are shown. Arbitrary color bars illustrate relative light intensity levels of firefly luciferase, ranging from low (blue) to high (red).

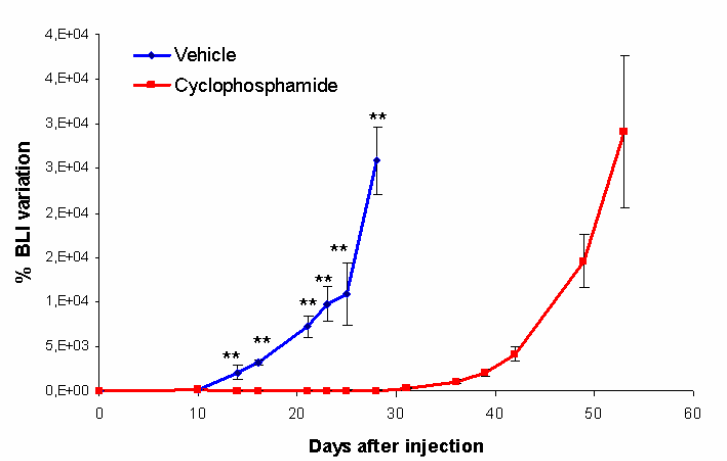

Figure 21. BLI variation curves over time in vehicle and cyclophosphamide-treated groups. Mice from the vehicle group were euthanized earlier than cyclophosphamide-treated mice due to weight loss. **P value < 0.01 (Mann-Whitney test).

Furthermore, Kaplan-Meier survival curves showed a significant increase in mouse survival time in the cyclophosphamide-treated group compared with the vehicle-administered group (**Figure 22**). Mice treated with cyclophosphamide were also euthanized because of the weight loss associated with relapse after drug withdrawal.

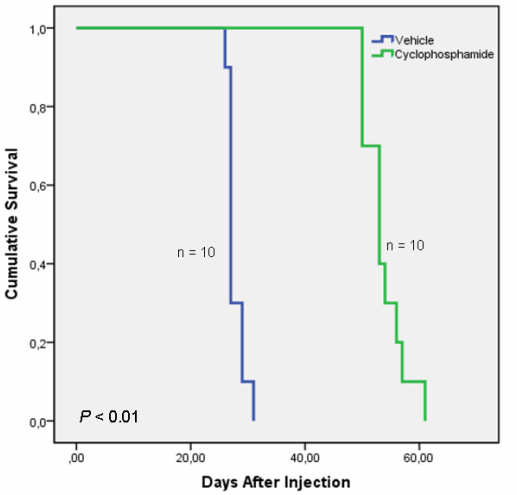

Figure 22. Kaplan-Meier survival curves of vehicle and cyclophosphamide-treated mice. Survival time was longer in the cyclophosphamide-treated mice than in the vehicle-treated mice. *P* value was calculated using the Log-rank test

Taken together, these results indicate that cyclophosphamide showed antitumor effect in our disseminated model of DLBCL, since this treatment induced lymphoma cell death leading to an increase in mouse survival time. Thus, the use of this disseminated DLBCL model for antitumor drug evaluation was successfully validated.

2. A NOVEL INHIBITOR OF FOCAL ADHESION INCREASES SURVIVAL IN A XENOGRAFT MODEL OF DLBCL WITH CENTRAL NERVOUS SYSTEM INVOLVEMENT

Based on the reported lack of benefit from current treatment in relapsed DLBCL patients with CNS affectation, we evaluated the antitumor effect of the focal adhesion inhibitor E7123 in a luminescent DLBCL model with CNS involvement. First, we will briefly introduce previous results obtained in our group and then we will describe the results of the evaluation of E7123 antitumor effect in the bioluminescent mouse model.

2.1 THE INTRAVENOUS INJECTION OF HT-SC CELLS GENERATED A DISSEMINATED DLBCL WITH CNS INFILTRATION

In previous studies of our group, we observed that the subcutaneous passage of the HT cell line significantly enhanced engraftment of the conditioned cells once intravenously injected in a new set of mice. All mice injected with subcutaneously conditioned cells HT-Sc (n=7) developed lymphoma with CNS infiltration and were euthanized between days 40 and 51 post-injection due to weight loss. In contrast, only 2 out of 10 HT intravenously injected mice (control) were euthanized, at days 78 and 89 after injection as a consequence of weight loss. The remaining mice in the HT control group were euthanized at day 100 without any sign of disease, and their histopathological analysis revealed lack of tumor development. The difference in survival times between both groups was statistically significant ($p<0.01$, Log-rank test) as revealed by the Kaplan-Meier survival analysis. In addition, it was also shown

that HT-Sc cells showed higher p130Cas and β1-integrin expression than HT cells, findings that could be associated with the enhanced CNS-tropism.

Most mice injected with HT-Sc cells showed motor difficulties before being euthanized and they showed an evident cranial inflammation. When analyzed microscopically, we observed that 100% of HT-Sc mice showed leptomeningeal brain infiltration (**Figure 23A-C**). Infiltrated brains of the HT-Sc mice were positive for CD10 (germinal center marker) immunostaining (**Figure 23C**), confirming that HT-Sc cells maintained the germinal center DLBCL phenotype found in the original HT cells.

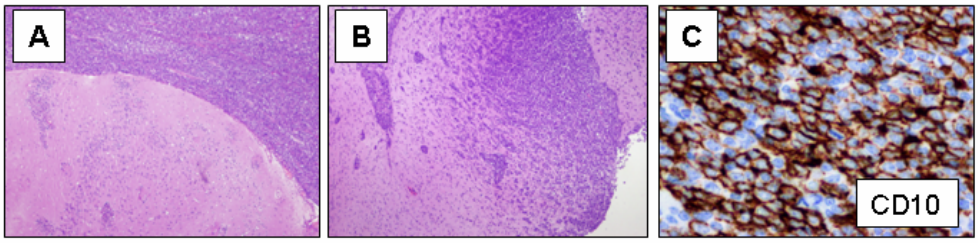

Figure 23. Histological and immunohistochemical phenotype in the brain of the disseminated DLBCL mouse model with CNS involvement. H&E staining of representative brains of mice injected with HT-Sc cells. Lymphoma cells infiltrated the leptomeninges in most mice (A), reaching the parenchyma in isolated cases (B). Original magnification x40. (C) Immunohistochemical analyses of CD10 in representative sections of HT-Sc infiltrated brains. Original magnification x400. CNS, central nervous system; H&E, hematoxylin and eosin.

However, this first DLBCL model with CNS involvement produced in our group was not luminescent so we could not monitor *in vivo* the dissemination of DLBCL cells or the effect of treatment with antitumor drugs. Therefore, HT luminescent cells were produced by lentiviral infection (as previously explained) and injected into NOD/SCID mice after the subcutaneous conditioning of the cells. The luminescent model replicated the clinico-pathological features that have been previously explained. Hence, this new

bioluminesncent model with CNS involvement could be used to evaluate the antitumor effect of the focal adhesion inhibitor E7123.

2.2 E7123 INCREASED SURVIVAL TIME IN THE DLBCL MOUSE MODEL WITH CNS INVOLVEMENT

In previous studies we reported that the focal adhesion inhibtor, E7123, showed antitumor effect in several DLBCL cell lines in culture and that the drug was able to decrease the growth of DLBCL subcutaneous tumors in mice.[173] Here, we use the luminescent model of DLBCL with CNS involvement to evaluate the antitumor effect of E7123 in terms of survival time and inhibition of CNS tumor growth.

To that aim, after the subcutaneous growth of HT tumors, the derived cell suspension was intravenously injected into 20 mice. Ten days after the intravenous injection of HT-Sc cells, mice were randomly allocated into two groups and treated orally with 75 mg/kg E7123 or vehicle (**Figure 24**). Mice were treated every day until they were euthanized for weight loss or signs of sickness. We used PEG-400:FBS 3:1 as a vehicle because it showed no toxicity in healthy mice and permitted the total solubilization of E7123 without changing its antitumor activity *in vitro.*

Once HT-Sc tumor cells were injected into mice, the bioluminescence emitted by the cells in this *in vivo* model was monitored once a week. The first CNS bioluminescent signal was observed in 3 vehicle-treated and 2 E7123-treated mice on day 17 after cell injection. CNS bioluminescence was observed in all mice between days 17 and 57 after cell injection. We observed that BLI signal in the CNS of vehicle-treated mice increased faster than in E7123-treated

mice. Representative BLI images of the CNS from vehicle and E7123-treated mice are shown in **Figure 25**. Vehicle-treated mouse showed a rapid BLI increase from week 6 to week 7 post-injection of cells and was euthanized on week 7. In contrast, the E7123-treated mouse presented a weak BLI signal in the CNS at week 6 post-injection of cells that was slowly increasing until week 13, when the mouse had to be euthanized.

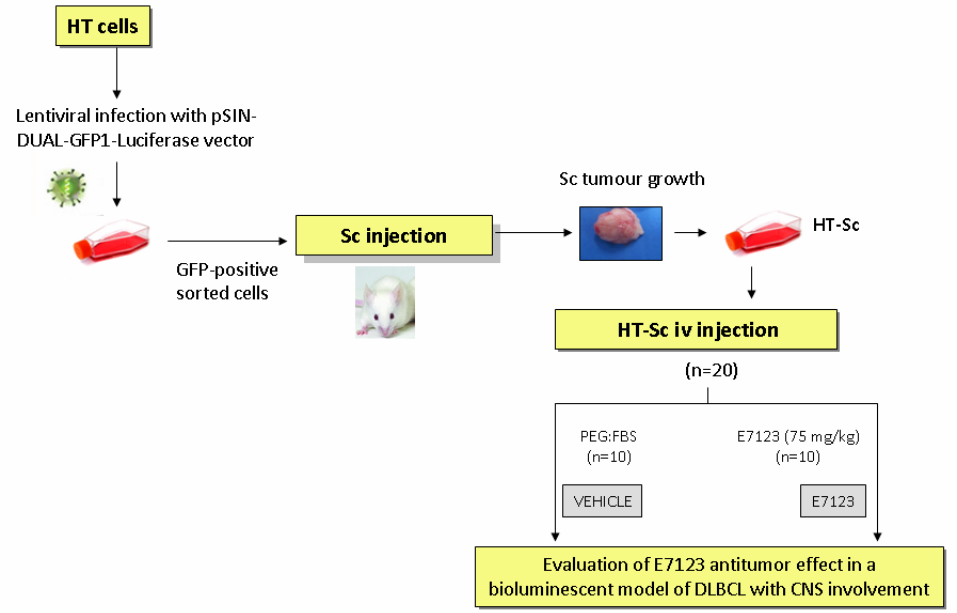

Figure 24. E7123-induced antitumor effect was evaluated in a bioluminescent DLBCL model with CNS involvement. Diagram of the experimental design.

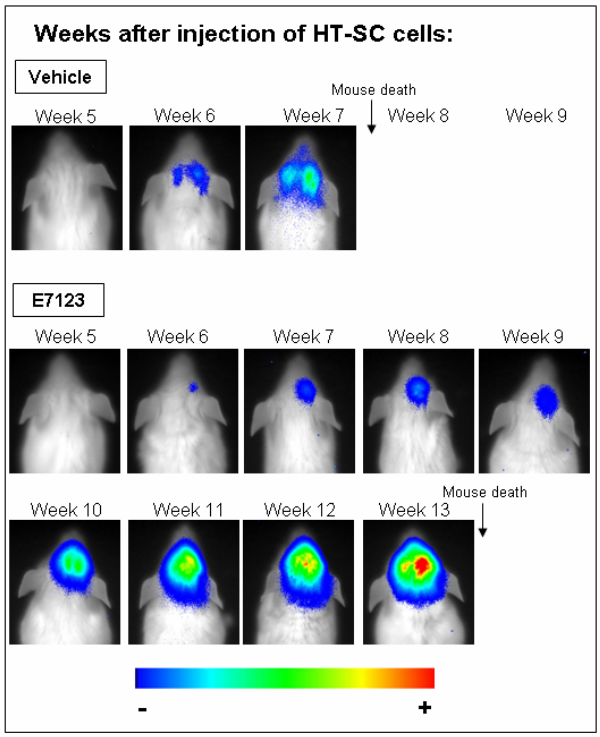

Figure 25. BLI images showing E7123 antitumor effect in a disseminated model of DLBCL with CNS involvement. Representative BLI images showing the kinetics of lymphoma HT-Sc cell growth in the CNS in vehicle (PEG:FBS) or E7123-treated (75 mg/kg) groups. Arbitrary color bars illustrate relative light intensity levels of firefly luciferase, ranging from low (blue) to high (red).

Curves of the mean BLI intensity for both groups are represented in **Figure 26.** At week six after tumor cell injection, one vehicle-treated mouse could not be evaluated for BLI because it showed signs of sickness that precluded the use of anesthesia (a procedure required for BLI quantitation). As observed in the plot, the mean BLI signal was higher in vehicle-treated than in E7123-treated mice at weeks 7 and 8 post-cell injection. At week 8, all mice from the vehicle group were already euthanized due to weight loss. In E7123-treated mice, the mean BLI signal was increasing over time from week 6 to week 12 after cell injection. After week 12, all the remaining mice from this group had to be also euthanized due to weight loss.

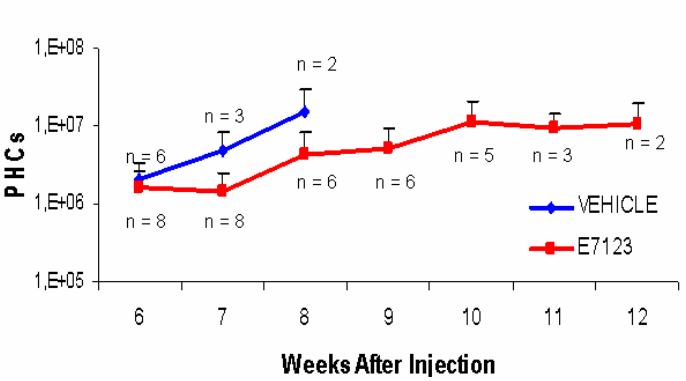

Figure 26. Kinetics of mean BLI intensity for vehicle and E7123-treated mice. BLI signal was followed every week to evaluate E7123 antitumor effect. Error bars represent the standard error.

E7123 treatment increased mice survival time in this model since vehicle-treated mice were euthanized between 36 and 58 days post-injection, whereas E7123-treated mice were euthanized between 48 and 91 days after cell injection (**Figure 27**). Two mice from each group were excluded from the experiment because they did not develop lymphoma. The histopathological features and clinical evolution of HT-Sc injected mice are detailed in **Table 14**. There were no significant differences in the number of mice with tumor cell infiltration in the CNS, LN or BM when comparing vehicle and E7123-treated mice at the end of the experiment.

In summary, we observed that DLBCL cell growth in the CNS was delayed in E7123-treated mice. However, E7123 did not block lymphoma cell invasion of the CNS since there were no significant differences in the time of initial detection of CNS BLI signal between groups. Interestingly, E7123 increased mouse survival time and slowed down the growth of lymphoma cells within the CNS. Hence, E7123 seems to be able to cross the blood brain barrier and reduce the growth of lymphoma cells (once they have colonized the CNS) by inducing their death or inhibiting their proliferation.

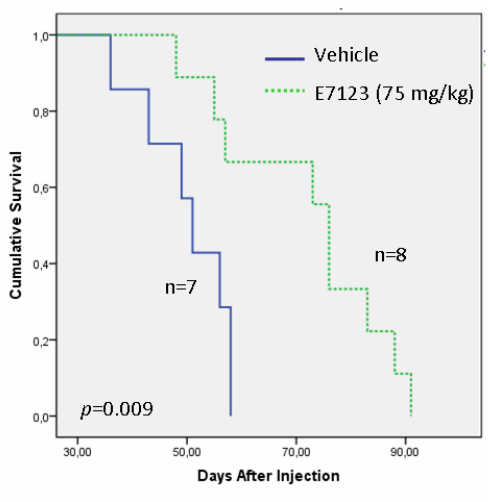

Figure 27. Survival time in E7123-treated HT-Sc mice was significantly higher than in control mice. *P* value was calculated using the Log-rank test. The Kaplan-Meier analysis showed a significant increase in the survival time of E7123-treated mice (*n*=8) compared with control mice (n=7).

Table 14. Histopathological features and clinical evolution of NOD/SCID mice intravenously injected with HT-Sc cells and treated with vehicle or E7123.

Clinical features	Vehicle	E7123	*P*
Survival time (days)[1] of CNS positive mice	50.1 ± 8.3	74 ± 14.8	0.009
Nº of positive mice, n (%)	8/10 (80)	8/10 (80)	-
Nº of positive mice with CNS infiltration, n (%)	7/8 (87.5)	8/8 (100)	1.000
Meningeal infiltration, n (%)	7/7 (100)	8/8 (100)	-
Parenchymal infiltration, n (%)	5/7 (71.4)	7/8 (87.5)	0.596
Nº of positive mice with LN infiltration, n (%)	0/8 (0)	2/8 (25)	0.471
Nº of positive mice with BM infiltration, n (%)	1/8 (12.5)	2/8 (25)	1.000

CNS positive mice were considered those that developed lymphoma in the brain. *P* values were calculated using the Log-rank test for survival time and the Fisher's exact test for categorical variables. CNS, central nervous system; LN, lymph node; BM, bone marrow. [1]Values represent the mean ± standard deviation.

3. ROLE OF CXCR4 EXPRESSION IN DLBCL CELLS

3.1 CXCR4 EXPRESSION AND REGULATION IN DLBCL CELL LINES

The chemokine receptor CXCR4 has been reported to be involved in the migration and trafficking of both normal and malignant B cells. Several studies have described the overexpression of CXCR4 in haematological tumors, but data concerning the role of this receptor in DLBCL are lacking. In the current thesis, we study the expression and regulation of the receptor CXCR4 in DLBCL cell lines and also in the disseminated DLBCL mouse models derived from the injection of these cell lines.

3.1.1 CXCR4 expression in DLBCL cell lines

We evaluated CXCR4 expression in DLBCL cell lines and found that the levels of CXCR4 mRNA (**Figure 28**) were the highest in OCI-Ly10 cells, followed by Toledo and RIVA cells. In contrast, CXCR4 mRNA was undetectable in the SUDHL-2 cell line.

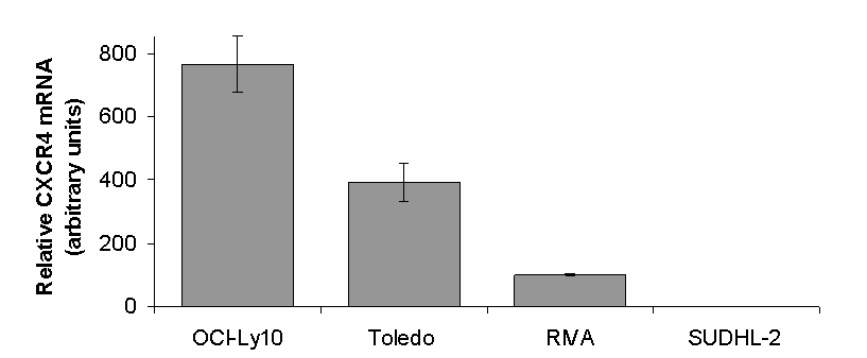

Figure 28. CXCR4 mRNA levels in DLBCL cell lines. Relative levels of CXCR4 mRNA were higher in OCI-Ly10 than in Toledo or RIVA cells. CXCR4 mRNA was undetectable in SUDHL-2 cells. Data are presented as mean ± standard deviation.

Membrane expression of the CXCR4 protein was also evaluated by FACS analysis and immunohistochemistry (**Figure 29**) and correlated with mRNA levels of the receptor obtained by RT-PCR.

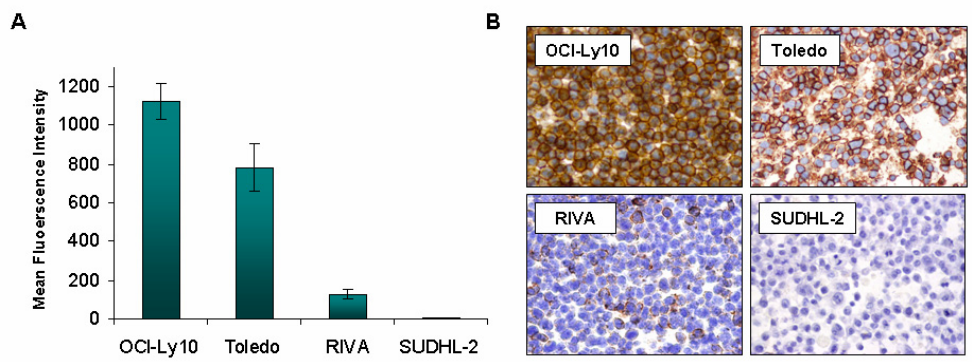

Figure 29. The levels of membrane expression of CXCR4 protein correlated with the levels of CXCR4 mRNA in DLBCL cell lines. (A) Levels of membrane expression of CXCR4 in OCI-Ly10, Toledo, RIVA and SUDHL-2 cell lines detected by flow cytometry. Data are represented as mean fluorescence intensity ± standard deviation. (B) CXCR4 expression in DLBCL cell lines detected by immunohistochemistry also correlated with CXCR4 mRNA levels.

3.1.2 SDF-1α-driven migration in DLBCL cell lines

The stromal cell derived factor (SDF-1α, also known as CXCL12) chemokine is a potent lymphocyte chemoattractant and is also the unique ligand known for CXCR4 receptor. The CXCR4/SDF-1 axis plays a critical role in hematopoiesis, in the homing and retention of B lymphocytes in the bone marrow, and also in the trafficking of these cells to sites of tissue inflammation and damage. A role for both, CXCR4 receptor and its ligand, has been described in the migration and trafficking of malignant B cells in haematological malignancies others than DLBCL.

Here, we evaluated the migration induced by the chemokine SDF-1α in DLBCL cell lines. OCI-Ly10, Toledo and RIVA cells significantly increased their

migration capacity towards a SDF-1α gradient (**Figure 30**), as compared to migration in the absence of the chemokine. In contrast, the SUDHL-2 cell line, which does not express CXCR4, migrated equally in the presence or absence of SDF-1α (data not shown). Hence, the migration towards SDF-1α observed in the different DLBCL cell lines correlated with the levels of CXCR4 expressed in their membrane.

To assess if SDF-1α-driven migration was dependent on the expression of CXCR4, we evaluated whether exposure to the CXCR4 antagonist AMD3100 inhibited this process. We found that AMD3100 significantly inhibited the migration stimulated by SDF-1α in OCI-Ly10, Toledo and RIVA cell lines (**Figure 30**). Hence, the migration of DLBCL cells towards SDF-1α chemotactic gradient was directed by the membrane CXCR4 receptor.

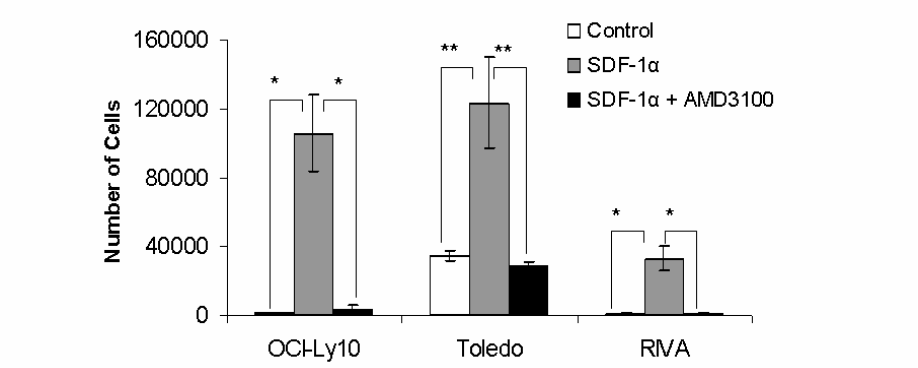

Figure 30. Migration assay in DLBCL cell lines. Cells were incubated in serum-free media in the presence or absence of AMD3100 (10 μg/ml) prior to and during the migration assay. SDF-1α (100 ng/ml) was added to the lower chambers of the transwells to stimulate cell migration. Cells unexposed to SDF-1α were used as control. Incubation of cells with AMD3100 induced a significant decrease in their migration. Data are presented as mean values ± standard deviation; **P* value <0.05, ***P* value <0.01 (Mann-Whitney test).

3.1.3 SDF-1α induces CXCR4 internalization in DLBCL cell lines

As DLBCL cells migrated towards a SDF-1α chemotactic gradient, we investigated the regulation of CXCR4 by this chemokine. To do this, we used the DLBCL cell lines OCI-Ly10, Toledo and RIVA, which expressed CXCR4 receptor in their membrane (**Figure 31A**, Control) and evaluated the effect of SDF-1α exposure on the chemokine receptor by cytometry analysis. When the cells were exposed to SDF-1α (100 ng/ml), there was a significant decrease in the levels of the receptor in membrane (**Figure 31A**, SDF-1α). After cell exposure to SDF-1α for 2 hours, CXCR4 was internalized from the membrane showing a dot-like staining (punctuated) in the cell cytosol, as shown in **Figure 31B** for Toledo, RIVA and OCI-Ly10 cell lines.

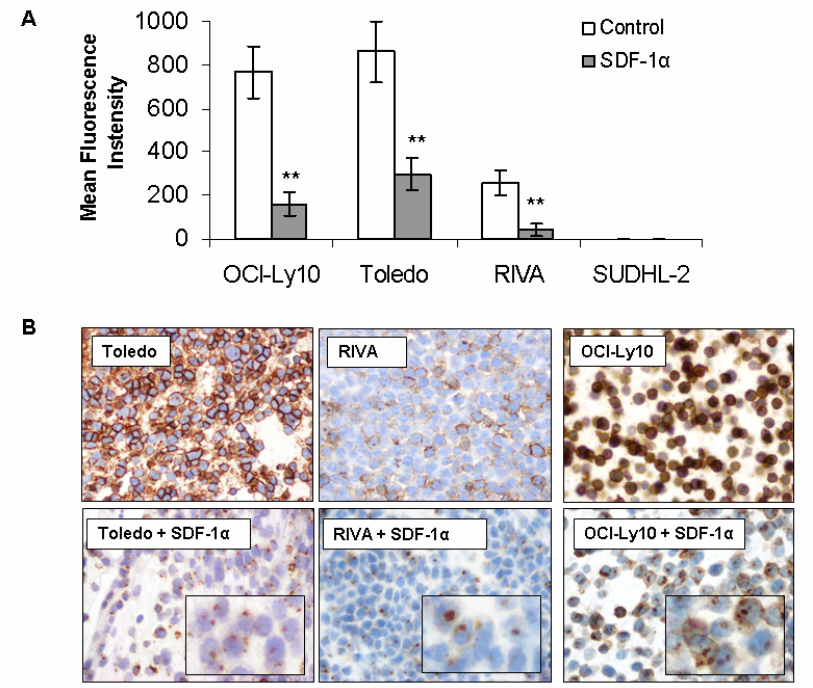

Figure 31. CXCR4 expression in DLBCL cell membrane and internalization induced by SDF-1α. (A) In the absence of SDF-1α, CXCR4 expression was detected by flow cytometry on the cell surface. However, in the presence of the chemokine, CXCR4 membrane expression significantly decreased. (B) Internalization of the receptor was observed by immunohistochemistry; a dot-like cytoplasmic staining of the receptor was observed in cells after 2 hours exposure to SDF-1α as compared to control cells. Original magnification x400. Data are presented as mean values ± standard deviation; **P* value <0.05, ***P* value <0.01 (Mann-Whitney test).

3.2 OVEREXPRESSION OF CXCR4 INCREASED MIGRATION OF DLBCL CELLS

Once we had determined that CXCR4 was expressed in RIVA, Toledo and OCI-Ly10 cells, that the receptor responded to SDF-1α–induced migration and also that its expression in the cell membrane was regulated by this chemokine, we performed a functional evaluation of CXCR4 overexpression in SUDHL-2 cell line.

3.2.1 Nucleofection of SUDHL-2 cells using pCXCR4 plasmid

We first evaluated the effect of CXCR4 overexpression in a DLBCL cell line. To that aim we used SUDHL-2 cells which do not express the receptor. As observed in **Figure 32A**, we transfected SUDHL-2 cells with the pCXCR4 plasmid by nucleofection. Then, CXCR4 expression was detected by cytometry to evaluate the efficacy of the nucleofection process. **Figure 32B** shows that transfected cells SUDHL-2 pCXCR4 successfully expressed this receptor in their membrane. The transfected cells that had incorporated the pCXCR4 plasmid were selected using geneticin to generate a stable cell line overexpressing the receptor. 24 hours after transfection, the cells were diluted with culture media and seeded in a 96-well culture plate to obtain different cell number (ranging from 1 to 2000 cells) in each plate column, and different antibiotic concentrations were added to the cells (from 0 to 1.4 mg/ml) in each row. The selection medium was refreshed every two days and after 30 days of incubation, the cells that remained alive were evaluated for CXCR4 expression by flow cytometry.

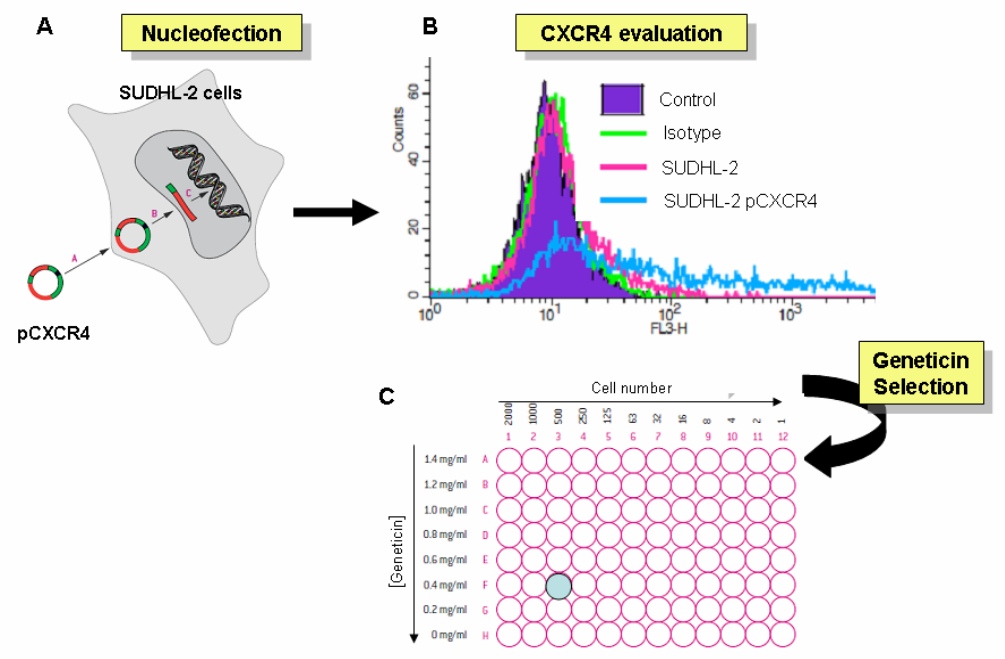

Figure 32. Nucleofection of SUDHL-2 cells with pCXCR4 plasmid and selection with geneticin. (A) SUDHL-2 cells were nucleofected with the pCXCR4 plasmid that contains a geneticin resistance gene. (B) CXCR4 expression was evaluated in SUDHL-2 transfected cells. Cytometry histograms to detect membrane CXCR4 are shown for control (SUDHL-2) and transfected cells (SUDHL-2 pCXCR4). (C) Cells were diluted with culture media in a 96-well plate and different concentrations of geneticin were added (0 – 1.4 mg/ml) to select the cells that had incorporated the plasmid. Cells growing in the F3 well (marked in blue) were the ones with the highest membrane CXCR4 levels.

Cells from different wells selected with different concentrations of geneticin were evaluated for CXCR4 expression. It is important to mention that the SUDHL-2 cell line was not able to grow when it was seeded at low densities, for that reason it was not possible to select CXCR4 positive cells growing from one single clone. The 500 cells growing in the F3 well and selected with 400 µg/ml of geneticin showed the highest levels of CXCR4 expression. These cells were further selected by cell sorting to obtain an enriched and homogeneous population expressing CXCR4. The levels of CXCR4 expression were evaluated in the transfected SUDHL-2 pCXCR4 cells and also in the CXCR4-sorted cells

(SUDHL-2 pCXCR4 F3 Sort). As observed in **Figure 33**, the sorted cells expressed higher levels of CXCR4 in their membrane than the non-sorted or than the parental cells. These cells were used for migration studies to assess the role of CXCR4 in this process.

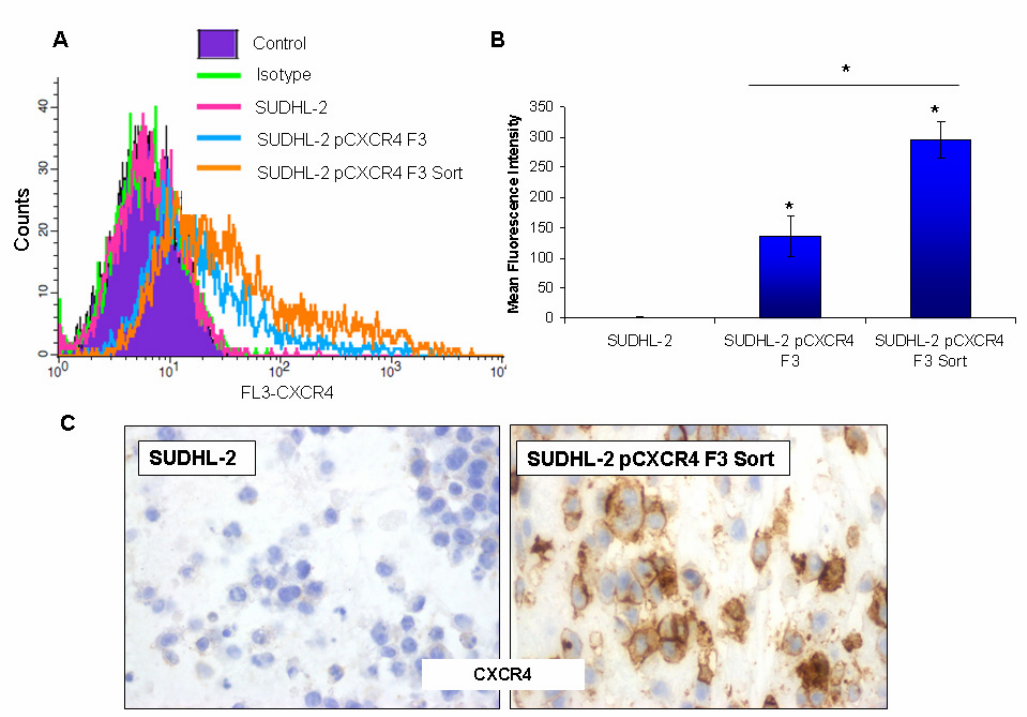

Figure 33. CXCR4 membrane expression in transfected SUDHL-2 pCXCR4 F3 cells. (A) Histogram and (B) bar-graph showing membrane CXCR4 detected by cytometry in transfected SUDHL-2 pCXCR4 F3 and in sorted cells. Data are presented as mean values ± standard deviation. *P value < 0.05 (Mann-Whitney test) (C) CXCR4 expression was also evaluated by IHC in control and transfected SUDHL-2 pCXCR4 F3 Sort cells. IHC, immunohistochemistry.

3.2.2 SUDHL-2 pCXCR4 cells migrated towards SDF-1α gradient

To evaluate the function of the CXCR4 receptor in the transfected cells, we assessed the migration towards an SDF-1α gradient of SUDHL-2 pCXCR4 F3 and sorted cells, and compare it with the migration of the non-transfected

counterparts. The transfected cells SUDHL-2 pCXCR4 F3 increased their migration in the presence of SDF-1α chemokine. In contrast, the parental cells SUDHL-2, which do not express CXCR4, did not present any difference in migration in the presence or absence of the chemokine. Furthermore, the transfected and sorted cells, SUDHL-2 pCXCR4 F3 Sort, significantly increased their migration capacity induced by the SDF-1α chemokine compared with the non-sorted SUDHL-2 pCXCR4 F3 cells or with the parental SUDHL-2 cell line (**Figure 34**). Hence, SDF-1α-driven migration in this cell line was dependent on the levels of CXCR4 expression in cell membrane.

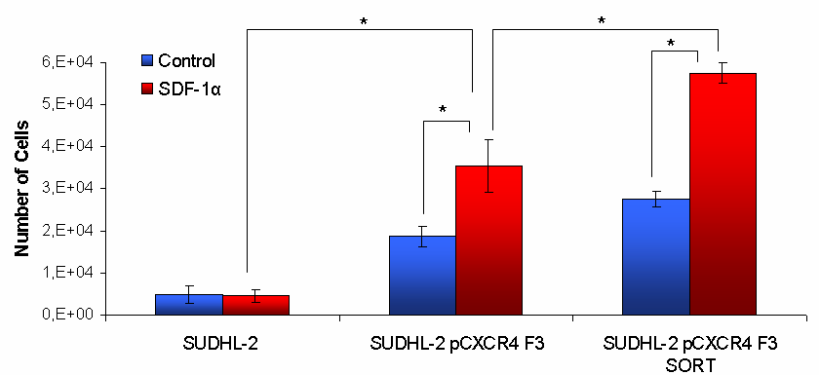

Figure 34. CXCR4 expression in SUDHL-2 cells correlated with SDF-1α driven migration. SUDHL-2 pCXCR4 F3 pre-sorter and post-sorter were used to perform the migration assay using the SUDHL-2 parental cells as control. Cells were incubated in serum-free media prior to and during the transwell migration assay. SDF-1α (100 ng/ml) was added to the lower chambers to stimulate cell migration. Cells unexposed to SDF-1α were also used as control. Data are presented as mean values ± standard deviation *P value < 0.05 (Mann-Whitney test).

Then, we evaluated whether exposure to the CXCR4 antagonist AMD3100 inhibited this process. As observed in **Figure 35**, AMD3100 significantly inhibited the migration stimulated by SDF-1α in SUDHL-2 pCXCR4 F3 Sort cells.

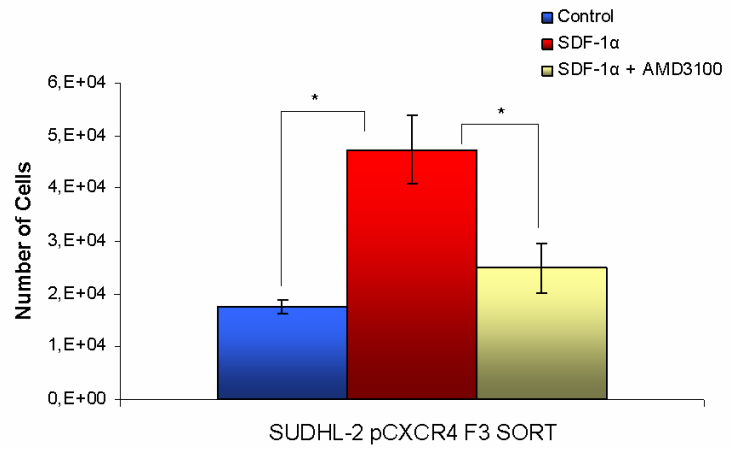

Figure 35. SDF-1α driven migration of SUDHL-2 pCXCR4 F3 Sort cells was inhibited by the CXCR4 antagonist AMD3100. Cells were incubated in serum-free media in the presence or absence of AMD3100 (10 μg/ml) prior to and during the transwell migration assay. SDF-1α (100 ng/ml) was added to the lower chambers to stimulate cell migration. Cells unexposed to SDF-1α were used as control. The incubation of cells with AMD3100 induced a significant decrease in their migration. Data are presented as mean values ± standard deviation. *P value < 0.05 (Mann-Whitney test).

Finally, we evaluated if membrane CXCR4 in SUDHL-2 pCXCR4 F3 Sort cells was regulated in the presence of SDF-1α. As observed in **Figure 36**, membrane CXCR4 was detected in control cells, whereas in the presence of the chemokine, the receptor was internalized from the membrane, as previously described for the rest of studied DLBCL cell lines.

Hence, we concluded that CXCR4 overexpression induced the migration of transfected SUDHL-2 pCXCR4 F3 Sort cells towards SDF-1α chemokine gradient. In addition, this CXCR4-directed migration was inhibited by exposure of the cells to the CXCR4 antagonist AMD3100.

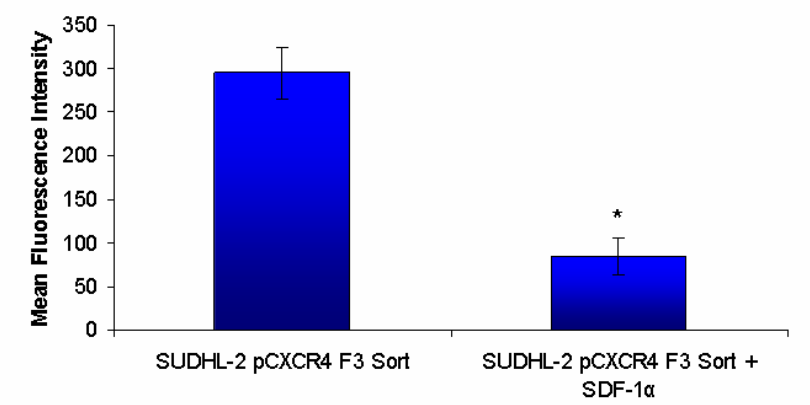

Figure 36. Membrane CXCR4 expression in SUDHL-2 pCXCR4 F3 Sort cells and internalization induced by SDF-1α. CXCR4 expression was detected by flow cytometry on the cell surface. However, in the presence of the chemokine, CXCR4 membrane expression significantly decreased**.** Data are presented as mean values ± standard deviation; **P* value <0.05 (Mann-Whitney test).

3.2.3 SUDHL-2 pCXCR4 cells increased their dissemination to lymph nodes

Finally, we wanted to evaluate if SUDHL-2 pCXCR4 F3 Sort cells increased their dissemination when intravenously injected in mice compared with SUDHL-2 cells. To that aim, a preliminary experiment was conducted by intravenously injecting SUDHL-2 and SUDHL-2 pCXCR4 F3 Sort cells in 6 and 2 mice, respectively. As observed in **Figure 37**, infiltration of LN was detected in one mouse (50% engraftment) injected with SUDHL-2 pCXCR4 F3 Sort cells, whereas no infiltration was detected in mice injected with SUDHL-2 cells. The engrafted mouse injected with SUDHL-2 pCXCR4 F3 Sort cells was euthanized 64 days after cell injection, whereas the rest of the mice were euthanized 120 days after cell injection without showing any signs of disease.

Hence, cells overexpressing CXCR4 receptor showed dissemination to maxilar lymph nodes in one mouse, whereas the parental SUDHL-2 cells, lacking

CXCR4 expression, did not infiltrate any organ. Althought this was just a preliminary study, the results are encouraging and a new experiment will be conducted again with a larger number of mice to verify the results. Nevertheless, the obtained results are in concordance with the previously described *in vitro* results.

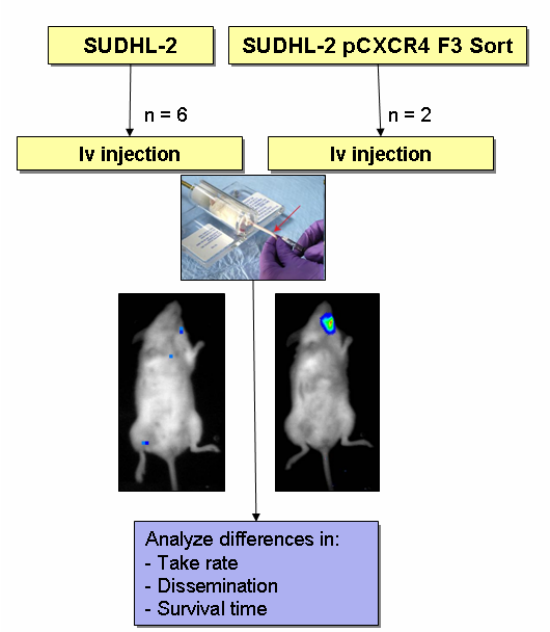

Figure 37. Analysis of dissemination in NOD/SCID mice injected with SUDHL-2 pCXCR4 F3 Sort or SUDHL-2 cells. One mouse injected with cells overexpressing CXCR4 showed dissemination to LN, whereas mice from the control group SUDHL-2 did not show any dissemination. LN, lymph nodes.

3.3 EVALUATION OF CXCR4 EXPRESSION IN DLBCL MOUSE MODELS

We have previously explained the development of disseminated DLBCL mouse models by intravenously injecting non-conditioned and subcutaneously preconditioned cells. Here, we evaluate membrane CXCR4 expression in the DLBCL mouse models and its role in cell dissemination and aggressiveness. We also evaluated the CXCR4 expression changes induced by the subcutaneous conditioning and its correlation with the aggressiveness of the models.

3.3.1 CXCR4 expression in DLBCL cell lines correlates with engraftment, dissemination and mouse survival time in xenograft models

As CXCR4 receptor is expressed in normal and malignant B cells and plays a pivotal role in cell migration and traficking, here, we compared the aggressiveness of DLBCL cell lines displaying different levels of CXCR4 expression in xenograft mouse models. We compared the OCI-Ly10 cell line, with high levels of membrane CXCR4 expression, with the SUDHL-2 cell line, which does not express de receptor. The intravenously injected OCI-Ly10 cell line, with a high expression of CXCR4, showed 100% of engraftment, rapid dissemination to lymph nodes (LN), bone marrow (BM) and central nervous system (CNS) in all mice, and mouse survival time of less than 30 days (**Table 12**). In contrast, SUDHL-2 injected cells, which do not express CXCR4 receptor, showed 50% of engraftment, and longer mouse survival time (67.3 ± 21.5 days). No infiltration of LN was detected in SUDHL-2 intravenously injected mice and only 33% of the animals presented BM infiltration. Bioluminescent images (BLI) of OCI-Ly10 and SUDHL-2 injected mice were acquired starting at the first week after cell injection (**Figure 38**).

In OCI-Ly10 injected mice, BLI was first observed 2 weeks after cell injection. As observed in the representative images, these lymphoma cells presented a rapid dissemination towards LN, BM and CNS. At week 4 after injection, the lymphoma was fully disseminated and mice had to be euthanized. In one of the engrafted SUDHL-2 mice, however, the BLI signal was not detected until week 6 after cell injection. The cells just disseminated towards the femur of the mouse and the BLI signal was localized in the femur until week 11, when the mouse was euthanized.

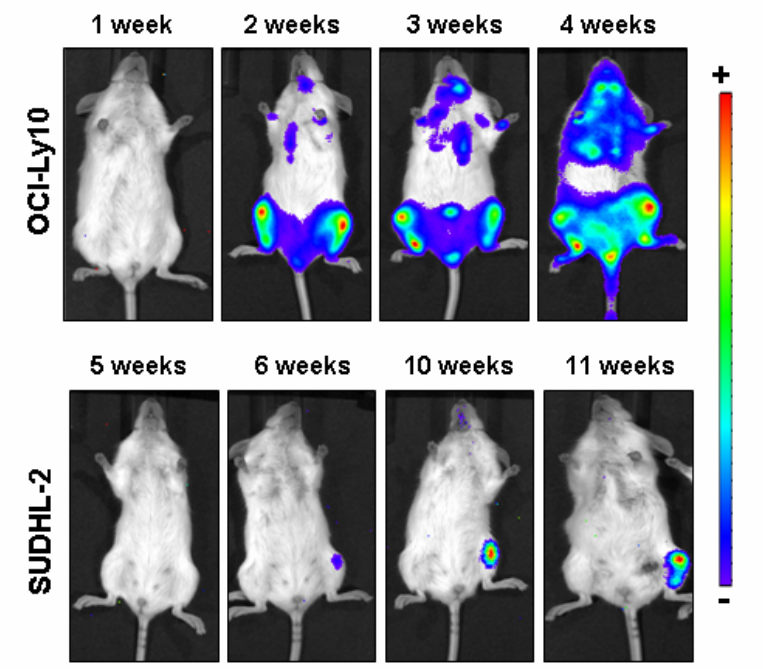

Figure 38. Representative bioluminescent images showing lymphoma dissemination in mice injected with OCI-Ly10 or SUDHL-2 cells. OCI-Ly10 cells (with high levels of CXCR4 expression) disseminated at a shorter time and infiltrated more organs (CNS, LN and BM) than SUDHL-2 cells (no CXCR4 expression). Arbitrary color bars illustrate relative light intensity levels of firefly luciferase, ranging from low (blue) to high (red).

The infiltration of LN, BM and CNS by lymphoma cells observed in BLI images was confirmed by histological analysis of the organs for both cell lines

(**Figure 39A-B**, H&E). Immunohistochemical analysis showed that membrane CXCR4 expression of OCI-Ly10 cells was maintained in cells surrounding the bone, infiltrating the CNS and in the external part of the LN (**Figure 39A**, CXCR4). Moreover, in the BM and in the center of the LN, CXCR4 expression showed a dot-like or punctuated cytoplasmic immunostaining indicating that the receptor was internalized from the cell membrane.

In agreement with the lack of CXCR4 expression in SUDHL-2 cells, the receptor was almost undetectable in infiltrated BM in this model. However, a minor infiltration detected in the BM is shown (**Figure 39B,** CXCR4).

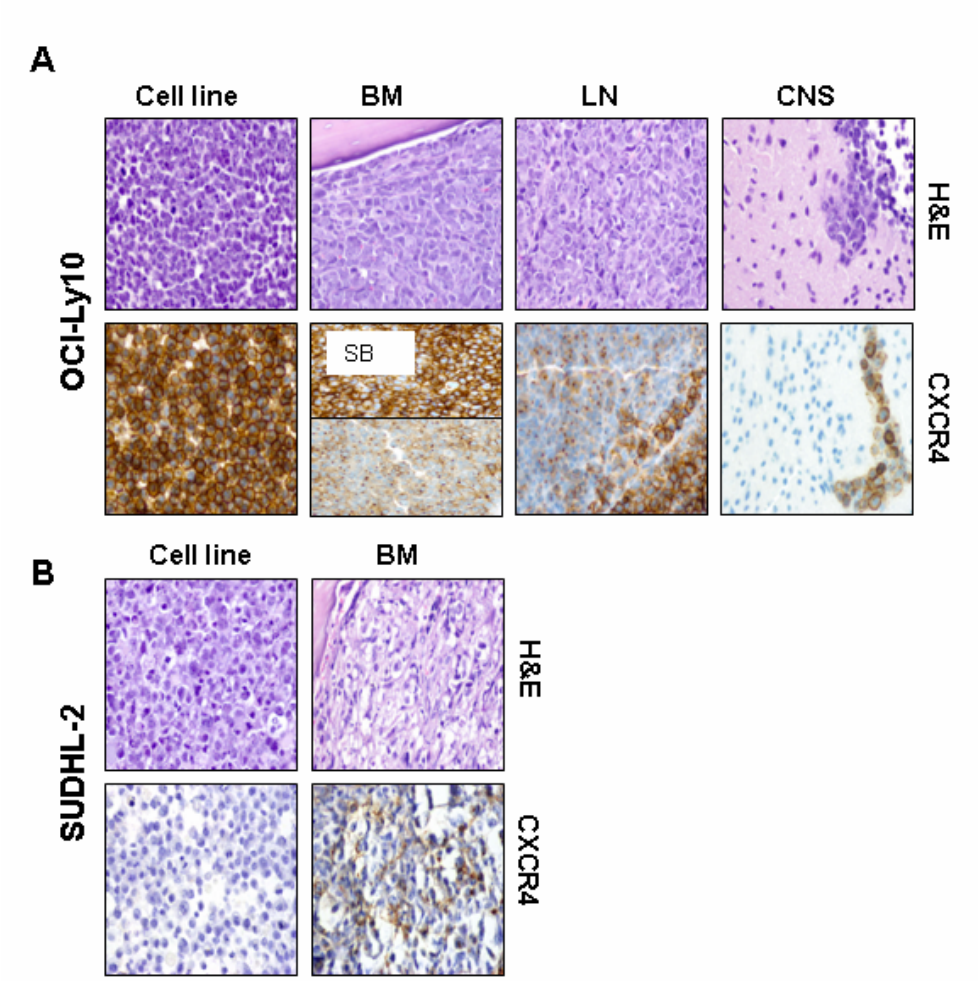

Figure 39. H&E staining and CXCR4 expression in cell lines and in infiltrated tissues of NOD/SCID mice intravenously injected with OCI-Ly10 or SUDHL-2 cells. (A) CXCR4 expression was detected by IHC in the membrane of OCI-Ly10 cell line and in cells surrounding the bone, infiltrating the CNS and in the external part of the LN. Dot-like staining of the receptor was detected in the center of the LN and inside the BM. (B) Expression of CXCR4 was almost undetectable by IHC in the infiltrated BM of SUDHL-2 injected mice and was undetetable in the cell line in culture. Original magnification x400. CNS, central nervous system; LN, lymph nodes; BM, bone marrow; SB, surrounding bone; H&E, hematoxylin and eosin; IHC, immunohistochemistry.

3.3.2 Subcutaneous preconditioning of DLBCL cells induced changes in CXCR4 expression that correlated with their aggressiveness

As previously explained, we developed disseminated lymphoma mouse models by performing subcutaneous preconditioning of the cells to increase their aggressiveness prior to their intravenous injection in mice. Here, we evaluated the effect of subcutaneous preconditioning of DLBCL cells on CXCR4 expression and its impact on engraftment, dissemination and survival time *in vivo*. CXCR4 expression in cell lines and infiltrated tissues was quantified by assigning an H-score (0-300), which is the result from the product of expression intensity (0-3) and the percentage of stained cells (0-100). We observed that CXCR4 expression was increased in subcutaneously conditioned RIVA and Toledo cells (Sc cells; **Table 15**). For both preconditioned cell lines, CXCR4 expression further increased in cells surrounding the BM. Moreover, mice injected with conditioned cells, RIVA-Sc and Toledo-Sc, showed a shorter survival time than mice injected with non-conditioned cells (**Table 12** and **Figure 17,** see "DLBCL MOUSE MODELS DEVELOPMENT AND VALIDATION"). This enhanced cell aggressiveness positively correlated with increased CXCR4 expression in their membrane.

In agreement with the higher aggressiveness of RIVA-Sc cells, CXCR4 expression was increased compared to the non-conditioned counterpart as shown by immunohistochemical analysis (**Figure 40**). Membrane expression of the receptor increased in infiltrated LN. Interestingly, the membrane expression of CXCR4 was highly increased in lymphoma cells surrounding the bone (SB) whereas CXCR4 expression was decreased in cells within the BM, in which a dot-like staining was observed. CXCR4 expression was also detected in cells

infiltrating the CNS although the expression was decreased compared with the subcutaneous preconditioned cells.

Table 15. CXCR4 expression (H Score) in lymphoma cells and in infiltrated tissues of NOD/SCID mice intravenously injected with DLBCL cell lines (iv) or with subcutaneously-conditioned cells (Sc-iv).

	H Score CXCR4 (intensity x %staining)							
	OCI-Ly10		**RIVA**		**SUDHL-2**		**Toledo**	
	iv	**Sc-iv**	**iv**	**Sc-iv**	**iv**	**Sc-iv**	**iv**	**Sc-iv**
Cell line	285		40		0		160	
Sc tumor	175		80		60		240	
Sc cells	160		100		20		210	
LN	187 + DL	60 + DL	255 + DL	167 + DL	*NA*	*NA*	20 + DL	30 + DL
BM	30 + DL	120 + DL	*NA*	20 + DL	5	*NA*	60 + DL	25 + DL
BM, SB	300	300	*NA*	300	*NA*	*NA*	300	270
CNS	200 + DL	270 + DL	240 + DL	20 + DL	*NA*	*NA*	210 + DL	150 + DL

Sc Tumor, subcutaneous tumor; Sc cells, cells disaggregated from subcutaneous tumors; CNS, central nervous system; LN, lymph nodes; BM, bone marrow; SB, surrounding bone; DL, presence of CXCR4 cytoplasmic Dot-Like staining; NA, not applicable, no infiltration of cells.

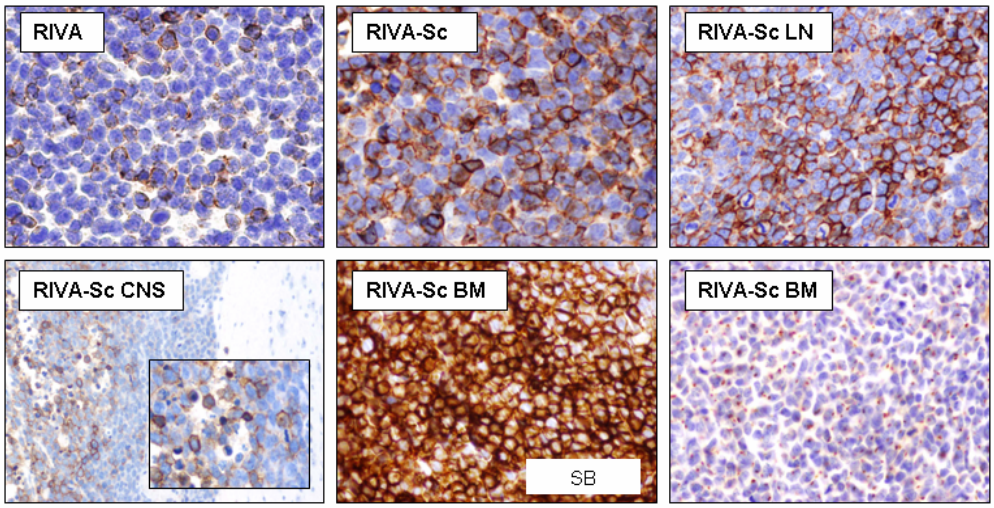

Figure 40. Immunohistochemical analysis of CXCR4 expression in RIVA, RIVA-Sc, and in representative LN, CNS and BM tissues infiltrated with RIVA-Sc cells. Original magnification x400. CNS, central nervous system; LN, lymph nodes; BM, bone marrow; SB, surrounding bone; H&E, hematoxylin and eosin.

Representative images of a RIVA-Sc injected mouse with macroscopic and microscopic infiltrations of LN are shown in **Figure 41**. BM and CNS were also infiltrated in some mice. In contrast, in the group of mice injected with RIVA cells, we observed infiltration of CNS and LN, but the BM of the vertebral column or femur was not infiltrated (**Table 12**).

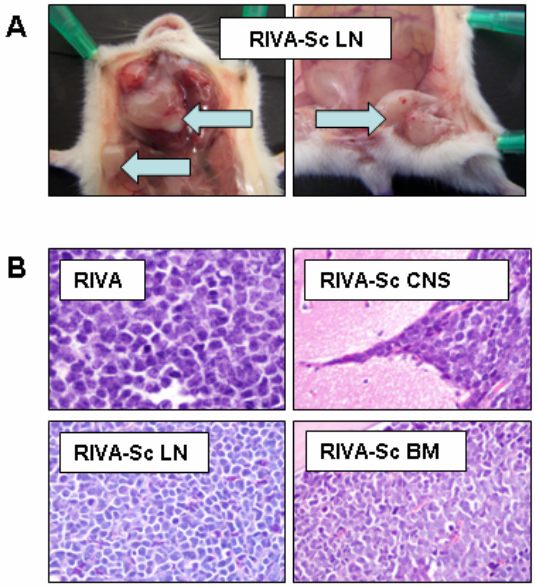

Figure 41. Macroscopic and microscopic infiltration of NOD/SCID mice injected with RIVA-Sc cells. (A) Macroscopic infiltration of cervical, axillar (left image) and caudal LN (right image) in RIVA-Sc NOD/SCID mice. (B) H&E staining of RIVA cells, representative CNS, LN and BM tissue infiltrated with RIVA-Sc cells. Original magnification x400. CNS, central nervous system; LN, lymph nodes; BM, bone marrow; H&E, hematoxylin and eosin.

BLI images were taken weekly to evaluate RIVA and RIVA-Sc cell dissemination in mice (**Figure 42**). In the top images, the BLI variation over the time is shown for a representative engrafted mouse injected with RIVA cells; the BLI signal was first detected 8 weeks after cell injection and the cells infiltrated only a maxilar lymph node in this mouse. The BLI signal increased over the time and after week 12 post-injection of cells, the mouse was euthanized due to weight loss. In contrast, in the representative mouse injected with RIVA-Sc cells (bottom images), the BLI signal appeared at week 5 and was located in the caudal lymph nodes. Over the time, the RIVA-Sc cells disseminated and reached the axilary and maxilar lymph nodes. Mice from this group were euthanized at week 7 post-injection of cells. Thus, RIVA-Sc cells,

which express higher levels of membrane CXCR4, presented higher and more rapid dissemination to LN than RIVA cells when injected into mice. Also they showed higher engraftment in the injected mice compare with the non-condicioned cells.

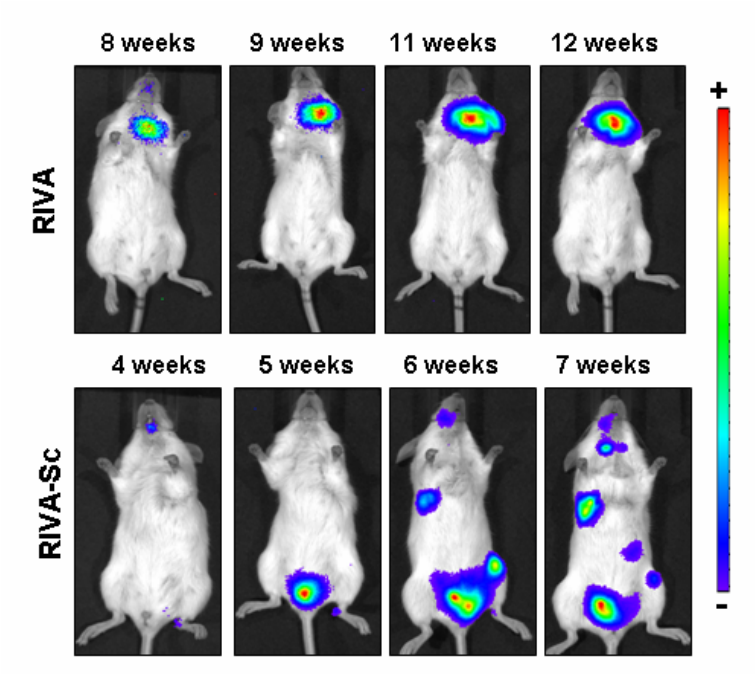

Figure 42. Bioluminescent images showing that subcutaneous preconditioning of RIVA cells increased their aggressiveness after their injection into mice. Mice injected with RIVA cells (top images) showed reduced dissemination and less organ infiltration than mice injected with cells obtained from the subcutaneous tumors, RIVA-Sc (bottom images). Arbitrary color bars illustrate relative light intensity levels of firefly luciferase, ranging from low (blue) to high (red).

The results of subcutaneous conditioning of Toledo cells were similar to those obtained for RIVA cells. As previously explained, when Toledo cells were intravenously injected, 100% of mice presented BM and CNS infiltration, whereas 88.8% of the animals presented LN infiltration (**Table 12**). Although the infiltration pattern of Toledo-Sc cells was similar to that in Toledo cells, survival time in mice injected with Toledo-Sc cells was shorter and correlated

with enhanced CXCR4 expression and cell aggressiveness (**Table 15 and Figure 43**). Toledo-Sc cells increased CXCR4 expression in the membrane, which was mantained in lymphoma cells of infiltrated tissues surrounding the bone. As observed in the images, we detected a CXCR4 dot-like staining in the infiltrated LN, within the BM and also in the CNS. Microscopic infiltration of LN, CNS and BM are shown in **Figure 44**.

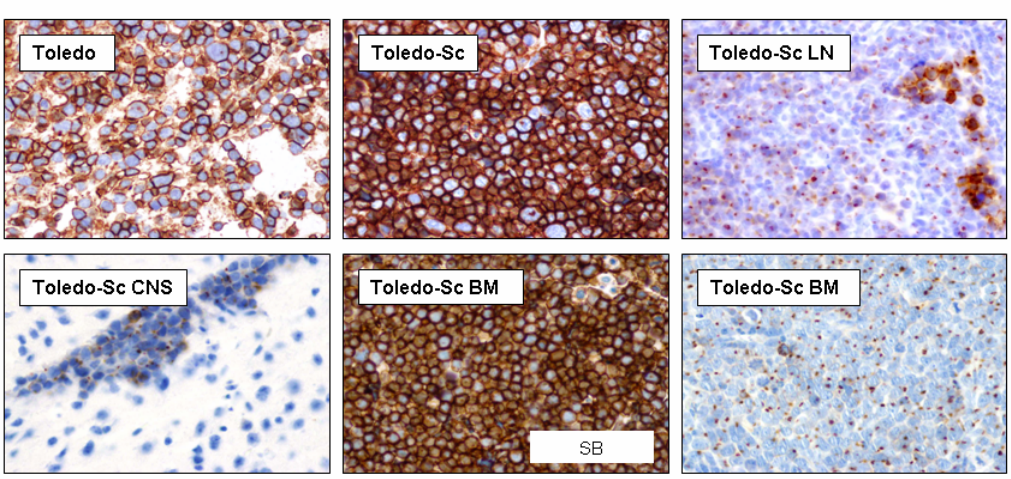

Figure 43. Immunohistochemical analysis of CXCR4 in Toledo, Toledo-Sc, and in infiltrated LN, BM and CNS. Original magnification x400. CNS, central nervous system; LN, lymph nodes; BM, bone marrow; SB, surrounding bone.

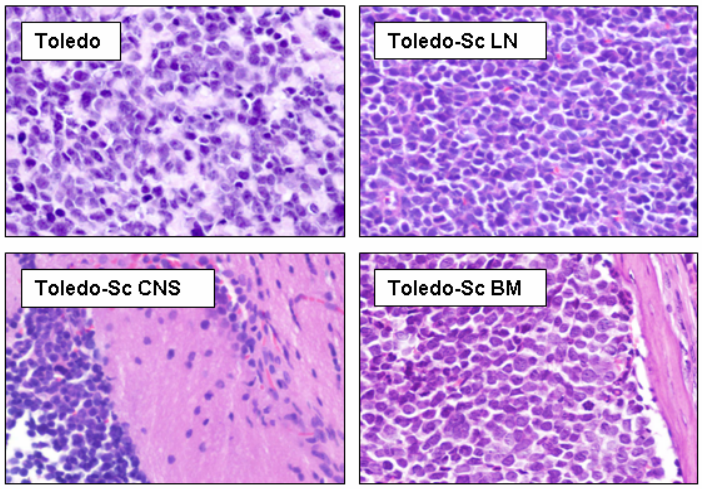

Figure 44. H&E staining of Toledo cell line and representative LN, BM and CNS infiltrated with Toledo-Sc cells. Original magnification x400. CNS, central nervous system; LN, lymph nodes; BM, bone marrow; H&E, hematoxylin and eosin.

As observed in the BLI images, mice injected with Toledo-Sc cells showed a more rapid dissemination compared with the mice injected with Toledo cells (**Figure 45**). At week 1 after cell injection, mice injected with Toledo cells presented a weak BLI signal, whereas mice injected with Toledo-Sc cells showed a higher BLI signal and cells were fully disseminated to LN, BM and CNS. However, mice injected with Toledo cells showed a slight BLI signal near the tail and in the CNS. Mice injected with Toledo-Sc cells were euthanized aproximately one week earlier than mice injected with Toledo cells. Hence, the subcutaneous conditioning of Toledo cells also increased the aggressiveness of this cell line.

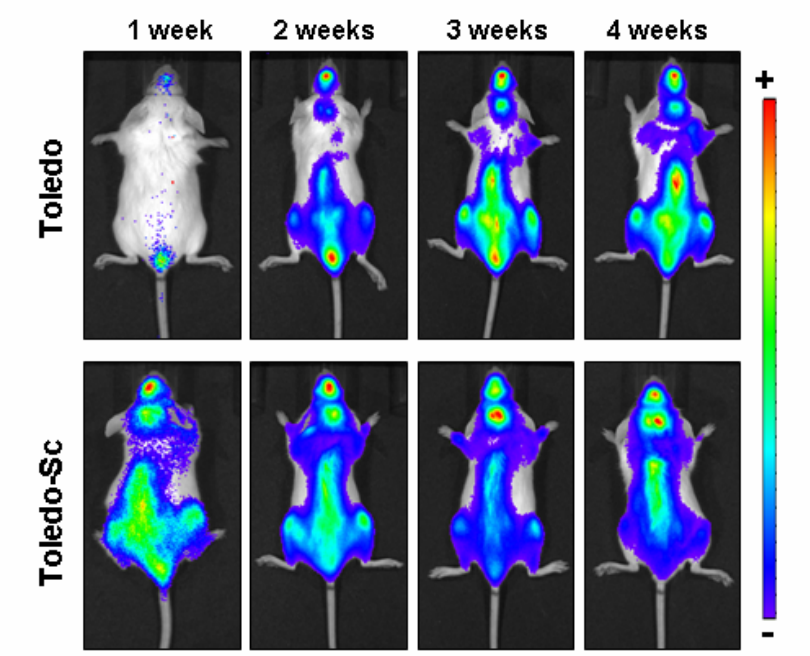

Figure 45. Bioluminescence images showing that subcutaneous preconditioning of Toledo cells increased their aggressiveness when injected in mice. Mice injected with Toledo cells (top images) took longer time to disseminate than mice injected with the subcutaneous conditioned Toledo-Sc cells (bottom images). Arbitrary color bars

illustrate relative light intensity levels of firefly luciferase, ranging from low (blue) to high (red).

In contrast to the results obtained with RIVA and Toledo cells, subcutaneous conditioning of OCI-Ly10 cells decreased CXCR4 expression in the membrane (**Table 14** and **Figure 46**) and was associated with a decreased dissemination of cells to LN and longer survival time of mice (**Table 12**). The immunohistochemical analysis showed that CXCR4 expression decreased in subcutaneously conditioned cells and this lower expression was mantained in cells infiltrating the LN. However, CXCR4 expression in the CNS and in cells that disseminated from the bone marrow to the surrounding tissues was similar to that observed in mice injected with the parental OCI-Ly10 cell line. As observed in other cell lines, there was a CXCR4 dot-like staining inside the BM and also in the infiltrated LN. In summary, the expression levels of CXCR4 also maintained a positive correlation with dissemination in this model, lower levels of expression of the receptor were associated with lower cell dissemination and increased mouse survival time.

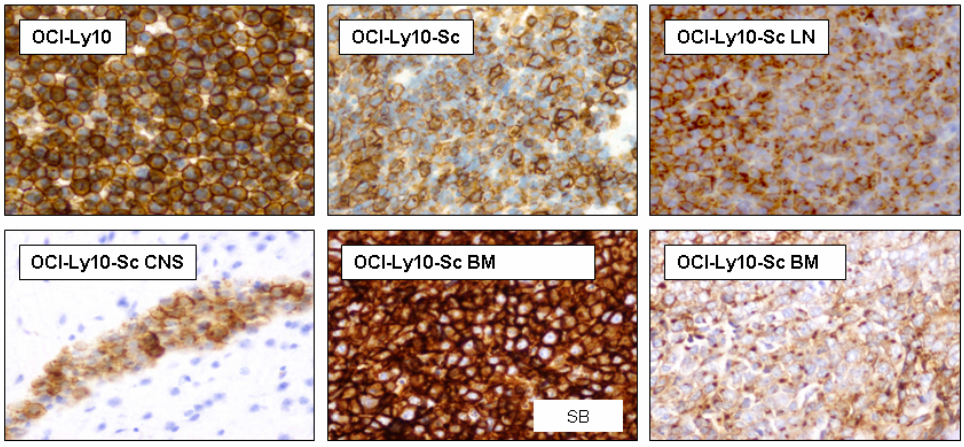

Figure 46. CXCR4 expression in OCI-Ly10, OCI-Ly10-Sc cells and in infiltrated organs. CXCR4 was highly expressed in OCI-Ly10 cell line and the expression was decreased when cells were subcutaneously injected in mice (OCI-Ly10-Sc). CXCR4 expression in the membrane was detected in infiltrated LN, CNS and BM of mice injected with OCI-Ly10-Sc cells. Dot-like staining of the receptor was detected in the center of the LN and

within the BM of the vertebral column. Original magnification x400. CNS, central nervous system; LN, lymph nodes; BM, bone marrow; SB, surrounding bone.

SUDHL-2 cells, which do not express CXCR4, showed low engraftment and dissemination when they were injected in mice (**Table 12**) and no statistical differences were observed when compared to SUDHL-2-Sc injected mice. CXCR4 expression was almost undetectable in SUDHL-2 and SUDHL-2-Sc cells, and in the infiltrated tissues (**Figure 47** and **Table 15**).

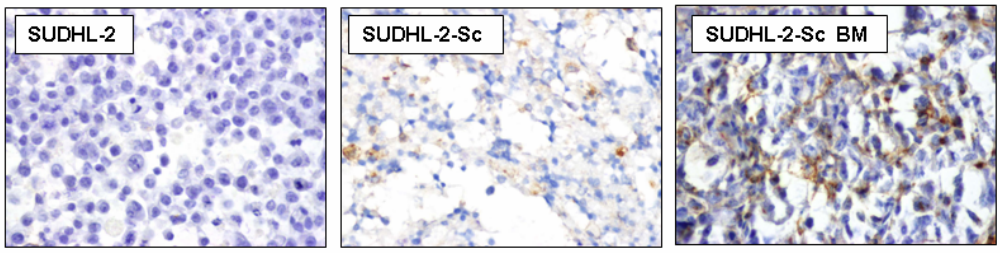

Figure 47. CXCR4 expression in SUDHL-2 cells and in infiltrated BM. CXCR4 was not expressed in SUDHL-2 cell line. The expression of the receptor was nearly undetectable in SUDHL-2-Sc cells and in the infiltrated BM. Original magnification x400. BM, bone marrow.

Thus, in this cell line, subcutaneous preconditioning did not enhance engraftment or dissemination, and it did not significantly increased CXCR4 expression. The absence of a change in CXCR4 expression correlated with the absence of significant changes in cell dissemination pattern.

Taken all together, these results show that in all DLBCL models there is a positive correlation between the levels of CXCR4 expression in membrane and cell aggressiveness. In addition, the subcutaneous preconditioning of the cells induced changes in CXCR4 expression that also correlated with the aggressiveness of the models.

3.3.3 Blockage of CXCR4 in a DLBCL mouse model decreased cell dissemination

The obtained results showed a positive correlation between membrane CXCR4 and aggressiveness of the DLBCL mouse models. Here, we wanted to functionally evalute the role of CXCR4 in dissemination by blocking the activity of the receptor with the CXCR4 antagonist AMD3100.

To that aim, we used the disseminated mouse model derived from OCI-Ly10 cell line that presented high CXCR4 expression in the infiltrated tissues and short survival time. As shown in **Figure 48**, two groups of mice were either intravenously injected with AMD3100-pretreated OCI-Ly10 cells or injected with untreated OCI-Ly10 cells. Moreover, to maintain the inhibition of membrane CXCR4, mice were daily administered with AMD3100 (10 mg/kg) in the experimental group or with saline solution in the control group. BLI images were taken every week to evaluate cell dissemination in both groups of mice.

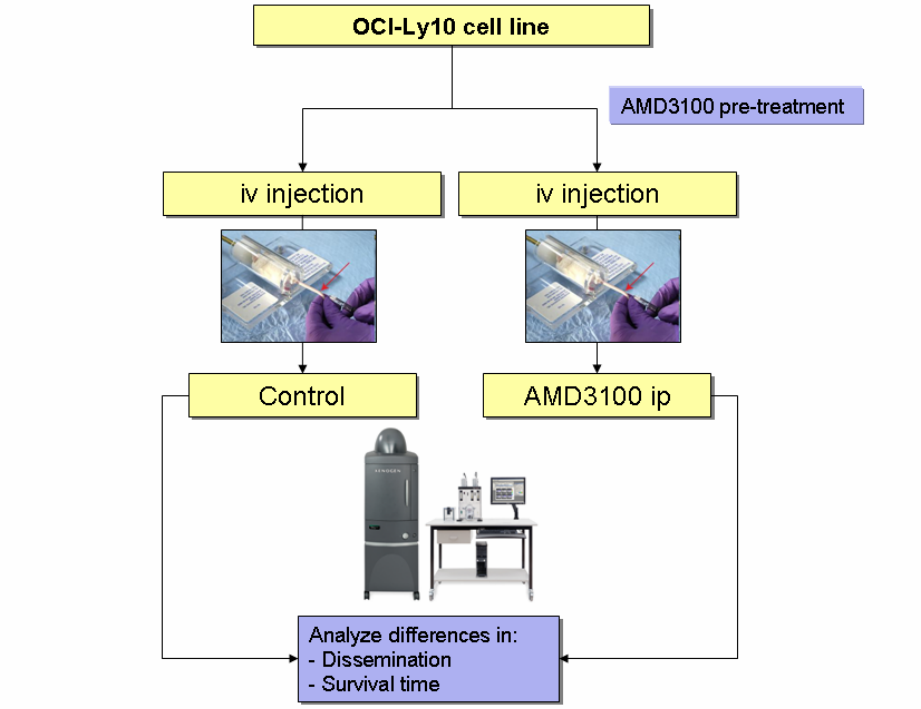

Figure 48. AMD3100 was used to assess its capacity to inhibit cell dissemination in a DLBCL mouse model. OCI-Ly10 cells pre-treated with AMD3100 were injected in NOD/SCID mice and mice were daily treated with the inhibitor. Non-pretreated cells were used as control and were injected in mice receiving saline solution instead of the inhibitor.

The BLI signal was observed in all mice from week 2 after injection of cells. The time course of the BLI signal in the AMD3100-treated group showed that DLBCL cells took longer time to disseminate than cells from the vehicle-treated mice. At week 2 after cell injection, mice from the AMD3100-treated group showed less dissemination than the vehicle-treated mice, with BLI signal being mainly located in the femurs. The BLI signal in the AMD3100-treated group slightly increased at week 3 and at week 4 the BLI was also detected in LN and in the BM from the vertebral column. Mice from the vehicle-treated group showed BLI signal in LN and BM from week 2 which increased over the time (**Figure 49**).

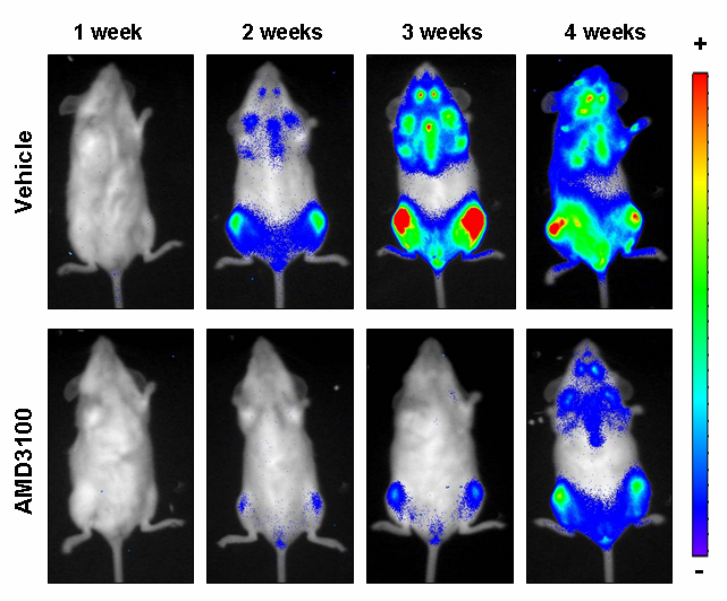

Figure 49. AMD3100 decreased dissemination of CXCR4-expressing cells in a DLBCL mouse model. Representative bioluminescent images showing dissemination of OCI-Ly10 cells in vehicle and AMD3100-treated mice. Mice from both groups were euthanized 4 weeks post-injection of cells. Arbitrary color bars illustrate relative light intensity levels of firefly luciferase, ranging from low (blue) to high (red).

Significant differences between groups were observed in the BLI curves from day 14 after cell injection. Quantification of mean photon count (PHC) was higher in the vehicle group than in the AMD3100-treated group of mice (**Figure 50**). Hence, the CXCR4 inhibitor decreased lymphoma cell dissemination in the DLBCL mouse model derived from OCI-Ly10 cells.

Furthermore, the LN infiltration was significantly decreased in the AMD3100-treated group. No infiltration of axillary or cervical LN was detected in AMD3100-treated mice, whereas 60% of mice presented infiltration of these LN in the vehicle-treated group (**Table 16**). In contrast, infiltration of BM and CNS were detected equally in both groups.

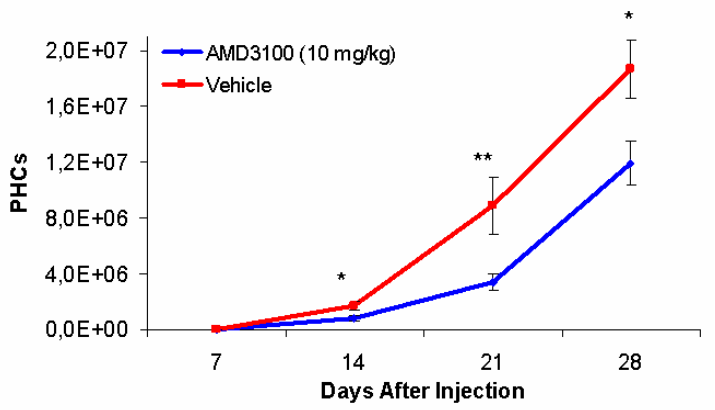

Figure 50. Bioluminescence quantification curves in vehicle and AMD3100-treated groups of mice. There is a higher slope of the bioluminescence curve in vehicle-treated mice compared to AMD3100-treated mice. Significant differences between groups started being detected at day 14 after cell injection and were maintained until the end of the experiment. The bioluminescence signal was quantified and expressed as Photon Counts (PHCs). Curves represent the kinetics of mean BLI intensity for each group. Error bars represent the standard error. *P < 0.05, **P < 0.01 (Mann-Whitney test).

Table 16. Histopathological features and clinical evolution of NOD/SCID mice injected with OCI-Ly10 cells after daily administration of vehicle or AMD3100.

Clinical features	Vehicle	AMD3100	*P*
Nº of positive mice, n (%)	10 (100)	10 (100)	1
Nº of positive mice with LN infiltration, n (%)	8/10 (80)	3/10 (30)	0.028*
Axillary or cervical LN infiltration, n (%)	6/10 (60)	0/10 (0)	0.004*
Renal LN infiltration, n (%)	6/10 (60)	3/10(30)	0.189
Nº of positive mice with BM infiltration, n (%)	10/10 (100)	10/10 (100)	1
Nº of positive mice with CNS infiltration, n (%)	10/10 (100)	10/10 (100)	1

Positive mice are those that developed lymphoma. P values were calculated using Fisher's exact test for categorical variables. LN, lymph nodes; BM, bone marrow; CNS, central nervous system. *P < 0.05

To ensure that the effect of pre-incubation with AMD3100 on cell infiltration was due to the inhibition of cell dissemination rather than to the induction of cell death, we evaluated whether the pre-treatment of OCI-Ly10 cells with AMD3100 affected cell viability. Cell apoptosis was assessed by detection of annexin-V and propidium iodide in culture cells. We observed that after 30 minutes of incubation, AMD3100 did not induce apoptosis (**Figure 51A**). More

than 95% of the cell population was composed of viable cells in control and AMD3100-treated samples.

Moreover, we evaluated CXCR4 membrane expression in OCI-Ly10 cells exposed to AMD3100. As observed in **Figure 51B**, AMD3100 induced the internalization of CXCR4 from the cell membrane to the cytosol. Thus, we observed that AMD3100 reduced the dissemination and decreased DLBCL cell migration to LN by down-regulating the membrane CXCR4 receptor without inducing cell death.

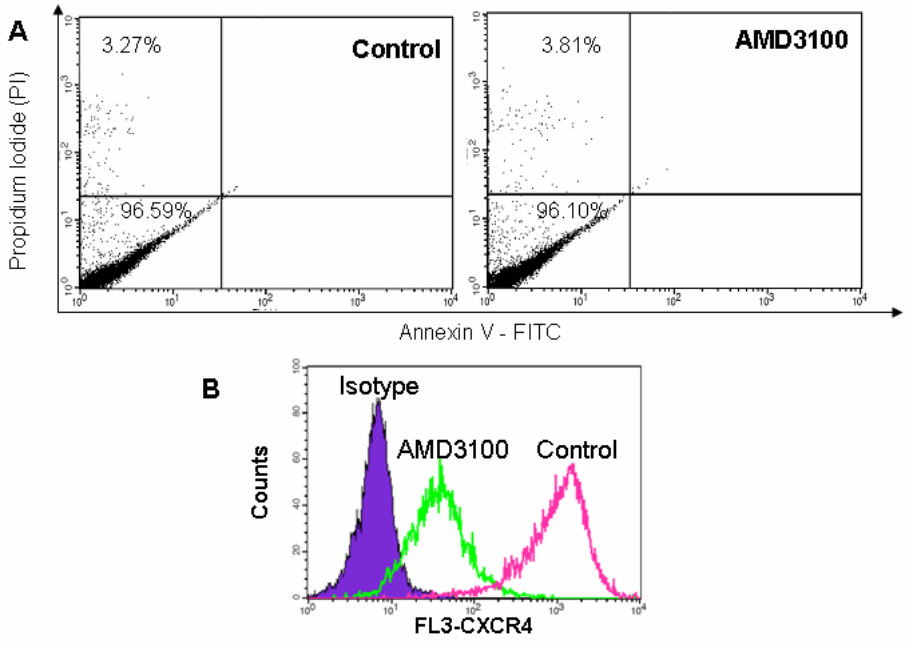

Figure 51. Evaluation of apoptosis and CXCR4-internalization in cells exposed to AMD3100 (10 µg/ml). (A) Representative histograms showing flow cytometry analysis of Annexin V-FITC/Propidium Iodide stained OCI-Ly10 cells. Cells were cultured in the absence (Control, left) or in the presence of CXCR4 inhibitor (AMD3100, right) for 30 minutes. AMD3100 did not induce cell apoptosis. (B) Flow cytometry analysis of surface expression of CXCR4 in control OCI-Ly10 cells and in AMD3100-treated cells. AMD3100 significantly reduced CXCR4 expression in the membrane. The coloured area represents the result of staining with isotype-matched control antibody.

3.4 EVALUATION OF CXCR4 IN DLBCL PATIENTS

We have described the role of CXCR4 in *in vitro* cell migration and also in cell dissemination in DLBCL mouse models. Then, we studied the expression of CXCR4 in DLBCL patients and evaluated its prognosis impact. Several authors have described the association between CXCR4 and decreased survival of oncology patients; moreover, in several neoplasms, CXCR4 is considered a prognostic marker that correlates with disease aggressiveness.[178] However, no data are available about CXCR4 involvement in DLBCL dissemination or its relevance as a prognostic marker in this disease.

We evaluated the expression of membrane CXCR4 in 42 lymph node biopsies from patients with primary nodal DLBCL that were diagnosed in our institution between 2007 and 2012. All 42 patients received rituximab in their treatment; 87% were treated with R-CHOP chemotherapy and 13% received other chemotherapeutic agents in combination with rituximab. The evaluated clinico-pathological features of these patients were: age, gender, bone marrow involvement, serum LDH, stage, ECOG performance status, IPI, chemotherapy, recurrence and DLBCL subtype (**Table 17)**.

As described in "*Materials and methods*", two tissue arrays containing duplicated tumor samples were generated using a tissue-array device and were evaluated by immunohistochemical analysis for CXCR4 expression in the cell membrane. Samples from normal lymphoid tissues were used as controls (tonsil, spleen, thymus and Peyer patches). We evaluated if CXCR4 was present or absent in the cell membrane of tumor samples of DLBCL patients and used dichotomized values for statistical analysis. Representative images of CXCR4 positive tumor samples (with high, medium or low expression levels), of CXCR4

negative tumor samples and of CXCR4 expression in normal lymphoid tissue are shown in **Figure 52**. Some biopsies presented a dot-like CXCR4 staining in the cytosol (**Figure 52D**), as we have previously shown for cell lines exposed to SDF-1α *in vitro* and in mouse infiltrated tissues. However, those samples were considered negative for CXCR4 expression; we just quantified membrane CXCR4 expression due to the previous demonstration that its implication in cell dissemination requires localization of this receptor on the cell membrane.

Table 17. Clinico-pathological features of DLBCL patients.

Clinico-pathological features of DLBCL patients	Number of patients
Age	
<60	20
≥60	22
Gender	
Male	21
Female	21
Bone marrow	
Negative	36
Positive	5
Serum LDH	
Normal	18
High	23
Stage	
I-II	23
III-IV	18
ECOG performance status	
0-2	34
> 2	8
IPI	
Low risk	17
Low/intermediate	8
High/intermediate	10
High risk	6
Chemotherapy	
R-CHOP	37
Others	4
Recurrence	
No	25
Yes	16
DLBCL subtype	
Non-GCB	16
GCB	17

LDH, lactate dehydrogenase; ECOG, Eastern Cooperative Group; IPI, International Prognostic Index; GCB, germinal center B-cell.

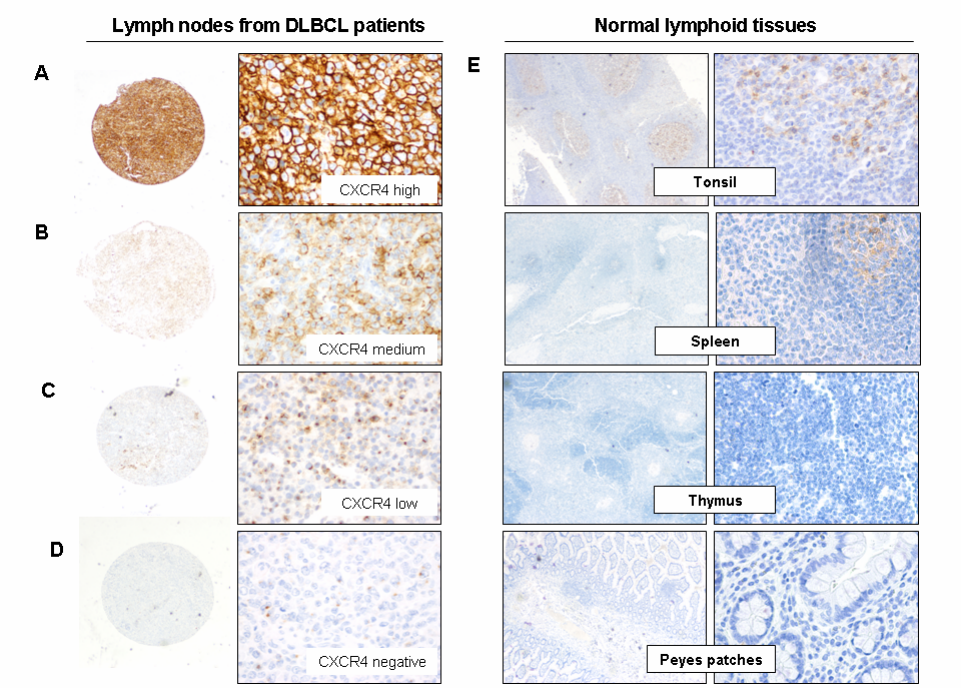

Figure 52. Immunohistochemical analysis of membrane CXCR4 expression in lymph nodes from DLBCL patients and in normal lymphoid tissues. Biopsies displaying high, medium or low levels of CXCR4 were considered positive samples. Dot-like immunostaining was considered negative. Dichotomized values, defined as positive or negative expression for membrane CXCR4, were used for statistical analysis.

The CXCR4 dichotomized values were used to evaluate if the receptor was associated with progression-free survival (PFS) or overall survival (OS) in DLBCL patients. Analysis using the Kaplan-Meier curves showed a significant decrease in PFS in patients with membrane CXCR4 expression in their LN (**Figure 53A**). Although Kaplan-Meier curves showed a trend towards decreased OS, no significant differences were obtained between dichotomized groups for CXCR4 expression (**Figure 53B**).

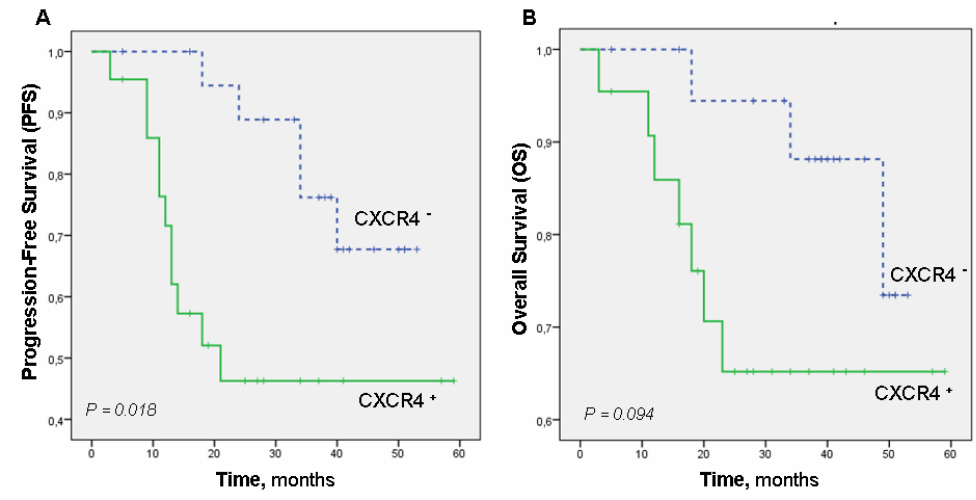

Figure 53. CXCR4 expression correlated with progression-free survival (A) and showed a trend towards decreased overall survival in DLBCL patients (B). *P* values were calculated using the Log-rank test for Kaplan-Meier survival analysis.

Stratification of membrane CXCR4 expression according to the clinical characteristics of the patients (**Table 18**) also showed a trend towards a correlation between recurrent patients and CXCR4-expressing tumors (*P* = 0.069). However, none of the other clinical features (age, gender, bone marrow, serum LDH, stage, ECOG, IPI, chemotherapy or DLBCL subtype) correlated with membrane CXCR4 expression in the tumors.

Table 18. Analysis of the correlation between CXCR4 expression and patients' clinico-pathological features.

	CXCR4 expression		
Clinico-pathological features	**Negative**	**Positive**	***P***
Age			
<60 *(n=20)*	11 (26)	9 (21)	0.537
≥60 *(n=22)*	9 (21)	13 (31)	
Gender			
Male *(n=21)*	10 (24)	11 (26)	1
Female *(n=21)*	10 (24)	11 (26)	
Bone marrow			
Negative *(n=36)*	19 (46)	17 (41)	0.343
Positive *(n=5)*	1 (2)	4 (10)	
Serum LDH			
Normal *(n=18)*	9 (22)	9 (22)	1
High *(n=23)*	11 (27)	12 (29)	
Stage			
I-II (n=23)	14 (34)	9 (22)	0.118
III-IV (n=18)	6 (15)	12 (29)	
ECOG performance status			
0-2 *(n=34)*	18 (43)	16 (38)	0.243
> 2 *(n=8)*	2 (5)	6 (14)	
IPI			
Low risk *(n=17)*	10 (24)	7 (17)	
Low/intermediate *(n=8)*	4 (10)	4 (10)	0.464
High/intermediate *(n=10)*	5 (12)	5 (12)	
High risk *(n=6)*	1 (2)	5 (12)	
Chemotherapy			
R-CHOP *(n=37)*	18 (44)	19 (46)	1
Others *(n=4)*	2 (5)	2 (5)	
Recurrence			
No *(n=25)*	15 (37)	10 (24)	0.069
Yes *(n=16)*	5 (12)	11 (27)	
DLBCL subtype			
Non-GCB *(n=16)*	10 (30)	6 (18)	0.491
GCB *(n=17)*	8 (24)	9 (27)	

n (%), patients considered for each studied variable. P values were calculated using Fisher's exact test. *P value <0.05. LDH, lactate dehydrogenase; ECOG, Eastern Cooperative Group; IPI, International Prognostic Index; GCB, germinal center B-cell.

We further evaluated the clinico-pathological features of DLBCL patients and their CXCR4 expression using survival models to relate the studied features with PFS or OS. These studies were done with one or more covariates using the univariate or the multivariate COX regression models, respectively. Only the significant factors identified in the univariate analysis were included in the multivariate analysis.

By applying a univariate COX analysis and as observed in the clinical setting, the Eastern Cooperative Oncology Group (ECOG, <2 *vs* ≥2) and the International Prognostic Index (IPI, 0-2 *vs* 3-4) were significant predictors for PFS. Interestingly, CXCR4 (positive *vs* negative expression in membrane) was also a significant predictor for PFS. Furhtermore, in the multivariate COX analysis both ECOG (<2 *vs* ≥2) and CXCR4 (positive *vs* negative) remained significant prognostic factors (**Table 19**) with a hazard ratio of 5.470 (95% IC, 1.903 - 15.720; *P* = 0.002) and 3.729 (95% CI, 1.202 to 11.574; *P* = 0.023), respectively.

In contrast, studies for the overall survival using the univariate COX regression showed that ECOG and IPI were significant predictors for OS (**Table 20**) but CXCR4 expression was not (*P* = 0.111). In addition, bone marrow infiltration (BM) showed a trend towards a correlation with OS (*P* = 0.055).

It is important to mention that these analyses were performed using a relative small group of lymph node samples. It will be clinically more valuable if the results could be validated in a separate and independent DLBCL dataset with higher number of patients also treated with R-CHOP. If the results are reproduced in an independent cohort of patients, CXCR4 could be used as a critical prognostic indicator in DLBCL patients.

Table 19. Univariate and multivariate COX regression analysis for progression-free survival in DLBCL patients.

	Progression-free survival			
	Univariate COX Regression		Multivariate COX Regression	
	HR (IC 95%)	*P*	HR (IC 95%)	*P*
CXCR4 (+ *vs* -)	3.387 (1.155 – 9.930)	0.026*	3.729 (1. 202 - 11.574)	0.023 *
ECOG (0-2 *vs* >2)	5.575 (2.052 – 15.144)	0.001*	5.470 (1.903 – 15.720)	0.002*
IPI (0-2 *vs* 3-5)	3.060 (1.106 – 8.466)	0.031*	2.636 (0.934 – 7.440)	0.067
Stage (I-II *vs* III-IV)	2.025 (0.747 – 5.486)	0.165		
LDH (normal *vs* high)	2.001 (0.692 – 5.784)	0.200		
BM (+ *vs* -)	1.843 (0.518 – 6.563)	0.345		
GCB (yes *vs* no)	1.073 (0.268 – 4.299)	0.920		
Age (< 60 *vs* ≥ 60)	1.522 (0.565 – 4. 099)	0.406		

Only significant factors identified in the univariate analysis were included in the multivariate analysis. HR, hazard ratio; 95% IC, 95% confidence interval of hazard ratio; ECOG, Eastern Cooperative Group; LDH, lactate dehydrogenase; IPI, International Prognostic Index; BM, bone marrow; GCB, germinal center B-cell. *P <0.05

Table 20. Univariate and multivariate COX regression analysis for overall survival in DLBCL patients.

	Overall Survival			
	Univariate COX Regression		Multivariate COX Regression	
	HR (IC 95%)	*P*	HR (IC 95%)	*P*
CXCR4 (+ *vs* -)	3.055 (0.773 – 12.077)	0.111		
ECOG (0-2 *vs* >2)	5.436 (1.558 – 18.962)	0.008*	4.719 (1.322 – 16.836)	0.017*
IPI (0-2 *vs* 3-5)	4.276 (1.098 – 16.644)	0.036*	3.845 (0.960 – 15.395)	0.057
Stage (I-II *vs* III-IV)	2.418 (0.674 – 8.670)	0.175		
LDH (normal *vs* high)	2.116 (0.546 – 8.201)	0.278		
BM (+ *vs* -)	3.912 (0.970 – 15.766)	0.055		
GCB (yes *vs* no)	1.881 (0.313 – 11.291)	0.490		
Age (< 60 *vs* ≥ 60)	2.921 (0.742 – 11.500)	0.125		

Only significant factors identified in the univariate analysis were included in the multivariate analysis. HR, hazard ratio; 95% IC, 95% confidence interval of hazard ratio; ECOG, Eastern Cooperative Group; LDH, lactate dehydrogenase; IPI, International Prognostic Index; BM, bone marrow; GCB, germinal center B-cell. *P <0.05

"The mystery of the beginning of all things seems insoluble by us"

“El misterio del comienzo de todas las cosas nos resulta irresoluble”

Charles Darwin

DISCUSSION

In this thesis we have generated novel mouse models of DLBCL that can now be used in the mechanistic study of lymphoma dissemination and in preclinical drug evaluation. Some of these models have been afterwards used to establish a role for the CXCR4 receptor in DLBCL dissemination, and consistently its prognostic value in DLBCL patients. In addition, the use of these models led to the identification of a candidate compound for preclinical development in DLBCL therapy.

1. NOVEL BIOLUMINESCENT MOUSE MODELS OF DISSEMINATED DLBCL

We have generated bioluminescent DLBCL cell lines to develop disseminated mouse models and non-invasively follow the lymphoma progression. The luminescent cells allowed us to generate DLBCL mouse models in which we could monitor the localization and dissemination of DLBCL cells *in vivo*. In addition the bioluminescent models are useful for the follow-up of lymphoma response to antitumor drugs during preclinical development. We have developed GCB-DLBCL models and also novel ABC-DLBCL models that reproduce the clinical features of the disease. The direct intravenous injection of several ABC-DLBCL cell lines (RIVA, OCI-Ly10, SUDHL-2) and GCB-DLBCL cell line (Toledo) into NOD/SCID mice generated disseminated lymphomas. The injection of OCI-Ly10 and Toledo cells generated mouse models displaying a more aggressive phenotype than RIVA or SUDHL-2 cells. OCI-Ly10 and Toledo cells presented almost the same dissemination pattern with infiltration of the same organs (CNS, BM, LN), a short survival time and a 100% of engraftment in mice. Although RIVA cells presented lower engraftment (83.3%), they also infiltrated CNS, BM and LN in several animals. In contrast, SUDHL-2 cells

presented a 50% of engraftment, and BM infiltration was detected in just 33% of the animals; no CNS or LN infiltration was detected in mice injected with this cell line. Thus, different cell lines generated models with distinc pattern of organ involvement and no specific pattern of dissemination was associated with the GCB or ABC subtypes.

The described bioluminescent GCB and ABC-DLBCL models might be useful tools to understand the molecular pathways associated with dissemination and aggressiveness of the disease. Furthermore, the models can be used to evaluate the efficacy of antitumor drugs. This *in vivo* evaluation of dissemination and drug effect can be easily and non-invasively conducted by following the luminescent cells using imaging systems. These models do represent an advance to solve the need of developing new models for some of the lymphoma subtypes so that drug development can be focused on specific biological questions and the identification of candidate targets. Several authors have described other xenograft DLBCL models that have been widely used for drug testing. However, these models are based on subcutaneous injection of the tumor cells and do not represent the disseminated malignancy.[99] Here, we provide luminescent models of disseminated DLBCL that do represent the clinical features observed in patients,[32] that are representative of either GCB or ABC lymphoma subtypes, and are useful for drug-testing or mechanistic studies.

Several authors have reported difficulties in developing disseminated DLBCL mouse models by intravenous injection of the cells due to their low engraftment and low dissemination when injected into immunodeficient mice.[179] As a consequence, strategies based on the subcutaneous growth of tumors or on the intravenous injection of aggressive cells were routenly used for preclinical drug testing or evaluation of molecular pathways, respectively.

Although measuring the volume of subcutaneous tumors is an easy method of evaluating the antitumor drugs effect, these models have localized tumors that do not reflect the disseminated pattern of DLBCL malignancy. In addition, one of the main limitations of the established disseminated models of human lymphomas is that they are based on the intravenous injection of the most aggresssive lymphoproliferative malignancy Burkitt lymphoma.[114] The direct intravenous injection of Burkitt cell lines generates an aggressive and disseminated lymphoma. However, these models do not reflect the DLBCL biology, because Burkitt lymphoma is a different lymphoproliferative entity with distinct biology, treatment and prognosis.[99] On the other side, different genetically engineered mice (GEM) have been reported that developed a disseminated lymphoma. Several GEM mouse models representing ABC or GCB-DLBCL have been described. The GEM models are based on conditional gain or loss-of-function mutagenesis in mice leading to deregulation of different proteins like Bcl6, Myc, NF-*k*B or other proteins implicated in the NF-*k*B pathway.[121,180-182] Other genetically engineered models are obtained by introducing genetic lesions that are not found in human tumors and, consequently, do not truthfully represent the malignancy. These models are useful tools to evaluate the function of particular genes in tumour progression. Nevertheless, GEM models present some limitations: they take long times to develop lymphoma (from 30 to 600 days), tumor engraftment is usually low (not higher than 25% in some models), and tumors can vary in their location and phenotype.[107] These limitations have to be considered when applying these models to the study of lymphomas. These GEM models are not suitable when comparing groups of mice to study antitumor drug effectiveness since their heterogeneity in lymphoma development precludes the achievement of statistically significant conclusions.

In the current thesis, we obtained DLBCL disseminated mouse models in a short period of time and just with a simple intravenous injection of several human cell lines. In addition, Toledo, OCI-Ly10 and RIVA cells presented high engraftment in mice (>80%) and infiltrated LN, BM and CNS, which is also observed in DLBCL patients.[32] The generated models are reproducible and the cells maintained the morphology and immunophenotype of their original counterparts. Moreover, this is the first time that a bioluminescent model for ABC DLBCL useful for mechanistic studies and drug evaluation has been generated.

Finally, we have validated the Toledo-derived DLBCL model for preclinical drug testing. We observed that cyclophosphamide enhanced mouse survival time and decreased lymphoma dissemination, mimicking the reponse to treatment observed in DLBCL patients. Thus, the use of this disseminated DLBCL model for antitumor drug evaluation was confirmed, indicating that it can be applied to the identification of novel drug candidates.

2. CELL-TYPE-DEPENDENT AGGRESIVENESS INDUCED BY SUBCUTANEOUS PRECONDITIONING OF DLBCL CELLS

Previous results obtained in our group revealed that the subcutaneous conditioning of DLBCL cells enhanced their aggressiveness. The aggressiveness of a GCB-DLBCL cell line (WSU-DLCL-2) increased after its subcutaneous preconditioning leading to higher engraftment, and decreased mouse survival time.[117] Similarly, a colorectal mouse model with increased invasion and metastatic dissemination was developed using the subcutaneous conditioning of the tumor cells.[183] In this thesis, we tested whether this finding could be generalized; thus, we followed the same strategy to generate luminescent and aggressive models of both GCB and ABC-DLBCL. We observed that the subcutaneous preconditioning of DLBCL cell lines increased or decreased their aggressiveness depending on the cell line. The subcutaneous conditioning of RIVA and Toledo cells before their intravenous injection increased their aggressiveness, whereas the subcutaneous conditioning of OCI-Ly10 and SUDHL-2 cells did not.

The main difference between the cells injected directly by the intravenous route and the subcutaneously preconditioned cells was the environment where they grew. Whereas the first ones grew *in vitro*, the second ones formed tumors in the mouse subcutis. Thus, the subcutaneous environment induced changes in the RIVA and Toledo lymphoma cells that conferred them a more aggressive phenotype. As these cell lines derived from either activated or germinal center B-cell counterparts the changes in cell aggressiveness are not associated with the cell of origin of these distinct DLBCL subtypes (GCB *or* ABC). Several authors have reported the influence of the tumor stroma on the growth and clonal adaptation of malignant cells.[184,185] In addition, it is well-known that

subpopulations of tumor cells with increased metastatic potential can be obtained by succesive *in vivo* passages of cells. Fidler *et al* revealed that injection of pancreatic carcinoma cells obtained from murine metastases, increased their motility and invasion capacities compared with non-conditioned cells.[186] Furthermore, it has also been described that tumor cell aggressiveness and metastatic behaviour acquired during *in vivo* passages decrease after prolonged *in vitro* culture and that these properties could be restored when cells were injected into new mice.[185,186] The reversibility of this process suggests that epigenetic reprogramming induced by the tumor microenvironment could contribute to phenotypic changes on the tumor cells. These epigenetically induced changes may determine the adaptation for each of the different tumor cell lines when transferred from the *in vitro* to the *in vivo* environment. The epigenetic reprogramming was previously described by Seftor *et al* in a melanoma mouse model.[187] Based on this proposal, we might think that the lymphoma cells obtained from tumors of patients lost their capacity to metastatize when they were adapted to the *in vitro* culture. However, when the cells were introduced into the subcutis of mice, they recovered, at least in part, their original epigenetic signature and phenotype. Hence, we hypothesized that the DLBCL cells obtained from tumors growing in mice and intravenously injected into new hosts, maintained the epigenetic changes induced by the subcutis. Consequently, when re-injected into the *in vivo* microenvironment, the cells recover their original aggressive phenotype. However, the mechanisms that regulate aggressiveness might also be determined by characteristics intrinsic to each particular lymphoma cell line.

Although RIVA and Toledo cells significantly increased their aggressiveness due to the subcutaneous preconditioning, SUDHL-2 and OCI-Ly10 cells did not. Morikawa *et al* reported that the behavior of tumor cells in immunodeficient

mice was influenced by the microenvironment of implantation but also by the nature of the tumor cells.[184] Thus, the differences observed in engraftment, dissemination and survival time in mice injected with subcutaneous preconditioned cells, might be in part attributed to properties intrinsic to the tumor cell lines. Some of the specific mutations that some lymphoma cells bear, may led to the deregulation of proteins that enhance their survival and capacity to disseminate to other organs, which may determine the acquisition of a more aggressive phenotype[188] Hence, the interplay between the mutations involved in lymphoma transformation, which are specific to each particular cell line, and the epigenetic reprograming induced by the subcutaneous conditioning may finally determine the mechanisms used to achieve higher capacity for survival and dissemination. These factors could explain the enhanced aggressiveness of some cells after their subcutaneous preconditioning. In contrast, the pathways activated by the mutations of other lymphoma cell lines may not be affected or even be inhibited by the subcutaneous environment. As a consequence, the subcutis does not promote survival or dissemination of these tumor cells and its subsequent ability to promote dissemination.

In summary, the subcutaneous preconditioning of DLBCL cells increased cell aggressiveness in RIVA and Toledo cell lines; however, in other lymphoma cell lines the subcutaneous preconditioning did not lead to this effect. This effect on dissemination seems to be independent of DLBCL subgroups and migt be explained by specific mutations associated with the cell lines and by epigenetic cell reprogramming induced by the environment.

3. EFFECTIVE TREATMENT OF A DLBCL MODEL WITH CNS AFFECTATION USING A FOCAL ADHESION INHIBITOR

One of the goals of this PhD work was to evaluate the *in vivo* antitumor effect of the focal adhesion inhibitor E7123 in a disseminated model of DLBCL with CNS involvement. This model was also developed by subcutaneous preconditioning of the HT lymphoma cells to increase their aggressiveness. The novel compound E7123 was obtained in our group by modifying the structure of its parental compound, celecoxib, in order to improve its antitumor activity without inhibiting COX-2. It was shown that E7123 induced higher cell death withouth inhibiting COX-2, avoiding the celecoxib-associated cardiovascular side effects. Our group showed the *in vitro* antitumor effect of the E7123 inhibitor in different DLBCL cell lines and also that the drug was able to decrease the growth of DLBCL subtutaneous tumors in mice. Furthermore, it was shown that the antitumor effect was based on inhibition of signaling through focal adhesion proteins.[173] In this thesis, we show that the oral administration of the focal adhesion inhibitor E7123 increases the survival of a disseminated DLBCL mouse model with CNS involvement. This luminescent model replicates the clinical features of DLBCL patients with CNS infiltration and thus can be used for *in vivo* evaluation of novel therapies and to further study the disease.

One of the most serious and usually fatal complication in DLBCL patients is the development of CNS metastasis. Althought the rate of CNS affectation in patients with DLBCL is relatively low, ranging from 3 to 5%, the associated mortality is high.[189] Furthermore, most drugs included in the standard therapy for DLBCL, included in the R-CHOP protocol, are not able to reach the CNS[190] and, as a consequence, they do not prevent CNS relapse. This affectation

usually involves the cerebrospinal fluid and meninges, but solid parenchymal brain infiltration can also occur. Based on the poor outcome reported in DLBCL patients with CNS occurrence and the reported lack of benefit from current prophylactic protocols in the rituximab era,[191] there is an urgent need to develop novel drugs able to cross the blood brain barrier to improve the current treatment of the patients.

Previously, our group developed a DLBCL mouse model with CNS involvement based on the subcutaneous preconditioning of a GCB-DLBCL cell line (HT). It was demonstrated that preconditioned cells showed higher β1-integrin and p130Cas expression that could be associated with the enhanced CNS-tropism. However, the model was not luminescent so we could not monitor *in vivo* the dissemination of DLBCL cells or evaluate novel antitumor drugs.

In this thesis, we have developed a luminescent mouse model with disseminated DLBCL and CNS involvement. The model showed high engraftment (80%), leptomeningeal brain infiltration in almost all mice with lymphoma and short survival time. Thus, the bioluminescent DLBCL model displays the clinico-pathological features observed in patients with CNS involvement, showing predominant meningeal infiltration. In the model, the lymphoma cells maintained their typical morphology and retained the germinal center DLBCL marker expression of their original HT lymphoma counterpart. In addition, the luminescent tumor cells could be followed *in vivo* by non-invasively monitoring the lymphoma progression. Thus, this DLBCL mouse model with CNS involvement can be useful for the preclinical evaluation or development of novel drugs in order to offer a therapeutic option for a clinical situation that is currently lacking therapy.

Until now the development of novel therapies for this pathology was dificulted by the lack of appropriate mouse models that recapitulated the clinico-pathological aspects of the CNS metastases. Some authors developed xenograft models of lymphoma affectation of the CNS by injection of Burkitt or DLBCL lymphoma cells directly into the brain,[192-196] whereas others performed intraocular or intracerebral injection of murine lymphoma cells into immunocompetent syngeneic hosts.[197,198] The syngeneic models might be useful to understand the process of tumor adherence to cerebral endothelial cells, and to study the influence of the immune infiltrate and the microenvironment.[199] However, they are technically difficult to perform and they do not use human DLBCL cells. Jiang *et al* injected lymphoma cells from a primary central nervous system lymphoma (PCNSL) patient into the subcutis of athymic mouse and observed a selective tropism of the cells to the CNS and its vasculature. However, this model was limited to the collection of human tumor samples from the CNS and the experiment was conducted with just one mouse due to the limited availability of tissue samples.[200] It is important to mention that our xenograft model is not representative of PCNSL. PCNSL is considered a distinct DLBCL entity that shows tropism for the CNS microenvironment. As we injected cells intravenously in mice rather than directly into the brain, our model represents a systemic DLBCL that is capable of undergoing dissemination to the CNS. This bioluminescent model complements currently available murine models and can be used in the study of the mechanisms of dissemination, colonization and growth of DLBCL cells into the CNS. Furthermore, it is a reproducible and convenient model to non-invasively follow the antitumor effect of novel therapies.

As previously mentioned, a report from our group described that the focal adhesion inhibitor, E7123, showed *in vitro* antitumor effect in different DLBCL

cell lines by inhibition of focal adhesion signaling, a pathway that was activated in the majority of human DLBCL patient samples.[173] In the current thesis, we evaluated the antitumor effect of E7123 in the HT-derived luminescent DLBCL model with CNS involvement.

We observed that the inhibitor E7123 increased the survival time of HT DLBCL mice with CNS involvement. However, the bioluminiscence images showed that there were no differences in the initial detection of the BLI signal in the CNS between the E7123-treated and the vehicle-treated groups. Hence, E7123 did not block infiltration or dissemination of lymphoma cells to the CNS, but it did delay the growth of the DLBCL cells once in the brain. These results suggested that E7123 was capable of crossing the blood-brain barrier as its parent compound celecoxib does. Hence, this orally bioavailable compound merits further studies as a potential treatment for DLBCL patients with CNS involvement.

Most drugs included in the standard therapy for DLBCL, R-CHOP, do not reach the CNS[190] and consequently, do not prevent CNS relapse. Wang *et al* evaluated E7123 parental compound, celecoxib, as a therapeutic agent in the treatment of a PCNSL xenograft mouse model. They reported that celecoxib was able to inhibit the CNS lymphoma growth and increased survival time of treated mice.[195] Interestingly, it was also reported that celecoxib was able to cross the blood brain barrier.[201] Hence, it seems that celecoxib inhibited lymphoma growth in the CNS by crossing the blood brain barrier and blocking proliferation or inducing cell apoptosis. In addition, phase II studies reported that the combination of celecoxib with cyclophosphamide was an effective therapy for patients with relapsed DLBCL.[202,203] However, the clinical use of celecoxib is associated with risk of cardiovascular side effects due to COX-2

inhibition and, as a consequence, the drug is only given to relapsed patients with aggressive DLBCL.

Results obtained in our group demonstrated that E7123 showed a higher *in vitro* antitumor effect against DLBCL cells compared to celecoxib. In addition, as E7123 did not inhibit COX-2, the associated cardiovascular side effects produced by celecoxib were avoided. When E7123 was given to healthy mice it showed no toxicity and the compound was well tolerated and effective when given to the disseminated DLBCL mouse model with CNS affectation. In addition, the oral bioavailability of the compound and the non-invasive administration of E7123 would represent an advantage for its potential clinical use in the treatment of DLBCL patients with CNS affectation.

Taken together, our findings suggest that E7123 could be effective for the treatment of DLBCL patients with CNS involvement without showing cardiovascular toxicity. Considering the unproven efficacy of current drugs in the CNS relapse treatment and the complexity of their intrathecal administration, orally administration of E7123 could be an alternative treatment in combination with current therapy to treat CNS involvement in DLBCL patients. However, further clinical investigations will be necessary to evaluate E7123 antitumor effect in patients.

4. PIVOTAL ROLE OF MEMBRANE CXCR4 IN DLBCL DISSEMINATION AND AGGRESSIVENESS OF MOUSE MODELS

Another goal of this thesis was to evaluate the expression of the CXCR4 receptor in DLBCL cells and in the generated xenograft models. We describe a positive correlation between CXCR4 expression in the membrane of DLBCL cells and their chemotactic migration *in vitro* and their dissemination *in vivo*. In addition, the subcutaneous precondioning of lymphoma cells induced changes in the levels of membrane CXCR4 that also correlated with cell aggressiveness. Further, we inhibited CXCR4 using an antagonist, AMD3100, and observed a decreased dissemination in a DLBCL bioluminescent model. Finally, we assessed the prognostic value of membrane CXCR4 levels in lymph node biopsies from DLBCL patients and found a significant correlation with progression-free survival.

The levels of membrane CXCR4 receptor in the different DLBCL cell lines may explain their migration *in vitro* and dissemination towards SDF-1α expressing organs such as bone marrow (BM), central nervous system (CNS) and lymph nodes (LN) in mice. We observed a positive correlation between CXCR4 levels in the membrane and *in vitro* migration of DLBCL cells towards a SDF-1α chemotactic gradient. Moreover, DLBCL cell lines expressing high levels of CXCR4 and directly injected into mice showed a more aggressive behaviour with higher engraftment and dissemination, and lower mouse survival time than cells expressing low levels or lacking expression of CXCR4. In addition, the subcutaneous preconditioning of lymphoma cells induced changes in membrane CXCR4 expression. Conditioned cells that increased their levels of

CXCR4 overexpression also showed enhanced dissemination and engraftment capacities, and decreased survival time when injected into mice (RIVA-Sc and Toledo-Sc). Furthermore, the subcutaneous preconditioned cells that down-regulated CXCR4 in the membrane, showed decreased aggressiveness (OCI-Ly10). Hence, the changes in membrane CXCR4 levels induced by the subcutaneous preconditioning of the cells also correlated with their dissemination and aggresiveness.

In the generated xenograft models, lymphoma cells displaying high levels of CXCR4 in their membrane disseminated and reached SDF-1α -rich areas of BM, CNS and LN. As described in the literature, SDF-1α gradients attract CXCR4-positive tumor cells to niches containing high levels of the chemokine.[132,204] In the BM, SDF-1α is mainly produced by osteoblasts lining the bone endosteum.[205,206] In the CNS, SDF-1α is produced by astrocytes, neurons, microglia and endothelia,[207,208] while in the LN it is constitutively produced by stromal cells.[131,209] SDF-1α is also detected on the luminal surface of high endothelial venules (HEVs), mediating the entry of circulating lymphocytes to the peripheral LN.[210] In our mouse models, we observed that lymphoma cells infiltrated the BM and CXCR4 receptor was internalized from cell membrane; the cells proliferated and induced osteolysis leading to invasion of adjacent tissues which was associated with a recovery of CXCR4 expression in the membrane. Hence, it seems that the concentration of SDF-1α was decreased in the areas surrounding the infiltrated BM. The absence or the low concentration of SDF-1α may be the reason for the maintenance of membrane CXCR4 overexpression in lymphoma cells located in the areas sourronding the BM or the LN. These CXCR4 overexpressing cells might maintain their high dissemination capacity, as we observed invasion of the muscle and fat tissues adjacent to the infiltrated BM.

Our results showing that membrane CXCR4 drives DLBCL cells towards SDF-1α expressing organs are in concordance with previous preclinical studies reported in models of breast cancer.[139] Based on other studies indicating that SDF-1α protein levels are higher in normal LN and BM than in the brain,[139] we hypothesize that first lymphoma cells may disseminate following the chemokine gradient produced by LN and BM stromal cells; once the cells have reached the LN and the BM, the stromal cells and their secreted factors may provide a selective advantage for the survival and proliferation of the tumor cells, as reported by several authors in other malignancies.[134,211,212] One possible explanation for the brain involvement woud be that lymphoma cells invade the brain from the adjacent BM of the cranium. Another possibility would be that, as observed in DLBCL patients, there might be an increased risk for CNS affectation in mice that presented an advanced disease and involvement of extranodal sites such as the BM.[75,213] However, these hypotheses have to be confirmed by performing further *in vivo* experiments to evaluate the dissemination of cells over the time for understanding their sequential cell infiltration pattern.

Previous studies also demonstrated that membrane CXCR4 increases dissemination to SDF-1α-expressing organs in some B-cell malignancies other than DLBCL, such as chronic lymphocytic leukaemia and mantle cell lymphoma.[154] Other authors reported high expression of CXCR4, together with CCR7 and CXCR5 receptors, in several B-cell neoplasms correlating with a wide dissemination to LN.[153] Studies in lung cancer have also found a correlation between CXCR4 expression and cell dissemination.[214] In accordance with these findings, our results suggest that overexpression of CXCR4 in the cell membrane was associated with enhanced dissemination of the lymphoma cells and aggressiveness in the derived DLBCL mouse models. However, functional

studies will be needed before confirming CXCR4 involvement in DLBCL dissemination.

The obserbations made in the described DLBCL models are reminiscent of previous work on normal B cell trafficking and homing, a non-random multistep process involving engagement of adhesion molecules and the activation through chemokine receptors.[215] It has been described that dissemination of lymphoma cells is controlled by the same molecular mechanisms that guide the trafficking of their normal lymphocyte counterparts.[215] These findings establish that, differently from other cancer types, lymphoma progression is in part a reflection of a conserved physiological behavior. The SDF-1α chemokine, which is constitutively expressed in BM and LN, together with CXCR4, plays a key role in the trafficking and homing of normal B cells to specific niches.[216] In physiological conditions, CXCR4 participates in homeostatic processes, including lymphocyte homing to secondary lymphoid organs. During the humoral immune response, subsets of activated B cells home to BM, most probably via CXCR4-dependent pathways.[135] Therefore, the migration of CXCR4-expressing B cells is at least partially induced by SDF-1α chemotactic gradients. Once the cells have reached the organ, SDF-1α binds to CXCR4 initiating divergent signaling pathways associated with chemotaxis, cell survival and/or proliferation. Then, the receptor is internalized from the cell membrane leading to CXCR4 desensitization[217] and degradation or recycling back to the membrane. SDF-1α binding to CXCR4 also affects retention of B cells in the organ;[137] studies have reported that SDF-1α binding triggers rapid integrin-dependent arrest inducing lymphocyte recruitment in the organ.[218,219] This physiological process is in agreement with our results in the DLBCL models where SDF-1α from LN and BM induced the internalization of CXCR4 from membrane (punctuated or dot-like immunostaining) and the consequent

retention of lymphoma cells in the organ niche. Hence, in physiological conditions and also in the tumor cells, membrane or internalized CXCR4 plays a pivotal role in the migration and retention of the cells, respectively.

The internalization of the receptor in response to SDF-1α observed in our mouse models is consistent with our *in vitro* results and also with reported studies in which the chemokine induced CXCR4 internalization in multiple myeloma cells[133] and in lymphoma cells.[131] This down-regulation of membrane CXCR4 when tumor cells reach SDF-1α-expressing organs has been considered a consequence of the contact between lymphoma and stromal cells, an event that leads to retention of the lymphoma cells in the colonized organ.[131] Furthermore, studies of tumor microenvironment reported that the interaction between membrane CXCR4 and the extracellular matrix proteins (such as laminin, fibronectin and collagen) also contributes to the metastatic spread of tumor cells.[220,221] Hence, it would be interesting to study the interaction between CXCR4 receptor expressed in lymphoma cells with the stromal cells and also with the extracellular matrix proteins. Understanding these interactions would elucidate the mechanism leading to CXCR4 internalization and desensitization. In addition, determining which interactions are required for CXCR4 recycling or maintenance in the membrane would help to further understand the process of DLBCL metastatic dissemination.

The DLBCL mouse models described in this thesis may be used to study the mechanism of CXCR4 deregulation in DLBCL malignancy. In other tumor types membrane CXCR4 overexpression associates with enhanced dissemination to SDF-1α expressing organs (BM, LN, lung), and for some of them the metastases to BM and LN have demonstrated to be SDF-1α-dependent.[222] The overexpression of CXCR4 may occur as a consequence of enhanced

transcription or blockade of the mechanism of CXCR4 ubiquitination that targets CXCR4 for proteosomal degradation, most likely altered by the mutations acquired during neoplastic transformation. Consistently, in different cancers, CXCR4 internalizes after SDF-1α binding, but instead of being targeted for lysosomal degradation it is estabilized and recycled back to the membrane. This has been reported for neuroblastoma,[223] gastric,[224] or breast cancer.[225] In DLBCL the disregulation of CXCR4 expression by oncogenic mutations is unknown and might be interesting to study.

Taken together and as previously mentioned, the microenvironment within BM and LN enhances lymphocyte recruitment in physiological conditions and also in the pathology of DLBCL. It would be interesting to understand not only the SDF-1α-driven migration of lymphoma cells but also how they are stimulated by stromal cells and their secreted factors in the LN, BM or CNS once the cells have infiltrated the target tissues. Particularly, it would be important to study how the microenvironment of the LN, BM or CNS influenced the expression and regulation of CXCR4 receptor in lymphoma cells and the consequences associated with tumor cell dissemination. Moreover, further studies will be needed to reveal if CXCR4 overexpression in DLBCL cells is a consequence of enhanced transcription or if particular oncogenic mutations disregulate the mechanism of lysosomal degradation of the receptor.

5. A CXCR4 INHIBITOR BLOCKS DLBCL DISSEMINATION: THERAPY IMPLICATIONS

We functionally evaluated the role of CXCR4 in lymphoma migration and dissemination by blocking the receptor using the specific CXCR4 antagonist, AMD3100. We showed that non-cytotoxic doses of AMD3100 inhibited the *in vitro* migration of lymphoma cells towards a SDF-1α gradient without inducing cell death. Moreover, we demonstrated that the AMD3100 inhibitor was able to block OCI-Ly10 dissemination *in vivo* leading to reduced cell aggressiveness. The administration of the antagonist, led to a significant decrease in DLBCL cell migration towards the LN.

Interestingly, we observed that at the end of the experiment the dissemination of DLBCL cells towards the LN was significantly decreased in AMD3100-treated mice, but the dissemination to BM and CNS was not. Although we did not observe differences in BM or CNS infiltration by histological analyses, based on the bioluminescence quantification, we observed that cell dissemination towards these organs was also decreased but not totally inhibited. These results suggest that there might be different molecular mechanisms involved in lymphoma cell colonization between the LN and the BM.

It is known that, in physiological conditions, homing of B lymphocytes is a multistep process that involves engagement of L-selectine, followed by activation of lymphocyte integrins and transmigration through the endothelial cell layer. Moreover, the receptor CXCR4 participates in homeostatic lymphocyte homing to LN and in activated B cells homing to BM during the humoral immune response.[135] Acummulating studies have established a key

role for 3 B-cell integrins in the normal trafficking of mature B cells to either the LN (LFA-1 ($\alpha_L\beta2$)) or the BM (VLA-4 ($\alpha4\beta1$) and $\alpha4\beta7$). The integrin LFA-1 plays a key role in B-cell migration to the LN. In contrast, the α4 integrins are associated with B-cell entry into the BM through interaction with the VCAM-1 adhesion molecule.[226,227] Similarly, CXCR4 in myeloma cells cooperates with VLA-4 integrins to home and grow in the BM where they induce osteolysis.[228-230] Furthermore, it has been reported that CXCR4 may favor VLA-4 integrin signalling by inducing migration of AML cells towards BM stromal cells.[151] Therefore, in physiological and in pathological conditions CXCR4 may cooperate with different adhesion molecules for the homing and colonization of different organs. The different molecular partners that cooperate with CXCR4 in colonizing the LN or the BM may be the basis for the differences in response to AMD3100 observed between these two organs in our DLBCL model.

Furthermore, we hypothesized that there might be other receptors expressed in lymphoma cells implicated in cell dissemination to the target organs. Recently, it was demonstrated that the chemokine SDF-1α also binds to CXCR7, a receptor for the CXCL11 chemokine (I-TAC, interferon-inducible T cell chemoattractant). This receptor forms heterodimers with CXCR4 and is upregulated in several malignant cells promoting tumor cell growth, survival and metastasis.[231,232] Recent studies have reported that the receptor CXCR7 is implicated in the SDF-1α-mediated tumor cell transendotelial migration in lymphoblastic leukaemia and Burkitt lymphoma.[233,234] Therefore, evaluation of CXCR7 expression and contribution to lymphoma cell dissemination induced by SDF-1α might be important to understand the metastatic process and to find an efficient strategy to inhibit SDF-1α-mediated tumor cell dissemination.

Our *in vivo* results showing decreased lymphoma migration towards the LN in AMD3100-treated mice, are consistent with our *in vitro* studies, in which

AMD3100 induced internalization of CXCR4 from the membrane, leading to inhibition of cell migration towards SDF-1α chemotactic gradient. Other authors have shown that a different inhibitor of the CXCR4 pathway (CTCE-9908) reduced the number of metastases in mouse models of osteosarcoma and melanoma.[163] Another group found that blocking CXCR4 expression by siRNAs inhibited metastasis in a breast cancer model.[235] Furthermore, subcutaneous administration of AMD3100 significantly inhibited LN metastasis in a mouse model of oral squamous cell carcinoma.[236] Other preclinical studies using CXCR4 inhibitors reported a decreased metastatic potential in different tumor types,[237] and that disruption of the interaction of cancer cells with the microenvironment lead to their sensitization to cytotoxic therapeutic agents.[238,239] In Burkitt lymphoma, it was reported by Bertolini *et al* that CXCR4 neutralization by monoclonal antibodies significantly delayed tumor growth of lymphoma cells.[152] Bleider *et al* showed that the CXCR4 inhibitor BKT140 induced apoptosis of Burkitt cells and cooperated with rituximab in inducing cell death showing a synergistic antitumor effect; moreover, they demonstrated that BKT140 inhibited the dissemination of lymphoma cells to the BM in a xenograft mouse model.[134] Furthermore, a study published by O'Collaghan *et al* reported that the cell-penetrating lipopeptide CXCR4 antagonist (pepducins), increased rituximab-induced apoptosis of Burkitt lymphoma cells both *in vitro* and *in vivo*.[240] In accordance with these studies and our previous results, we conclude that membrane CXCR4 receptor plays a critical role in the dissemination of DLBCL cells and also that AMD3100 is able to inhibit this process. AMD3100 seems also to be important for inducing cell death in other malignancies; however, we did not observe that this drug induced lymphoma cell death in our model. Further studies will be needed to address this issue.

AMD3100 is the most studied CXCR4 antagonist and after the initial studies as an anti-HIV agent,[241] it was discovered that it was able to mobilize stem cells from the BM.[242] In physiological conditions, CXCR4-positive hemotopoietic stem cells are retained within the BM due to the SDF-1α gradients produced by the stromal cells (paracrine signals); the SDF-1α chemokine binds to the CXCR4 receptor preventing the migration of stem cells outside the BM. The CXCR4 antagonist AMD3100 binds to the CXCR4 receptor blocking the binding of SDF-1α. Hence, stem cells are induced to leave the BM and enter the bloodstream because in the presence of AMD3100 they are unable to respond to the SDF-1α retention signal.[243] The antagonist AMD3100 has already been used in the clinic to mobilize stem progenitors within transplantation protocols in various haematological malignancies, including NHL.[124] Later and based on preclinical studies, the antitumor activity of AMD3100 has been identified as an attractive therapeutic approach in several neoplasms.[244] The effect of CXCR4 inhibitors on DLBCL shoud be further investigated to consider their use in the treatment of patients.

Currently, in the clinical setting, novel CXCR4 antagonists to be given alone or in combination with other antitumor drugs are currently in clinical trials (phase I-II) to treat patients with multiple myeloma, leukaemia and refractory solid tumors.[243] However, AMD3100 inhibitor has not been used for the treatment of DLBCL patients. Evaluation of a dose scalation protocol for this inhibitor may determine whether AMD3100 is able not only to inhibit lymphoma dissemination but also to inhibit the colonization of the tumor cells by inducing cell death. The drug could be given in combination with the standard R-CHOP chemotherapy to induce chemosensitization of tumor cells. However, as CXCR4 is also expressed in healthy tissues, studies are needed to

evaluate the associated side effects of CXCR4-targeted therapeutics. The ongoing clinical trials in other malignancies may help to address this issue.

6. CXCR4 AS A PROGNOSTIC FACTOR IN DLBCL PATIENTS

Finally, after showing the pivotal role of membrane CXCR4 receptor in the migration and dissemination of DLBCL cells, we evaluated the expression of membrane CXCR4 in lymph node biopsies of patients with primary nodal DLBCL.

Dichotomized values of CXCR4 expression in the membrane (absence or presence) were obtained by immunohistochemical analysis of the biopsies and used to correlate with clinical parameters and statistical analysis. Only membrane CXCR4 staining, and not dot-like staining, was considered for the immunohistochemical evaluation due to the implication of the receptor in cell dissemination only when it is localized in the cell membrane.

We found for the first time a strong correlation between membrane expression of CXCR4 receptor and progression-free survival (PFS) in DLBCL patients. In addition, we found a trend towards worse overall survival (OS) in patients that expressed membrane CXCR4. These results suggest that a longer period of clinical follow-up of the patients and/or a higher number of biopsies may convert the observed trend towards reduced OS into a statistically significant finding. However, this evaluation has to be repeated in the near future using the same DLBCL biopsies and updated clinical information to confirm this hypothesis.

Furthermore, by applying survival models we observed that in the univariate COX analysis, membrane CXCR4, IPI and ECOG were significant predictors for PFS. These results for IPI and ECOG were expected because of the implication of both clinical variables in predicting the progression of DLBCL patients. The prognostic value of these standard factors determines that the

cohort of DLBCL patients used for the study was representative of the DLBCL patient population, so the obtained results could be generalized. In addition, multivariate COX analysis indicated that membrane CXCR4 is an independent prognostic marker associated with a higher risk of relapse in DLBCL patients. Our results revealed that patients with CXCR4 expression in their lymph nodes are three times more likely to die or relapse than patients showing lack of CXCR4 expression.

Our findings are consistent with previous studies in which CXCR4 expression was described as a prognostic factor associated with poor outcome in solid neoplasms such as breast,[147,245] colorectal,[149,246] or small cell lung cancers.[150,214] CXCR4 expression has also been described as a prognostic factor in haematological malignancies such as acute myelogenous leukaemia[148] and chronic lymphocytic leukaemia.[247] In some B-cell neoplasms, expression of CXCR4 has been associated with widespread involvement of LN[153] or BM infiltration,[248] however, this has not been described for DLBCL. Although the expression of CXCR4 has been described in DLBCL cell lines and in patient samples,[249,250] its prognostic value has not been reported before in this lymphoma subtype.

Moreover, it is important to mention that, as explained in the "*Introduction*", the prognosis of newly diagnosed DLBCL patients depends on clinical and biological features defined in the IPI factor that was developed almost 20 years ago.[251] As the prognosis of patients within the IPI groups is highly diverse, novel biomarkers that show a strong association with outcome are needed to refine and update the predictive scores.[252] As described in this thesis, biological markers involved in cell dissemination such as the CXCR4 receptor seem to merit particular attention.

In conclusion, the results obtained in this thesis indicate the urgent need to further understand CXCR4 regulation and implication in DLBCL aggressiveness. As shown, this novel prognostic marker thus constitutes a potentially valuable clinical tool for determining the risk of relapse in DLCBL patients. However, as our study involved a limited number of patients, studies using a larger and independent cohort will be necessary to validate these results. If the results are further confirmed, CXCR4 receptor could improve the current staging of DLBCL patients or become a potential therapeutic target for DLBCL treatment.

"…the day you win a Nobel Prize is the day I begin my research on the drag coefficient of tassels on flying carpets …"

"… el día que ganes el premio Nobel, será el día que comience mi investigación sobre el coeficiente de arrastre de las borlas en las alfombras voladoras…"

Sheldon Cooper, Chapter 9 - The Cooper-Hofstadter Polarization

CONCLUSIONS

1. We have developed bioluminescent xenograft models of disseminated DLBCL that derive from the GCB and ABC subtypes, by using Toledo, RIVA and OCI-Ly10 cell lines. These models reflect the clinical features observed in DLBCL patients and can be used to study cell dissemination and the effect of novel antitumor drugs.
2. The subcutaneous conditioning of Toledo and RIVA cell lines generates mouse models with increased dissemination and aggressiveness when compared with their direct intravenous injection.
3. Cyclophosphamide shows antitumor effect and increases the survival time of a DLBCL mouse model generated by the subcutaneous conditioning of Toledo cells prior to their injection. Hence, this model is useful for testing new treatments for DLBCL.
4. The focal adhesion inhibitor E7123 increases survival time in a mouse model of DLBCL with CNS involvement. This drug delays the growth of DLBCL metastasis in the brain.
5. The levels of CXCR4 in the membrane positively correlate with the migration of DLBCL cell lines *in vitro*.
6. High levels of CXCR4 in the membrane correlate with increased dissemination and aggressiveness in *in vivo* models generated after intravenous injection of DLBCL cells. Moreover, the changes induced by the subcutaneous preconditioning of DLBCL cells maintain the positive association observed between CXCR4 levels and cell dissemination or aggressiveness.
7. The CXCR4 antagonist, AMD3100, inhibits migration *in vitro* and dissemination in DLBCL mouse models.
8. CXCR4 protein level in the membrane is a significant predictor of progression-free survival (PFS) in DLBCL patients.

”Attitude is a little thing that makes a big difference”

“La actitud es una pequeña cosa que hace una gran diferencia”

Winston Churchill

BIBLIOGRAPHY

1. Roman E, Smith AG. Epidemiology of lymphomas. *Histopathology*. 2010;58(1):4-14.
2. Baris D, Zahm SH. Epidemiology of lymphomas. *Curr Opin Oncol*. 2000;12(5):383-394.
3. Lenz G, Staudt LM. Aggressive lymphomas. *N Engl J Med*. 2010;362(15):1417-1429.
4. Hennessy BT, Hanrahan EO, Daly PA. Non-Hodgkin lymphoma: an update. *Lancet Oncol*. 2004;5(6):341-353.
5. Bosetti C, Levi F, Ferlay J, Lucchini F, Negri E, La Vecchia C. Incidence and mortality from non-Hodgkin lymphoma in Europe: the end of an epidemic? *Int J Cancer*. 2008;123(8):1917-1923.
6. Ekstrom-Smedby K. Epidemiology and etiology of non-Hodgkin lymphoma--a review. *Acta Oncol*. 2006;45(3):258-271.
7. Alexander DD, Mink PJ, Adami HO, et al. The non-Hodgkin lymphomas: a review of the epidemiologic literature. *Int J Cancer*. 2007;120 Suppl 12:1-39.
8. Skarin AT, Dorfman DM. Non-Hodgkin's Lymphomas: Current classification and management. *CA Cancer J Clin*. 1997;47(6):351-372.
9. The Non-Hodgkin's Lymphoma pathologic classification project: National Cancer Institute study of classifications on non-Hodgkin's lymphoma: Summary and description of a working formulation for clinical usage. *Cancer*. 1982;49:2112-2135.
10. Harris NL, Jaffe ES, Stein H, et al. A revised European-American classification of lymphoid neoplasms: a proposal from the International Lymphoma Study Group. *Blood*. 1994;84(5):1361-1392.
11. A clinical evaluation of the International Lymphoma Study Group classification of non-Hodgkin's lymphoma. The Non-Hodgkin's Lymphoma Classification Project. *Blood*. 1997;89(11):3909-3918.
12. Armitage JO. Staging non-Hodgkin lymphoma. *CA Cancer J Clin*. 2005;55(6):368-376.
13. Chan JK. The new World Health Organization classification of lymphomas: the past, the present and the future. *Hematol Oncol*. 2001;19(4):129-150.
14. Jaffe ES. The 2008 WHO classification of lymphomas: implications for clinical practice and translational research. *Hematology Am Soc Hematol Educ Program*. 2009:523-531.
15. Ollila J, Vihinen M. B cells. *Int J Biochem Cell Biol*. 2005;37(3):518-523.
16. Rajewsky K. Clonal selection and learning in the antibody system. *Nature*. 1996;381(6585):751-758.
17. MacLennan I. Germinal centers. *Annu Rev Immunol*. 1994;12:117-139.
18. Liu YJ, Zhang J, Lane PJ, Chan EY, MacLennan IC. Sites of specific B cell activation in primary and secondary responses to T cell-dependent and T cell-independent antigens. *Eur J Immunol*. 1991;21(12):2951-2962.

19. Janeway CA, Jr., Travers P, Walport M, Shlomchik MJ. Immunobiology: The Immune System in Health and Disease. 5th edition. New York: Garland Science; 2001.
20. Kuppers R. Mechanisms of B-cell lymphoma pathogenesis. *Nat Rev Cancer*. 2005;5(4):251-262.
21. Sagaert X, Sprangers B, De Wolf-Peeters C. The dynamics of the B follicle: understanding the normal counterpart of B-cell-derived malignancies. *Leukemia*. 2007;21(7):1378-1386.
22. Kuppers R, Klein U, Hansmann ML, Rajewsky K. Cellular origin of human B-cell lymphomas. *N Engl J Med*. 1999;341(20):1520-1529.
23. Wang JH, Gostissa M, Yan CT, et al. Mechanisms promoting translocations in editing and switching peripheral B cells. *Nature*. 2009;460(7252):231-236.
24. Chua KF, Alt FW, Manis JP. The function of AID in somatic mutation and class switch recombination: upstream or downstream of DNA breaks. *J Exp Med*. 2002;195(9):F37-41.
25. Shaffer AL, Rosenwald A, Staudt LM. Lymphoid malignancies: the dark side of B-cell differentiation. *Nat Rev Immunol*. 2002;2(12):920-932.
26. Kuppers R, Dalla-Favera R. Mechanisms of chromosomal translocations in B cell lymphomas. *Oncogene*. 2001;20(40):5580-5594.
27. Stevenson FK, Sahota SS, Ottensmeier CH, Zhu D, Forconi F, Hamblin TJ. The occurrence and significance of V gene mutations in B cell-derived human malignancy. *Adv Cancer Res*. 2001;83:81-116.
28. Janeway C, Murphy K, Travers P, Walport M, Shlomchik MJ. The development and survival of lymphocytes. Janeway's Immunobiology. 7th ed. New York, NY: Garland Science; 2008. .
29. De Paepe P, De Wolf-Peeters C. Diffuse large B-cell lymphoma: a heterogeneous group of non-Hodgkin lymphomas comprising several distinct clinicopathological entities. *Leukemia*. 2007;21(1):37-43.
30. Swerdlow SH, Campo E, Jaffe ES, et al. WHO Classification of Tumours of Haematopoietic and Lymphoid Tissues. Lyon: IARC; 2008.
31. Gatter K, Pezella F. Diffuse large B-cell lymphoma. *Diagnostic histopathology*. 2010;16(2):69-75.
32. Flowers CR, Sinha R, Vose JM. Improving outcome for patients with diffuse large B-cell lymphoma. *CA Cancer J Clin*. 2010;60(6):393-408.
33. Friedberg JW, Fisher RI. Diffuse large B-cell lymphoma. *Hematol Oncol Clin North Am*. 2008;22(5):941-952, ix.
34. Kufe DW, Pollock RE, Weichselbaum RR. Holland-Frei Cancer Medicine. 6th edition. Hamilton (ON). BC Decker; 2003.
35. Blinder V, Fisher SG, Lymphoma Research Foundation NY. The role of environmental factors in the etiology of lymphoma. *Cancer Invest*. 2008;26(3):306-316.

36. Vardiman JW. The World Health Organization (WHO) classification of tumors of the hematopoietic and lymphoid tissues: an overview with emphasis on the myeloid neoplasms. *Chem Biol Interact*. 2008;184(1-2):16-20.
37. Shaffer AL, 3rd, Young RM, Staudt LM. Pathogenesis of human B cell lymphomas. *Annu Rev Immunol*. 2012;30:565-610.
38. Pasqualucci L. The genetic basis of diffuse large B-cell lymphoma. *Curr Opin Hematol*. 2013;20(4):336-344.
39. Hartmann EM, Ott G, Rosenwald A. Molecular biology and genetics of lymphomas. *Hematol Oncol Clin North Am*. 2008;22(5):807-823, vii.
40. Klapproth K, Wirth T. Advances in the understanding of MYC-induced lymphomagenesis. *Br J Haematol*. 2010;149(4):484-497.
41. Kramer MH, Hermans J, Wijburg E, et al. Clinical relevance of BCL2, BCL6, and MYC rearrangements in diffuse large B-cell lymphoma. *Blood*. 1998;92(9):3152-3162.
42. Ladanyi M, Offit K, Jhanwar SC, Filippa DA, Chaganti RS. MYC rearrangement and translocations involving band 8q24 in diffuse large cell lymphomas. *Blood*. 1991;77(5):1057-1063.
43. Johnson NA, Slack GW, Savage KJ, et al. Concurrent expression of MYC and BCL2 in diffuse large B-cell lymphoma treated with rituximab plus cyclophosphamide, doxorubicin, vincristine, and prednisone. *J Clin Oncol*. 2012;30(28):3452-3459.
44. Hermine O, Haioun C, Lepage E, et al. Prognostic significance of bcl-2 protein expression in aggressive non-Hodgkin's lymphoma. Groupe d'Etude des Lymphomes de l'Adulte (GELA). *Blood*. 1996;87(1):265-272.
45. Hill ME, MacLennan KA, Cunningham DC, et al. Prognostic significance of BCL-2 expression and bcl-2 major breakpoint region rearrangement in diffuse large cell non-Hodgkin's lymphoma: a British National Lymphoma Investigation Study. *Blood*. 1996;88(3):1046-1051.
46. Thieblemont C, Briere J. MYC, BCL2, BCL6 in DLBCL: impact for clinics in the future? *Blood*;121(12):2165-2166.
47. Horn H, Ziepert M, Becher C, et al. MYC status in concert with BCL2 and BCL6 expression predicts outcome in diffuse large B-cell lymphoma. *Blood*. 2013;121(12):2253-2263.
48. Khodabakhshi AH, Morin RD, Fejes AP, et al. Recurrent targets of aberrant somatic hypermutation in lymphoma. *Oncotarget*. 2012;3(11):1308-1319.
49. Monti S, Chapuy B, Takeyama K, et al. Integrative analysis reveals an outcome-associated and targetable pattern of p53 and cell cycle deregulation in diffuse large B cell lymphoma. *Cancer Cell*. 2012;22(3):359-372.
50. Lenz G, Davis RE, Ngo VN, et al. Oncogenic CARD11 mutations in human diffuse large B cell lymphoma. *Science*. 2008;319(5870):1676-1679.

51. Witzig TE, Hu G, Offer SM, et al. Epigenetic mechanisms of protein tyrosine phosphatase 6 suppression in diffuse large B-cell lymphoma: implications for epigenetic therapy. *Leukemia*. 2013.
52. Clozel T, Yang S, Elstrom RL, et al. Mechanism-Based Epigenetic Chemosensitization Therapy of Diffuse Large B-Cell Lymphoma. *Cancer Discov*. 2013;3(9):1002-1019.
53. Stocklein H, Smardova J, Macak J, et al. Detailed mapping of chromosome 17p deletions reveals HIC1 as a novel tumor suppressor gene candidate telomeric to TP53 in diffuse large B-cell lymphoma. *Oncogene*. 2008;27(18):2613-2625.
54. Wang XM, Greiner TC, Bibikova M, et al. Identification and functional relevance of de novo DNA methylation in cancerous B-cell populations. *J Cell Biochem*. 2010;109(4):818-827.
55. Le Gouill S, Talmant P, Touzeau C, et al. The clinical presentation and prognosis of diffuse large B-cell lymphoma with t(14;18) and 8q24/c-MYC rearrangement. *Haematologica*. 2007;92(10):1335-1342.
56. A predictive model for aggressive non-Hodgkin's lymphoma. The international non-Hodgkin's lymphoma prognostic factors project. *The New England Journal of Medicine*. 1993;329(14):987-994.
57. Oken MM, Creech RH, Tormey DC, et al. Toxicity and response criteria of the Eastern Cooperative Oncology Group. *Am J Clin Oncol*. 1982;5(6):649-655.
58. Feugier P, Van Hoof A, Sebban C, et al. Long-term results of the R-CHOP study in the treatment of elderly patients with diffuse large B-cell lymphoma: a study by the Groupe d'Etude des Lymphomes de l'Adulte. *J Clin Oncol*. 2005;23(18):4117-4126.
59. Pfreundschuh M, Trumper L, Osterborg A, et al. CHOP-like chemotherapy plus rituximab versus CHOP-like chemotherapy alone in young patients with good-prognosis diffuse large-B-cell lymphoma: a randomised controlled trial by the MabThera International Trial (MInT) Group. *Lancet Oncol*. 2006;7(5):379-391.
60. Rosenwald A, Wright G, Chan WC, et al. The Use of Molecular Profiling to Predict Survival after Chemotherapy for Diffuse Large-B-Cell Lymphoma. *The New England Journal of Medicine*. 2002;346(25):1937-1947.
61. Iqbal J, Sanger WG, Horsman DE, et al. BCL2 translocation defines a unique tumor subset within the germinal center B-cell-like diffuse large B-cell lymphoma. *Am J Pathol*. 2004;165(1):159-166.
62. Iqbal J, Greiner T, Patel K, et al. Distinctive patterns of BCL6 molecular alterations and their functional consequences in different subgroups of diffuse large B-cell lymphoma. *Leukemia*. 2007;21(11):2332-2343.

63. Compagno M, Lim WK, Grunn A, et al. Mutations of multiple genes cause deregulation of NF-kappaB in diffuse large B-cell lymphoma. *Nature*. 2009;459(7247):717-721.
64. Hans CP, Weisenburger DD, Greiner TC, et al. Confirmation of the molecular classification of diffuse large B-cell lymphoma by immunohistochemistry using a tissue microarray. *Blood*. 2004;103(1):275-282.
65. Choi WW, Weisenburger DD, Greiner TC, et al. A new immunostain algorithm classifies diffuse large B-cell lymphoma into molecular subtypes with high accuracy. *Clin Cancer Res*. 2009;15(17):5494-5502.
66. Salles G, de Jong D, Xie W, et al. Prognostic significance of immunohistochemical biomarkers in diffuse large B-cell lymphoma: a study from the Lunenburg Lymphoma Biomarker Consortium. *Blood*. 2011;117(26):7070-7078.
67. Zelenetz AD, Abramson JS, Advani RH, et al. NCCN Clinical Practice Guidelines in Oncology: non-Hodgkin's lymphomas. *J Natl Compr Canc Netw*. 2010;8(3):288-334.
68. Fisher RI, Gaynor ER, Dahlberg S, et al. Comparison of a standard regimen (CHOP) with three intensive chemotherapy regimens for advanced non-Hodgkin's lymphoma. *N Engl J Med*. 1993;328(14):1002-1006.
69. McKelvey EM, Gottlieb JA, Wilson HE, et al. Hydroxyl- daunomycin (adriamycin) combination chemotherapy in malignant lymphoma. *Cancer*. 1976;38(4):1484–1493.
70. Cultrera JL, Dalia SM. Diffuse large B-cell lymphoma: current strategies and future directions. *Cancer Control*. 2012;19(3):204-213.
71. Reyes F, Lepage E, Ganem G, et al. ACVBP versus CHOP plus radiotherapy for localized aggressive lymphoma. *N Engl J Med*. 2005;352(12):1197-1205.
72. Ujjani C, Cheson BD. Monoclonal antibodies in advanced B-cell lymphomas. *Oncology (Williston Park)*. 2010;24(2):156-166.
73. Pfreundschuh M, Kuhnt E, Trümper L, et al. CHOP-like chemotherapy with or without rituximab in young patients with good-prognosis diffuse large-B-cell lymphoma: 6-year results of an open-label randomised study of the MabThera International Trial (MInT) Group. *Lancet Oncol*. 2011;12(11):1013-1022.
74. Armitage JO. How I treat patients with diffuse large B-cell lymphoma. *Blood*. 2007;110(1):29-36.
75. Tai WM, Chung J, Tang PL, et al. Central nervous system (CNS) relapse in diffuse large B cell lymphoma (DLBCL): pre- and post-rituximab. *Ann Hematol*. 2011;90(7):809-818.
76. Armitage JO. My treatment approach to patients with diffuse large B-cell lymphoma. *Mayo Clin Proc*. 2012;87(2):161-171.

77. Boehme V, Schmitz N, Zeynalova S, Loeffler M, Pfreundschuh M. CNS events in elderly patients with aggressive lymphoma treated with modern chemotherapy (CHOP-14) with or without rituximab: an analysis of patients treated in the RICOVER-60 trial of the German High-Grade Non-Hodgkin Lymphoma Study Group (DSHNHL). *Blood*. 2009;113(17):3896-3902.
78. Coiffier B. State-of-the-art therapeutics: diffuse large B-cell lymphoma. *J Clin Oncol*. 2005;23(26):6387-6393.
79. Kewalramani T, Zelenetz AD, Nimer SD, et al. Rituximab and ICE as second-line therapy before autologous stem cell transplantation for relapsed or primary refractory diffuse large B-cell lymphoma. *Blood*. 2004;103(10):3684-3688.
80. Philip T, Guglielmi C, Hagenbeek A, et al. Autologous Bone Marrow Transplantation as Compared with Salvage Chemotherapy in Relapses of Chemotherapy-Sensitive Non-Hodgkin's Lymphoma. *N Engl J Med*. 1995;333(23):1540-1545.
81. Oliansky DM, Czuczman M, Fisher RI, et al. The role of cytotoxic therapy with hematopoietic stem cell transplantation in the treatment of diffuse large B cell lymphoma: update of the 2001 evidence-based review. *Biol Blood Marrow Transplant*. 2010;17(1):20-47 e30.
82. Coiffier B, Lepretre S, Pedersen LM, et al. Safety and efficacy of ofatumumab, a fully human monoclonal anti-CD20 antibody, in patients with relapsed or refractory B-cell chronic lymphocytic leukemia: a phase 1-2 study. *Blood*. 2008;111(3):1094-1100.
83. Morschhauser F, Leonard JP, Fayad L, et al. Humanized anti-CD20 antibody, veltuzumab, in refractory/recurrent non-Hodgkin's lymphoma: phase I/II results. *J Clin Oncol*. 2009;27(20):3346-3353.
84. Micallef IN, Maurer MJ, Wiseman GA, et al. Epratuzumab with rituximab, cyclophosphamide, doxorubicin, vincristine, and prednisone chemotherapy in patients with previously untreated diffuse large B-cell lymphoma. *Blood*. 2011;118(15):4053-4061.
85. Advani R, Forero-Torres A, Furman RR, et al. Phase I study of the humanized anti-CD40 monoclonal antibody dacetuzumab in refractory or recurrent non-Hodgkin's lymphoma. *J Clin Oncol*. 2009;27(26):4371-4377.
86. Ruan J, Martin P, Furman RR, et al. Bortezomib plus CHOP-rituximab for previously untreated diffuse large B-cell lymphoma and mantle cell lymphoma. *J Clin Oncol*. 2010;29(6):690-697.
87. Morschhauser F, Dreyling M, Rohatiner A, Hagemeister F, Bischof Delaloye A. Rationale for consolidation to improve progression-free survival in patients with non-Hodgkin's lymphoma: a review of the evidence. *Oncologist*. 2009;14 Suppl 2:17-29.
88. Frese KK, Tuveson DA. Maximizing mouse cancer models. *Nat Rev Cancer*. 2007;7(9):645-658.

89. de Jong M, Maina T. Of mice and humans: are they the same?--Implications in cancer translational research. *J Nucl Med*. 2010;51(4):501-504.
90. Richmond A, Su Y. Mouse xenograft models vs GEM models for human cancer therapeutics. *Dis Model Mech*. 2008;1(2-3):78-82.
91. Bos PD, Nguyen DX, Massague J. Modeling metastasis in the mouse. *Curr Opin Pharmacol*. 2010;10(5):571-577.
92. Sausville EA, Burger AM. Contributions of human tumor xenografts to anticancer drug development. *Cancer Res*. 2006;66(7):3351-3354, discussion 3354.
93. Maina T, Nock BA, Zhang H, et al. Species differences of bombesin analog interactions with GRP-R define the choice of animal models in the development of GRP-R-targeting drugs. *J Nucl Med*. 2005;46(5):823-830.
94. Gopinathan A, Tuveson DA. The use of GEM models for experimental cancer therapeutics. *Dis Model Mech*. 2008;1(2-3):83-86.
95. Belizário J. Immunodeficient mouse models: An overview. *The Open Immunology Journal*. 2009(2):79-85.
96. Lock RB, Liem N, Farnsworth ML, et al. The nonobese diabetic/severe combined immunodeficient (NOD/SCID) mouse model of childhood acute lymphoblastic leukemia reveals intrinsic differences in biologic characteristics at diagnosis and relapse. *Blood*. 2002;99(11):4100-4108.
97. Rubio-Viqueira B, Jimeno A, Cusatis G, et al. An in vivo platform for translational drug development in pancreatic cancer. *Clin Cancer Res*. 2006;12(15):4652-4661.
98. Becher OJ, Holland EC. Genetically engineered models have advantages over xenografts for preclinical studies. *Cancer Res*. 2006;66(7):5555-3359.
99. O'Connor OA, Toner LE, Vrhovac R, Budak-Alpdogan T, Smith EA, Bergman P. Comparative animal models for the study of lymphohematopoietic tumors: strengths and limitations of present approaches. *Leuk Lymphoma*. 2005;46(7):973-992.
100. Macor P, Secco E, Zorzet S, Tripodo C, Celeghini C, Tedesco F. An update on the xenograft and mouse models suitable for investigating new therapeutic compounds for the treatment of B-cell malignancies. *Curr Pharm Des*. 2008;14(21):2023-2039.
101. Bernardi R, Grisendi S, Pandolfi PP. Modelling haematopoietic malignancies in the mouse and therapeutical implications. *Oncogene*. 2002;21(21):3445-3458.
102. Illidge T, Honeychurch J, Howatt W, Ross F, Wilkins B, Cragg M. A new in vivo and in vitro B cell lymphoma model, pi-BCL1. *Cancer Biother Radiopharm*. 2000;15(6):571-580.
103. Chaise C, Itti E, Petegnief Y, et al. [F-18]-Fluoro-2-deoxy-D: -glucose positron emission tomography as a tool for early detection of immunotherapy

response in a murine B cell lymphoma model. *Cancer Immunol Immunother*. 2007;56(8):1163-1171.
104. Passineau MJ, Siegal GP, Everts M, et al. The natural history of a novel, systemic, disseminated model of syngeneic mouse B-cell lymphoma. *Leuk Lymphoma*. 2005;46(11):1627-1638.
105. Slavin S, Strober S. Spontaneous murine B-cell leukaemia. *Nature*. 1978;272(5654):624-626.
106. Kim KJ, Kanellopoulos-Langevin C, Merwin RM, Sachs DH, Asofsky R. Establishment and characterization of Balb/c lymphoma lines with B cell properties. *The Journal of Immunology*. 1979;122(2):549-554
107. Donnou S, Galand C, Touitou V, Sautes-Fridman C, Fabry Z, Fisson S. Murine models of B-cell lymphomas: promising tools for designing cancer therapies. *Adv Hematol*. 2011;2012:701704.
108. Morse HCrd, Anver MR, Fredrickson TN, et al. Bethesda proposals for classification of lymphoid neoplasms in mice. *Blood*. 2002;100(1):246-258.
109. Fusetti L, Pruneri G, Gobbi A, et al. Human myeloid and lymphoid malignancies in the non-obese diabetic/severe combined immunodeficiency mouse model: frequency of apoptotic cells in solid tumors and efficiency and speed of engraftment correlate with vascular endothelial growth factor production. *Cancer Res*. 2000;60(9):2527-2534.
110. Baersch G, Möllers T, Hötte A, et al. Good engraftment of B-cell precursor ALL in NOD-SCID mice. *Klin Padiatr*. 1997;209(4):178-185.
111. Hudson WA, Li Q, Le C, Kersey JH. Xenotransplantation of human lymphoid malignancies is optimized in mice with multiple immunological defects. *Leukemia* 1998;12(12):2029-2033.
112. Steele JP, Clutterbuck RD, Powles RL, et al. Growth of human T-cell lineage acute leukemia in severe combined immunodeficiency (SCID) mice and non-obese diabetic SCID mice. *Blood*. 1997;90(5):2015-2019.
113. Kawata A, Yoshida M, Okazaki M, Yokota S, Barcos M, Seon BK. Establishment of new SCID and nude mouse models of human B leukemia/lymphoma and effective therapy of the tumors with immunotoxin and monoclonal antibody: marked difference between the SCID and nude mouse models in the antitumor efficacy of monoclonal antibody. *Cancer Res*. 1994;54(10):2688-2694.
114. Ghetie MA, Richardson J, Tucker T, Jones D, Uhr JW, Vitetta ES. Disseminated or localized growth of a human B-cell tumor (Daudi) in SCID mice. *Int J Cancer*. 1990;45(3):481-485.
115. Griffiths GL, Mattes MJ, Stein R, et al. Cure of SCID mice bearing human B-lymphoma xenografts by an anti-CD74 antibody-anthracycline drug conjugate. *Clin Cancer Res*. 2003;9(17):6567-6571.
116. DiJoseph JF, Dougher MM, Kalyandrug LB, et al. Antitumor efficacy of a combination of CMC-544 (inotuzumab ozogamicin), a CD22-targeted cytotoxic

immunoconjugate of calicheamicin, and rituximab against non-Hodgkin's B-cell lymphoma. *Clin Cancer Res*. 2006;12(1):242-249.
117. Bosch R, Moreno MJ, Dieguez-Gonzalez R, et al. Subcutaneous passage increases cell aggressiveness in a xenograft model of diffuse large B cell lymphoma. *Clin Exp Metastasis*. 2012;29(4):339-347.
118. Adams JM, Harris AW, Strasser A, Ogilvy S, Cory S. Transgenic models of lymphoid neoplasia and development of a pan-hematopoietic vector. *Oncogene*. 1999;18(38):5268-5277.
119. Adams JM, Harris AW, Pinkert CA, et al. The c-myc oncogene driven by immunoglobulin enhancers induces lymphoid malignancy in transgenic mice. *Nature*. 1985;318(6046):533-538.
120. Strasser A, Harris AW, Cory S. E mu-bcl-2 transgene facilitates spontaneous transformation of early pre-B and immunoglobulin-secreting cells but not T cells. *Oncogene*. 1993;8(1):1-9.
121. Cattoretti G, Pasqualucci L, Ballon G, et al. Deregulated BCL6 expression recapitulates the pathogenesis of human diffuse large B cell lymphomas in mice. *Cancer Cell*. 2005;7(5):445-455.
122. Cardiff RD, Anver MR, Gusterson BA, et al. The mammary pathology of genetically engineered mice: the consensus report and recommendations from the Annapolis meeting. *Oncogene*. 2000;19(8):968-988.
123. Schmitt CA, McCurrach ME, de Stanchina E, Wallace-Brodeur RR, Lowe SW. INK4a/ARF mutations accelerate lymphomagenesis and promote chemoresistance by disabling p53. *Genes Dev*. 1999;13(20):2670-2677.
124. Domanska UM, Kruizinga RC, Nagengast WB, et al. A review on CXCR4/CXCL12 axis in oncology: no place to hide. *Eur J Cancer*. 2012;49(1):219-230.
125. Ransohoff R. Chemokines and chemokine receptors: standing at the crossroads of immunobiology and neurobiology. *Immunity*. 2009;31(5):711-721.
126. Zlotnik A, Yoshie O. Chemokines: a new classification system and their role in immunity. *Immunity*. 2000;12(2):121-127.
127. Sun X, Cheng G, Hao M, et al. CXCL12/CXCR4/CXCR7 chemokine axis and cancer progression. *Cancer Metastasis Rev*. 2010;29(4):709-722.
128. Rot A, von Andrian UH. Chemokines in innate and adaptive host defense: basic chemokines grammar for immune cells. *Annu Rev Immunol*. 2004;22:891-928.
129. Burger JA, Kipps TJ. CXCR4: a key receptor in the crosstalk between tumor cells and their microenvironment. *Blood*. 2006;107(5):1761-1767.
130. Burns JM, Summers BC, Wang Y, et al. A novel chemokine receptor for SDF-1 and I-TAC involved in cell survival, cell adhesion, and tumor development. *J Exp Med*. 2006;203(9):2201-2213.

131. Arai J, Yasukawa M, Yakushijin Y, Miyazaki T, Fujita S. Stromal cells in lymph nodes attract B-lymphoma cells via production of stromal cell-derived factor-1. *Eur J Haematol*. 2000;64(5):323-332.
132. Busillo JM, Benovic JL. Regulation of CXCR4 signaling. *Biochim Biophys Acta*. 2007;1768(4):952-963.
133. Alsayed Y, Ngo H, Runnels J, et al. Mechanisms of regulation of CXCR4/SDF-1 (CXCL12)-dependent migration and homing in multiple myeloma. *Blood*. 2007;109(7):2708-2717.
134. Beider K, Ribakovsky E, Abraham M, et al. Targeting the CD20 and CXCR4 pathways in non-hodgkin lymphoma with rituximab and high-affinity CXCR4 antagonist BKT140. *Clin Cancer Res*. 2013;19(13):3495-3507.
135. Stein JV, Nombela-Arrieta C. Chemokine control of lymphocyte trafficking: a general overview. *Immunology*. 2005;116(1):1-12.
136. Werner L, Guzner-Gur H, Dotan I. Involvement of CXCR4/CXCR7/CXCL12 Interactions in Inflammatory bowel disease. *Theranostics*. 2013;3(1):40-46.
137. Balkwill F. The significance of cancer cell expression of the chemokine receptor CXCR4. *Semin Cancer Biol*. 2004;14(3):171-179.
138. Teicher BA, Fricker SP. CXCL12 (SDF-1)/CXCR4 pathway in cancer. *Clin Cancer Res*. 2010;16(11):2927-2931.
139. Muller A, Homey B, Soto H, et al. Involvement of chemokine receptors in breast cancer metastasis. *Nature*. 2001;410(6824):50-56.
140. Kuhne MR, Mulvey T, Belanger B, et al. BMS-936564/MDX-1338: a fully human anti-CXCR4 antibody induces apoptosis in vitro and shows antitumor activity in vivo in hematologic malignancies. *Clin Cancer Res*;19(2):357-366.
141. Sun X. CXCL12/CXCR4/CXCR7 Chemokine Axis and Cancer Progression. *Cancer Metastasis Rev*. 2010;29(4):709-722.
142. do Carmo A, Patricio I, Cruz MT, Carvalheiro H, Oliveira CR, Lopes MC. CXCL12/CXCR4 promotes motility and proliferation of glioma cells. *Cancer Biol Ther*. 2010;9(1):56-65.
143. Taichman R, Cooper C, Keller ET. Use of the stromal cell-derived factor-1/CXCR4 pathway in prostate cancer metastasis to bone. *Cancer Res*. 2002;62(6):1832-1837.
144. De Falco V, Guarino V, Avilla E, et al. Biological role and potential therapeutic targeting of the chemokine receptor CXCR4 in undifferentiated thyroid cancer. *Cancer Res*. 2007;67(24):11821-11829.
145. Bartolome RA, Ferreiro S, Miquilena-Colina ME, et al. The chemokine receptor CXCR4 and the metalloproteinase MT1-MMP are mutually required during melanoma metastasis to lungs. *Am J Pathol*. 2009;174(2):602-612.
146. Zeelenberg IS, Ruuls-Van Stalle L, Roos E. The chemokine receptor CXCR4 is required for outgrowth of colon carcinoma micrometastases. *Cancer Res*. 2003;63(13):3833-3839.

147. Hiller DJ, Meschonat C, Kim R, Li BD, Chu QD. Chemokine receptor CXCR4 level in primary tumors independently predicts outcome for patients with locally advanced breast cancer. *Surgery*. 2011;150(3):459-465.
148. Spoo AC, Lübbert M, Wierda WG, Burger JA. CXCR4 is a prognostic marker in acute myelogenous leukemia. *Blood*. 2007;109(2):786-791.
149. Ottaiano A, Franco R, Aiello Talamanca A, et al. Overexpression of both CXC chemokine receptor 4 and vascular endothelial growth factor proteins predicts early distant relapse in stage II-III colorectal cancer patients. *Clin Cancer Res*. 2006:12(19):2795-2803.
150. Spano JP, Andre F, Morat L, et al. Chemokine receptor CXCR4 and early-stage non-small cell lung cancer: pattern of expression and correlation with outcome. *Ann Oncol*. 2004;15(4):613-617.
151. Burger JA, Spoo A, Dwenger A, Burger M, Behringer D. CXCR4 chemokine receptors (CD184) and alpha4beta1 integrins mediate spontaneous migration of human CD34+ progenitors and acute myeloid leukaemia cells beneath marrow stromal cells (pseudoemperipolesis). *Br J Haematol*. 2003;122(4):579-589.
152. Bertolini F, Dell'Agnola C, Mancuso P, et al. CXCR4 neutralization, a novel therapeutic approach for non-Hodgkin's lymphoma. *Cancer Res*. 2002;62(11):3106-3112.
153. López-Giral S, Quintana NE, Cabrerizo M, et al. Chemokine receptors that mediate B cell homing to secondary lymphoid tissues are highly expressed in B cell chronic lymphocytic leukemia and non-Hodgkin lymphomas with widespread nodular dissemination. *J Leukoc Biol*. 2004;76(2):462-471.
154. Trentin L, Cabrelle A, Facco M, et al. Homeostatic chemokines drive migration of malignant B cells in patients with non-Hodgkin lymphomas. *Blood*. 2004;104(2):502-508.
155. Burger JA, Peled A. CXCR4 antagonists: targeting the microenvironment in leukemia and other cancers. *Leukemia*. 2009;23(1):43-52.
156. Nervi B, Ramirez P, Rettig MP, et al. Chemosensitization of acute myeloid leukemia (AML) following mobilization by the CXCR4 antagonist AMD3100. *Blood*. 2009;113(24):6206-6214.
157. Zeng Z, Shi YX, Samudio IJ, et al. Targeting the leukemia microenvironment by CXCR4 inhibition overcomes resistance to kinase inhibitors and chemotherapy in AML. *Blood*. 2009;2009(113):24.
158. Kuhne MR, Mulvey T, Belanger B, et al. BMS-936564/MDX-1338: a fully human anti-CXCR4 antibody induces apoptosis in vitro and shows antitumor activity in vivo in hematologic malignancies. *Clin Cancer Res*. 2013;19(2):357-366.
159. Vicenzi E, Lio P, Poli G. The puzzling role of CXCR4 in human immunodeficiency virus infection. *Theranostics*. 2013;3(1):18-25.

160. DiPersio JF, Micallef IN, Stiff PJ, et al. Phase III prospective randomized double-blind placebo-controlled trial of plerixafor plus granulocyte colony-stimulating factor compared with placebo plus granulocyte colony-stimulating factor for autologous stem-cell mobilization and transplantation for patients with non-Hodgkin's lymphoma. *J Clin Oncol*. 2009;27(28):4767-4773.
161. Uy GL, Rettig MP, Motabi IH, et al. A phase 1/2 study of chemosensitization with the CXCR4 antagonist plerixafor in relapsed or refractory acute myeloid leukemia. *Blood*. 2012;119(17):3917-3924.
162. Andritsos L, Byrd JC, Jones JA, et al. Preliminary Results From A Phase I Dose Escalation Study to Determine the Maximum Tolerated Dose of Plerixafor In Combination with Rituximab In Patients with Relapsed Chronic Lymphocytic Leukemia. *Blood (ASH Annual Meeting Abstracts)*. 2010;116. Abstract 2450

163. Kim SY, Lee CH, Midura BV, et al. Inhibition of the CXCR4/CXCL12 chemokine pathway reduces the development of murine pulmonary metastases. *Clin Exp Metastasis*. 2008;25(3):201-211.
164. Arber N, Eagle CJ, Spicak J, et al. Celecoxib for the prevention of colorectal adenomatous polyps. *N Engl J Med*. 2006;355(9):885-895.
165. Morak MJ, Richel DJ, van Eijck CH, et al. Phase II trial of Uracil/Tegafur plus leucovorin and celecoxib combined with radiotherapy in locally advanced pancreatic cancer. *Radiother Oncol*. 2011;98(2):261-264.
166. Gilbert MR, Gonzalez J, Hunter K, et al. A phase I factorial design study of dose-dense temozolomide alone and in combination with thalidomide, isotretinoin, and/or celecoxib as postchemoradiation adjuvant therapy for newly diagnosed glioblastoma. *Neuro Oncol*. 2010;12(11):1167-1172.
167. Pierga JY, Delaloge S, Espie M, et al. A multicenter randomized phase II study of sequential epirubicin/cyclophosphamide followed by docetaxel with or without celecoxib or trastuzumab according to HER2 status, as primary chemotherapy for localized invasive breast cancer patients. *Breast Cancer Res Treat*. 2010;122(2):429-437.
168. Bhatt RS, Merchan J, Parker R, et al. A phase 2 pilot trial of low-dose, continuous infusion, or "metronomic" paclitaxel and oral celecoxib in patients with metastatic melanoma. *Cancer*. 2010;116(7):1751-1756.
169. Chan E, Lafleur B, Rothenberg ML, et al. Dual blockade of the EGFR and COX-2 pathways: a phase II trial of cetuximab and celecoxib in patients with chemotherapy refractory metastatic colorectal cancer. *Am J Clin Oncol*. 2011;34(6):581-586.
170. Buckstein R, Kerbel RS, Shaked Y, et al. High-Dose celecoxib and metronomic "low-dose" cyclophosphamide is an effective and safe therapy in patients with relapsed and refractory aggressive histology non-Hodgkin's lymphoma. *Clin Cancer Res*. 2006;12(17):5190-5198.

171. Casanova I, Parreno M, Farre L, et al. Celecoxib induces anoikis in human colon carcinoma cells associated with the deregulation of focal adhesions and nuclear translocation of p130Cas. *Int J Cancer*. 2006;118(10):2381-2389.
172. Casanova I, Bosch R, Lasa A, et al. A celecoxib derivative inhibits focal adhesion signaling and induces caspase-8-dependent apoptosis in human acute myeloid leukemia cells. *Int J Cancer*. 2008;123(1):217-226.
173. Bosch R, Dieguez-Gonzalez R, Cespedes MV, et al. A novel inhibitor of focal adhesion signaling induces caspase-independent cell death in diffuse large B-cell lymphoma. *Blood*. 2011;118(16):4411-4420.
174. Giancotti FG, Ruoslahti E. Integrin signaling. *Science*. 1999;285(5430):1028-1032.
175. Carbonell WS, Ansorge O, Sibson N, Muschel R. The Vascular Basement Membrane as "Soil" in Brain Metastasis. *PLoS One*. 2009;4(6):e5857.
176. Yoshimasu T, Sakurai T, Oura S, et al. Increased expression of integrin alpha3beta1 in highly brain metastatic subclone of a human non-small cell lung cancer cell line. *Cancer Sci*. 2004;95(2):142-148.
177. del Zoppo GJ, Milner R. Integrin-matrix interactions in the cerebral microvasculature. *Arterioscler Thromb Vasc Biol*. 2006;26(9):1966-1975.
178. Balkwill F. The significance of cancer cell expression of the chemokine receptor CXCR4. *Semin Cancer Biol*. 2004;14(3):171-179.
179. Yan JS, Chen XY, Li WP, Yang Y, Song ZL. Establishing SCID mouse models of B-cell non-Hodgkin's lymphoma. *Ai Zheng*. 2009;28(2):181-183.
180. Calado DP, Zhang B, Srinivasan L, et al. Constitutive canonical NF-kappaB activation cooperates with disruption of BLIMP1 in the pathogenesis of activated B cell-like diffuse large cell lymphoma. *Cancer Cell*. 2010;18(6):580-589.
181. Ranger AM, Zha J, Harada H, et al. Bad-deficient mice develop diffuse large B cell lymphoma. *Proc Natl Acad Sci U S A*. 2003;100(16):9324-9329.
182. Mandelbaum J, Bhagat G, Tang H, et al. BLIMP1 is a tumor suppressor gene frequently disrupted in activated B cell like diffuse large B cell lymphoma. *Cancer Cell*. 2010;18(6):568-579.
183. Alamo P, Gallardo A, Pavon MA, et al. Subcutaneous preconditioning increases invasion and metastatic dissemination in colorectal cancer models. *Dis Model Mech*. 2014:[Epub ahead of print].
184. Morikawa K, Walker SM, Nakajima M, Pathak S, Jessup JM, Fidler IJ. Influence of organ environment on the growth, selection, and metastasis of human colon carcinoma cells in nude mice. *Cancer Res*. 1988;48(23):6863-6871.
185. Aubert C. Metastatic variants of the B16 melanoma: metastasis is related to environmental conditions. Genetic and metabolic effects. *Melanoma Res*. 1994;4(4):225-233.

186. Andreassen K, Mortensen B, Winberg JO, Huseby NE. Increased resistance towards oxidative stress accompanies enhancement of metastatic potential obtained by repeated in vivo passage of colon carcinoma cells in syngeneic rats. *Clin Exp Metastasis*. 2002;19(7):623-629.
187. Seftor EA, Meltzer PS, Kirschmann DA, Margaryan NV, Seftor RE, Hendrix MJ. The epigenetic reprogramming of poorly aggressive melanoma cells by a metastatic microenvironment. *J Cell Mol Med*. 2006;10(1):174-196.
188. Fidler I. Selection of successive tumour lines for metastasis. *Nat New Biol*. 1973;242(118):148-149.
189. Bunn PA, Jr., Schein PS, Banks PM, DeVita VT, Jr. Central nervous system complications in patients with diffuse histiocytic and undifferentiated lymphoma: leukemia revisited. *Blood*. 1976;47(1):3-10.
190. Siegal T, Goldschmidt N. CNS prophylaxis in diffuse large B-cell lymphoma: if, when, how and for whom? *Blood Rev*. 2012;26(3):97-106.
191. Kumar A, Vanderplas A, LaCasce AS, et al. Lack of benefit of central nervous system prophylaxis for diffuse large B-cell lymphoma in the rituximab era: findings from a large national database. *Cancer*. 2012;118(11):2944-2951.
192. Kadoch C, Dinca EB, Voicu R, et al. Pathologic correlates of primary central nervous system lymphoma defined in an orthotopic xenograft model. *Clin Cancer Res*. 2009;15(6):1989-1997.
193. Kim JA, Kim SJ, Do IG, et al. Hypoxia-associated protein expression in primary central nervous system diffuse large B-cell lymphoma: does it predict prognosis? *Leuk Lymphoma*. 2011;52(2):205-213.
194. Muldoon LL, Lewin SJ, Dosa E, et al. Imaging and therapy with rituximab anti-CD20 immunotherapy in an animal model of central nervous system lymphoma. *Clin Cancer Res*. 2011;17(8):2207-2215.
195. Wang W, Kardosh A, Su YS, Schonthal AH, Chen TC. Efficacy of celecoxib in the treatment of CNS lymphomas: an in vivo model. *Neurosurg Focus*. 2006;21(5):E14.
196. Li Z, Qiu Y, Personett D, et al. Pomalidomide shows significant therapeutic activity against CNS lymphoma with a major impact on the tumor microenvironment in murine models. *PLoS One*. 2013;8(8).
197. Mineo JF, Scheffer A, Karkoutly C, et al. Using human CD20-transfected murine lymphomatous B cells to evaluate the efficacy of intravitreal and intracerebral rituximab injections in mice. *Invest Ophthalmol Vis Sci*. 2008;49(11):4738-4745.
198. Assaf N, Hasson T, Hoch-Marchaim H, et al. An experimental model for infiltration of malignant lymphoma to the eye and brain. *Virchows Arch* 1997;431(6):459-467.
199. Galand C, Donnou S, Molina TJ, Fridman WH, Fisson S, Sautès-Fridman C. Influence of Tumor Location on the Composition of Immune Infiltrate and Its

Impact on Patient Survival. Lessons from DCBCL and Animal Models. *Front Immunol*. 2012;3(98).
200. Jiang L, Marlow LA, Cooper SJ, et al. Selective central nervous system tropism of primary central nervous system lymphoma. *Int J Clin Exp Pathol*. 2010;3(8):763-767.
201. Dembo G, Park SB, Kharasch ED. Central nervous system concentrations of cyclooxygenase-2 inhibitors in humans. *Anesthesiology*. 2005;102(2):409-415.
202. El Bary NA, Hashem T, Metwally H, Ghany AA, El Mageed HA. A phase II study of high-dose celecoxib and metronomic 'low-dose' cyclophosphamide and methotrexate in patients with relapsed and refractory lymphoma. *Hematol Oncol Stem Cell Ther*. 2010;3(1):13-18.
203. Buckstein R, Kerbel RS, Shaked Y, et al. High-Dose celecoxib and metronomic "low-dose" cyclophosphamide is an effective and safe therapy in patients with relapsed and refractory aggressive histology non-Hodgkin's lymphoma. *Clin Cancer Res*. 2006;12(17):5190-5198.
204. Teicher BA, Fricker SP. CXCL12 (SDF-1)/CXCR4 pathway in cancer. *Clin Cancer Res*. 2010;16(11):2927-2931.
205. Sun X, Cheng G, Hao M. CXCL12/CXCR4/CXCR7 Chemokine Axis and Cancer Progression. *Cancer Metastasis Rev*. 2010;29(4):709-722.
206. Jung Y, Wang J, Schneider A, et al. Regulation of SDF-1 (CXCL12) production by osteoblasts; a possible mechanism for stem cell homing. *Bone*. 2006;38(4):497-508.
207. Biber K, Zuurman MW, Dijkstra IM, Boddeke HW. Chemokines in the brain: neuroimmunology and beyond. *Curr Opin Pharmacol*. 2002;2(1):63-68.
208. Reaux-Le Goazigo A, Van Steenwinckel J, Rostene W, Melik Parsadaniantz S. Current status of chemokines in the adult CNS. *Prog Neurobiol*. 2013;104:67-92.
209. Barbieri F, Bajetto A, Pattarozzi A, et al. The Chemokine SDF1/CXCL12: A Novel Autocrine/Paracrine Factor Involved In Pituitary Adenoma Development. *The Open Neuroendocrinology Journal*. 2011(4):64-76
210. Bleul C, Fuhlbrigge R, Casasnovas J. A highly efficacious lymphocyte chemoatractant, stromal cell-derived factor 1 (SDF-1). *Journal of Experimental Medicine*. 1996;184(3):1101-1109.
211. LeBedis C, Chen K, Fallavollita L, Boutros T, Brodt P. Peripheral lymph node stromal cells can promote growth and tumorigenicity of breast carcinoma cells through the release of IGF-I and EGF. *Int J Cancer*. 2002;100(1):2-8.
212. Wong SY, Hynes RO. Tumor-lymphatic interactions in an activated stromal microenvironment. *J Cell Biochem*. 2007;101(4):840-850.
213. van Besien K, Ha CS, Murphy S, et al. Risk factors, treatment, and outcome of central nervous system recurrence in adults with intermediate-grade and immunoblastic lymphoma. *Blood*. 1998;91(4):1178-1184.

214. Gangadhar T, Nandi S, Salgia R. The role of chemokine receptor CXCR4 in lung cancer. *Cancer Biol Ther*. 2010;9(6):409-416.
215. Pals ST, de Gorter DJ, Spaargaren M. Lymphoma dissemination: the other face of lymphocyte homing. *Blood*. 2007;110(9):3102-3111.
216. Olson TS, Ley K. Chemokines and chemokine receptors in leukocyte trafficking. *Am J Physiol Regul Integr Comp Physiol*. 2002;283(1):R7-28.
217. Teicher B, Fricker S. CXCL12 (SDF-1)/CXCR4 pathway in cancer. *Clin Cancer Res*. 2010;16(11):2927-2931.
218. Campbell JJ, Hedrick J, Zlotnik A, Siani MA, Thompson DA, Butcher EC. Chemokines and the arrest of lymphocytes rolling under flow conditions. *Science*. 1998;279(5349):381-384.
219. Ma Q, Jones D, Springer T. The chemokine receptor CXCR4 is required for the retention of B lineage and granulocytic precursors within the bone marrow microenvironment. *Immunity*. 1999;10(4):463-471.
220. Engl T, Relja B, Marian D, et al. CXCR4 chemokine receptor mediates prostate tumor cell adhesion through alpha5 and beta3 integrins. *Neoplasia*. 2006;8(4):290-301.
221. Sun YX, Fang M, Wang J, Cooper CR, Pienta KJ, Taichman RS. Expression and activation of alpha v beta 3 integrins by SDF-1/CXC12 increases the aggressiveness of prostate cancer cells. *Prostate*. 2007;67(1):61-73.
222. Burger JA, Kipps TJ. CXCR4: a key receptor in the crosstalk between tumors cells and their microenvironment. *Blood*. 2006;107(5):1761-1767.
223. Carlisle AJ, Lyttle CA, Carlisle RY, Maris JM. CXCR4 expression heterogeneity in neuroblastoma cells due to ligand-independent regulation. *Mol Cancer*. 2009;8(123).
224. Zhu S, Hong J, Tripathi MK, Sehdev V, Belkhiri A, El-Rifai W. Regulation of CXCR4-mediated invasion by DARPP-32 in gastric cancer cells. *Mol Cancer Res*. 2013;11(1):86-94.
225. Mukherjee D, Zhao J. The Role of chemokine receptor CXCR4 in breast cancer metastasis. *Am J Cancer Res*. 2013;3(1):46-57.
226. Koni PA, Joshi SK, Temann UA, Olson D, Burkly L, Flavell RA. Conditional vascular cell adhesion molecule 1 deletion in mice: impaired lymphocyte migration to bone marrow. *J Exp Med*. 2001;193(6):741-754.
227. Berlin-Rufenach C, Otto F, Mathies M, et al. Lymphocyte migration in lymphocyte function-associated antigen (LFA)-1-deficient mice. *J Exp Med*. 1999;189(9):1467-1478.
228. Bataille R, Harousseau JL. Multiple myeloma. *N Engl J Med*. 1997;336(23):1657-1664.
229. Mundy GR. Myeloma bone disease. *Eur J Cancer*. 1998;34(2):246-251.
230. Sanz-Rodriguez F, Hidalgo A, Teixido J. Chemokine stromal cell-derived factor-1alpha modulates VLA-4 integrin-mediated multiple myeloma cell adhesion to CS-1/fibronectin and VCAM-1. *Blood*. 2001;97(2):346-351.

231. Decaillot FM, Kazmi MA, Lin Y, Ray-Saha S, Sakmar TP, Sachdev P. CXCR7/CXCR4 heterodimer constitutively recruits beta-arrestin to enhance cell migration. *J Biol Chem*. 2011;286(37):32188-32197.
232. Singh A, Arya R, Trivedi A. Chemokine receptor trio: CXCR3, CXCR4 and CXCR7 crosstalk via CXCL11 and CXCL12. *Cytokine Growth Factor Rev*. 2013;24(1):41-49.
233. Zabel BA, Wang Y, Lewen S, et al. Elucidation of CXCR7-mediated signaling events and inhibition of CXCR4-mediated tumor cell transendothelial migration by CXCR7 ligands. *J Immunol*. 2009;183(5):3204-3211.
234. Zabel BA, Lewen S, Berahovich RD, Jaen JC, Schall TJ. The novel chemokine receptor CXCR7 regulates trans-endothelial migration of cancer cells. *Mol Cancer*. 2011;10:73.
235. Liang Z, Yoon Y, Votaw J. Silencing of CXCR4 blocks breast cancer metastasis. *Cancer Res*. 2005;65(3):967-971.
236. Uchida D, Onoue T, Kuribayashi N. Blockade of CXCR4 in oral squamous cell carcinoma inhibits lymph node metastases. *Eur J Cancer*. 2010;47(3):452-459.
237. Cojoc M, Peitzsch C, Trautmann F, Polishchuk L, Telegeev G, Dubrovska A. Emerging target in cancer management: role of the CXCL12/CXC4 axis. *Onco Targets Ther*. 2013;6:1347-1361.
238. Azab AK, Runnels JM, Pitsillides C, et al. CXCR4 inhibitor AMD3100 disrupts the interaction of multiple myeloma cells with the bone marrow microenvironment and enhances their sensitivity to therapy. *Blood*. 2009;113(18):4341-4351.
239. Zeng Z, Samudio IJ, Munsell M, et al. Inhibition of CXCR4 with the novel RCP168 peptide overcomes stroma-mediated chemoresistance in chronic and acute leukemias. *Mol Cancer Ther*. 2006;5(12):3113-3121.
240. O'Callaghan K, Lee L, Nguyen N, et al. Targeting CXCR4 with cell-penetrating pepducins in lymphoma and lymphocytic leukemia. *Blood*. 2012;119(7):1717-1725.
241. Labrosse B, Brelot A, Heveker N, et al. Determinants for sensitivity of human immunodeficiency virus coreceptor CXCR4 to the bicyclam AMD3100. *J Virol*. 1998;72(8):6381-6388.
242. Larochelle A, Krouse A, Metzger M, et al. AMD3100 mobilizes hematopoietic stem cells with long-term repopulating capacity in nonhuman primates. *Blood*. 2006;107(9):3772-3778.
243. Ramsey D, McAlpine S. Halting metastasis through CXCR4 inhibition. *Bioorg Med Chem Lett*. 2013;23(1):20-25.
244. Peled A, Wald O, Burger J. Development of novel CXCR4-based therapeutics. *Expert Opin Investig Drugs*. 2012;21(3):341-353.
245. Hiller D, Chu QD. CXCR4 and axillary lymph nodes: review of a potential biomarker for breast cancer metastasis. *Int J Breast Cancer*. 2011;2011:420981.

246. Kim J, Takeuchi H, Lam ST, et al. Chemokine receptor CXCR4 expression in colorectal cancer patients increases the risk for recurrence and for poor survival. *J Clin Oncol*. 2005;23(12):2744-2753.
247. Ishibe N AM, Jilani IB, Goldin LR, Marti GE, Caporaso NE. CXCR4 expression is associated with survival in familial chronic lymphocytic leukemia, but CD38 expression is not. *Blood*. 2002;100(3):1100-1101.
248. Deutsch AJ, Steinbauer E, Hofmann NA, et al. Chemokine receptors in gastric MALT lymphoma: loss of CXCR4 and upregulation of CXCR7 is associated with progression to diffuse large B-cell lymphoma. *Mod Pathol*. 2013;26(2):182-194.
249. Brault L, Menter T, Obermann EC, et al. PIM kinases are progression markers and emerging therapeutic targets in diffuse large B-cell lymphoma. *Br J Cancer*. 2012;107(3):491-500.
250. Katia B, Ribakovsky E, Abraham M, et al. Targeting the CD20 and CXCR4 Pathways in Non Hodgkin Lymphoma with Rituximab and high affinity CXCR4 antagonist BKT140. *Clin Cancer Res*. 2013;19(13):3495-3507.
251. Ghielmini M, Vitolo U, Kimby E, et al. ESMO Guidelines consensus conference on malignant lymphoma 2011 part 1: diffuse large B-cell lymphoma (DLBCL), follicular lymphoma (FL) and chronic lymphocytic leukemia (CLL). *Ann Oncol*. 2012;24(3):561-576.
252. Perry AM, Mitrovic Z, Chan WC. Biological prognostic markers in diffuse large B-cell lymphoma. *Cancer Control*. 2012;19(3):214-226.

”Many of life failures are people who did not realized how close they were to success when they gave up”

“Muchos de los fracasos de la vida son de personas que no se dieron cuenta cuán cerca estaban del éxito cuando se dieron por vencidos”

Thomas Edison

APPENDIX 1

WHO classification of the mature B-cell, T-cell, and NK-cell neoplasms (2008)

MATURE B-CELL NEOPLASMS
B-cell chronic lymphocytic leukaemia/small lymphocytic lymphoma
B-cell prolymphocytic leukaemia
Splenic marginal zone lymphoma
Hairy cell leukaemia
Splenic lymphoma/leukaemia, unclassifiable*
Splenic diffuse red pulp small B-cell lymphoma*
Hairy cell leukaemia-variant*
Lymphoplasmacytic lymphoma
Waldenström macroglobulinemia
Heavy chain diseases
Alpha heavy chain disease
Gamma heavy chain disease
Mu heavy chain disease
Plasma cell myeloma/Plasmacytoma
Solitary plasmacytoma of bone
Extraosseous plasmacytoma
Extranodal marginal zone lymphoma of mucosa-associated lymphoid tissue (MALT lymphoma)
Nodal marginal zone lymphoma
Pediatric nodal marginal zone lymphoma*
Follicular lymphoma
Pediatric follicular lymphoma
Primary cutaneous follicle center lymphoma
Mantle cell lymphoma
Diffuse large B-cell lymphoma (DLBCL), not otherwise specified
T-cell/histiocyte rich large B-cell lymphomas
Primary DLBCL of the CNS
Primary cutaneous DLBCL, leg type
EBV+ DLBCL of the elderly*
DLBCL associated with chronic inflamation
Lymphomatoid granulomatosis
Primary mediastinal (thymic) large B-cell lymphoma
Intravascular large B-cell lymphoma
ALK+ large B-cell lymphoma
Plasmablastic lymphoma
Large B-cell lymphoma arising in HHV8-associated multicentric Castleman disease
Primary effusion lymphoma
Burkitt lymphoma
B-cell lymphoma, unclassifiable, with features intermediate between diffuse large B-cell lymphoma and Burkitt lymphoma
B-cell lymphoma, unclassifiable, with features intermediate between diffuse large B-cell lymphoma and classical Hodgkin lymphoma

MATURE T-CELL AND NK-CELL NEOPLASMS
T-cell prolymphocytic leukaemia
T-cell granular lymphocytic leukaemia
Chronic lymphoproliferative disorder of NK cells*
Aggressive NK-cell leukaemia
Systemic EBV+ T-cell lymphoproliferative disease of childhood
Hydroa vacciniforme-like lymphoma
Adult T-cell leukaemia/lymphoma/
Extranodal NK/T-cell lymphoma, nasal type
Enteropathy-associated T-cell lymphoma
Hepatosplenic T-cell lymphoma
Subcutaneous panniculitis-like T-cell lymphoma
Mycosis fungoides
Sezary's syndrome
Primary cutaneous CD30+ T-cell lymphoproliferative disorders
Lymphomatoid papulosis
Primary cutaneous anaplastic large cell lymphoma
Primary cutaneous gamma-delta T-cell lymphoma
Primary cutaneous CD8+ aggressive epidermotropic cytotoxic T-cell lymphoma*
Primary cutaneous CD4+ small/medium T-cell lymphoma*
Peripheral T-cell lymphoma, NOS
Angioimmunoblastic T-cell lymphoma
Anaplastic large cell lymphoma, ALK-
Anaplastic large cell lymphoma, ALK+
HODGKIN LYMPHOMA
Nodular lymphocyte-predominant Hodgkin lymphoma
Classical Hodgkin lymphoma
Nodular sclerosis classical Hodgkin lymphoma
Lymphocyte-rich classical Hodgkin lymphoma
Mixed cellularity classical Hodgkin lymphoma
Lymphocyte-depleted classical Hodgkin lymphoma
POST-TRANSPLANTATION LYMPHOPROLIFERATIVE DISORDERS (PTLD)
Early lesions
Plasmacytic hyperplasia
Infectious mononucleosis-like PTLD
Polymorphic PTLD
Monomorphic PTLD (B-and T/NK-cell types)[1]
Classical Hodgkin lymphoma PTLD[1]

* Provisional entities for which the WHO Working Group felt there was insufficient evidence to recognize as distinct diseases at this time

[1] These lesions are classified according to the leukaemia or lymphoma to which they correspond.

”El éxito ocurre cuando tus sueños son más grandes que tus excusas”

“Success occurs when your dreams are bigger than your excuses”

Anonymous

APPENDIX 2

The results obtained during this PhD have been described in the following papers:

- **CXCR4 expression enhances dissemination and risk of relapse in diffuse large B-cell lymphoma.** Moreno MJ, Bosch R, Dieguez-Gonzalez R, Novelli S, Mozos A, Gallardo A, Pavón MA, Céspedes MV, Grañena A, Sierra J, Mangues R and Casanova I. 2014 [Under review]

- **A novel orally available inhibitor of focal adhesion signaling increases survival in a xenograft model of diffuse large B-cell lymphoma with central nervous system involvement**. Bosch R*, Moreno MJ*, Dieguez-Gonzalez R, Céspedes MV, Gallardo A, Trias M, Grañena A, Sierra J, Casanova I, Mangues R. Haematologica. 2013 Aug;98(8):1242-9. * These authors contributed equally to this manuscript.

During this period other papers have also been published:

- **Focal adhesion proteins expression in human diffuse large B cell lymphoma.** Bosch R, Dieguez-Gonzalez R, Moreno MJ, Gallardo A, Novelli S, Espinosa I, Céspedes MV, Pavón MA, Briones J, Grañena A, Sierra J, Mangues R, Casanova I. Histopathology. 2014 [Epub ahead of print]

- **Subcutaneous passage increases cell aggressiveness in a xenograft model of diffuse large B cell lymphoma**. Bosch R, Moreno MJ, Dieguez-Gonzalez R, Céspedes MV, Gallardo A, Nomdedeu J, Pavón MA, Espinosa I, Mangues MA, Sierra J, Casanova I, Mangues R. Clin Exp Metastasis. 2012 Apr;29(4):339-47.


If at first you
don't succeed,
try two more times
so that your failure
is ...
Statistically Significant!

APPENDIX 3

Desarrollo de un modelo murino de linfoma difuso de célula grande B y papel de CXCR4 en diseminación

Development of diffuse large B-cell lymphoma mouse models and role of CXCR4 in dissemination

RESUMEN DE LA TESIS DOCTORAL

INTRODUCCIÓN

El linfoma difuso de célula grande B (LDCGB) es el tipo de linfoma no Hodgkin más común en la población, representa un 30% de los casos. La incorporación de rituximab al tratamiento estándar CHOP (ciclofosfamida, doxorubicina, vincristina y prednisona) ha aumentado la supervivencia de los pacientes. Aún así, hay un elevado porcentaje de pacientes que recaen y es necesario desarrollar nuevos fármacos. Para ello es necesario disponer de modelos animales que reproduzcan las características clínicas observadas en pacientes y que permitan estudiar la enfermedad y desarrollar nuevos tratamientos. Por otro lado, también es necesario obtener nuevos biomarcadores capaces de predecir el pronóstico en pacientes de LDCGB.

Actualmente, el diagnóstico de pacientes con LDCGB se basa en la valoración de 5 factores: la edad, el estadio, el estado funcional de acuerdo con los criterios del *Eastern Cooperative Oncology Group* (ECOG), los niveles de LDH (lactato deshidrogenasa) y la afección extranodal. Por cada uno de estos factores se otorga una puntuación que define el estado clínico del paciente. La suma de todos estos factores se denominó IPI (*International Prognostic Index*) e

identificó grupos de pacientes con diferente pronóstico. Aunque el IPI se definió hace casi 20 años, continúa siendo el único método validado para definir el diagnóstico y consecuente pronóstico de los pacientes de LDCGB. Sin embargo, existe una gran variabilidad en cuanto a pronósico entre los subgrupos de pacientes definidos por el IPI. Por ese motivo, es necesario establecer nuevos marcadores biológicos, y no solo clínicos, que permitan clasificar a los pacientes en función de la agresividad de su afectación. Los marcadores biológicos implicados en señalización y tráfico celular son de gran interés; entre ellos se encuentra el receptor de quimioquinas CXCR4 que ha sido descrito en el tráfico de linfocitos B y en la diseminación de varias neoplasias.

El receptor de quimioquinas CXCR4 y su ligando SDF-1 (stromal cell-derived factor-1, también conocido como CXCL12), juegan un papel importante en el tráfico de linfocitos normales. CXCR4 funciona como un receptor de quimioquinas clásico en los adultos, y junto a su ligando, es esencial en procesos de organogénesis y hematopoyesis. Su expresión se ha detectado en varios tejidos y es predominante en las células hematopoyéticas. CXCR4 y SDF-1 también están implicados en el desarrollo de las células B normales y en varios de sus procesos homeostáticos como la retención de células B precursoras en la médula ósea y el *homing* de las células B hacia los ganglios linfáticos.

Además, el receptor y su ligando se han descrito en la migración y diseminación de células B tumorales en varias neoplasias hematológicas como en el linfoma de Burkitt, en el linfoma folicular y en la leucemia linfocítica crónica. La expresión del receptor CXCR4 se ha asociado con una disminución de la supervivencia de pacientes en varias neoplasias y también con la agresividad tumoral. En el LDCGB no se han publicado datos sobre la

implicación del receptor en la diseminación del linfoma ni tampoco su valor pronóstico en esta neoplasia.

Como hemos mencionado previamente, para poder desarrollar nuevos fármacos y estudiar la enfermedad, es necesario generar modelos murinos que reproduzcan las características clínicas observadas en pacientes con LDCGB. Los actuales modelos murinos de linfoma difuso de células grande (LDCGB) se generan mediante inyección intraperitoneal o subcutánea de las células tumorales, o bien por inyección intravenosa directa de células de linfomas agresivos como el linfoma de Burkitt. La primera estrategia genera linfomas localizados mientras que la segunda genera linfomas diseminados que no se asemejan al LDCGB. Además, la elevada heterogeneidad de los linfomas en cuanto a patogenia y respuesta a tratamiento dificulta la generación de modelos animales representativos de cada subtipo de linfoma. Por otro lado, el uso de modelos subcutáneos con enfermedad localizada, no diseminada, limita la traslación clínica de los resultados puesto que los linfomas, incluido el LDCGB, son neoplasias diseminadas. Así, es necesario generar nuevos modelos animales con LDGCB diseminado para el estudio de los mecanismos implicados en la diseminación del linfoma y la identificación de nuevos fármacos para su tratamiento.

Finalmente y en referencia al tratamiento de los pacientes, es importante seguir un protocolo terapeutico adecuado a la agresividad del linfoma. Generalmente el tratamiento estándar que se utiliza en pacientes con LDCGB es el R-CHOP, pero en caso de que el linfoma esté diseminado o el paciente haya recaído, se procede al transplante de médula ósea. Aún así, existen pacientes de LDCGB que presentan metástasis en el sistema nervioso central (SNC); aunque la incidencia es relativamente baja, 3-5%, esta afectación suele ser

mortal. Por este motivo, los pacientes con LDCGB diseminado que presentan alto riesgo de desarrollar metástasis en el SNC reciben terapia preventiva. Los protocolos preventivos se basan en la administración intratecal de metotrexato combinada o no con inyección intravenosa de altas dosis del mismo fármaco antitumoral. Sin embargo, el uso de este protocolo es aún controvertido debido a la compleja ruta de administración del fármaco y la falta de demostración de un claro beneficio.

En esta tesis se presenta la generación de modelos animales de LDCGB diseminado derivados de líneas celulares para el estudio de la enfermedad y para la evaluación de nuevas terapias. También evaluamos el efecto antitumoral de un inhibidor de adhesiones focales, E7123, en un modelo de LDCGB con afectación del sistema nervioso central. Además, basándonos en el papel de CXCR4 tanto en el tráfico de linfocitos B normales como en la diseminación de varias neoplasias, evaluamos la implicación de CXCR4 en la diseminación de LDCGB. Estos estudios se complementan con la evaluación de la expresión de CXCR4 y su valor pronóstico en biopsias ganglionares de pacientes con LDCGB.

RESULTADOS

1. GENERACIÓN Y VALIDACIÓN DE UN MODELO MURINO DE LINFOMA DIFUSO DE CÉLULAS GRANDES (LDCGB)

1.1. Obtención de células de LDCGB luminiscentes: Para generar un modelo de LDCGBB en el que pudiéramos realizar el seguimiento *in vivo* de las células tumorales fue necesario establecer líneas celulares de LDCGB que expresaran de manera constitutiva el gen de la *Luciferasa*. De este modo, se puede realizar el seguimiento por bioluminiscencia de la diseminación de las células de linfoma y evaluar la efectividad de fármacos antitumorales *in vivo* utilizando el sistema de imagen IVIS (*In vivo Imaging System*®, Caliper).

1.1.1 Generación de lentivirus que contienen el vector pSIN-DUAL-GFP1-Luciferasa: Debido a la dificultad de transfectar células de origen hematológico mediante las técnicas habituales de transfección, hemos generado lentivirus capaces de infectar las células y hacer que éstas expresen las proteínas de interés, GFP para el seguimiento *in vitro* y Luciferasa para el seguimiento *in vivo*.

1.1.2 Generación de líneas de linfoma que expresan GFP-Luciferasa: Una vez producidas y tituladas las partículas víricas, se infectaron las diferentes líneas de linfoma. El porcentaje de infección de cada línea celular se obtuvo mediante cuantificación de las células que expresaban GFP por citometría (FACS Calibur, BD). A continuación, las células positivas para GFP fueron seleccionadas mediante separación celular (FACSAaria, BD) para enriquecer la población fluorescente y que por tanto expresa el gen de la Luciferasa. Los porcentajes de GFP para cada línea celular antes y después del sorter se muestran en la **Tabla**

1. Las líneas celulares que han sido transducidas con el gen de la Luciferasa mediante infección con lentivirus son las siguientes: células de CG-LDCGB) TOLEDO, HT, OCI-Ly19, KARPAS-422, y las de ABC-LDCGB) OCI-Ly10, RIVA y SUDHL-2.

Tabla 1. Porcentajes de células GFP+ en las diferentes líneas celulares de LDCGB antes y después del proceso de separación.

Línea celular	%GFP Pre-sorter	%GFP Post-sorter
SUDHL-2	10.24	95.20
RIVA	28.81	98.93
OCI-Ly-10	14.89	94.29
OCI-Ly-19	17.75	96.39
TOLEDO	10.27	92.12
KARPAS-422	6.51	91.41
HT	8.32	92.71

1.2. Generación del modelo murino de LDCGB: La mayoría de células de linfoma inyectadas por vía intravenosa en ratones NOD/SCID, presentan una baja tasa de injerto y un tiempo de supervivencia demasiado largo para establecer un modelo animal útil para el estudio de la enfermedad. Nuestro grupo ha demostrado que el pase subcutáneo de las células de CG-LDCGB aumenta su agresividad y tasa de injerto. Con el objetivo de generar nuevos modelos que mejoren los establecidos en nuestro laboratorio, utilizamos el condicionamiento subcutáneo para evaluar la tasa de injerto y el patrón de diseminación de las células de LDCGB.

1.2.1 Evaluación del crecimiento subcutáneo de las líneas luminiscentes de LDCGB: Inicialmente evaluamos si las líneas celulares eran capaces de crecer subcutáneamente en los ratones NOD/SCID. Para ello, se realizó la inyección subcutánea de 7 líneas celulares luminiscentes de LDCGB. Las líneas inyectadas fueron TOLEDO, HT, OCI-Ly19, KARPAS-422, OCI-Ly10, RIVA y SUDHL-2. Las líneas celulares que generaron mayor número de tumores subcutáneos y que

además crecieron más rápidamente fueron SUDHL-2, RIVA, OCI-Ly10, TOLEDO y HT (**Tabla 2**). Estas líneas celulares se utilizaron para experimentos *in vivo* en los que estudiamos la diseminación de las células o el efecto antitumoral de un nuevo fármaco.

Tabla 2. Porcentaje de tumores subcutáneos (Sc) que crecieron por línea celular y tiempo que tardaron en alcanzar un volumen de 800-900 mm^3.

Línea celular	% Tumores Sc	Tiempo (días)
SUDHL-2	83.3	24
RIVA	75	28
OCI-Ly-10	91.6	25
TOLEDO	87.5	34
OCI-Ly-19	25	42
KARPAS-422	31.3	85
HT	48.8	56

1.2.2 Comparación de la agresividad de células de LDCGB con y sin condicionamiento subcutáneo: Los tumores subcutáneos de las líneas SUDHL-2, RIVA, OCI-Ly10 y TOLEDO fueron extraídos y disgregados mecánicamente. Posteriormente, las células se inyectaron por vía intravenosa en 6-10 ratones por cada línea celular. Además, se inyectaron también por vía intravenosa células sin condicionamiento subcutáneo en ratones NOD/SCID para evaluar las diferencias en tasa de injerto, diseminación y tiempo de supervivencia entre grupos (**Figura 1**). Los resultados obtenidos demuestran que el pase subcutáneo de las líneas celulares RIVA y Toledo, aumenta su agresividad. En estas líneas observamos que el pase subcutáneo provoca una disminución significativa del tiempo de supervivencia de los ratones (**Tabla 3**). Además, en la línea RIVA también observamos que el condicionamiento subcutáneo induce un aumento en la tasa de injerto y en la diseminación a ganglios linfáticos (GL), a médula ósea (MO) y al sistema nervioso central (SNC). Sin embargo, en la línea celular OCI-Ly10 observamos que el pase subcutáneo producía una disminución en su agresividad, que se traducía en un aumento de la supervivencia de los

ratones. Por último, la línea celular SUDHL-2 presentó la menor tasa de inserto (50%, **Tabla 3**) en ratones inyectados por vía intravenosa; además, el pase subcutáneo no produjo ningún cambio significativo en esta línea celular en cuanto a tiempo de supervivencia, tasa de injerto o diseminación.

Así, observamos que el efecto del pase subcutáneo en la agresividad depende de la línea celular. Además, disponemos de varios modelos luminiscentes de LDCGB, tanto CG como ABC, que nos permitirán estudiar los mecanismos de diseminación del linfoma y evaluar nuevos fármacos antineoplásicos.

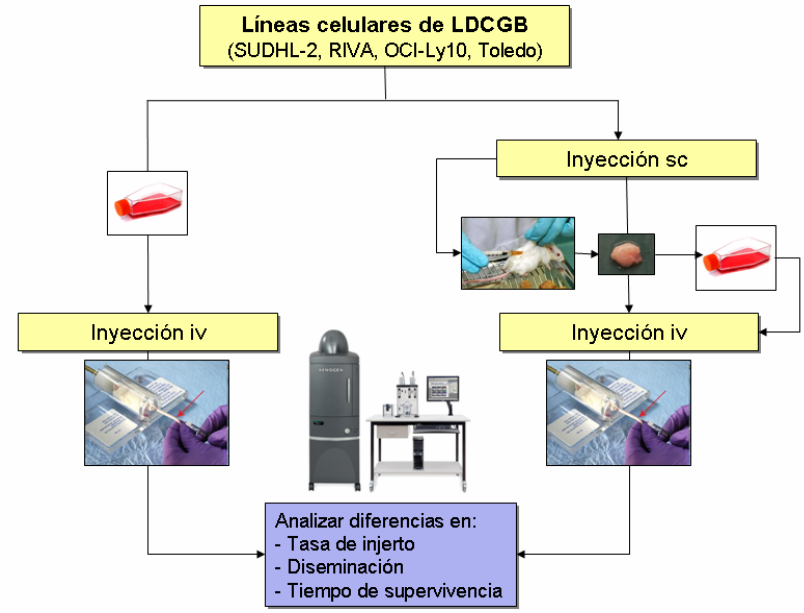

Figura 1. Esquema de los experimentos *in vivo* realizados con las células SUDHL-2, RIVA, OCI-Ly10 y Toledo.

Tabla 3. Características histopatológicas y clínicas de ratones NOD/SCID inyectados por vía intravenosa (iv) con células de LDCGB o con las células condicionadas subcutáneamente (Sc-iv).

	OCI-Ly10 (CXCR4 elevado)		**RIVA** (CXCR4 medio)		**SUDHL-2** (No CXCR4)		**Toledo** (CXCR4 elevado)	
	iv	**Sc-iv**	**iv**	**Sc-iv**	**iv**	**Sc-iv**	**iv**	**Sc-iv**
Ratones positivos, n(%)	6/6 (100)	6/6 (100)	5/6 (83.3)	6/6 (100)	3/6 (50)	2/6 (33)	9/9 (100)	10/10 (100)
Tiempo de supervivencia, días	29.6 ± 0.5	37.4 ± 0.8*	81.6 ± 9.5	52.7 ± 8.1*	67.3 ± 21.5	52 ± 35.4	37.8 ± 6.2	27.7 ± 1.5*
Ratones con infiltración de GL, n(%)	6/6 (100)	4/6 (66)	3/5 (60)	6/6 (100)	0/6 (0)	0/6 (0)	8/9 (88.8)	8/10 (80)
Ratones con infiltración de MO, n(%)	6/6 (100)	6/6 (100)	5/6 (83.3)	6/6 (100)	2/6 (33)	1/6 (16)	9/9 (100)	10/10 (100)
Columna o femur, n(%)	6/6 (100)	6/6 (100)	0/6 (0)	5/6 (83)*	2/6 (33)	0/6 (0)	9/9 (100)	10/10 (100)
Cráneo, n(%)	6/6 (100)	6/6 (100)	5/6 (83.3)	6/6 (100)	1/6 (16.6)	0/6 (0)	9/9 (100)	10/10 (100)
Ratones con infiltración del SNC, n(%)	6/6 (100)	6/6 (100)	5/6 (83.3)	6/6 (100)	0/6 (0)	0/6 (0)	9/9 (100)	10/10 (100)

Los ratones positivos son aquellos que desarrollan linfoma. Los valores de P se calcularon con el test Log rank para el tiempo de supervivencia y con el test exacto de Fisher para variables categóricas. Los valores se presentan como la media ± desviación estándar. *P <.05 cuando las características de ratones inyectados con células LDCGB por vía intravenosa (iv) fueron comparados con la inyección intravenosa de células con condicionamiento subcutáneo (Sc-iv). Los niveles de expresión de CXCR4 en membrana se indican entre paréntesis para cada línea celular. GL, ganglios linfáticos; MO, médula ósea; SNC, Sistema nervioso central.

1.3. Validación del modelo de LDCGB con ciclofosfamida: La ciclofosfamida, junto con otros agentes quimioterapicos, se utiliza habitualmente para el tratamiento de linfomas. Con el objetivo de evaluar si nuestro modelo de LDCGB diseminado era válido para el estudio de fármacos, evaluamos el efecto antitumoral de la ciclofosfamida. Previamente hicimos estudios de toxicidad

utilizando ratones sanos para determinar la pauta de administración. El modelo se validó con la línea celular Toledo condicionada subcutáneamente.

1.3.1 Ensayos de toxicidad *in vivo* de la ciclofosfamida (Genoxal®): Hicimos un ensayo de toxicidad utilizando ratones NOD/SCID sanos para determinar la dosis máxima tolerada (DMT) del fármaco. En base a la bibliografía, determinamos varias pautas y dosis de administración del fármaco. A partir de estos ensayos de toxicidad, decidimos administrar 60 mg/kg de ciclofosfamida por vía intravenosa cada 2 días por un total de 7 administraciones.

1.3.2 Validación del modelo de LDCGB: Una vez determinada la DMT de la ciclofosfamida, se evaluó su actividad antitumoral en el modelo Toledo-Sc. La administración se inició 7 días después de la inyección de las células. Los ratones fueron administrados por vía intravenosa con ciclofosfamida (grupo tratado) o con suero fisiológico (grupo control). Como se observa en la **Figura 2A**, la BLI aumenta más rápidamente en el grupo control. Además, la diseminación de las células es menor en el grupo tratado (**Figura 2B**) y la supervivencia de este grupo es mayor (**Figura 2C**). Por lo tanto, hemos demostrado que nuestro modelo murino de LDCGB responde al tratamiento con ciclofosfamida. Así, el modelo es apto para el estudio de la diseminación y para evaluar la eficacia de nuevos fármacos antitumorales.

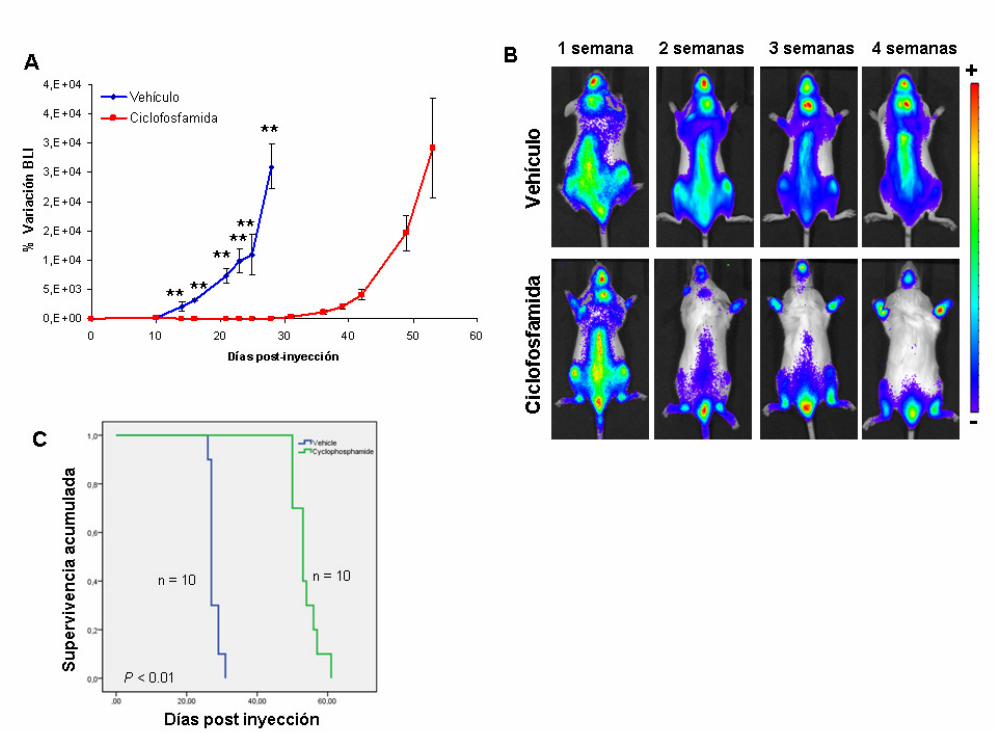

Figura 2. Validación del modelo murino de LDCGB con ciclofosfamida. **(A)** Curvas de cuantificación de la bioluminiscencia (BLI) en ratones administrados con vehículo (azul) o con Genoxal® (rojo). **(B)** Diseminación de células Toledo-Sc en ratones NOD/SCID administrados con vehículo (panel superior) o ciclofosfamida (panel inferior). La señal BLI disminuye a lo largo del tiempo para el grupo de ratones tratados con el fármaco. **(C)** Curvas de Kaplan-Meier de los ratones administrados con vehículo o ciclofosfamida. El tiempo de supervivencia fue superior en los ratones tratados con ciclofosfamida. El valor *P* fue calculado mediante el test Log-rank, **P < 0.01.

2. EVALUACIÓN DEL EFECTO DE UN INHIBIDOR DE ADHESIONES FOCALES, E7123, EN UN MODELO DE LDCGB CON AFECTACIÓN DEL SISTEMA NERVIOSO CENTRAL

2.1. Resultados previos: Mediante la inyección intravenosa de células HT condicionadas subcutáneamente, conseguimos generar un modelo murino de LDCGB con afectación del sistema nervioso central (SNC). Además, nuestro grupo demostró previamente que un fármaco inhibidor de las adhesiones focales, el E7123, induce apoptosis en líneas celulares de LDCGB y es capaz de reducir el volumen de tumores subcutáneos *in vivo*. En esta tesis, evaluamos el efecto del E7123 en un modelo bioluminiscente derivado de la línea celular HT con afectación del SNC.

2.2. Efecto antitumoral del E7123 en el modelo de LDCGB con afectación del SNC: Para evaluar el efecto antitumoral del E7123, inyectamos por vía intravenosa las células HT condicionadas subcutáneamente (HT-Sc) en 20 ratones NOD/SCID. Después de 10 días los animales fueron distribuidos en 2 grupos aleatoriamente y administrados diariamente con E7123 (75 mg/kg) o con vehículo (PEG:FBS) por vía oral. En la **Figura 3A** podemos observar imágenes de BLI del SNC representativas de cada grupo. Tanto en el ratón del grupo vehículo como en el del grupo tratado, la señal de BLI aparece en la semana 6 post-inyección de las células, pero en el grupo tratado la señal de BLI aumenta más lentamente. En el gráfico de cuantificación de la BLI (**Figura 3B**), observamos que los valores de BLI son superiores en el grupo vehículo que en el tratado con E7123. Además, la supervivencia del grupo de ratones tratado es significativamente superior a la del grupo vehículo (**Figura 3C**). Por lo tanto, el nuevo fármaco E7123 es capaz de atravesar la barrera hematoencefálica

produciendo una reducción del crecimiento del tumor en el SNC y aumentando la supervivencia de los ratones.

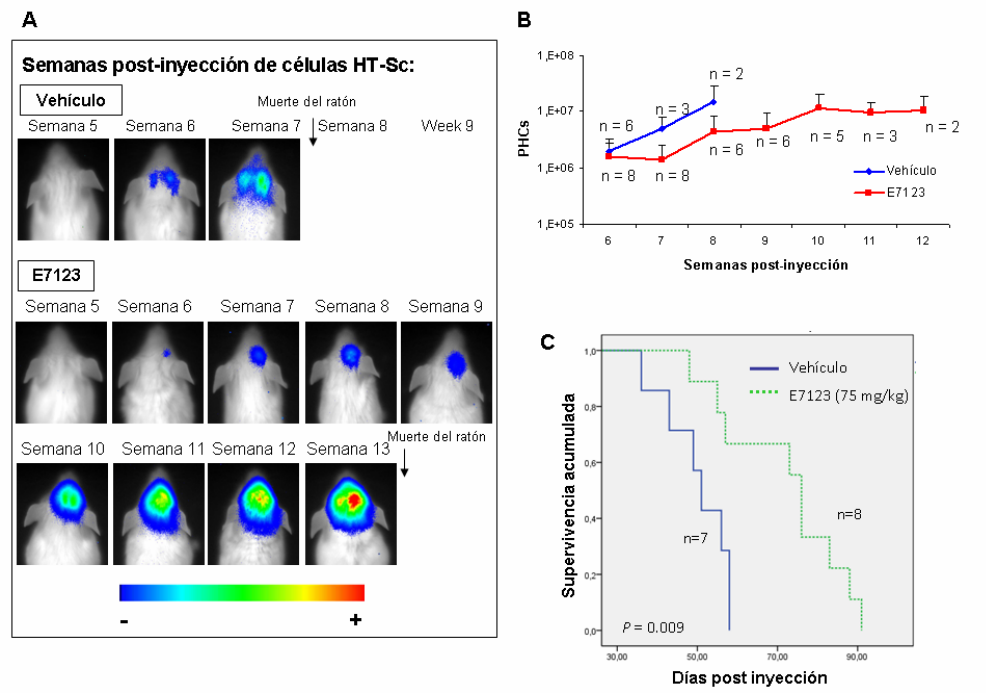

Figura 3. Efecto antitumoral del E7123 en un modelo de LDCGB con afectación de SNC. **(A)** Imágenes representativas de bioluminiscencia (BLI) muestran la infiltración del SNC de las células HT-Sc en ratones tratados con vehículo (PEG:FBS) o con E7123 (75 mg/kg). **(B)** Curvas de cuantificación de la señal de BLI para los ratones administrados con vehículo o con fármaco. La señal de BLI se expresa como *Photon Counts* (PHCs) ± desviación estándar. Las curvas representan la cinética de la intensidad media de BLI para cada uno de los grupos. Las barras de error representan el error estándar. **(C)** Las curvas Kaplan-Meier muestran que el tiempo de supervivencia en los ratones inyectados con las células HT-Sc es mayor en los ratones tratados con E7123 (75 mg/Kg) que en el grupo de ratones tratados con vehículo. El valor *P* fue calculado mediante el test Log-rank.

3. EVALUACIÓN DEL PAPEL DEL RECEPTOR CXCR4 EN LA MIGRACIÓN Y DISEMINACIÓN DE LDCGB

CXCR4 es un receptor de quimioquinas que se expresa preferentemente en células hematopoyéticas. Junto a su ligando SDF-1, está implicado en procesos de organogénesis, hematopoyesis y tráfico/diseminación de las células B. Además, en más de 20 neoplasias se ha asociado la expresión de CXCR4 con la agresividad tumoral. Por ello, hemos estudiado el papel de CXCR4 en la migración y diseminación de LDCGB.

3.1. Resultados *in vitro:*

3.1.1 Expresión de CXCR4 en células de LDCGB: Hemos evaluado la expresión del receptor tanto a nivel de mRNA como de proteína, en las líneas de LDCGB. Todas las líneas celulares expresan el receptor, a excepción de las SUDHL-2. Las líneas celulares OCI-Ly10 y Toledo son las que presentan niveles más elevados de CXCR4, y la línea celular RIVA presenta unos niveles intermedios. Además, existe una clara correlación entre los niveles de mRNA detectados por RT-PCR (**Figura 4A**) con los niveles del receptor obtenidos por immunohistoquímica y citometría (detección de la proteína en la membrana celular, **Figura 4B-C**).

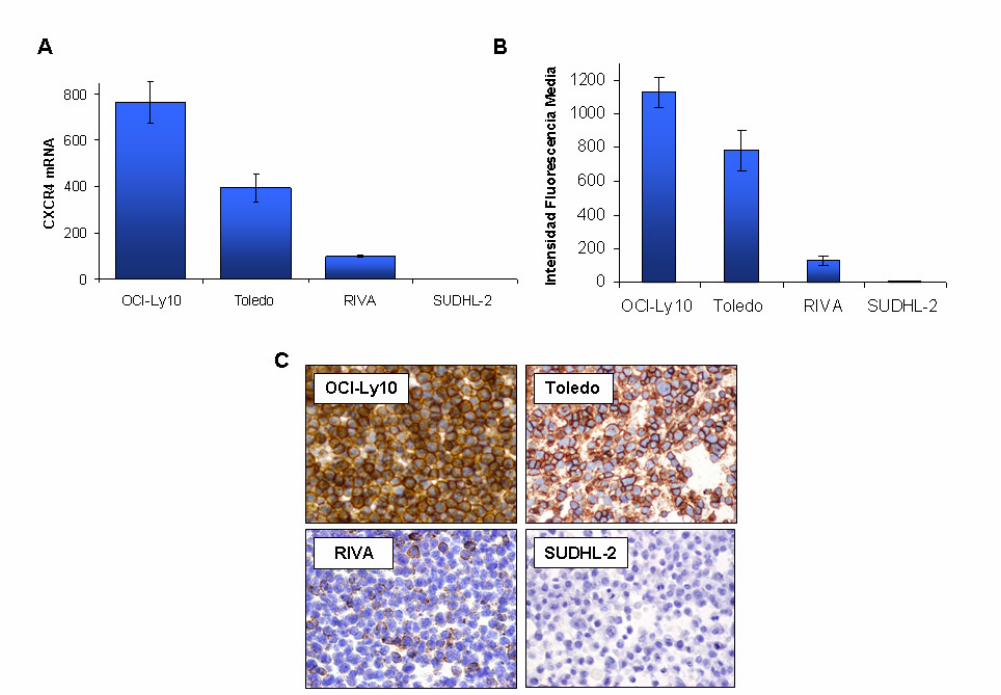

Figura 4. Expresión de CXCR4 en líneas celulares de LDCGB. **(A)** Niveles de mRNA CXCR4 en las líneas celulares de LDCGB. La expression relativa de mRNA CXCR4 es mayor en las células OCI-Ly10 seguidas de Toledo y RIVA. La línea celular SUDHL-2 no expresa el receptor. **(B)** Análisis mediante citometría de la expresión de CXCR4 en membrana de OCI-Ly10, Toledo, RIVA y SUDHL-2. Los niveles de expresión de CXCR4 en membrana correlacionan con los niveles de mRNA detectados. Datos presentados como la media ± desviación estándar. **(C)** Expresión de CXCR4 detectado mediante IHQ también correlaciona con los niveles de mRNA CXCR4. IHQ, immunohistoquímica.

3.1.2 Ensayos de migración en células de LDCGB: A continuación, evaluamos el papel del receptor en la migración *in vitro* de las células de LDCGB. Evaluamos si la quimioquina SDF-1α inducía la migración de las células que expresaban el receptor CXCR4 en comparación con las células en ausencia de estímulo. El nivel de migración de cada una de las líneas celulares correlacionaba con los niveles de expresión del receptor. Así, como se observa en la **Figura 5A**, OCI-Ly10 y Toledo presentaban una mayor migración que la línea celular RIVA. Además, la línea celular SUDHL-2, que no expresa CXCR4, no presentó

migración hacia SDF-1α. Para verificar que la migración era inducida por la quimiotaxis de las células que expresan CXCR4 hacia el gradiente de SDF-1α, utilizamos un antagonista específico de CXCR4, AMD3100. El antagonista AMD3100 inhibía la migración de todas las células que expresan el receptor CXCR4 (**Figura 5A**).

3.1.3 Regulación de CXCR4 mediada por SDF-1α en las líneas celulares de LDCGB: Por otra parte, evaluamos el efecto que producía la quimioquina SDF-1α en el receptor CXCR4. Incubamos las líneas de LDCGB en presencia de SDF-1α y posteriormente evaluamos la expresión del receptor mediante citometría e immunohistoquímica (IHQ). La exposición de las células a la quimioquina produce una significativa disminución de la expresión del receptor en membrana (**Figura 5B**). Además, mediante análisis por IHQ se detectó la internalización de CXCR4 inducida por SDF-1α. En la **Figura 5C** observamos un patrón punteado de tinción (*Dot-like*) en la línea celular Toledo. También vimos este patrón de tinción en las líneas RIVA y OCI-Ly10 expuestas a la quimioquina.

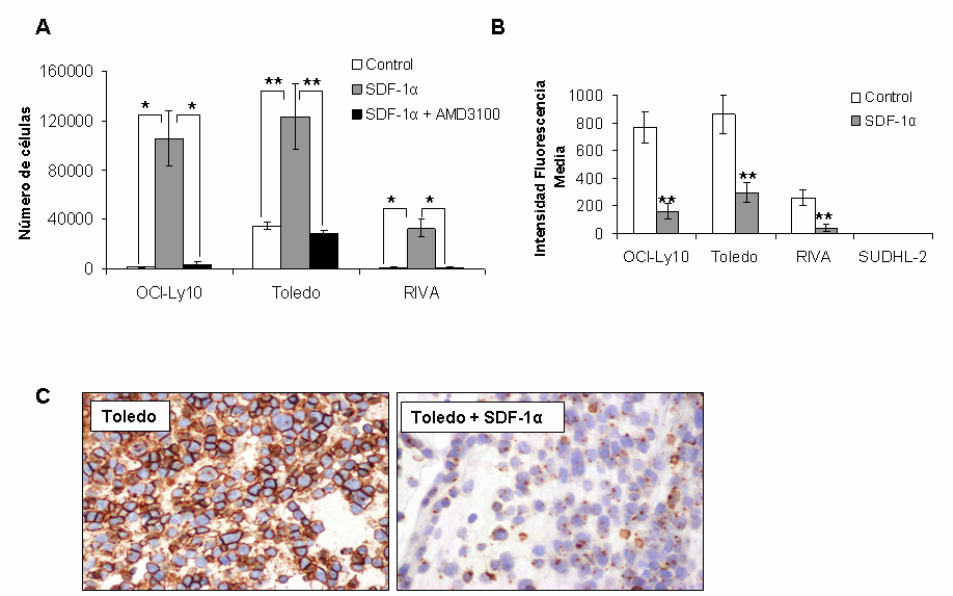

Figura 5. Migración de células de LDCGB y regulación de CXCR4 mediada por SDF-1α. **(A)** Ensayo de migración en presencia o ausencia de SDF-1α. Las células se incubaron en presencia o ausencia de AMD3100 (10 µg/ml) antes y durante el ensayo de migración. Se añadió SDF-1α (100 ng/ml) para estimular la migración y como control se utilizaron células no expuestas a la quimioquina. La incubación de las células con AMD3100 indujo una disminución significativa en la migración celular. **(B)** Regulación de CXCR4 mediada por SDF-1α. En ausencia de SDF-1α, se detectó expresión de CXCR4 en la membrana celular. En cambio, en presencia de la quimioquina, se detectó una significativa disminución en la expresión de CXCR4 en la membrana celular. **(C)** Mediante inmunohistoquímica se detectó la internalización de CXCR4 (tinción punteada) en el citoplasma tras la exposición de las células a SDF-1α (Toledo + SDF-1α). Datos presentados como la media ± desviación estándar; **P* <.05, ***P* <.01

3.1.4 Transfección de las células SUDHL-2 con plásmido pCXCR4: Mediante nucleofección transfectamos la línea celular SUDHL-2 con el plásmido pCXCR4 y seleccionamos los clones positivos mediante selección con antibióticos. Además, para obtener una población homogénea seleccionamos las células que expresaban CXCR4 mediante sorter celular. En la **Figura 6A** se muestra la expresión de CXCR4 en células transfectadas y control. El objetivo era evaluar si al inducir la expresión de CXR4 las células adquirían capacidad de migración inducida por SDF-1α. Como se observa en la **Figura 6B**, las células con expresión

del receptor, presentan una mayor capacidad de migración inducida por SDF-1α. Además, esta migración se inhibe en presencia del antagonista de CXCR4, AMD3100 (**Figura 6C**). Por otro lado, hicimos un ensayo preliminar en el que inyectamos ratones NOD/SCID con la línea celular SUDHL-2 y con las células SUDHL-2 pCXCR4 F3 Sort. Observamos el 50% de los ratones inyectados con las células que expresan el receptor presentan una infiltración de ganglios mientras que los ratones inyectados con las células parentales no presentan infiltración; aún así, se trata de un ensayo realizado con pocos ratones y habría que repetirlo para verificar estos resultados.

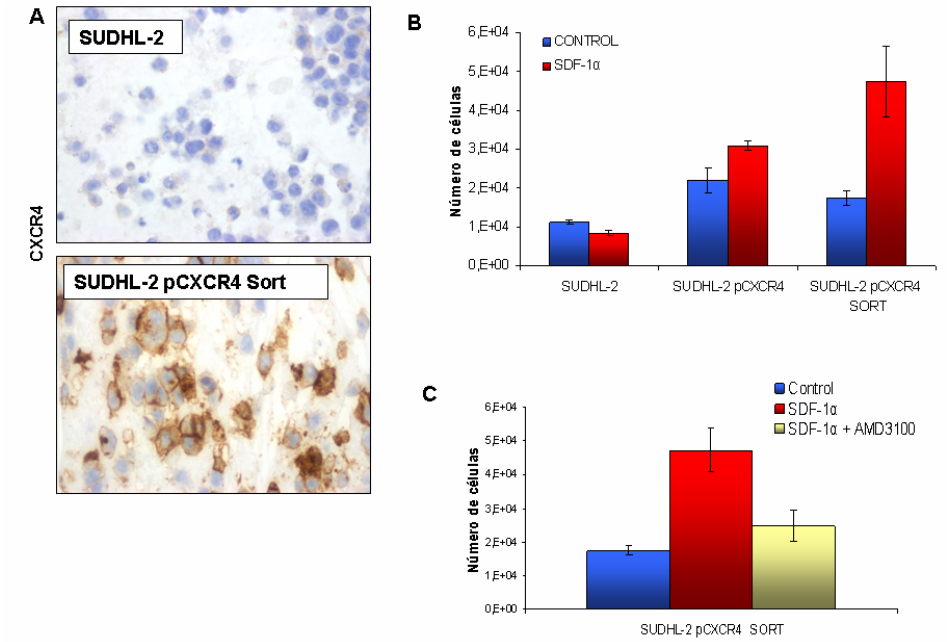

Figure 6. Expresión de CXCR4 y migración en las células SUDHL-2 transfectadas con pCXCR4. **(A)** Expresión de CXCR4 en los transfectantes SUDHL-2 pCXCR4 Sort en comparación con la línea parental SUDHL-2. Detección mediante immunohistoquímica. **(B)** La expresión de CXCR4 correlaciona con la migración de las células inducida por SDF-1α. **(C)** AMD3100 inhibe la migración de las células transfectantse SUDHL-2 pCXCR4 Sort expuestas a SDF-1α.

3.2 Resultados *in vivo:* Tras demostrar la relevancia de CXCR4 en la migración *in vitro* nos propusimos evaluar el papel de CXCR4 en la diseminación de las células de LDCGB en ratones NOD/SCID.

3.2.1 La expresión de CXCR4 correlaciona con agresividad en el modelo de LDCGB: Analizamos mediante IHQ la expresión del receptor en las líneas celulares, en las líneas con condicionamiento subcutáneo y en los órganos infiltrados. Las líneas celulares con mayor expresión de CXCR4 (Toledo y OCI-Ly10) presentan mayor agresividad, con elevada tasa de injerto y diseminación, y menor tiempo de supervivencia al ser inyectadas por vía intravenosa en ratones (**Tabla 1**). En cambio, la línea celular RIVA, con niveles intermedios de expresión del receptor, presenta una menor agresividad y un tiempo de supervivencia mayor al ser inyectada en ratones. Por último, la línea celular SUDHL-2, que no expresa CXCR4, presenta una tasa de injerto baja, un largo tiempo de supervivencia y poca diseminación en los ratones. En la **Figura 7A** podemos observar la evolución de la BLI en ratones inyectados con una de las líneas celulares con mayor expresión de CXCR4 (OCI-Ly10) en comparación con otra línea celular que no expresa el receptor (SUDHL-2). La señal de BLI aparece antes en los ratones inyectados con OCI-Ly10 y, además, la diseminación es mayor que en los ratones inyectados con las células SUDHL-2. También observamos una alta expresión de CXCR4 en la línea celular OCI-Ly10 y en las células tumorales que rodean el hueso de la MO, así como en células que infiltran el SNC y la parte externa de los GL. Además, se observa un patrón de tinción punteada (dot-like) de CXCR4 en la parte central de los GL y dentro de la MO, asociado con la internalización del receptor (**Figura 7B**). Por el contrario, no se detecta expresión de CXCR4 en la línea SUDHL-2 y fue prácticamente indetectable en los tejidos que infiltra (**Figura 7C**).

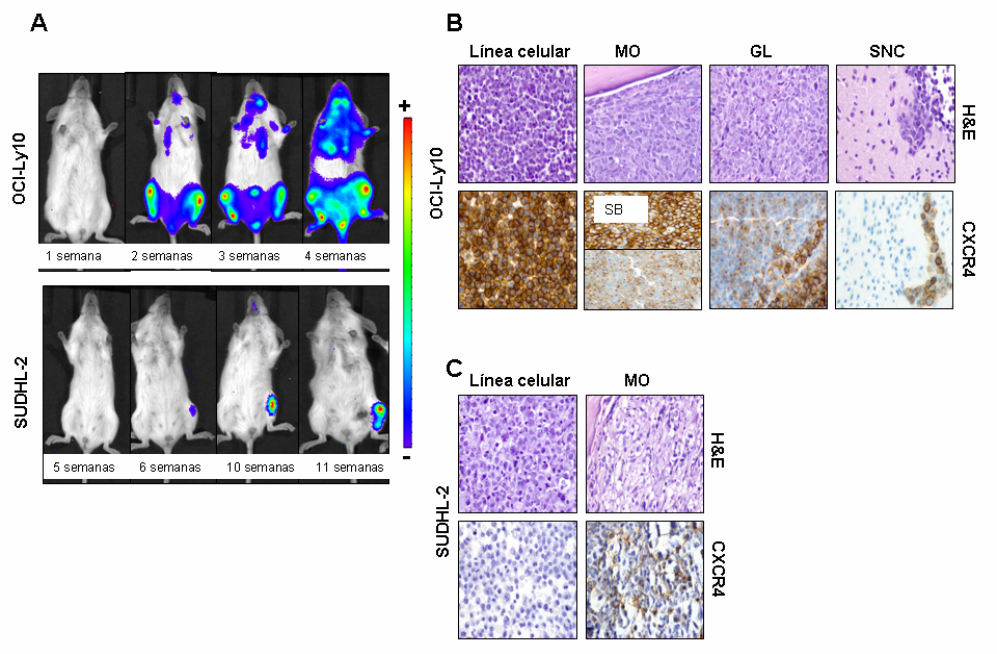

Figura 7. Los niveles de expresión de CXCR4 en las células OCI-Ly10 y SUDHL-2 correlacionan con su agresividad tras ser inyectadas en ratones. **(A)** Las imágenes de bioluminiscencia (BLI) muestran la diseminación de las células de linfoma en ratones inyectados con las células OCI-Ly10 o SUDHL-2. Las células OCI-Ly10 diseminan en un tiempo más corto e infiltran más órganos que las células SUDHL-2. **(B)** La expresión de CXCR4 en membrana se detectó en la línea celular OCI-Ly10 y en células tumorales que rodean el hueso de la MO, así como en células que infiltran el SNC y la parte externa de los GL. Se detectó una tinción puntuada del receptor en la parte central de los GL y dentro de la MO. También se muestran los órganos infiltrados por las células OCI-Ly10 (H&E) **(C)** La expresión de CXCR4 fue prácticamente indetectable en la MO infiltrada de ratones inyectados con las células SUDHL-2. También se muestran los órganos infiltrados por las células SUDHL-2 (H&E). SNC, sistema nervioso central; GL, ganglios linfáticos; MO, médula ósea; AH, alrededor del hueso; H&E, tinción hematoxilina-eosina.

3.2.2 El pase subcutáneo aumenta la expresión de CXCR4 y la agresividad en RIVA y Toledo: Analizamos si la expresión de CXCR4 se alteraba mediante el condicionamiento subcutáneo. Mediante el análisis de las líneas celulares condicionadas subcutáneamente, observamos que el nivel de CXCR4 aumentaba en las líneas Toledo y RIVA. Este aumento en la expresión del receptor, correlaciona con el aumento de agresividad observado al inyectar

estas líneas con condicionamiento subcutáneo en nuevos ratones. En la **Figura 8A** podemos ver como la BLI en los ratones inyectados con la línea celular RIVA condicionada subcutáneamante (RIVA-Sc), aparece antes y presenta mayor diseminación que en los ratones inyectados con RIVA. Además, los ratones inyectados con la línea condicionada RIVA-Sc, presentan una disminución significativa de la supervivencia (**Figura 8B**). La infiltración ganglionar tanto macroscópica como microscópica de estas células en los ratones inyectados se observa en la **Figura 8C-D**. También se muestra como la expresión de CXCR4 aumenta al hacer el pase subcutáneo y como este aumento se mantiene en los tejidos infiltrados (**Figura 8E**). En MO, GL y SNC, se detecta una tinción puntuada del receptor tal y como habíamos observado en los experimentos *in vitro* (tinción Dot-like, que indica la internalización de CXCR4). Resultados muy parecidos se obtuvieron para la línea celular Toledo (**Figura 9**). En cambio, el condicionamiento subcutáneo en la línea OCI-Ly10, produjo una disminución en la expresión del receptor CXCR4. Esta disminución correlaciona con la disminución en la agresividad de las células, que se traduce en un mayor tiempo de supervivencia de los ratones inyectados (**Tabla 3**). Por último, no observamos ninguna diferencia significativa en la expresión de CXCR4 en la línea celular SUDHL-2 comparada con la línea condicionada subcutáneamente y con los tejidos infiltrados por la misma línea. En esta línea celular, el condicionamiento subcutáneo no produce ningún cambio en el patrón de agresividad de la línea celular, coincidiendo con la no alteración la expresión del receptor CXCR4 (**Tabla 3**).

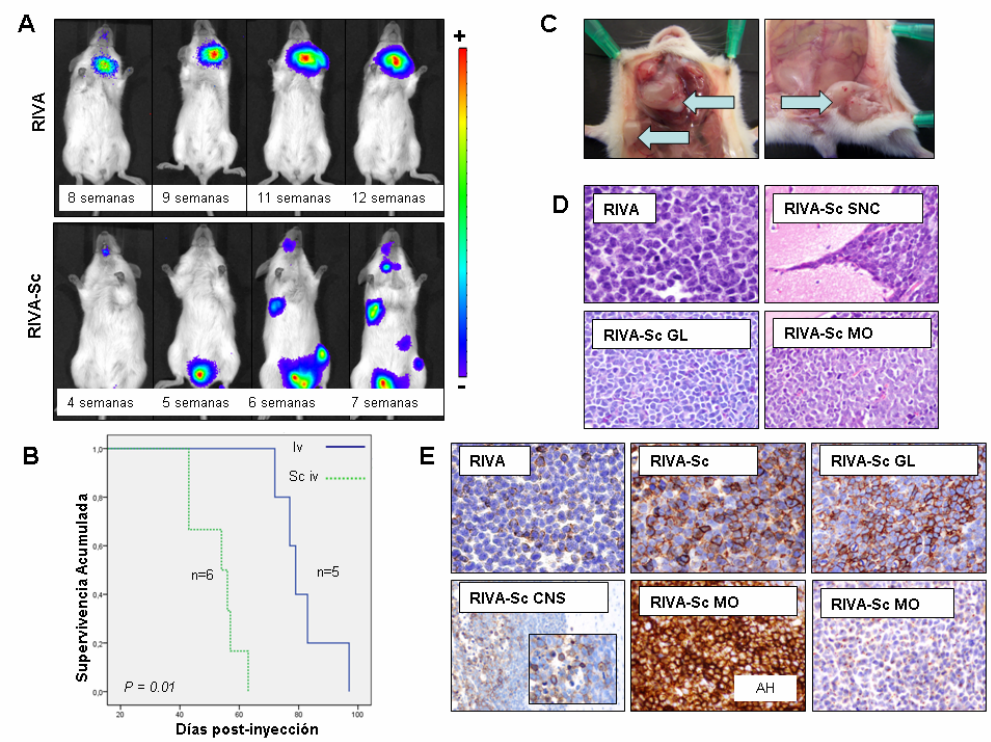

Figura 8. El condicionamiento subcutáneo de las células RIVA aumenta su agresividad tras ser inyectadas en ratones. **(A)** La diseminación de las células de linfoma en ratones inyectados con células RIVA fue menor que en ratones inyectados con células condicionadas subcutáneamente, RIVA-Sc. **(B)** Las curvas de Kaplan-Meier muestran una significativa reducción del tiempo de supervivencia en ratones inyectados con RIVA-Sc en comparación con ratones inyectados con las células RIVA, valor *P* calculado con el test Log-Rank. **(C)** Infiltración macroscópica de GL cervical, axilar (izquierda) y caudal (derecha) en ratones inyectados con células RIVA-Sc. **(D)** Tinción H&E de RIVA y secciones de SNC, GL y MO infiltradas con las células RIVA-Sc. **(E)** Immunoreactividad de CXCR4 en RIVA, RIVA-Sc, y en secciones representativas de GL, SNC y MO infiltradas con las células RIVA-Sc. Magnificación original x400. SNC, sistema nervioso central; GL, ganglios linfáticos; MO, médula ósea; AH, alrededor del hueso; H&E, tinción hematoxilina-eosina.

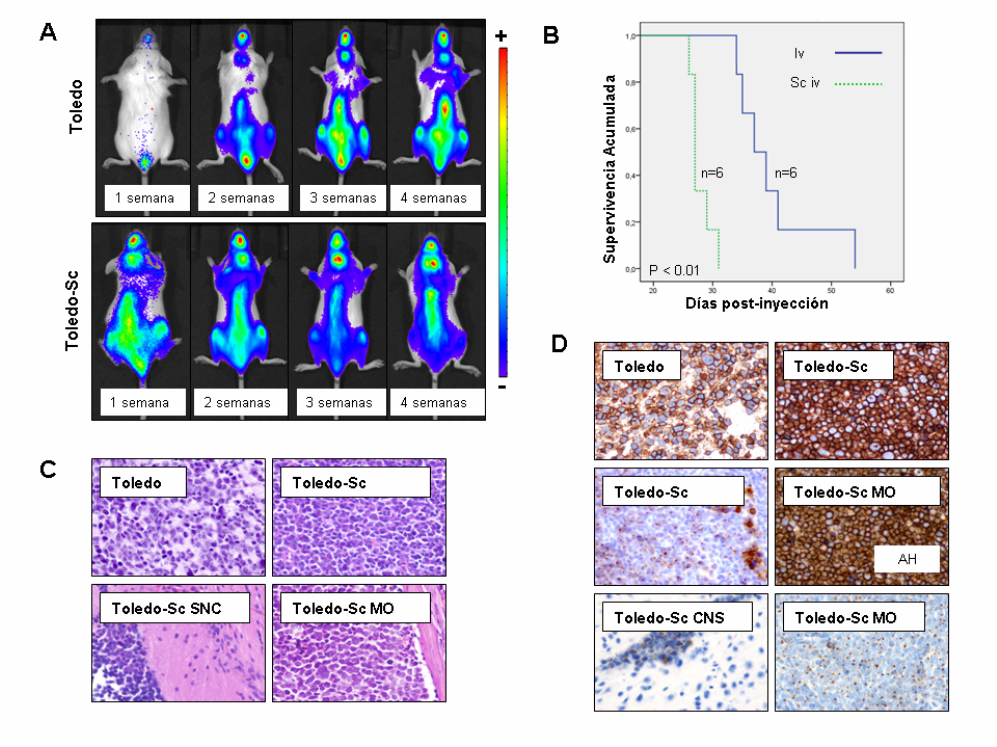

Figura 9. El condicionamiento subcutáneo de las células Toledo aumenta su agresividad tras ser inyectadas en ratones. **(A)** En las imágenes de BLI se observa una menor diseminación de las células de linfoma en los ratones inyectados con las células Toledo que en los ratones inyectados con Toledo-Sc. **(B)** El análisis de supervivencia mediante Kaplan-Meier muestra una significativa reducción en el tiempo de supervivencia en los ratones inyectados con las células Toledo-Sc en comparación con los ratones inyectados con Toledo. Valor *P* calculado con el test Log-Rank. **(C)** Tinción H&E de las células Toledo y secciones representativas de GL, MO y SNC infiltrados con células Toledo-Sc. **(D)** Inmunoreactividad de CXCR4 en Toledo, Toledo-Sc, y en secciones infiltradas de GL, MO y SNC. Magnificación original x400. SNC: sistema nervioso central; GL: ganglios linfáticos; MO: médula ósea; AH, alrededor del hueso; H&E, tinción hematoxilina-eosina.

3.2.3 El bloqueo de CXCR4 disminuye la diseminación de células de LDCGB: Por último, hicimos un ensayo funcional *in vivo* para demostrar que las diferencias observadas en diseminación estaban relacionadas con el receptor CXCR4. Primero hicimos ensayos *in vitro* para confirmar que el inhibidor de CXCR4,

AMD3100, no inducía muerte celular. Posteriormente, inyectamos células OCI-Ly10 (altos niveles de CXCR4) con o sin pretratamiento con el inhibidor por vía intravenosa en ratones NOD/SCID. Los ratones inyectados con células pretratados fueron administrados diariamente por vía intraperitoneal con AMD3100 (10 mg/kg). Además, se utilizó un grupo de ratones control a los que se le administró diariamente suero fisiológico. Como podemos observar en la **Figura 10A-B**, la diseminación de las células es menor en el grupo de ratones tratados con AMD3100. Además, en los ratones tratados se observó menor diseminación a ganglios de las células de LDCGB. Así, podemos concluir que el bloqueo de CXCR4 disminuye la diseminación de las células de LDCGB *in vivo*.

3.3 Resultados con pacientes de LDCGB: Hemos evaluado la expresión de CXCR4 mediante inmunohistoquímica en 42 biopsias ganglionares de pacientes con LDCGB nodal primario. Como se observa en la **Figura 10C**, las curvas de Kaplan-Meier muestran una significativa disminución en la supervivencia libre de progresión (SLP) en los pacientes que expresan CXCR4 en membranaLas curvas de Kaplan-Meier también muestran una tendencia hacia una disminución de la supervivencia global (**Figura 10D**) en los pacientes que expresan el receptor; aun así, las diferencias observadas en SG entre los grupos dicotomizados no fueron significativas.

La estratificación de la expresión de CXCR4 en función de los parámetros clínicos de los pacientes de LDCGB (**Tabla 4**), también muestra una tendencia hacia la correlación entre pacientes que expresan el receptor y el riesgo de recaída (P = 0.069). El análisis univariante de COX indicó que el *Eastern Cooperative Oncology Group* (ECOG, <2 *vs* ≥2), el *International Prognosis Index* (IPI, 0-2 *vs* 3-4) y la expresión de CXCR4 (positivo *vs* negativo), son predictores

de la SLP. Además, el análisis multivariante de COX, mostró que tanto ECOG (<2 *vs* ≥2) como CXCR4 (positivo *vs* negativo) seguían siendo factores que predicen la SLP (**Tabla 5**) con un *Hazard ratio* de 5.470 (95% IC, 1.903 - 15.720; *P* = 0.002) y 3.729 (95% CI, 1.202 - 11.574; *P* = 0.023), respectivamente. En el análisis de COX para la supervivencia global, IPI y ECOG son predictores significativos de supervivencia pero la expresión de CXCR4 no presentó significación estadística (*P* = 0.111).

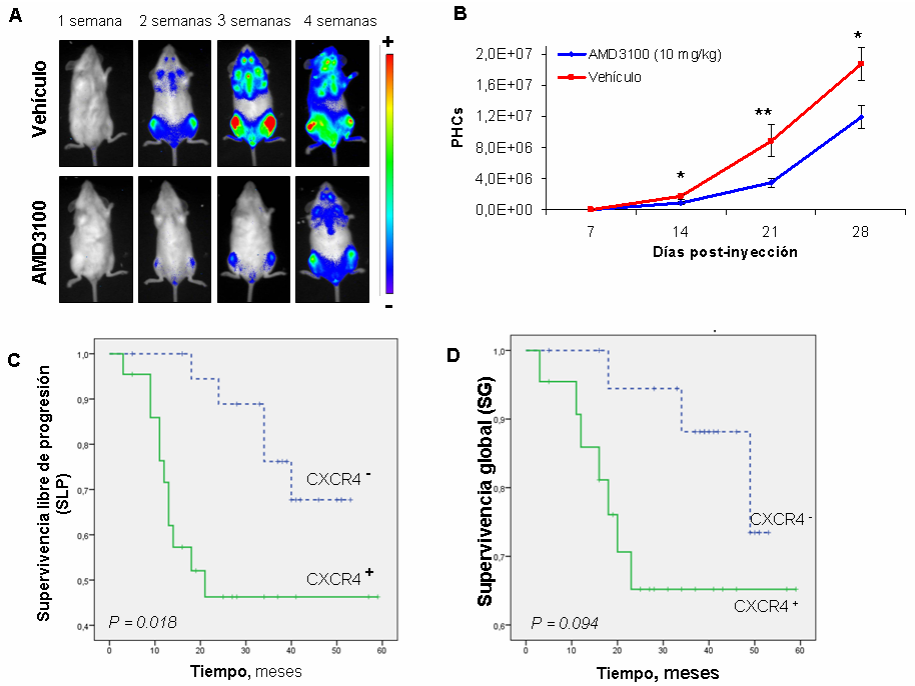

Figura 11. AMD3100 disminuye la diseminación de las células de LDCGB en ratones NOD/SCID y la expresión de CXCR4 correlaciona con recaída en pacientes de LDCGB. **(A)** Diseminación de células OCI-Ly10 en ratones NOD/SCID administrados con vehículo (panel superior) o AMD3100 (panel inferior). La señal BLI aparece más tarde en el grupo de ratones tratados con el antagonista de CXCR4. **(B)** Curvas de cuantificación de la bioluminiscencia (BLI) en ratones administrados con vehículo o con AMD3100. La señal de BLI del grupo de ratones vehículo es mayor que la del grupo de ratones tratados con AMD3100. La señal de BLI se expresa como *Photon Counts* (PHCs) ± desviación estándar. El valor *P* fue calculado mediante el test de Mann-Whitney, *<0.05, **<0.01. **(C)** Los pacientes con expresión de CXCR4 muestran un mayor riesgo de muerte o recidiva que los pacientes que no expresan el receptor. **(D)** Las curvas de Kaplan-Meier de supervivencia global indican que aunque se observa una menor supervivencia de los

pacientes que expresan CXCR4, no hay diferencias significativas entre grupos. Valor *P* calculado mediante el test Log-rank.

Tabla 4. Correlación entre la expresión de CXCR4 y las características clínico-patológicas de los pacientes de LDCGB.

	Expresión CXCR4		
Características clinico-patológicas	**Negativo**	**Positivo**	***P***
Edad			
<60 *(n=20)*	11 (26)	9 (21)	0.537
≥60 *(n=22)*	9 (21)	13 (31)	
Género			
Hombre *(n=21)*	10 (24)	11 (26)	1
Mujer *(n=21)*	10 (24)	11 (26)	
Médula ósea			
Negativa *(n=36)*	19 (46)	17 (41)	0.343
Positiva *(n=5)*	1 (2)	4 (10)	
LDH suero			
Normal *(n=18)*	9 (22)	9 (22)	1
Elevado *(n=23)*	11 (27)	12 (29)	
Estadío			
I-II (n=23)	14 (34)	9 (22)	0.118
III-IV (n=18)	6 (15)	12 (29)	
ECOG performance status			
0-2 *(n=34)*	18 (43)	16 (38)	0.243
> 2 *(n=8)*	2 (5)	6 (14)	
IPI			
Bajo riesgo *(n=17)*	10 (24)	7 (17)	
Bajo/Intermedio *(n=8)*	4 (10)	4 (10)	0.464
Alto/Intermedio *(n=10)*	5 (12)	5 (12)	
Alto riesgo *(n=6)*	1 (2)	5 (12)	
Quimioterapia			
R-CHOP *(n=37)*	18 (44)	19 (46)	1
Others *(n=4)*	2 (5)	2 (5)	
Recaída			
No *(n=25)*	15 (37)	10 (24)	0.069
Si *(n=16)*	5 (12)	11 (27)	
Subtipo de LDCGB			
No-GCB *(n=16)*	10 (30)	6 (18)	0.491
GCB *(n=17)*	8 (24)	9 (27)	

n (%), pacientes para cada variable evaluada. Los valores de P se calcularon con el test exacto de Fisher. *P <0.05. LDH, lactate dehydrogenase; ECOG, Eastern Cooperative Group; IPI, International Prognostic Index.

Tabla 5. Regresiones de COX univariante y multivariante para analizar la supervivencia libre de progresión en pacientes de LDCGB.

	Supervivencia Libre de Progresión			
	Regression COX Univariante		**Regression COX Multivariante**	
	HR (IC 95%)	***P***	**HR (IC 95%)**	***P***
CXCR4 (+ *vs* -)	3.387 (1.155 – 9.930)	0.026*	3.729 (1. 202 - 11.574)	0.023 *
ECOG (0-2 *vs* >2)	5.575 (2.052 – 15.144)	0.001*	5.470 (1.903 – 15.720)	0.002*
IPI (0-2 *vs* 3-5)	3.060 (1.106 – 8.466)	0.031*	2.636 (0.934 – 7.440)	0.067
Stage (I-II *vs* III-IV)	2.025 (0.747 – 5.486)	0.165		
LDH (normal *vs* alto)	2.001 (0.692 – 5.784)	0.200		
BM (+ *vs* -)	1.843 (0.518 – 6.563)	0.345		
GCB (si *vs* no)	1.073 (0.268 – 4.299)	0.920		
Age (< 60 *vs* ≥ 60)	1.522 (0.565 – 4. 099)	0.406		

Sólo las variables significativas para el análisis univariante se incluyeron en el análisis de COX multivariante. HR, hazard ratio; 95% IC, intervalo de confianza para el hazard ratio; ECOG, Eastern Cooperative Group; LDH, lactate dehydrogenase; IPI, International Prognostic Index; MO, médula ósea; GC, centro germinal. *P <0.05

DISCUSIÓN

1. GENERACIÓN DE NUEVOS MODELOS MURINOS BIOLUMINISCENTES DE LINFOMA DIFUSO DE CÉLULAS GRANDES (LDCGB) CON PATRÓN DISEMINADO

En esta tesis, se han generado líneas celulares bioluminiscentes de LDCGB tanto derivadas de centro germinal (CG) como activadas (ABC). La inyección intravenosa de estas células bioluminiscentes en ratones NOD/SCID ha permitido generar varios modelos de LDCGB que reproducen las características clínicas observadas en pacientes. Además, la bioluminiscencia nos ha permitido monitorizar de manera no agresiva y mediante técnicas de captación de imagen, la diseminación de las células de linfoma así como también la respuesta a fármacos de los modelos.

Mediante la inyección intravenosa de varias líneas celulares de LDCGB-ABC (RIVA, OCI-Ly10, SUDHL-2) y de LDCGB-CG (Toledo) en ratones NOD/SCID, hemos generado diferentes modelos de LDCGB con patrón diseminado. Las líneas celulares OCI-Ly10 y Toledo presentaron un patrón más agresivo, con diseminación hacia ganglios linfáticos (GL), médula ósea (MO) y sistema nervioso central (SNC); además, presentaron una tasa de injerto del 100% y un tiempo de supervivencia corto al ser inyectadas en ratones. Aunque la línea celular RIVA presentó una menor tasa de injerto (83.3%), también generó un linfoma difuso diseminado con afectación de GL, MO y SNC en varios animales. Por el contrario, la línea celular SUDHL-2 presentó un 50% de tasa de injerto e infiltración de MO en sólo un 33% de los ratones inyectados; esta línea no generó infiltración en CNS ni en GL.

Los modelos bioluminiscentes generados en esta tesis son útiles para estudiar los mecanismos moleculares implicados en la diseminación y en la agresividad tumoral, así como también para la evaluación de nuevos fármacos antitumorales. Es importante mencionar que los modelos de LDCGB previamente descritos en la literatura se basan en la injección intravenosa o subcutánea de líneas celulares agresivas; mayoritariamente se utilizan células derivadas del linfoma de Burkitt que no representan la patología del LDCGB puesto que se trata de una neoplasia totalmente distinta, caracterizada por otros procesos moleculares y con diferente tratamiento.

Además, evaluamos si el pase subcutáneo aumentaba la agresividad en todas las líneas celulares de LDCGB; para ello comparamos la agresividad de las células con y sin condicionamiento subcutáneo al ser inyectadas por vía intravenosa en ratones NOD/SCID. Observamos que algunas líneas celulares, (Toledo y RIVA) aumentaban su agresividad, mientras que otras (SUDHL-2 y OCI-Ly10) no lo hacían. Los resultados obtenidos indican que los cambios inducidos por el condicionamiento subcutáneo son independientes del origen de las células (CG vs ABC), y que, por lo tanto, otros mecanismos deben estar implicados. Los mecanismos implicados pueden derivar de las mutaciones concretas que contiene cada una de las líneas celulares y la reprogramación epigénetica inducida por el ambiente. El microambiente tumoral puede inducir que se recupere la firma epigenética que originalmente estaba presente en el tumor del cual fueron extraídas las células. Así pues, tanto las mutaciones específicas de las células como mecanismos epigenéticos, deben estar implicados en la adaptación clonal, crecimiento y diseminación de aquellas líneas tumorales que aumentan su agresividad mediante el condicionamiento subcutáneo.

Finalmente, con objeto de evaluar si nuestros modelos de LDCGB con patrón diseminado eran válidos para el estudio de fármacos, probamos el efecto antitumoral de la ciclofosfamida en el modelo generado con la línea celular Toledo. Observamos que la administración de ciclofosfamida prolongó el tiempo de supervivencia de los ratones y además disminuyó la diseminación del linfoma, tal y como se observa en los pacientes. Por ese motivo, los modelos generados mediante una simple inyección intravenosa de las células de LDCGB con o sin precondicionamiento subcutáneo, son aptos para la evaluación de nuevos fármacos antitumorales.

2. EVALUACIÓN DEL EFECTO ANTITUMORAL DE UN INHIBIDOR DE ADHESIONES FOCALES, E7123, EN UN MODELO DE LDCGB CON AFECTACIÓN DEL SISTEMA NERVIOSO CENTRAL

La afectación del sistema nervioso central (SNC) en pacientes con LDCGB se observa en el 3-5% de los casos y, aunque esta afectación es minoritaria, suele ser fatal. Además, los fármacos incluídos en la terapia estándar para el tratamiento de los pacientes, R-CHOP, no son capaces de travesar la barrera hemato-encefálica, con lo cual no pueden prevenir ni tratar la afectación del SNC. Por ello es de extrema necesidad desarrollar y evaluar nuevos fármacos que permitan tratar o prevenir la afectación del SNC en estos pacientes.

En esta tesis evaluamos el efecto antitumoral de un nuevo fármaco inhibidor de las adhesiones focales, el E7123, en un modelo de LDCGB diseminado con afectación del SNC. Este fármaco se obtuvo mediante modificación de la estructura del celecoxib y previamente demostró tener una mayor capacidad antitumoral en células de LDCGB tanto *in vitro* como en tumores subcutáneos crecidos en ratones immunodeprimidos.

Con el fin de evaluar el efecto antitumoral del E7123 utilizamos un modelo bioluminiscente de LDCGB diseminado con afectación del SNC basado en el condicionamiento subcutáneo de las línea celular HT (previamente descrito por nuestro grupo). Observamos que el E7123 aumenta el tiempo de supervivencia de los ratones y que, aunque no es capaz de inhibir la diseminación tumoral, enlentece el crecimiento de las células de linfoma una vez que estas han colonizado el cerebro. De este modo, este fármaco es capaz de cruzar la barrera hemato-encefálica y ejercer su efecto antitumoral en ratones con afectación del SNC. Además, el fármaco es bien tolerado y su administración oral facilita que pueda ser evaluado en análisis clínicos con pacientes de LDCGB que presentan afectación del SNC.

Finalmente, destacamos que el modelo luminiscente de LDCGB con afectación del SNC es una herramienta útil para desarrollar y evaluar nuevas terapias. Este modelo se obtiene mediante una simple inyección intravenosa de las células precondicionadas subcutáneamente, una ventaja respecto a otros modelos descritos en la literatura en los que se inyectan por vía intratecal células agresivas, generalmente de Burkitt, que acaban generando un linfoma localizado en el SNC en vez de un linfoma diseminado con afectación del SNC. Nuestro modelo bioluminiscente permite el seguimiento del linfoma *in vivo* mediante técnicas de captación de imagen. Además, el modelo reproduce las características clínicas observadas en pacientes con afectación mayoritaria de leptomeninges y, en consecuencia, es apto para estudiar mecanismos moleculares implicados en la patología y nuevos fármacos antitumorales.

Basándonos en los resultados obtenidos, el inhibidor de adhesiones focales, E7123, merece más investigación para su futura administración en pacientes de

LDCGB que no responden al tratamiento convencional o que recaen después del tratamiento.

3. PAPEL DEL RECEPTOR CXCR4 EN LA DISEMINACIÓN Y AGRESIVIDAD DE LOS MODELOS DE LDCGB

En esta tesis describimos el importante papel que juega el receptor de quimioquinas CXCR4 en la migración de células de LDCGB *in vitro* y en la diseminación de las mismas al ser inyectadas en ratones NOD/SCID. Observamos que las células con mayor expresión de CXCR4 en membrana (Toledo y OCI-Ly10, seguidas de RIVA) presentan una mayor migración inducida por la quimioquina SDF-1α en ensayos de migración. Además, al inyectar las células por vía intravenosa en ratones NOD/SCID, las células con mayor expresión de CXCR4 en membrana presentan una mayor tasa de injerto así como una mayor diseminación e infiltración de órganos que expresan la quimioquina SDF-1α, como médula ósea (MO) y ganglios linfáticos (GL). Los ratones inyectados con células que tienen elevados niveles de CXCR4 en membrana presentan un menor tiempo de supervivencia.

Nuestros resultados coinciden con otros artículos en los que se demuestra que tanto la MO como los GL presentan niveles elevados de la quimioquina SDF-1; también se ha descrito que las células que expresan CXCR4 en membrana son atraídas por gradientes de la quimioquina hasta el tejido diana. Además, se han descrito otros modelos animales, como un modelo murino de cáncer de mama, en el que también se observa como las células tumorales con expresión de CXCR4 en membrana metastatizan a órganos que contienen elevados niveles de la quimioquina SDF-1. Basándonos en la literatura, se ha descrito que los órganos con mayor concentración de SDF-1α son la MO y los

GL. Nuestra hipótesis en cuanto al patrón de diseminación de las células de linfoma sería que éstas primero colonizan los GL y la MO, y posteriormente, por proximidad al cerebro (donde también hay expresión de SDF-1α) acaban infiltrando el órgano. Esta propuesta tendría que ser estudiada mediante nuevos experimentos para poder entender el proceso metastásico que siguen las células de linfoma.

También observamos en nuestros modelos de LDCGB que el pase subcutáneo alteraba los niveles de CXCR4 en la membrana de las células. Estos cambios inducidos por el condicionamiento subcutáneo correlacionaban con la agresividad de las células; las células en las que el subcutis inducía mayor expresión de CXCR4 presentaban un fenotipo más agresivo con mayor diseminación y tasa de injerto, así como un menor tiempo de supervivencia de los ratones inyectados.

Nuestros resultados correlacionan con otros estudios en los que se ha demostrado que la expresión de CXCR4 en membrana aumenta la diseminación en varias neoplasias de células B como por ejemplo en leucemia linfocítica crónica y en linfoma del manto. Otros autores también han descrito el receptor CXCR4 en la diseminación ganglionar en otras neoplasias hematológicas. Aunque nuestros resultados indican que CXCR4 juega un papel importante en la agresividad del LDCGB y correlacionan con estudios descritos en la literatura, es necesario seguir investigando para confirmar estos resultados. Nuestros modelos bioluminiscentes pueden ser una herramienta útil para estudiar los mecanismos moleculares implicados en la desregulación de CXCR4 en la neoplasia, especialmente en términos de internalización (patrón de tinción punteada), desensibilización y reciclaje del receptor. También sería interesante

estudiar como el entorno tumoral en los tejidos infiltrados (MO, GL y SNC) puede contribuir en el proceso de metástasis.

Finalmente, para demostrar funcionalmente el papel del receptor CXCR4 en la agresividad del LDCGB, utilizamos un antagonista de CXCR4, AMD3100. Demostramos que el AMD3100 bloquea la migración inducida por SDF-1α *in vitro* y, además, es capaz de disminuir la diseminación de las células a GL en uno de los modelos murinos generados. Demostramos que las dosis de AMD3100 utilizadas no inducen muerte celular sino que inhiben la diseminación tumoral. Además, observamos que aunque el AMD3100 enlentece la diseminación de las células tumorales a MO y SNC, el inhibidor no consigue bloquear la diseminación a estos órganos. Por ello, sería interesante estudiar otros receptores de quimioquinas o moléculas de adhesión que puedan estar implicados en la diseminación de las células y/o colonización de estos órganos; también sería importante estudiar como el microambiente de GL, MO y SNC regula la expresión del receptor CXCR4 para así poder enteneder las consecuencias asociadas con diseminación tumoral.

Nuestros resultados correlacionan con otros experimentos descritos en la literatura en los que se han utilizado varios inhibidores de CXCR4 para inhibir la diseminación de las células tumorales en modelos de osteosarcoma, melanoma y cáncer de mama, entre otros. Además, también se han descrito otros estudios pre-clínicos en los que se utilizan inhibidores de CXCR4 para inhibir el crecimiento tumoral, inducir apoptosis o sensibilizar las células frente a agentes citotóxicos. Por último, es importante mencionar que el inhibidor de CXCR4, AMD3100, ya ha sido utilizado en pacientes para inducir la mobilización de células progenitoras con el objetivo de transplantar a pacientes con neoplasias hematológicas. Actualmente, el efecto antitumoral del AMD3100 está siendo

evaluado en ensayos clínicos para tratar pacientes de mieloma multiple, leucemia y algunos tumores sólidos recidivantes. Con lo cual, sería interesante evaluar si el inhibidor AMD3100 proporciona beneficios al ser combinado con fármacos de la terapia estándar actual para mejorar el tratamiento de pacientes con LDCGB; para ello es necesario establecer las dosis adecuadas y valorar si el inhibidor es capaz de inducir muerte celular o bloquear la diseminación y/o colonización de las células de linfoma.

Por último, en esta tesis hemos evaluado la expresión de CXCR4 en biopsias ganglionares de pacientes de LDCGB primario. Describimos por primera vez la correlación positiva entre expresión de CXCR4 en membrana y una significativa disminución en la supervivencia libre de progresión (SLP) en los pacientes de LDCGB. Además, hay una tendecia hacia la significación entre la expresión de CXCR4 en membrana y la supervivencia global (SG) de los pacientes. Estos resultados indican que probablemente aumentando el número de muestras y/o el seguimiento de los pacientes, la tendencia ganaría significación. Los análisis de COX multivariante indican que CXCR4 es un marcador independiente que predice la SLP en pacientes de LDCGB. Estos resultados concuerdan con el valor pronóstico del marcador CXCR4 descrito en otras neoplasias tanto sólidas (cáncer de mama, colon, pulmón) como hematológicas (leucemia mieloide aguda, leucemia linfocítica crónica).

Nuestros resultados indican que CXCR4 es un marcador pronóstico que podría ser incorporado en la clínica para determinar el riesgo de recaída de los pacientes con LDCGB. Aún así, sería conveniente validar estos resultados en una serie independiente de pacientes y utilizar un mayor número de muestras.